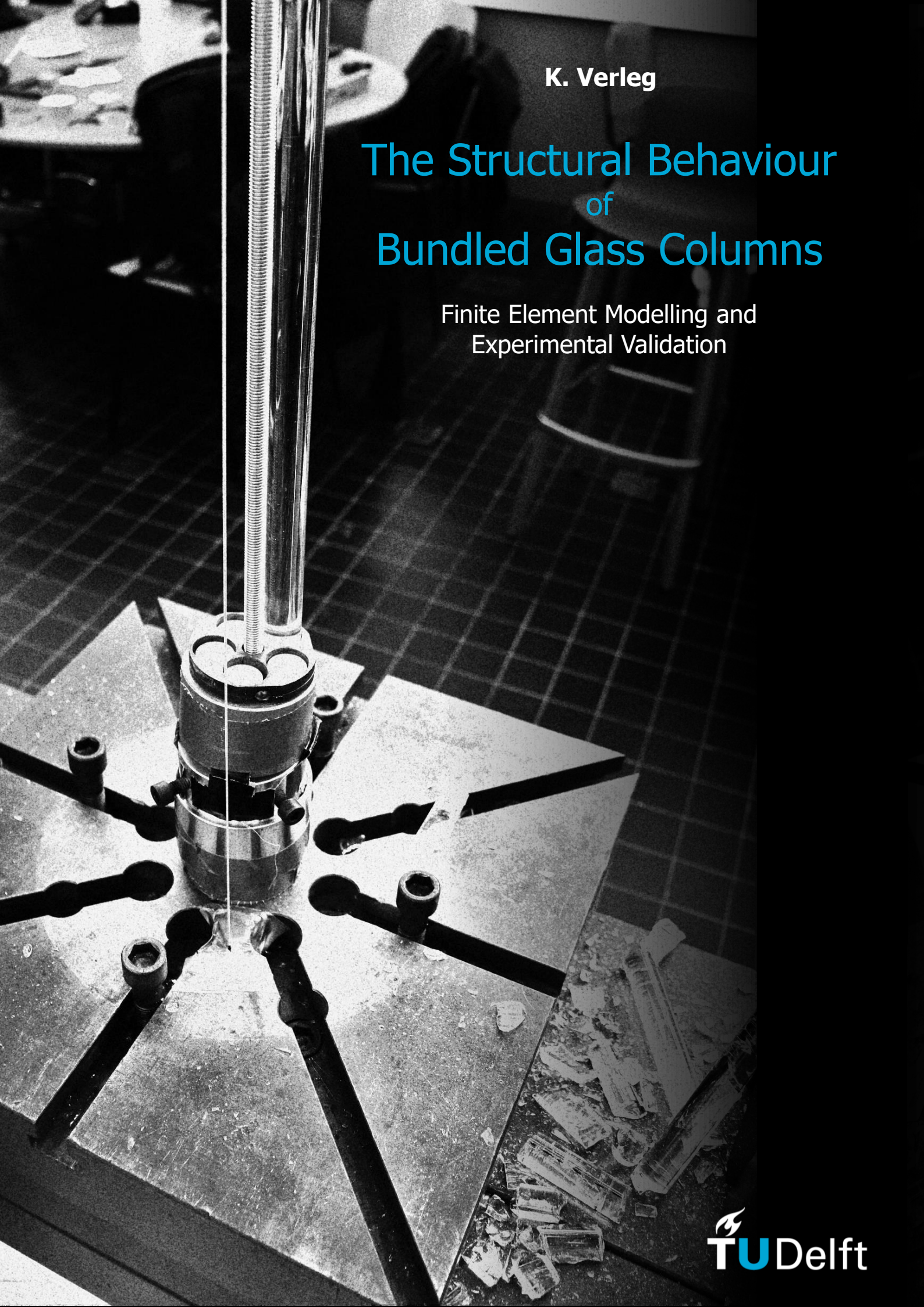

K. Verleg

The Structural Behaviour of Bundled Glass Columns

Finite Element Modelling and Experimental Validation

TU Delft

The Structural Behaviour of Bundled Glass Columns

Finite Element Modelling and Experimental Validation

by

Katinka Verleg

To obtain the degree of Master of Science in Structural Engineering
at Delft University of Technology,
to be defended publicly on Friday November 29th, 2019 at 15:00.

Student number: 4213211
Project duration: February 26, 2019 – November 29, 2019

Assessment Committee

Chairman:	Prof. dr. A.V. Metrikine,	Structural Mechanics (TU Delft)
Daily supervisors:	Prof. ir. R. Nijsse,	Building Engineering (TU Delft)
	Dr. F. Messali,	Structural Mechanics (TU Delft)
	Dr. J.M. De Oliveira Barbosa,	Structural Mechanics (TU Delft)
	Dr. ir. F.A. Veer,	Structural Design & Mechanics (TU Delft, Faculty of Architecture)

TU Delft Delft University of Technology

Preface

Katinka Verleg
Delft, November 2019

This document you are holding right now represents for me the end of an amazing phase of my life as a TU Delft student. But nevertheless, it also represents the beginning of new adventures and opportunities in the future. My choice to study Civil Engineering as a bachelors and Structural Engineering as a masters enabled me to find the interesting topic that is elaborated in this thesis.

The main subject of this research is structural glass, but originally the topic was structural dynamics. This was due to the desired knowledge of the dynamic behaviour of the Glass Truss Bridge. During the beginning of this studies, it was found that, to gain knowledge about the behaviour of a structure on itself, it is necessary to know what the structural behaviour of its individual structural components are. The diagonals of the Glass Truss Bridge consisted of bundled glass columns. Since the structural behaviour of these columns was practically unknown, it was necessary to start researching those before diving into the structural behaviour of the bridge itself. Although it was hard for me at the beginning to let go of the original goal of this research, I am happy to say that the change of topic to the structural behaviour of bundled glass columns resulted in a thesis that I am proud to present.

The events above led to an interesting assessment committee with a structural dynamics expert as chairman. I would like to thank Andrei Metrikine for his mechanical questions and feedback of the behaviour of the bundled glass columns and for helping me to make the decision to switch the topic. João de Oliveira Barbosa helped me from my very first day of the graduation process and kept giving good insights during the progress meetings, I would like to thank him for that. Furthermore, I would like to thank Rob Nijsse for giving me the topic of this research to begin with and for allowing me to perform the spectacular tests I did on the Bend & Break columns. I would like to thank Fred Veer for helping me with all the tests. Thanks to Fred I have learned a lot about the practical issues that occur during testing and how to solve them. Furthermore, his thorough research on the failure behaviour of structural glass helped me a lot during my own research. Last but not least, I would like to thank Francesco Messali for helping me with my finite element modelling and the programming needed to make my models. Francesco was always there to give a second opinion about the various assumptions I made, which resulted in the finite element models presented in this thesis.

I would like to acknowledge multiple individuals who helped me to successfully perform the experiments. Ewoud Veltmeijer for helping me straightening the columns before testing. Lars Duindam, Siddhesh Rajadhyaksha, José Abad and Stijn de Vreede for letting me use their GoPro cameras. Paul Vermeulen for attaching the strain gauges. Pim Buskermolen and Arthur de Groot for assisting me during the experiments.

At last, I would like to thank my family and friends for their support throughout my graduation.

Abstract

A group of researchers from Delft University of Technology is currently investigating new designs for slender and transparent glass columns. These researchers came up with a design that consists of bundled glass rods that can bear axial loads. The first application of such columns was to use them as diagonals in a truss footbridge located at the campus of the university. The safety of the bridge was ensured by, among others, compression tests on the diagonals. These tests, however, gave limited information about the structural behaviour and ultimate capacity of the columns. The behaviour of bundled glass columns was only briefly researched, which led to insecurities regarding the capacities of bundled glass columns in general. In this thesis two types of bundled glass column designs are investigated when subjected to a compressive load until failure. This knowledge can be used for future calculations of structures that consist of such glass columns. Furthermore, the findings give guidelines on how the designs of bundled glass columns can be improved.

In order to simulate the structural behaviour of bundled glass columns, finite element models are created. For one of the bundled glass column designs, the 'Bend & Break columns', these finite element models were validated using compression tests until failure of twenty of such columns. The design of these columns consists of five separate glass rods with a diameter of 20 mm. The general failure mode of the columns appeared to be buckling, which causes tensile stresses in the glass that lead to failure. A new approach to model structural glass until failure is proposed in this study, where all the finite elements have a different tensile strength drawn from a statistical (Weibull) distribution. This new approach is based on studies regarding the failure stresses of glass. These failure stresses are difficult to determine, since they are dependent on microscopic flaws at the surface of the glass. The variety of flaws cause differences in tensile strength along the glass. At this point in time, insufficient studies are available regarding the choice of statistical distribution to estimate these tensile stresses perfectly. Since the knowledge used to create the finite element models is limited, these finite element results only represent a part of experimentally obtained data. However, since the finite element results lay in line with the experimental results, this new finite element modelling approach shows potential for future calculations with structural glass. Especially when bearing in mind that the results are already this accurate without the desired prior knowledge.

The experimental results of the Bend & Break columns showed maximum capacities of the columns varying between 58 kN and 93 kN. With knowledge gained from the finite element models and these experiments, it was concluded that these differences were mainly caused by an inequality in stress distribution over the glass rods within the columns. This is caused by, among others, differences in rod lengths. To simulate this, simplified finite element models were created where glass rods were removed in different configurations. The experimental results showed intermediate results between the finite element results of those configurations. By assigning the experimental results in rod configuration groups, estimations are made regarding the probability of occurrence of a column having a certain capacity.

The same principle was used to create finite element models for the design used for the Glass Truss Bridge diagonals. They consist of a glass hollow star-shaped profile encircled with six circular glass rods with a diameter of 22 mm that are glued to the star-shaped profile. Unfortunately, the finite element models of the Glass Truss Bridge diagonals can only be partly validated. However, using this partial validation, it is expected that the models are trustworthy. This resulted in the knowledge that the design of the Glass Truss Bridge diagonals have a load bearing capacity that is approximately 4 times higher than that of the Bend & Break column design. This difference in capacity is caused by the larger cross-sectional area of the Glass Truss Bridge diagonals, but also due to the ability to transfer loads from one glass rod to another within the column. It is, among others, recommended to improve the design of bundled glass columns such that the stress distribution over the rods is as equal as possible. This will decrease the range in variety of structural behaviour of the columns.

Contents

I

Introduction

1

Introduction

This chapter gives an introduction to this graduation project. The objectives and the methodology to reach those objectives are described. Additionally, a scheme showing the outline of this thesis is presented which can be used as reading guide for this thesis.

1.1. Introduction to the Research

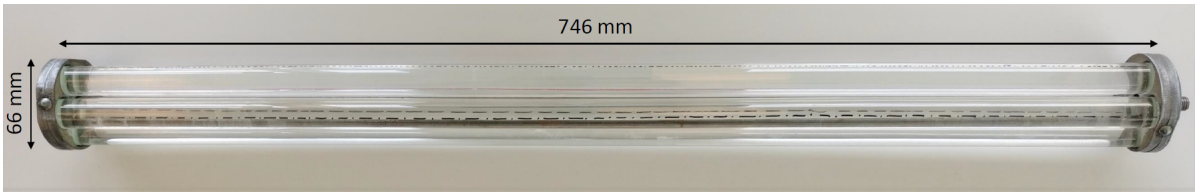

Figure 1.1: A bundled glass column consisting of 5 borosilicate glass rods.

Buildings which consist largely of glass are generally considered aesthetically attractive. The more glass, the more open and light a structure will appear. Typically, glass used in structures does not have any structural function, it merely gives resistance to a wind load when it is for example used in a façade. Researchers of Delft University of Technology are currently investigating new designs of structural glass elements, including transparent bundled glass columns which can take axial forces [1]. One application of these glass columns is the implementation of these elements as diagonals in a truss footbridge bridge, see Figure 1.2. The theoretical strength of glass is very high due to the chemical bonds within the glass, namely ±17 GPa [2]. Also from a sustainability point of view, building with glass is attractive due to its recyclable nature and non-corrosive behaviour. This raises the question of why glass, a strong material that is aesthetically more attractive in comparison to other building materials, is not used more often structurally.

The problem with using glass for structural elements is that glass fails in a brittle and relatively unpredictable way. This makes glass appear as an unsafe structural material and is, therefore, not generally used in structural applications. The thorough knowledge of the structural behaviour of more conventional building materials, such as steel or concrete, makes those for most engineers the best design choice. Furthermore, the strength of the glass in practice is around 1000 times smaller than its theoretical strength [2]. This is due to geometrical imperfections such as bubbles in the glass, scratches or microscopic flaws at the surface, which cause a significant decrease of tensile strength of the glass at those points. The guidelines that are currently available to design with structural glass are too conservative due to the uncertainties regarding the failure strength of glass. Conservative designs are less economical and less sustainable and, therefore, make glass a less attractive building material. With more knowledge available regarding the structural behaviour of newly designed structural glass elements, like the bundled glass diagonals shown in Figure 1.2, it is likely that the threshold for designing with glass structural elements will be lowered.

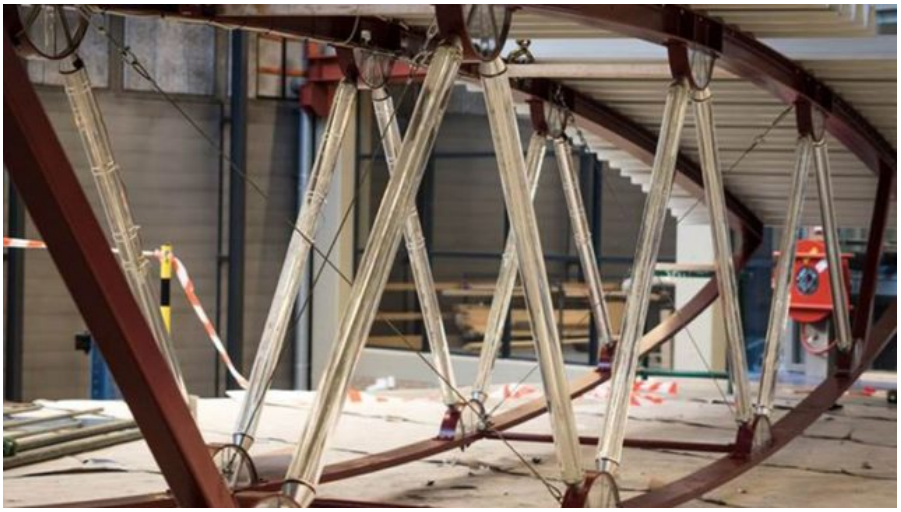

Figure 1.2: Picture of the Glass Truss Bridge designed by researchers of Delft University of Technology before erection. The diagonals consist of bundled glass rods [3].

Before this study, however, little was known about the structural behaviour of the bundled glass columns (or diagonals) created by the researchers of Delft University of Technology. The diagonals in the Glass Truss Bridge were tested to prove their structural capacity to be sufficient. Furthermore, static and dynamic tests on the bridge itself after erection were performed to validate its safety. Although those tests proved that the design was safe, it did not give information about the maximum capacity or the structural behaviour of the diagonals. During this graduation project the structural behaviour of bundled glass columns was studied. This knowledge can be used for future calculations of structures that consist of such glass columns, like the Glass Truss Bridge. Furthermore, the findings give guidelines on how the designs of bundled glass columns can be improved.

In this research two types of bundled glass column designs were investigated. The first type is the design shown in Figure 1.1, the 'Bend & Break column'. Since it was possible to perform tests on already fabricated columns with this design, these were studied most thoroughly. The other investigated design is the one belonging to the diagonals in the Glass Truss Bridge. It was not possible to perform tests on that type of bundled glass column, since the creation of new columns was too expensive in both time and costs. As a result, the studies regarding the Glass Truss Bridge diagonals is limited to partly validated finite element (FE) models and conclusions.

1.2. Objectives and Methodology

The overall goal of this research and the research questions are given here. Furthermore, the methodology used to accomplish the objective is presented.

1.2.1. Objective

The objective of this research is to understand the structural behaviour of two particular types of bundled glass column designs that are subjected to a compressive load until failure.

To achieve this objective, finite element models of the *'Bend & Break'* bundled glass column design are created. Those models are validated by experimental results obtained as part of this research. These particular columns were tested in compression until total failure. After validation of the finite element models, the used finite element modelling method was implemented to make models that could predict the behaviour of the *'Glass Truss Bridge diagonals'* when loaded in compression until failure. This methodology will be elaborated in more detail in the following subsection.

To help achieving the objective, the following research question and subquestions are answered in this study:

How do two particular designs of bundled glass columns behave structurally, when subjected to a compressive load until failure?

- What are the material properties of the glass used in the two bundled glass column designs?
- How can the failure behaviour of structural glass be modelled?
- What is the failure behaviour of the two bundled glass column designs?
- What are the buckling and maximum loads of the two bundled glass column designs?
- What are the differences in the structural behaviour of the two bundled glass column designs?

1.2.2. Methodology

Literature research

Using literature, information is obtained regarding the mechanical properties of glass as a structural material. Especially the failure behaviour of glass is investigated, since this differs from other, more conventional, building materials. Previous studies that include examples of finite element modelling of (structural) glass, shows that finite element modelling of this material until failure is a challenge. Using the obtained knowledge regarding the structural behaviour of glass, a new method to model structural glass until failure using finite element modelling is proposed.

Experimental research

The material properties of the glass used in both bundled glass column designs are validated by measuring and calculating the Young's modulus using ultrasonic pulse velocity testing. Furthermore, experiments were performed on the Bend & Break columns using displacement controlled compression tests until failure. This was done for twenty of such columns, to determine the failure behaviour and structural capacity. The collected results (force-displacement diagrams, measured strains, fracture patterns and video footage) were used to validate the finite element models of the Bend & Break columns.

Numerical research

Multiple finite element models of the Bend & Break columns are created in order to gain knowledge about the variety in structural behaviour between the tested columns. By comparing the results of the experimental research with the finite element results, the models and the way of modelling the structural glass within the columns is validated. Next, using the same material properties and the same modelling principles as done in the finite element model of the Bend & Break columns, finite element models of the Glass Truss Bridge diagonals are created. These are used to predict the behaviour of these diagonals when they are subjected to compressive loads until failure, while also giving additional information about the structural behaviour of these bundled glass column designs.

The experimental and numerical research described above helped answering the questions regarding the buckling loads, failure loads and failure behaviour of bundled glass columns. Comparison between the two kinds of finite element models gave estimations on the differences in structural behaviour between the two kinds of bundled glass column designs, which answers the last research question.

1.3. Outline

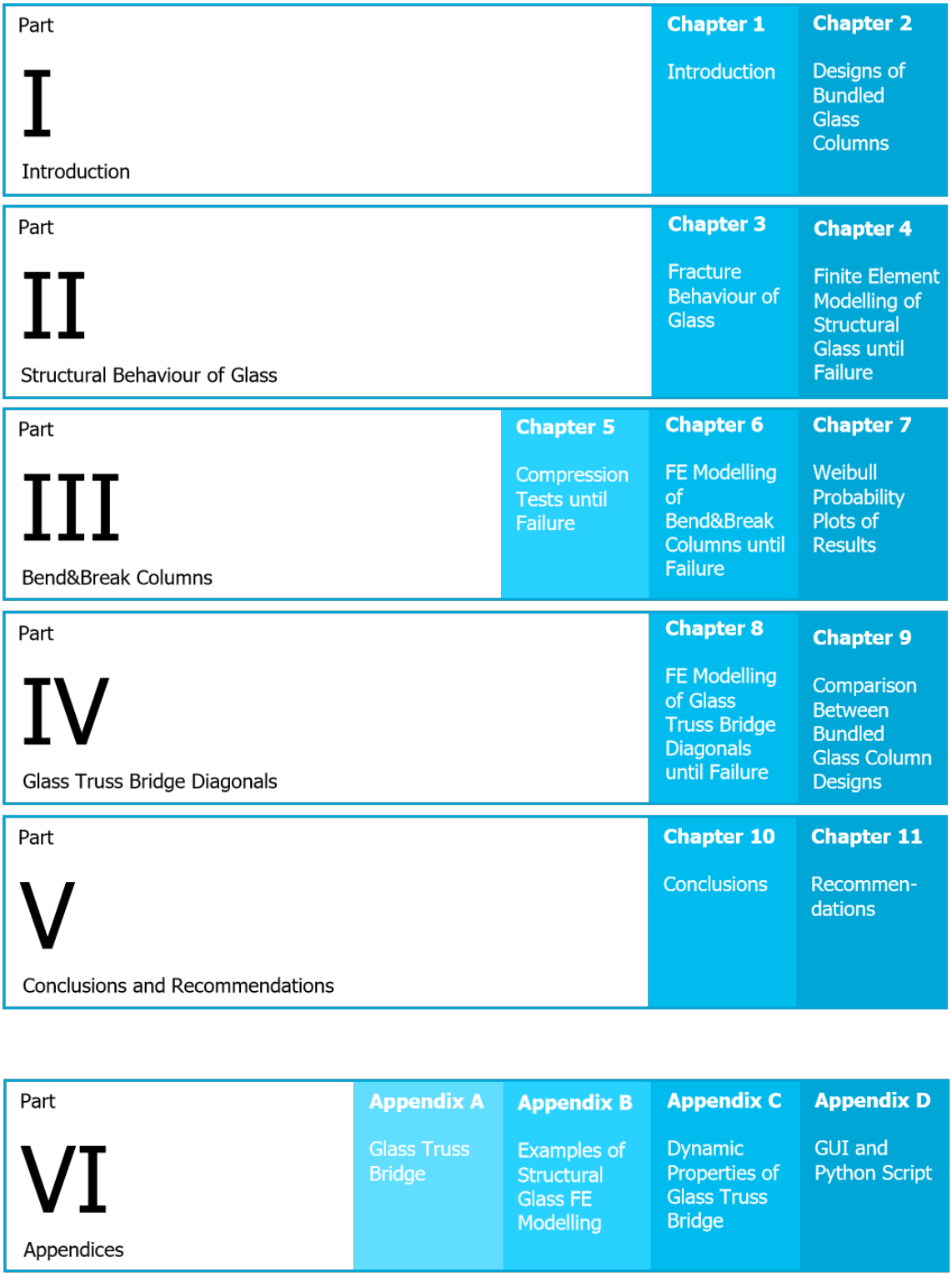
Part
I
Introduction
Chapter 1
Introduction
Chapter 2
Designs of Bundled Glass Columns
Part
II
Structural Behaviour of Glass
Chapter 3
Fracture Behaviour of Glass
Chapter 4
Finite Element Modelling of Structural Glass until Failure
Part
III
Bend&Break Columns
Chapter 5
Compression Tests until Failure
Chapter 6
FE Modelling of Bend&Break Columns until Failure
Chapter 7
Weibull Probability Plots of Results
Part
IV
Glass Truss Bridge Diagonals
Chapter 8
FE Modelling of Glass Truss Bridge Diagonals until Failure
Chapter 9
Comparison Between Bundled Glass Column Designs
Part
V
Conclusions and Recommendations
Chapter 10
Conclusions
Chapter 11
Recommen-dations
Part
VI
Appendices
Appendix A
Glass Truss Bridge
Appendix B
Examples of Structural Glass FE Modelling
Appendix C
Dynamic Properties of Glass Truss Bridge
Appendix D
GUI and Python Script

2

Designs of Bundled Glass Columns

Researchers at the Glass Department of Delft University of Technology are working on the design of slender and transparent glass columns. In the past, designs of glass columns have been realised and used in buildings. These glass columns mainly consist of laminated glass panels of which an example is shown in Figure 2.1(a). However, the application of such glass columns is rare. The glass column designs made at Delft University of Technology consist of circular glass rods that are bundled together to form a single column, see Figure 2.1(b) where one of the so called 'Bend & Break columns' is depicted. By bundling the glass rods instead of using one solid glass column, the safety of the design is increased since there is more than one way to bear the load. Furthermore, the fabrication of multiple smaller glass rods is easier and therefore results in glass of better quality, while the production prices stay relatively low due to automation [4].

(a) Glass column made of laminated glass panels at the Danfoss headquarters in Nordborg, Denmark. Architect: Schmidt Hammer Lassen Architects. Contractor: H.S. Hansen [5].

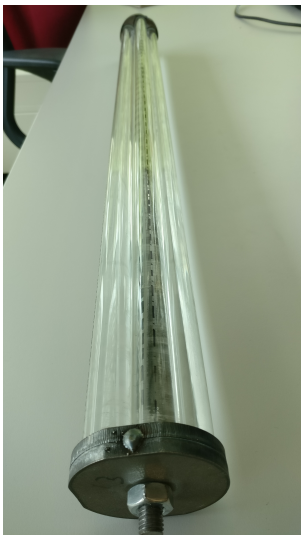

(b) Bend & Break bundled glass columns consisting of 5 glass rods designed by Delft University of Technology.

Figure 2.1: Structural glass columns.

Glass is a difficult material to use in engineering, due to, among others, its poor behaviour when it is subjected to tension. It is, however, very strong in compression. The bundled glass columns are, therefore, designed in such a way that the glass will be subjected to compressive forces only. How this is accomplished is shown in this chapter. Furthermore, this chapter describes the designs of the bundled glass columns made by the researchers of Delft University of Technology. Three designs are

discussed, which are chosen to show different phases in the design of the bundled glass columns. Firstly, the initial bundled glass column design is shown, on which compression tests were performed on various column lengths in 2016 [4]. Secondly, the design of the Glass Truss Bridge diagonals is elaborated. That design shows great resemblance with the initial bundled glass column design. At last, the design of the so called 'Bend & Break columns' is discussed. This design is relatively new and different to the previous designs.

The glass used in all of the presented bundled glass column designs is borosilicate glass. This type of glass is known for its high resistance against heat and chemicals in comparison with, more commonly used, soda-lime glass. In comparison with soda-lime glass it has lower Young's modulus, mass density and generally also a lower failure (tensile) strength. The latter also highly depends on the manufacturing process of the glass, which influences the quality and, therefore, the occurrence of bubbles in the glass and the size and amount of surface flaws. Those flaws cause differences in strength along the glass; this will be elaborated in more detail in Part II of this thesis. Table 2.1 shows the material properties of the borosilicate glass according to the glass producer SCHOTT. During this thesis project the Young's modulus given in this table was validated using ultrasonic pulse velocity testing, see Figure 2.2. When the geometry and density of a certain material is known, the Young's modulus can be determined by measuring the travelling speed of sound through that material. Using this method it was proven that the Young's modulus of the glass was indeed around 63 GPa. Therefore, it can be assumed that the other material properties given in Table 2.1 are correct as well.

	Unit	**Value**
Young's modulus	GPa	63
Poisson's ratio	-	0.2
Mass density	kg/m^3	2230
Thermal expansion coefficient	10^{-6} K^{-1}	3.3

Table 2.1: Material properties of the borosilicate glass used in the bundled glass column designs according to the glass producer SCHOTT [6].

Figure 2.2: Determining the Young's modulus of a borosilicate glass rod using ultrasonic pulse velocity testing.

2.1. Initial Bundled Glass Column Design

This section shows the initial bundled glass column design and the results of the performed compression tests as described in the paper of F. Oikonomopoulou et al. [4]. Since this design is similar to the design of the Glass Truss Bridge diagonals, the test results shown in this section are used to partly validate the finite element models of the Glass Truss Bridge diagonals presented in Chapter 8.

2.1.1. Design

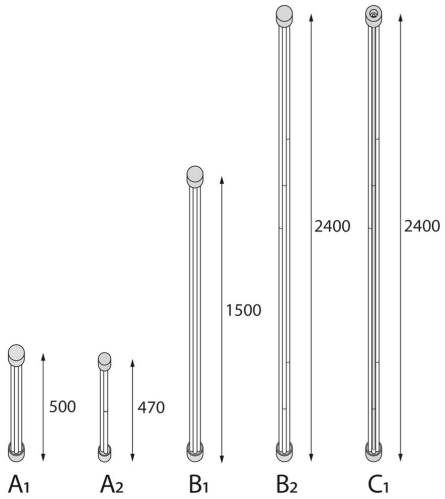

(a) Specimen series that are tested in compression. Lengths depicted in mm.

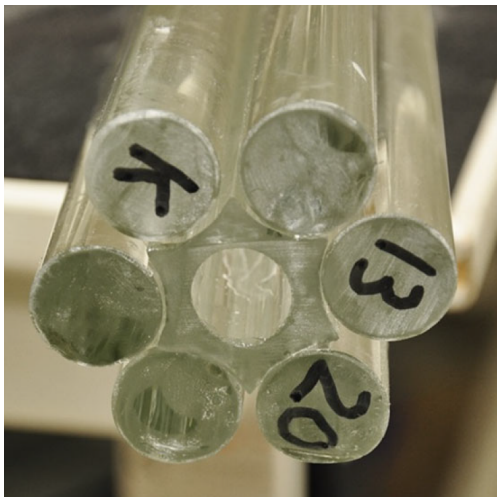

(b) Cross-section showing six circular glass rods and one hollow star-shaped glass profile in the centre. They are glued together using a UV-curing adhesive.

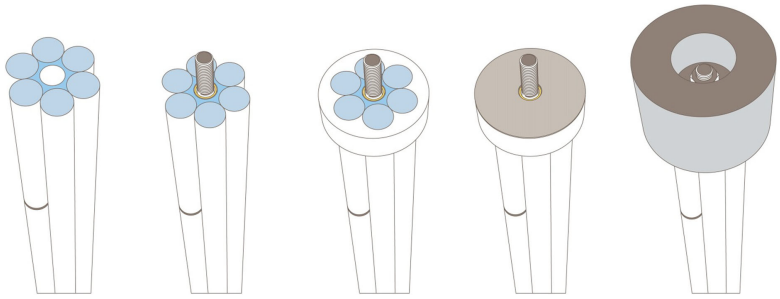

(c) Configuration of the glass rods and the head detail needed to introduce the post-tensioning of configuration C_1.

Figure 2.3: Configurations of earlier bundled glass column designs tested in compression in the labs of Delft University of Technology in 2016 [4].

In 2016 lab tests were performed on one of the first bundled glass column designs. Here, compression tests were done on different column configurations. Those configurations are shown in Figure 2.3(a). In Figure 2.3(b) the cross-section of those columns is shown, which is the same for every configuration. Here it can be observed that the glass rods on the outside have circular cross-sections, while the glass rod in the middle has a hollow star-shaped cross-section. The circular rods are glued to the star-shaped profile in the middle using a UV-curing adhesive. The glass profiles are made by the company SCHOTT. The six circular solid rods are of the *DURAN*® series and have a diameter of 22(±0.45) mm. While the hollow star shaped profile is of the *CONTURAX*® series and has an inner diameter of 17(±2.00) mm and an external diameter of 30(±2.00) mm. The latter profile is only commercially available in the mentioned parameters. The six circular solid rods were chosen to match the star-shaped profile. These glass rods should be able to work together as one solid glass column. As mentioned previously, this is accomplished by gluing the circular rods to the star-shaped profile with an adhesive. The chosen adhesive is a UV-curing acrylate adhesive with medium viscosity. *DELO*® *PHOTOBOND*® *4468* is used due to its colourless nature, similar refraction index to glass, fast application and impressive mechanical properties [4] [7].

Special care is taken for the boundary conditions of such columns, since it is important to avoid peak stresses when transferring loads from the boundary towards the glass rods. Direct contact of the glass rods with steel can cause such peak stresses and will lead to fracturing of the glass rods ends. Figure 2.3(c) shows the head detail of the right-most configuration (C_1) of Figure 2.3(a). This configuration is

a post-tensioned column as opposed to the other depicted configurations. That post-tensioned configuration is high-lighted, since both the Glass Truss Bridge diagonals and the 'Bend & Break columns' are post-tensioned in a similar fashion. Post-tensioning of the columns is advantageous, since it ensures the glass to be in compression. This post-tensioning is realised by placing a steel rod in the centre of the column with nuts at both ends. By turning of the nuts, the post-tensioning is applied. The other configurations in Figure 2.3(a) show, from left to right, a relatively short column (A_1), a relatively short column with spliced connections along the length of the rods (A_2), a medium length column (B_1), a relatively long column with spliced connections along the length of the rods (B_2) and at last the post-tensioned column which has the same spliced design in glass rods as configuration B_2 (C_1). The spliced connections were made to enable the creation of longer columns, since the glass manufacturer only produces the glass rods up to a length of 1500 mm. Since both the Glass Truss Bridge diagonals and the 'Bend & Break columns' are smaller than 1500 mm, those spliced connections are not used in these designs [4]. The configurations of the initial bundled glass columns that show most resemblance to the Glass Truss Bridge diagonals, are configurations B_1 and C_1. This is due to its length and the post-tensioning of the configuration respectively.

2.1.2. Compression Tests

Series	Spec. no.	Length [mm]	End connections	Post-tension	Approx. load where first crack was observed	F_{max} [kN]	λ
B_1	1	1500	Clamped	No	N.R.	331.0	47
	2				260	389.4	
	3				120	508.8	
B_2	1	2400	Pinned	No	45	63.0	151
	2				N.R.	75.0	
	3				70	90.0	
C_1	1	2400	Pinned	Yes	N.R.	69.0	151
	2				N.R.	64.4	
	3				N.R.	62.7	

Table 2.2: Dimensions and strength values of B_1, B_2 and C_1 series of specimens [4].

Figures 2.4 and 2.5 show load-displacement diagrams which resulted from the compression tests of configurations B_1, B_2 and C_1. In the latter figure, stage 1 represents the setting of the machine. In stage 2 the column is slightly compressed. Stage 3 shows that the lead layer in the columns is compressed. In stage 4 the glass is loaded in compression; stage 5 shows the initiation of buckling. In addition, the specifics and strength values of the specimen of the B_1, B_2 and C_1 series are given in Table 2.2. It is chosen to show the results of these configurations, since those are most similar to the Glass Truss Bridge diagonal designs. It is interesting to observe from the load-displacement diagrams that configuration C_1 shows a more ductile behaviour in the buckling stage. This is due to the post-tensioning of the column. Figure 2.6 shows the failure pattern of a specimen of configuration C_1. It can be seen that the failure of the column is mostly in the glass and not in the adhesive layer. This means that the capacity of the glue is larger than the capacity of the structural material; the glass. This type of adhesive was therefore a good design choice.

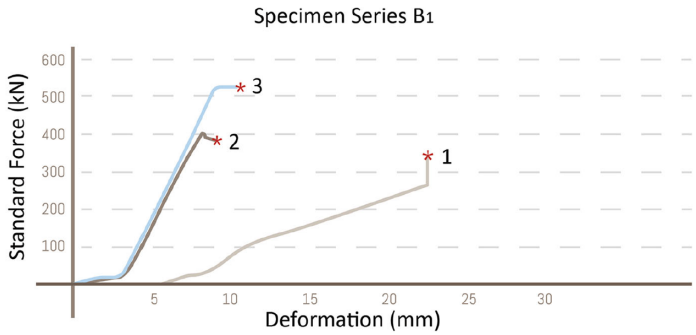

Figure 2.4: Load-displacement diagrams of the B_1 series the first bundled glass columns made by researchers of Delft University of Technology [4].

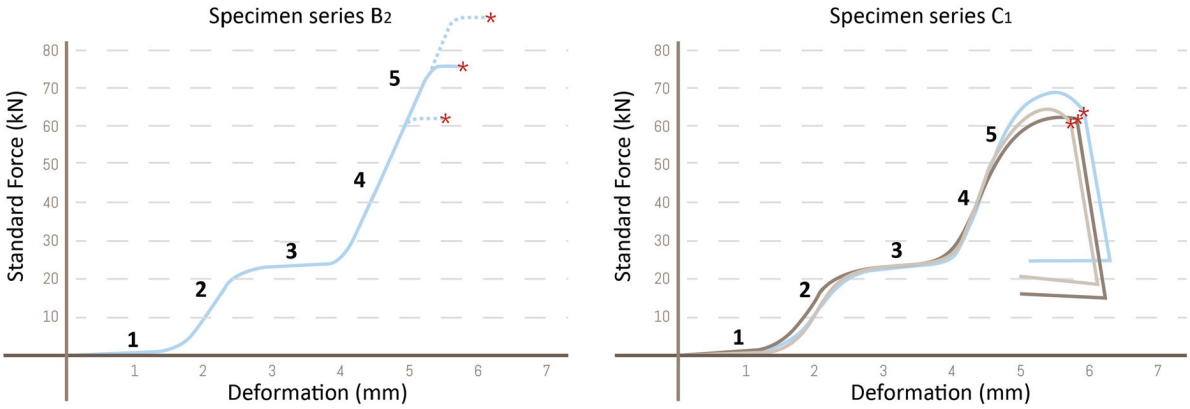

Figure 2.5: Load-displacement diagrams of the B_2 and C_1 series of the first bundled glass columns made by researchers of Delft University of Technology. The difference between the two series is that C_1 is post-tesioned while B_2 is not. In both graphs 5 different stages are indicated which are elaborated in the previous paragraph [4].

Figure 2.6: The failure pattern of a specimen of configuration C_1 [4].

2.2. Glass Truss Bridge Diagonals

Figure 2.7: Picture of the Glass Truss Bridge located at the Delft University of Technology campus. The diagonals are made of bundled glass rods. The left-most and right-most diagonals are steel. The bridge has a span of 14 meters [1].

After the lab tests that were performed on the bundled glass columns as described in the previous section, it was decided that it was time to use such columns in a real structure. This idea was executed by means of the creation of a truss footbridge, of which the diagonals in the truss would be bundled glass 'columns'. This footbridge, which is called the Glass Truss Bridge (see Figure 2.7), was realised in 2017 and is located at the campus of the university. This section describes the design of these diagonals.

Compression tests were performed on the diagonals before they were installed in the bridge. Those tests and the obtained results are discussed as well. More information about the Glass Truss Bridge itself can be found in Appendix A.

2.2.1. Design

The Glass Truss Bridge diagonals have the same cross-section as the initial bundled glass columns as described in the previous chapter, see Figure 2.8. The same type of glass profiles were used from the same glass manufacturer, the adhesive used to glue the rods together is the same as well. The boundary conditions are, however, slightly different.

Glass is, as a material, very sensitive to imperfections. Where small imperfections are present, stresses will accumulate which will cause the glass to break at a relatively low applied force in a brittle way [8]. The connection has to be made in such a way to avoid peak stresses. Such peak stresses can occur in the contact area between steel and glass. Therefore, the boundary conditions shown in Figure 2.9 are chosen to avoid such peak stresses. The left-most image shows the green, star-shaped PLA centering ring, which ensures the steel rod to stay in the centre of the diagonal to avoid direct contact with the glass. The next image shows the soft aluminium ring which guarantees that no peak stresses occur in the glass. A steel ring is placed on top of this aluminium ring to spread the loads. After that, the extension nut is placed on the steel rod to enable post-tensioning. The aluminium ring has a star-shaped hole in the middle which exactly matches the green PLA centering ring. The load transfers from the steel plate through the aluminium, avoiding the PLA ring. This causes the load to be transferred to the circular rods only. In this way, large stresses in the relatively fragile legs of the star-shaped glass profile are avoided [1].

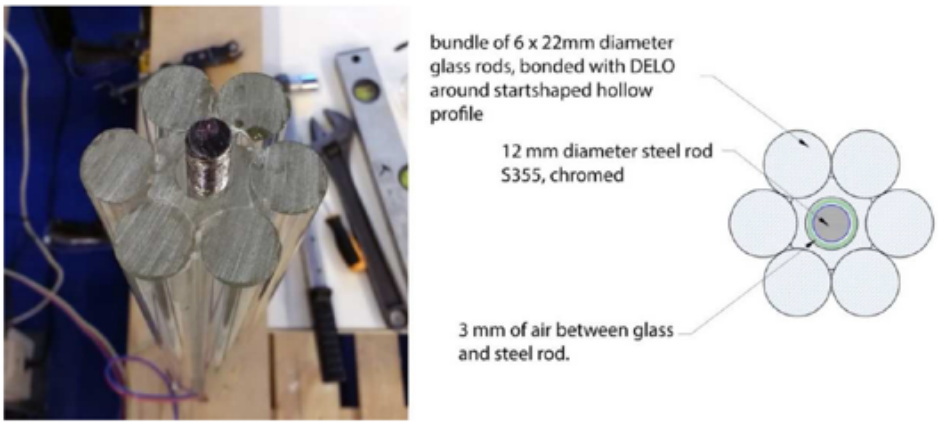

Figure 2.8: Cross-section and configuration of a bundled glass diagonal [1].

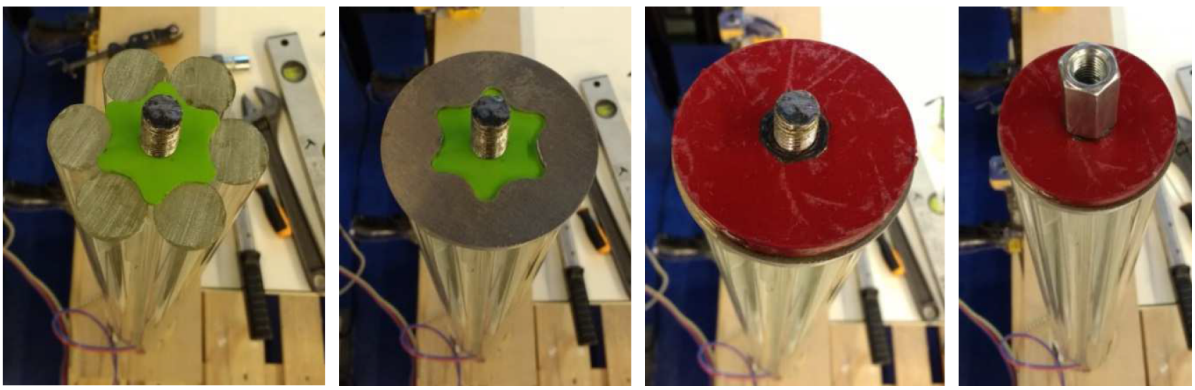

Figure 2.9: (a) Steel pre-tension rod and PLA centering ring. (b) Soft aluminium ring to avoid peak stresses. (c) Steel ring to spread load. (d) Extension nut to enable post-tensioning [1].

The glass diagonals are post-tensioned in order to ensure a compression force in the glass at all times, since tension is an unfavourable load condition for glass. The post-tensioning could be realised by placing a 12 mm chrome coated, steel rod in the centre of each bundled glass diagonal. A post-tensioning force on these steel rods was applied; the well designed steel to glass connections enabled these forces to transfer through the glass. The steel rods and the post-tensioning were necessary, since in a truss structure some diagonals will be in tension, while others are in compression. Whether a certain diagonal is in tension or compression can change in time when different load cases are present on the bridge. Therefore, every diagonal must be able to resist tension and compression. The steel rods can transfer the tension forces in the diagonals without the need to transfer these tension forces through the glass. The applied post-tensioning force is as much as the maximum tension force in a diagonal that was calculated in the design stage [1].

2.2.2. Compression Tests

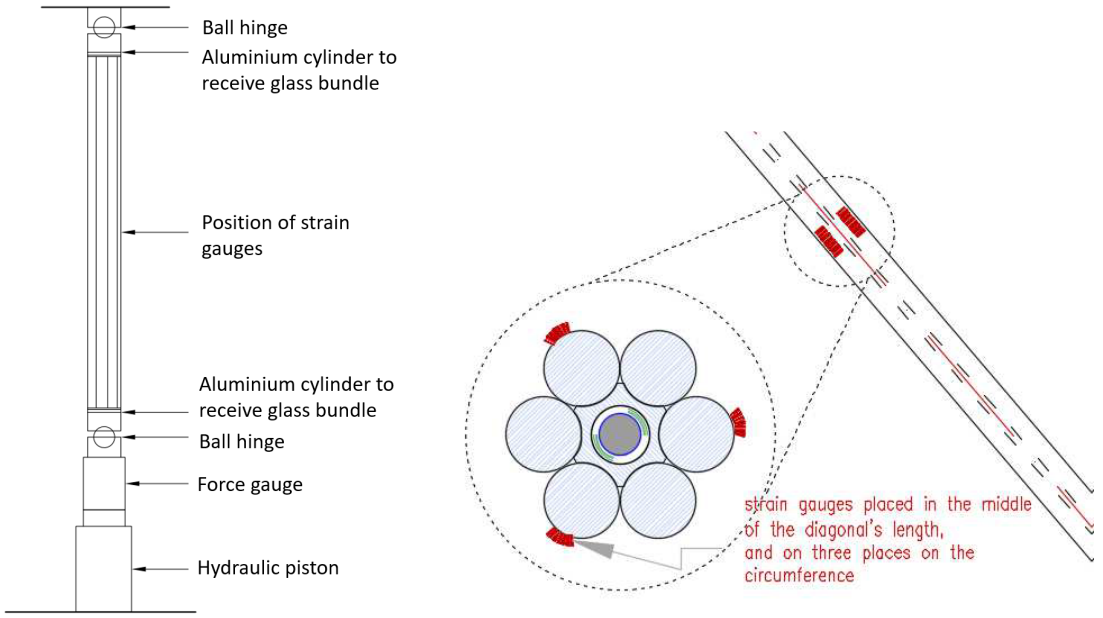

(a) Schematised drawing of lab tests setup [9].

(b) Position of the three strain gauges, all the strain gauges are placed in the middle of the diagonals [1].

Figure 2.10: Test setup of the compression tests on the Glass Truss Bridge diagonals.

In March 2017 the Glass Truss Bridge diagonals were created and tested before they were placed in the bridge structure. They were subjected to compression tests in the Stevin II laboratory of Delft University of Technology. A drawing of this test setup is illustrated in Figure 2.10(a). All the diagonals were loaded twice the amount of the maximum expected load. The loads were maintained for 10 minutes after which the diagonals were gradually unloaded [1]. Examples of the output of the tests are shown in Figure 2.11, where a force-microstrain [m/μm] plot is given for two of the diagonals. It can be seen that three lines are plotted, since each diagonal was supplied with three strain gauges. The position of those strain gauges is shown in Figure 2.10(b). The applied post-tension is not included in the graphs, since the strain gauges were positioned after post-tensioning.

It can be seen from Figure 2.11 that the diagonals show a linear stress-strain relation for the applied forces. Furthermore, small plastic deformation occurs, which is probably caused by the deformation of the aluminium ring [1] shown in Figure 2.9. The slopes of the graphs sometimes differ per strain gauge although they belong to the same diagonal. The explanation of this phenomenon is given in Chapter 8 where, furthermore, test results for all diagonals are shown.

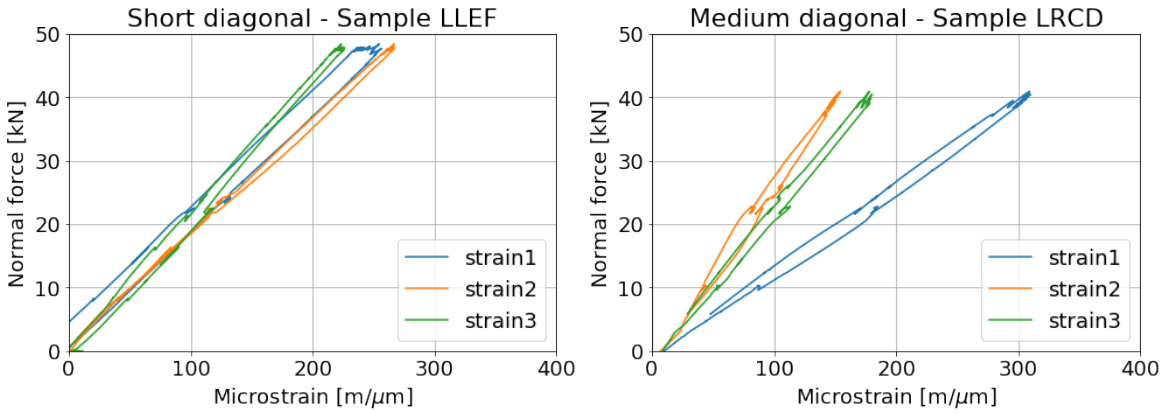

(a) Example where the slopes of the plots are approximately equal.

(b) Example where the slopes of the plots differ per strain gauge.

Figure 2.11: Examples of the output of the compression tests performed on the Glass Truss Bridge diagonals in 2017. The results are given as force-strain diagrams.

2.3. Bend & Break Columns

The use of glue in the previously described designs will make decomposition and, therefore, recycling of the glass in the columns impossible. For this reason, designs of bundled glass columns without the use of an adhesive are studied. This is why the 'Bend & Break column' design differs from the previously shown designs. The 'Bend & Break columns' were, again, designed by researchers of Delft University of Technology. However, the production was done by bachelor students of the university in 2017. The creation of these columns was part of a minor program at the faculty of Civil Engineering which is called Bend & Break. Therefore, these glass columns are referred to as 'Bend & Break columns'. In total 46 of those columns were created. Twenty of those were tested in compression until failure as part of this graduation project.

2.3.1. Design

The Bend & Break columns consist of five borosilicate glass rods of approximately 728 mm which have a diameter of 20 mm. These glass rods are from the same glass manufacturer, SCHOTT, as the rods of the previously discussed designs. The hollow star-shaped profile is not present in this design. However, the steel rod that enables post-tensioning is present in this design as well. The configuration is such that direct contact between the glass rods or the steel rod is avoided as shown in Figure 2.13(b). To avoid steel to glass contact within the column, POM (polyoxymethylene) discs with a thickness of ±2 mm are placed between the steel endplates and the glass rods ends. These discs will prevent the occurrence of peak stresses in the glass rods ends and are, therefore, an important aspect of the design of the columns. In the other bundled glass column designs this was done by including a lead sheet or a aluminium ring in between the steel and the glass rods ends. This layer of lead used in the initial bundled glass column design was too soft and, therefore, got pressed outwards, decreasing the thickness of the layer of lead between the steel and the glass more and more. The POM discs have a lower Poisson's ratio in comparison to lead; ν = 0.42 for lead and ν = 0.37 for POM. Therefore, that material was chosen to use in the Bend & Break column design as an improvement of the boundary conditions in comparison to the lead or aluminium rings.

Figure 2.12: Initial twist in one of the Bend & Break columns.

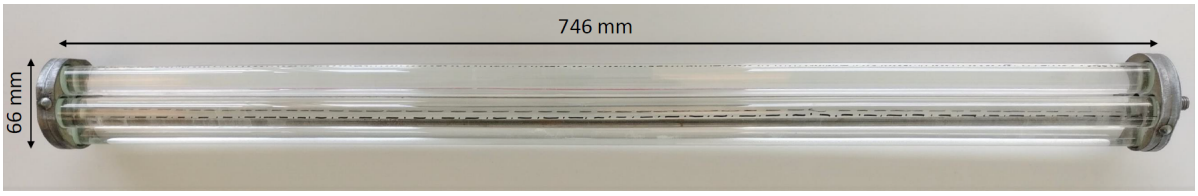

(a) A Bend & Break column. The five glass rods inside the column have an average length of 728 mm.

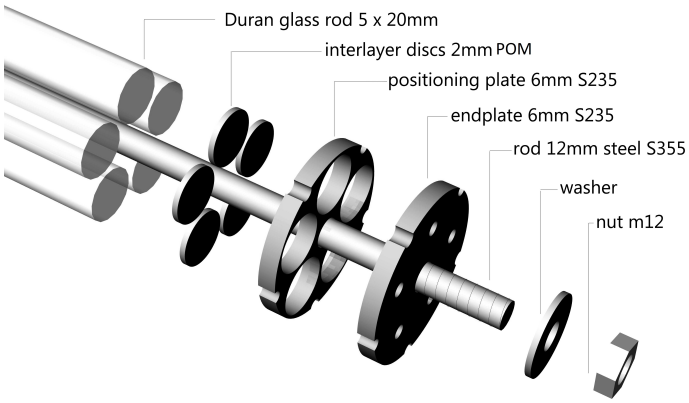

(b) Design of the Bend & Break columns.

Figure 2.13: The configuration of the Bend & Break columns.

The steel rod in the middle of the columns together with the nuts on the ends of the columns and the holes in the endplates will ensure that the glass rods stay in place. Furthermore, by twisting the nut post-tension can be applied in the column. The downside with this particular bundled glass column design is that when the nut is twisted to apply some post-tensioning, the column itself will twist with it, which is undesirable. The severity of the twist in some of the columns beforehand can be seen in Figure 2.12. The white bar laying on the end of the column should be horizontal if the column had no twist, here a twist angle of approximately 45° can be observed. Before testing of the columns, this twist was reduced as much as possible by turning of the nut. By removing the twist of the columns, the post-tension of the rods was almost completely removed. Therefore, it can be assumed that the stresses caused by post-tensioning in the tested Bend & Break columns was negligible.

2.4. Comparison between Designs

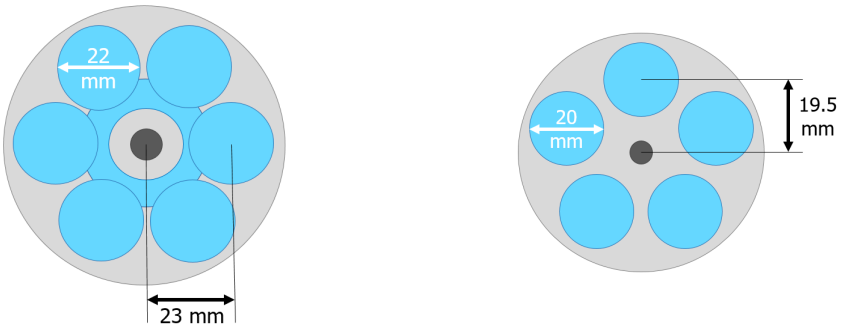

(a) Cross-section of a Glass Truss Bridge diagonal.

(b) Cross-section of a Bend & Break column.

Figure 2.14: The configuration of a Glass Truss Bridge diagonal versus that of a Bend & Break column.

In this section the focus is on the designs of the Glass Truss Bridge diagonals and the Bend & Break columns only. These are the bundled glass column designs that are tested and modelled in this study. It is important to know the design differences, since it was only possible to perform experiments on the Bend & Break columns. That means that the experimental results given previously in this chapter are the only means to validate the finite element models that are created for the Glass Truss Bridge diagonals. The experimental results belonging to the initial bundled glass column design and the obtained results regarding the Bend & Break columns can, however, give indications about the accuracy of the Glass Truss Bridge diagonals finite element models.

The Bend & Break columns have a smaller and simpler geometry than the diagonals of the Glass Truss Bridge. First of all, the Bend & Break columns consist of five glass rods with a diameter of 20 mm. While the diagonals of the Glass Truss Bridge consist of six circular glass rods ($d = 22$ mm) with an additional star-shaped glass profile in the middle, see Figure 2.14. In the diagonals of the Glass Truss Bridge, the glass profiles were glued together using a UV-curing adhesive. No adhesives are used in the Bend & Break columns. At last, the material that prevents the glass rods to be in direct contact with steel, differs per design. In the Glass Truss Bridge diagonals soft aluminium is used, while in the design of the Bend & Break columns POM (polyoxymethylene) is used. These materials are incorporated to balance the stresses and, therefore, avoid peak stresses in the glass rods ends. A summary of the differences in designs can be found in Table 2.3.

	Glass Truss Bridge diagonals	**Bend & Break columns**
Length [mm]	1251 / 1339 / 1408	746
Number of rods	6	5
Diameter of rods [mm]	22	20
Star-shaped profile	Yes	No
Use of adhesive	Yes	No
Stress balancing material	Soft aluminium	POM

Table 2.3: Differences between the configurations of the diagonals of the Glass Truss Bridge and the Bend & Break columns.

II

Structural Behaviour of Glass

3

Fracture Behaviour of Glass

Unlike most building materials, the failure behaviour of glass is mainly dependent on geometrical imperfections instead of the material properties of the glass itself [8]. For clarification, the behaviour of glass will be compared to the behaviour of steel; a more commonly used structural material. When steel is loaded in tension, the steel starts to yield at a particular stress, the yield strength, which is a known material property of that type of steel. Glass, however, has theoretically a very high ultimate strength due to the chemical bonds within the glass, but fails in reality at a very low tensile stress. This is due to geometrical imperfections within the glass, such as scratches, bubbles or microscopic flaws on the surface which cause significant decreases in tensile strength at those particular points. Therefore, knowing the theoretical material properties, like the ultimate strength of glass, is not enough to predict the failure behaviour of a piece of glass.

It has been shown, in practice, that failure of glass due to exceedance of the compressive strength is extremely rare. However, due to the minor flaws and cracks at the surface of the glass, stress peaks can occur which cause the glass to fail. The cause of failure is the exceedance of the tensile strength of the glass, which is low at those points. A failure mode that is likely to occur in glass panels as well as glass columns is buckling due to its slenderness. Buckling in its turn causes tensile stresses and, therefore, also fracture of the glass [10].

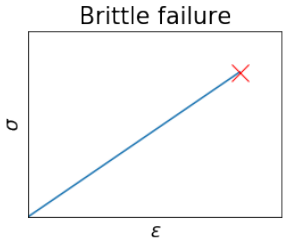

Figure 3.1: Stress-strain diagram showing brittle failure behaviour.

Glass experiences brittle failure, which means it will break suddenly without any warning. This is, therefore, a dangerous failure mode and makes glass a tricky material to use in a structural sense. For clarification Figure 3.1 shows the stress-strain diagram of brittle failure behaviour. It can be seen that the material behaves linear elastically up to a certain point where it exceeds the ultimate stress/strain. There it suddenly loses all its capacity to carry a load.

In this chapter the fracture behaviour of glass, which is relatively hard to predict, is described by means of statistics. Fracture mechanics, on the other hand, may give information about the origination and propagation of a crack, but it is limited to a local level for glass [11]. Since this study focuses on the global behaviour of glass columns, the statistical approach is of more value and is, therefore, highlighted in this chapter.

3.1. The Strength of Glass

As mentioned before, the theoretical strength of glass is very high, ±17 GPa in both tension and compression. This is estimated on the basis of the breaking of atomic bonds [2] [12]. Due to geometrical

imperfections within the glass, this theoretical strength is, however, never reached in reality. As previously mentioned, glass never appears to break to an exceedance of the compressive strength. It is, therefore, assumed that the imperfections influence the tensile strength only.

These flaws on the surface of the glass are often very small and can, therefore, not be seen by the naked eye. Figure 3.2 shows how small a surface flaw is in comparison with a real scratch. Due to the fact that surface flaws are often too small to be observed, it is difficult to predict where the tensile stresses in the glass will be lowest without looking at the glass on a microscopic level. Looking at glass with that much detail is not preferable due to time and cost related matters. From this, it can be concluded that the fabrication process and the care in handling of glass products after production, have great influence on the strength of the glass. This all makes it very difficult to predict what the strength of a glass product actually is.

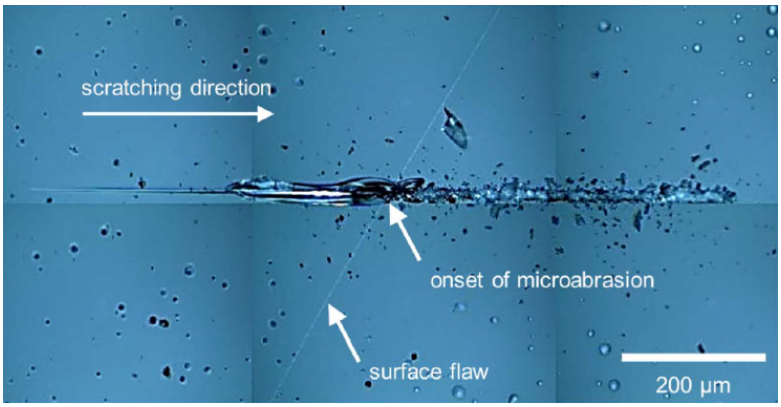

Figure 3.2: Microscopic picture of a scratch and a surface flaw on glass [13].

The strength of most materials that show brittle failure behaviour can be estimated using a statistical Weibull distribution. More information about this distribution is given in the following subsection. According to F.A. Veer, a glass engineering expert of Delft University of Technology, decades of research have been performed regarding the failure of glass. Unfortunately, it appears that the Weibull distribution on itself is not enough to estimate the failure stresses of glass. However, recent studies indicate that it can be approximated using multiple Weibull distributions [8]. This has all to do with the flaw sizes and orientation within the glass. Subsection 3.1.2 discusses these studies.

3.1.1. The Weibull Distribution

The Weibull distribution states that the fracture behaviour of a material is linked to the most significant defect within that material, this is the so called 'weakest link theory' [13]. Equations 3.1 and 3.2 give the probability density function and the cumulative distribution function of a 2-parameter Weibull distribution respectively.

$$f(x;\lambda,k) = \begin{cases} \frac{k}{\lambda}\left(\frac{x}{\lambda}\right)^{k-1} e^{-(x/\lambda)^k} & x \geq 0, \\ 0 & x < 0 \end{cases} \tag{3.1}$$

$$F(x;k,\lambda) = 1 - e^{-(x/\lambda)^k} \tag{3.2}$$

This 2-parameter Weibull distribution is used in this study, with the parameters k and λ. k defines the shape of the Weibull distribution, of which the differences can be clearly seen in Figure 3.3. It is sometimes also referred to as the Weibull parameter. This parameter is a characteristic of the glass and its surface preparation. λ on the other hand is dependent on the surface area and can be seen as a scaling factor or the mean strength of the glass, particularly for values of k near 5, when the probability density function shows resemblance with that of a normal distribution.

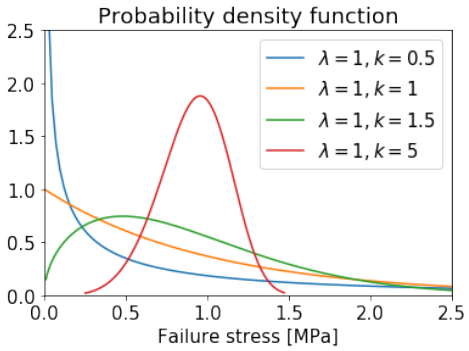

(a) Probability density functions.

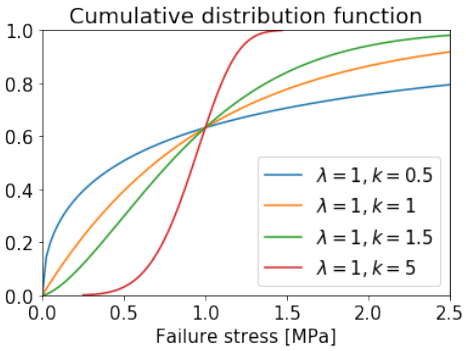

(b) Cumulative distribution functions.

Figure 3.3: Examples of 2-parameter Weibull distributions with varying k.

It can be seen that the Weibull distribution shows different shapes for different values of k, therefore, it is important to pay attention to the determination of these values. $k < 1$ indicates that the failure rate of a certain material decreases over time. If $k = 1$ the failure rate is constant over time. When $k > 1$, the failure rate increases over time [14]. The latter is most likely for glass, since glass is more likely to fail as time goes on due to increase in flaw sizes and flaw quantity.

3.1.2. Weibull Fit of Experimental Results

In studies done by F.A. Veer and Y.M. Rodichev [8], tests were performed on rectangular glass panels where on one of the broad sides a diamond scratch had been made. Four point bending tests were performed where the specimens were either placed vertically (standing tests) or horizontally (flat tests), see Figure 3.4. A distinction was made between whether the scratch was on the top or bottom side (for the flat tests) or on the left or right side (for the standing tests) of the glass. In these tests the load at failure was recorded, with which the failure (bending) stresses in the glass were calculated. The goal of these tests was to find whether or not these results could be fitted on a Weibull scale.

(a) Flat tests.

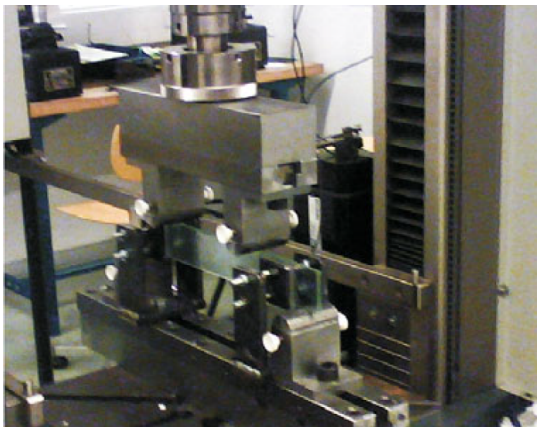

(b) Standing tests.

Figure 3.4: The test setups for both the flat tests and the standing tests [8].

In order to see whether the failure stresses of the tested specimens can be fitted to a Weibull distribution, these points can be plotted on a Weibull scale. With the failure stresses on the horizontal axis, which is a log-scale, and the Weibull scale on the vertical axis (which is different for each type of probability distribution) the values will make a good fit if they show a linear distribution. This is done for all the measured failure stresses for both tests. By means of an example, the focus will from now on be on the flat tests with the diamond scratch upwards only. The results are shown in Figure 3.5, which

is an adjusted version of the plot provided in the literature [8], used to find the Weibull parameters k and λ. It can be seen that it was not possible to fit a linear Weibull plot in between the data. Therefore, multiple lines are plotted belonging to different Weibull distributions in order to make a better fit. It can be stated that the failure stresses of these glass specimens can be fitted to a multi-linear Weibull distribution.

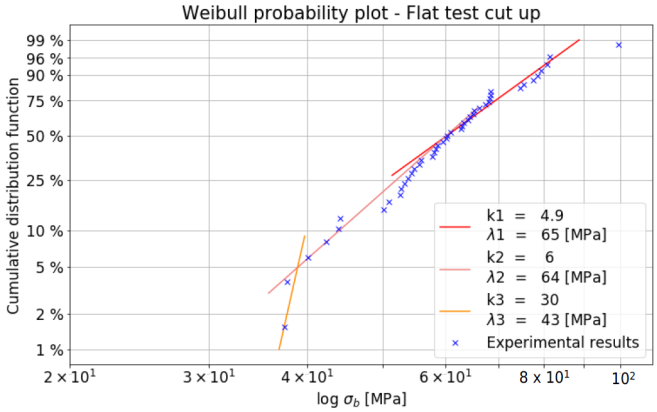

Figure 3.5: Weibull plot of flat test results with the diamond cut upwards. The horizontal axis depicts the failure (bending, tensile) stresses [8].

There is no single statistical descriptor that gives a universal fit on all the test results in practice [8]. However, when the cracks of these particular test specimen are explored in more detail, a distinction can be made between fracture that starts from the left side and fracture that starts from the right side. When these test results are all plotted in a different graph, a linear Weibull plot does match the results fairly accurately. This can be seen in Figure 3.6.

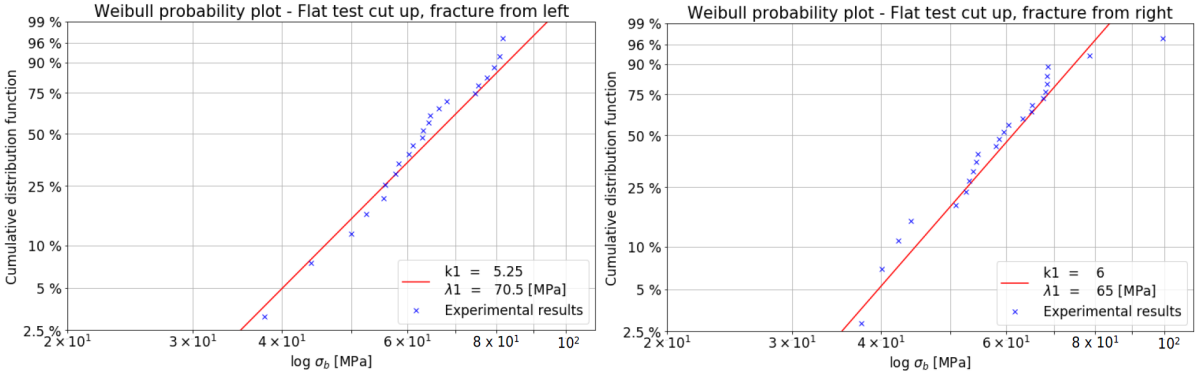

(a) Fracture from left.

(b) Fracture from right.

Figure 3.6: Weibull plots of flat tests results with cut upwards for fracture from the left and from the right [8].

From this example it can be concluded that the failure stresses of glass can be approximated by using a Weibull distribution, but only if a distinction is made between the crack origin and propagation. This, on its turn, gives information about the flaw size and orientation. The influence of flaw orientation can be explained in a simplified way with the help of Figure 3.7. Here, a schematised image of a microscopic flaw is depicted, showing two different stress directions. The failure stress will be smaller if the stress is directed in the direction of $\sigma 1$, than if it would be directed in the direction of $\sigma 2$. A different stress direction, will, furthermore, cause a crack to originate from a different corner of the flaw. This behaviour can be compared with a piece of paper with a similar shaped cut. When pulling the paper in the direction of $\sigma 2$, more force is needed to rip the paper than if the paper is pulled in the direction of $\sigma 1$. Furthermore, the ripping will start in a different corner of the cut. This phenomenon explains why not only the flaw size but also the flaw orientation influences the strength of glass.

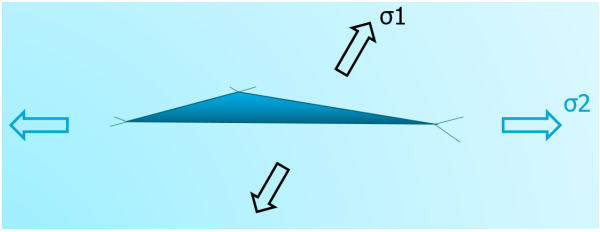

Figure 3.7: Schematised figure of a microscopic flaw within the glass. $\sigma 1$ and $\sigma 2$ represent two different stress directions.

All of the above indicates that there are a lot of factors which influence the strength of glass. Flaw size, orientation and quantity affect it, which on its turn are influenced by the type of glass manufacturing and the care in handling of the glass after production. These are all factors that are difficult to regulate. Furthermore, determining what the exact effect of a certain flaw is on the tensile strength is a great challenge that is still being researched. The experiments described in this section are an example of such a research. The multi-linear Weibull fits are part of the solution, but still more thorough knowledge is needed to obtain correct statistical distributions.

Figure 3.8 shows images that were very recently created by using a new advanced microscope of Delft University of Technology by F.A. Veer. This microscope is able to capture the 3-dimensional microstructure of the flaws within the glass by generating pictures that are taken on various distances from the specimen. It is expected that with the use of this microscope current research regarding the types of flaws within the glass, and what they mean for the tensile strengths of the glass, can be extended in the near future.

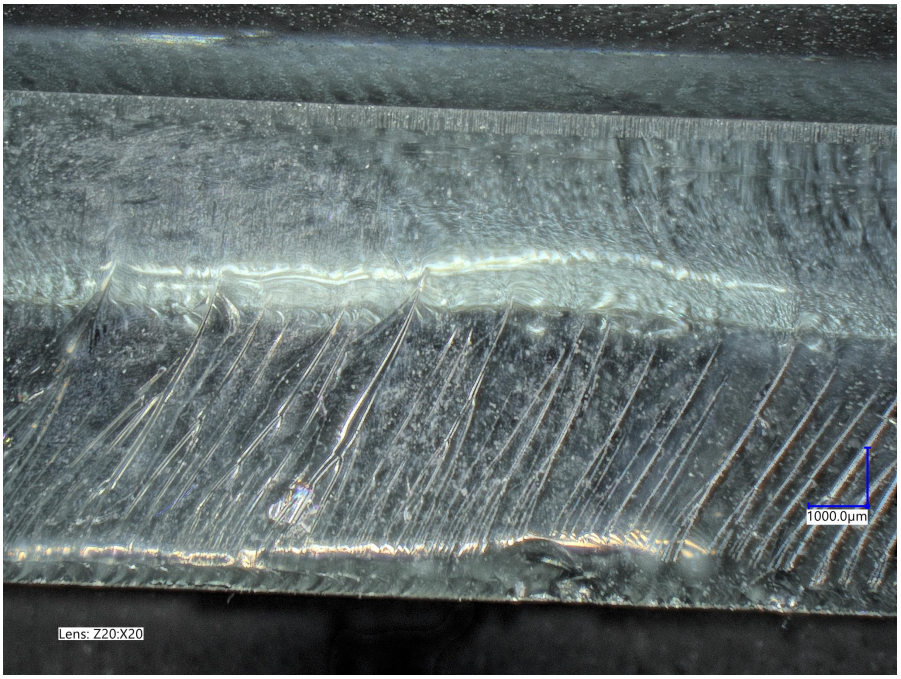

(a) Scratches that result from the cuts made to break the glass panel.

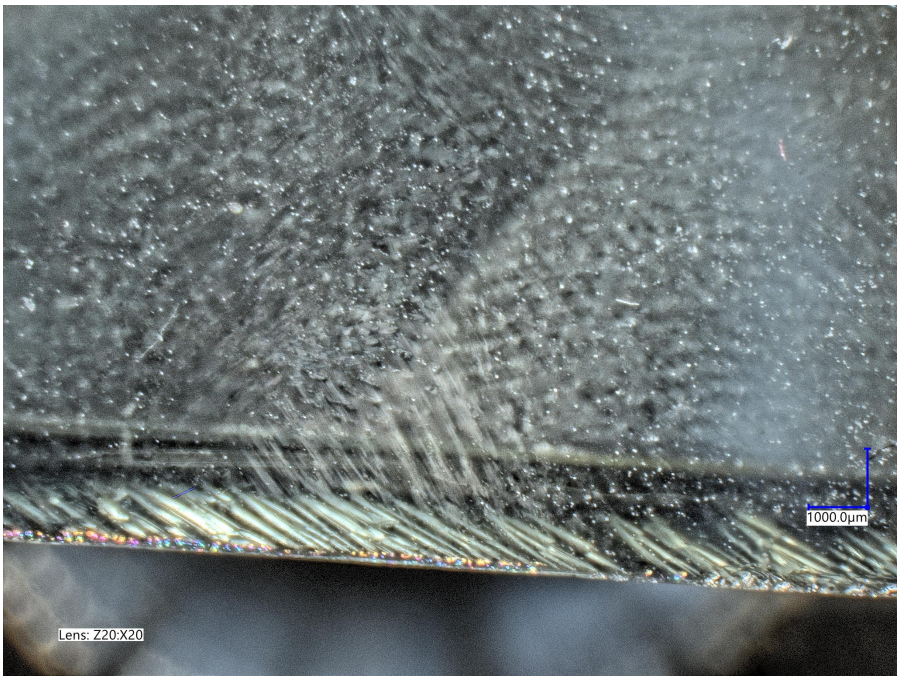

(b) Picture showing bubbles in the glass that can not be identified with a normal microscope.

Figure 3.8: Microscopic images of edges of cut glass panels made by F.A. Veer in November 2019. By making pictures of the glass from multiple heights this microscope is able to generate images that show the 3D structure of micro flaws within the glass.

4

Finite Element Modelling of Structural Glass until Failure

In Chapter 3 an introduction is given to the Weibull distribution; it was pointed out that the failure stresses of glass can be fitted to multi-linear Weibull distributions. In this studies, this knowledge is used to present a new approach for modelling the failure of structural glass using the finite element method. Here, varying tensile strengths are drawn from Weibull distributions to assign to the various finite elements. This finite element modelling method shows potential in predicting the failure load of glass elements more accurately than before. The finite element models of the bundled glass columns are created using this method.

The first section of this chapter elaborates the new way of modelling structural glass. Here a brief example will be given by a model of a glass rod. Section 4.2 will show finite element models and results of the experiments on the glass panels of Section 3.1.2. The latter will show the potential of this new finite element modelling approach in comparison to the conventional way where a single, low value tensile strength is given to all the elements. Even these conventional finite element models are rarely used when making calculations for glass. Examples of finite element modelling of glass from literature are given in Appendix B. Modelling glass for civil engineering purposes is normally limited to a loading stage below the failure load of the glass. However, modelling until the failure load is possible and done in, for example, models for car windows. In these cases the origin of the crack is known, since the position of an (impact) load is prescribed. In reality the position of the fracture origin will not be known beforehand. The glass can even start to fail simultaneously at multiple points within the same structural glass element. This new method of glass finite element modelling, indeed, does show cracks originating at different points along the piece of glass. This can be observed in the example given in Section 4.2 and in the bundled glass column finite element models presented in Chapters 6 and 8.

4.1. A New Approach to Model Glass

As mentioned before, glass fails in a certain way due to cracks and/or flaws on the surface or bubbles within the glass. Due to the variety in geometrical imperfections, the failure stress of every piece of glass is different. Glass fails due to tensile stresses that exceed the ultimate tensile strength where a critical flaw is present in the glass. From this point of view, it could be stated that the variety of geometrical imperfections along a piece of glass causes a variety of tensile strengths along that piece of glass. Hence, the geometrical flaws of the glass are translated into physical flaws. When a certain geometrical imperfection is large, e.g. a big scratch, the tensile strength will be relatively low at that particular point.

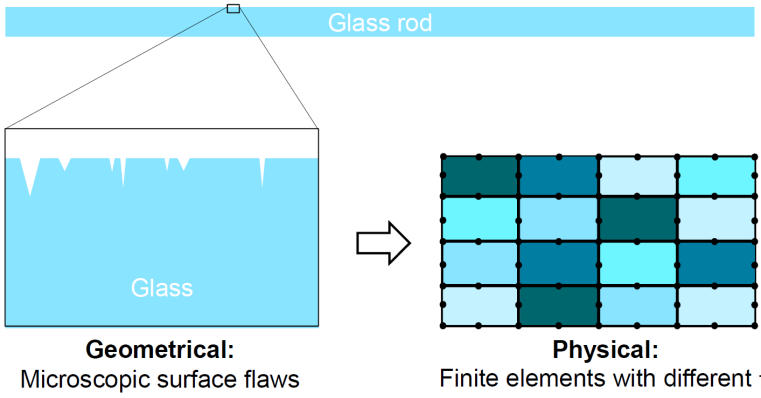

Figure 4.1: Translation of geometrical surface flaws into physical finite element properties. This principle is used in the method presented in this thesis to model the fracture behaviour of structural glass.

For this study, the flaws in glass are modelled by using the finite element method. The glass will be divided into a finite number of elements, which all have a certain ultimate tensile strength. The tensile strengths of the various finite elements are drawn from a Weibull distribution to account for the variety in imperfections. As depicted in Figure 4.1, the varying geometrical surface flaws in the glass will be translated to varying physical (material) properties of each finite element. The latter refers to varying ultimate tensile strengths, while keeping the other material properties of the glass identical for all elements. A simplification that is made in this method, is that only one Weibull distribution to describe the differences between imperfections along the glass is used. In reality, but often neglected in literature, the size of the flaws as well as the orientation will result in at least two different Weibull distributions.

The following subsection will show an example to elaborate this method of finite element modelling of structural glass until failure. This example shows the geometrical model and generated mesh for a glass rod like the ones the bundled glass columns are composed of. This example is merely to elaborate how the finite element models are created.

4.1.1. Finite Element Modelling of a Glass Rod

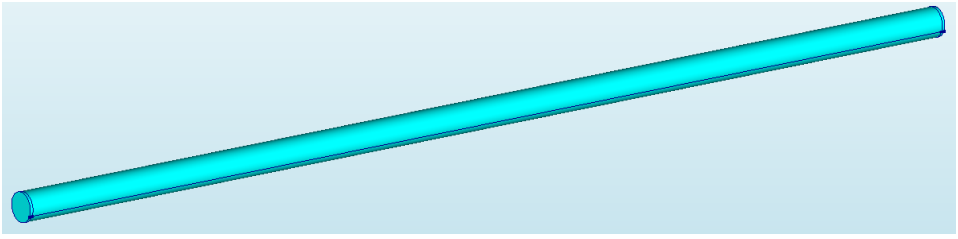

(a) Finite element geometry of the glass rod.

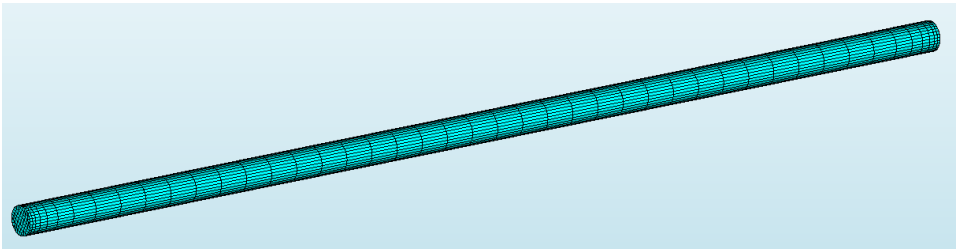

(b) Finite element mesh of the glass rod.

Figure 4.2: Finite element geometry and mesh of a glass rod with a diameter of 20 mm and a length of 728 mm.

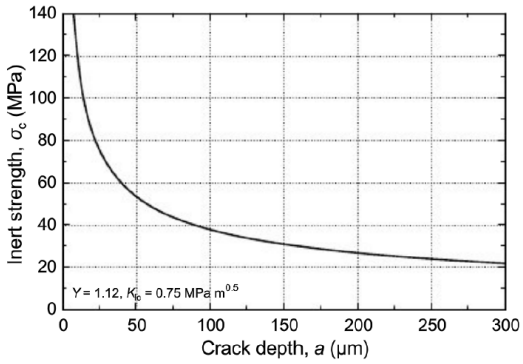

Figure 4.3: Dependence of the flaw depth in the glass on the tensile strength according to Haldimann et al. [10].

A circular glass rod is modelled in the finite element program DIANA, the geometry of the model is given in Figure 4.2(a). This model represents one of the rods used in the configuration of the bundled glass columns. The rod is of high quality glass and, therefore, the surface of the glass contains little and only shallow flaws. However, the rods that were produced by the manufacturer were longer than they should have been, so the rods were cut off at the right length. These cuts left the surfaces of the ends of the rod to be rough. It is, therefore, logical to presume that the finite elements at the ends of the rods have a lower failure strength than the rest of the finite elements. So the finite elements at the ends have tensile stresses drawn from a different Weibull distribution, with a lower mean, than the other elements.

The probability density functions of the Weibull distributions from which the elements are drawn for this example are given in Figure 4.4. The horizontal axis represents the (failure) tensile strength. On the vertical axis the probability of occurrence is depicted. The green graph represents the distribution for the rods ends. The red graph refers to the distribution belonging to the other elements (core). The dots along the graphs represent the tensile strengths (f_t) drawn from the distributions that will be used in the finite element model.

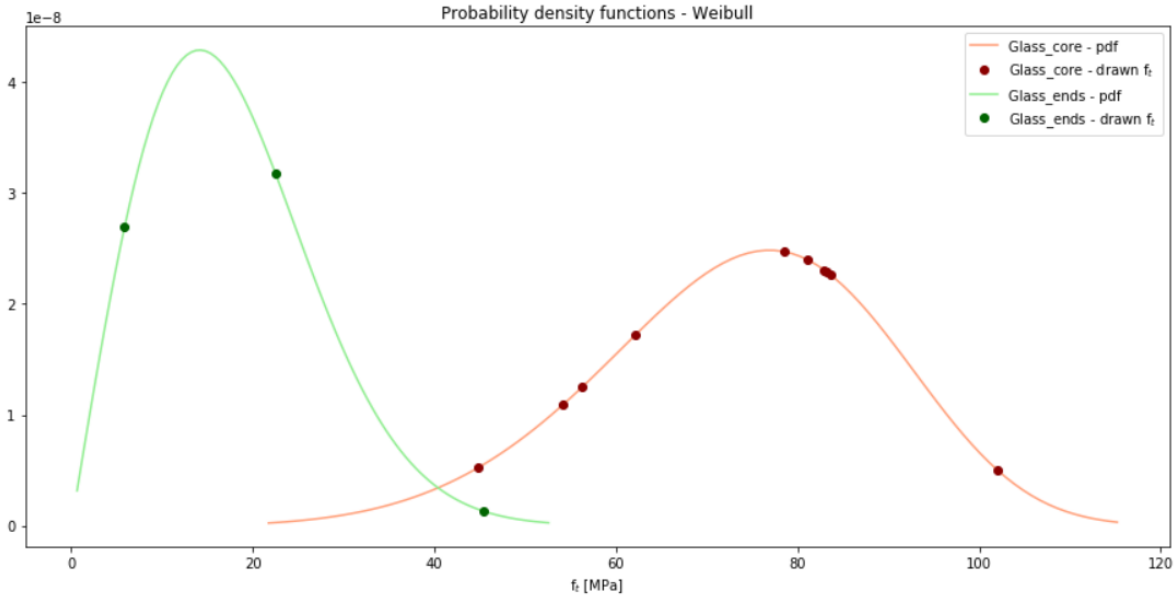

Figure 4.4: Probability density functions of the Weibull distributions used to model the glass rod with the dots referring to the drawn values of f_t. The green plot belongs to the glass ends with parameters $\lambda = 20$ MPa and $k = 2$. The red plot belongs to the rest of the glass elements (the core) and has parameters $\lambda = 80$ MPa and $k = 5.3$.

The Weibull parameters λ and k are estimated based on examples in literature. The values of λ are chosen by looking into the graph given in Figure 4.3, where the dependence of the flaw depth versus the tensile strength of glass is given according to Haldimann et al. [10]. Large flaw depths give a tensile strength that converges towards 20 MPa, which is used as a basis for the rods ends. A safe estimate for the strength of the rest of the rod is 80 MPa. The value of k is more difficult to predict. However,

from the University of Arizona a lecture about the Weibull distribution in the strength of glass given by E. Salamin [12] is available. Here an example is given on how to determine the Weibull parameters when a certain number of stresses at fracture in standard grade zinc sulfide discs are known. This gave a value of k = 5.3. This value of k is chosen as a starting point, although this example was for zinc sulfide instead of glass. Both the chosen values of λ and k are optimised for the finite element models of the bundled glass columns. This was done using the experimental results presented in Chapter 5.

It can be seen in Figure 4.4 that there are only limited values of f_t drawn from the distribution. Instead of giving all the finite elements a different random value, some tensile strengths are drawn from the distribution which will form a material set. All the finite elements will be randomly placed into a certain material set that belongs to a specific tensile strength. To visualise this, the elements that belong to a certain material set (a.k.a. have a certain tensile strength) have an assigned colour, see Figure 4.5. In this example the ends of the rod have three different material sets, and the rest of the rod has ten material sets. This can also be seen by the three green dots and the ten red dots in Figure 4.4. Furthermore, the figure shows that one of the drawn f_t for the rod ends has a very low probability of occurrence (f_t = ±45 MPa). Therefore, less elements will get this value in comparison with the other drawn values based on the probabilities of occurrence. This can also be seen in Figure 4.5(b). Here the elements of the rods ends are assigned light/pastel colours of which only 2 are coloured red, which indicates the rare tensile strength of ±45 MPa. The same procedure holds for the f_t drawn for the other glass elements (glass core); if the probability of occurrence of a certain value of f_t is high, a lot of elements will have that value. If the probability of occurrence is low, few elements will have that value.

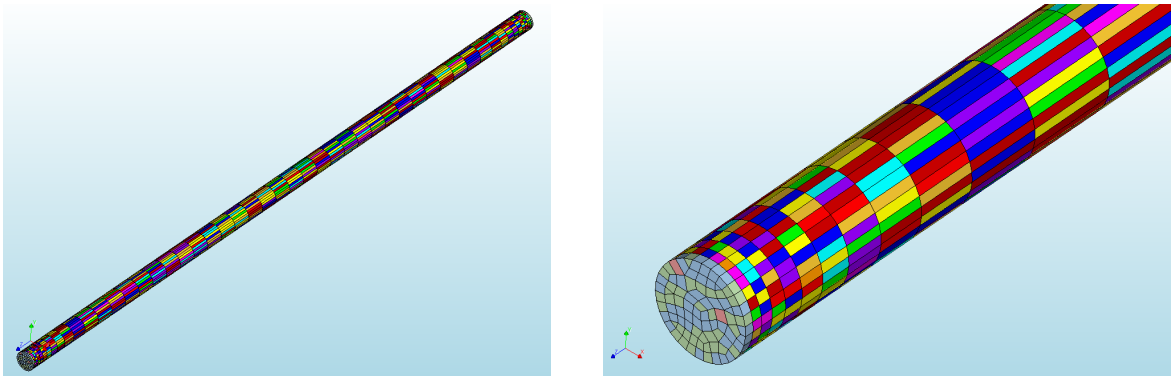

(a) Finite element mesh.

(b) Zoom-in on glass rod ends.

Figure 4.5: Finite element mesh of glass rod showing the different material sets by different colours. Each material set has its own value for the tensile strength (f_t).

4.1.2. Additional Comments

The example given in this section shows one possibility on how flaws on a glass rod can be distributed. In reality the rod that needs to be analysed can have flaws on different places that are unknown. Therefore, in order to make a good estimation of the failure stress of such a glass rod, it is needed to perform multiple analyses of different model. Each model will have different drawn tensile strengths assigned to randomised finite elements in the model. Every analysis will give a different outcome of the failure load. This is shown in Section 4.2 and done for the finite element models of the Bend & Break columns.

The finite element program, DIANA, does not have a built-in feature that randomises the elements as described in this chapter. In order to do so, a Python script is created which draws random numbers from the chosen Weibull distributions. Thereafter, it randomises the order of the glass finite elements in the finite element model data file and assigns them a certain tensile strength. The probability of occurrence of each drawn value determines how many elements are assigned to that particular material set. In this way, each created model has material sets with different tensile strengths, a different number of elements per set and elements at different locations that are assigned to each set. This all is accomplished by rewriting the input data file (a text file ending with .dat) of the DIANA finite

element model created by the user. The script is written in such a way that it creates a user-friendly GUI (Graphical User Interface) so that it can be used by others for future structural glass calculations. The script as well as the GUI are shown in Appendix D.

4.2. Finite Element Modelling of Glass Panels subjected to Bending

In Subsection 3.1.2 of Chapter 3 experiments done by F.A. Veer and Y.M. Rodichev [8] on glass panels were elaborated. To get an impression of what finite element results may look like when using the previously explained finite element modelling method, it was decided to make finite element models of the flat tests with the diamond scratch upwards. The Weibull plot showing the failure stresses belonging to these tests are shown in Figure 4.6(a). A similar plot was made for the flat tests with the diamond scratch downwards in Figure 4.6(b). It should be noted that the experimental results plotted in these graphs are 1.25 times higher than the failure stresses shown in Figure 3.5 of Chapter 3. The reason for this relies on the relation that is used to calculate the failure stresses from the measured applied force on the panels. In the literature [8] tables are given of the measured applied force at failure, together with the calculated failure stresses that are plotted in the graph of Figure 3.5. The used relation between applied force and failure (bending) stress is given in Equation 4.1. Where the value of 0.8 is used to account for nonlinear geometrical behaviour of the glass panels according to the author of the paper, F.A. Veer. For the creation of the finite element models this factor of 0.8 is not used, since the finite element method will account for these nonlinearities. This leads to the linear relation between force and bending stress as given in Equation 4.2, which explains the multiplication of the previous failure stresses and λ's by $\frac{1}{0.8} = 1.25$.

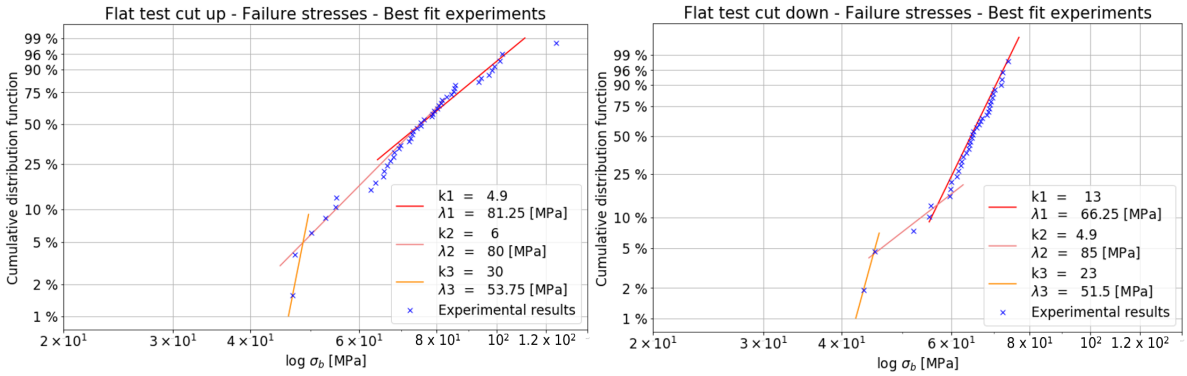

(a) Diamond scratch upwards.

(b) Diamond scratch downwards.

Figure 4.6: Weibull probability plots of flat tests results for the diamond scratch upwards and downwards [8].

$$\sigma_b = 0.8\frac{3FL}{4bh^2} \quad \text{[MPa]} \tag{4.1}$$

$$\sigma_b = \frac{3FL}{4bh^2} \quad \text{[MPa]} \tag{4.2}$$

With
$L = 350$ [mm] $b = 40$ [mm] $h = 6$ [mm] F [N]

The glass panels were subjected to bending; which means that the top of the panels will be in compression, while the bottom is in tension. According to literature, glass in reality always fails in tension and never in compression [10]. This is why it is assumed that for the tests with the diamond scratch upwards, the failure stresses are the original tensile strengths of the glass panels. While for the diamond scratch downwards, the failure stresses belong to the reduced failure strength due to the scratch. For the tensile strength of the glass panels in the finite element models, it is, therefore, chosen to draw the tensile strengths from the Weibull distributions on which most experimental results

are depicted in Figure 4.6(a). This will be the red line with $k1$ = 4.9 and $\lambda 1$ = 81.25 MPa. The reduced tensile strength of the diamond cut in the finite element model will be drawn from the distribution belonging to the red line in Figure 4.6(b), with $k1$ = 13 and $\lambda 1$ = 66.25 MPa.

The following subsections will show the finite element models and their results. Using those, conclusions can be drawn regarding this particular method of finite element modelling of structural glass until failure and the choice of Weibull distributions using experimental results as is done in this example.

4.2.1. Finite Element Model

Figure 4.7 shows the details of the finite element models. This is an example of one of the models, since for every model the tensile strengths will be different. The rest of the details shown in the figure will, however, be the same for all models. In total 20 models were created in order to get an appropriate image of the statistical distribution of failure stresses.

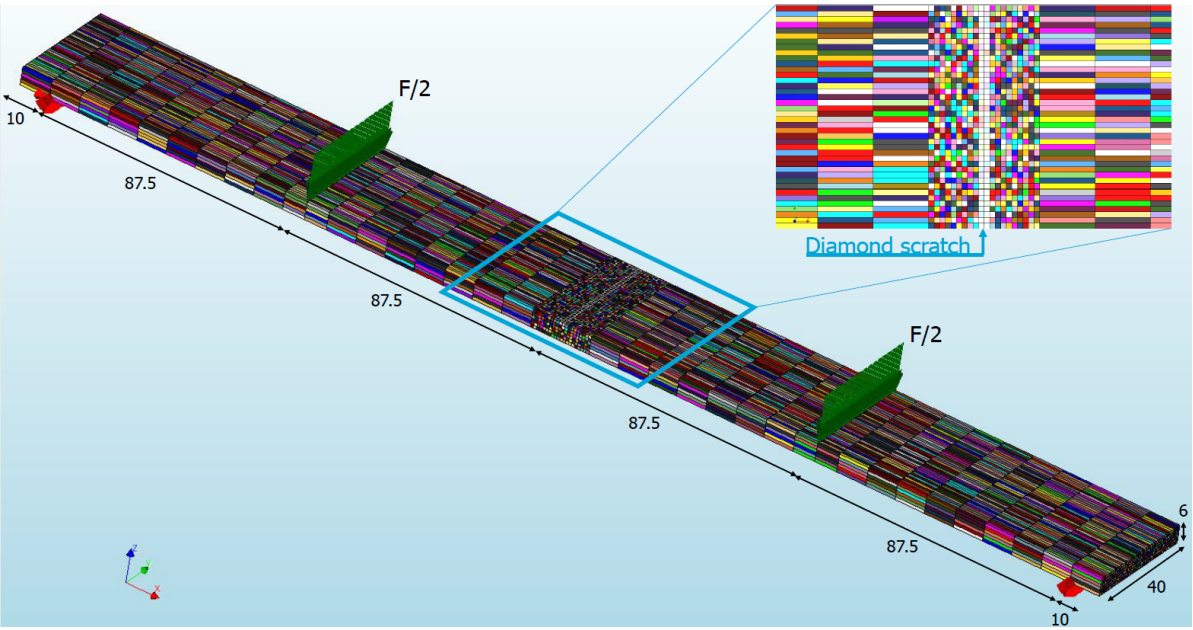

(a) 3D image of the finite element model with a close-up of the scratch. The light/pastel coloured elements refer to the scratch. The given dimensions are the same as the ones of the tests according to the literature and are given in mm.

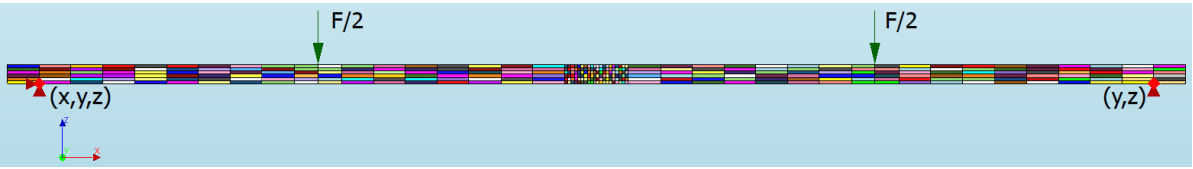

(b) Side view of the finite element model. The loads and supports are shown. Both are line loads/supports and extend over the whole width of the glass panel. The left support is fully hinged, while the right support is movable in horizontal (X) direction.

Figure 4.7: Details of one of the finite element models of the flat tests with the cut upwards. The different colours per element refer to different tensile strengths (f_t). These are different for every model.

The loads that are shown in the figure are in the finite element model represented as prescribed displacements in order to enable displacement controlled analysis. This displacement started at zero and was increased with 1 mm per load step. The supports are such that they represent a simply supported structure, hinged on one side and movable in horizontal (X) direction on the other side.

Smaller element sizes are chosen in the middle of the panel. These elements are 1 mm^3, while the rest of the elements are 10 mm x 1 mm x 1 mm (L x W x H). This is done, since it is expected that the panel will fail in the middle of the span first. Smaller elements will give more accurate results in case nonlinear behaviour, such as cracking, occurs. The stroke of elements belonging to the diamond

scratch consist of 2 x 40 x 1 elements. The analyses enabled both physical as geometrical nonlinearity.

Table 4.1 shows the material properties used for the glass panels in the finite element models. The properties of float glass are different than that of borosilicate glass, which is used in the bundled glass columns. The properties of the glass panels are chosen as given on the website of a car glazing manufacturer called Saint-Gobain [15], which are in agreement with the properties as given in the literature presented in Appendix B.

	Unit	Value	Type
Glass			
Young's modulus	GPa	70	
Poisson's ratio	-	0.2	
Compressive behaviour			Linear elastic
Tensile behaviour			Brittle (no residual strength)
Crack model			Smeared cracking (rotating)
Mass density	kg/m^3	2500	

Table 4.1: Material properties used in the FE calculations [15]. (The influence of gravity is neglected in the models).

Figure 4.8 shows the Weibull distributions for both the diamond scratched part of the glass and the rest of the glass as probability density functions. Both distributions refer to the red lines in Figures 4.6(a) and (b). The dots in the graph represent the drawn values of one of the models, those are different for all of the 20 models. For the elements of the diamond scratch, 20 different values of f_t are drawn. For the rest of the elements 50 different values are chosen.

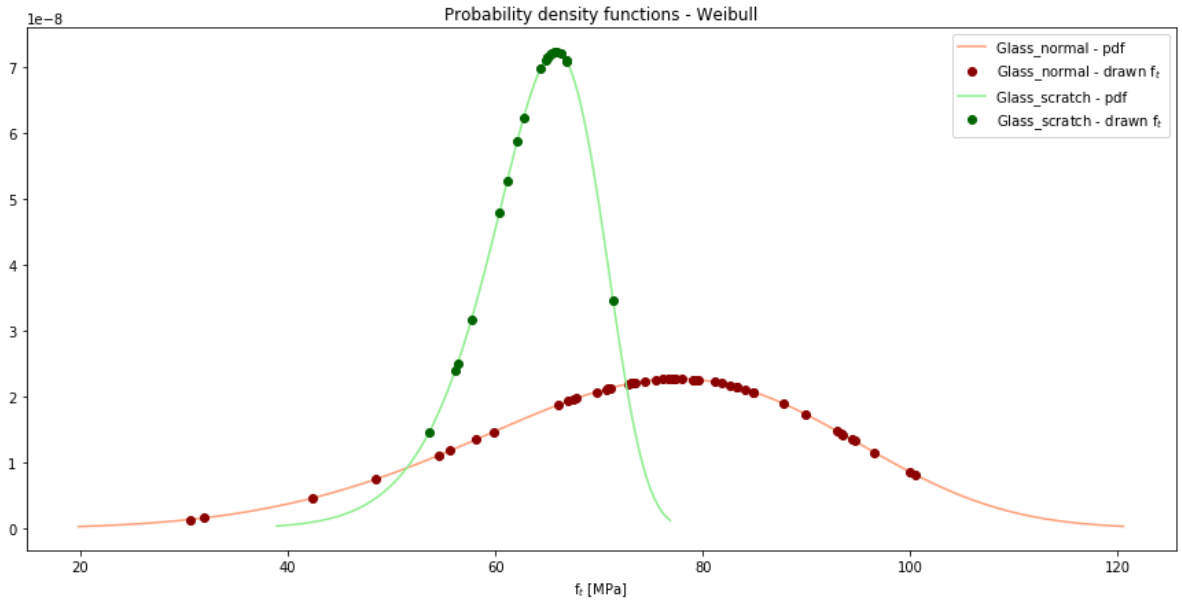

Figure 4.8: Probability density functions of the Weibull distributions used to model the panels with the dots referring to an example of drawn values of f_t. The green plot belongs to the diamond scratch with parameters $\lambda = 66.25$ MPa and $k = 13$. The red plot belongs to the rest of the glass elements and has parameters $\lambda = 81.25$ MPa and $k = 4.9$.

4.2.2. Finite Element Results

The results of the finite element models are presented by means of the fracture behaviour and by Weibull probability plots like the ones belonging to the experimental results shown in Figure 4.6. Furthermore, a table is given with the calculated failure (bending) stresses and the accompanying failure load (F). The failure loads are direct results of the finite element models; the stresses result from these loads by using the relation given in Equation 4.2.

Fracture Behaviour

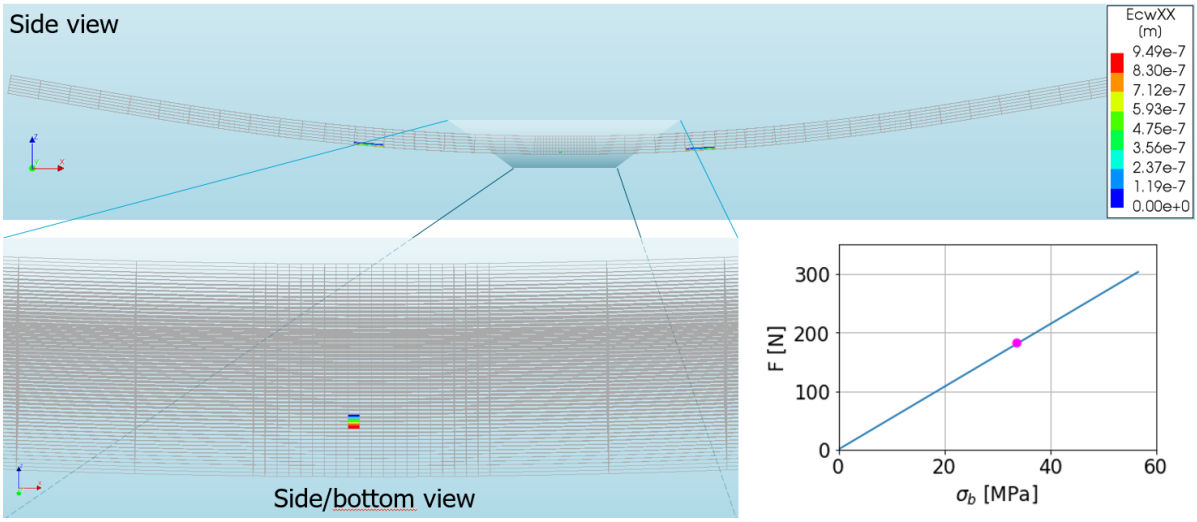

(a) First micro cracks.

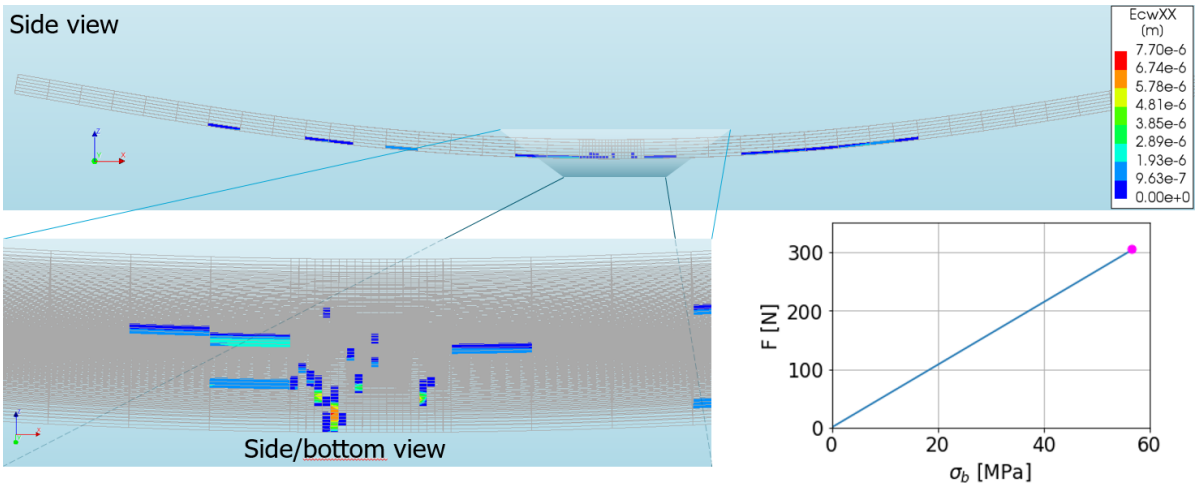

(b) Just before total failure.

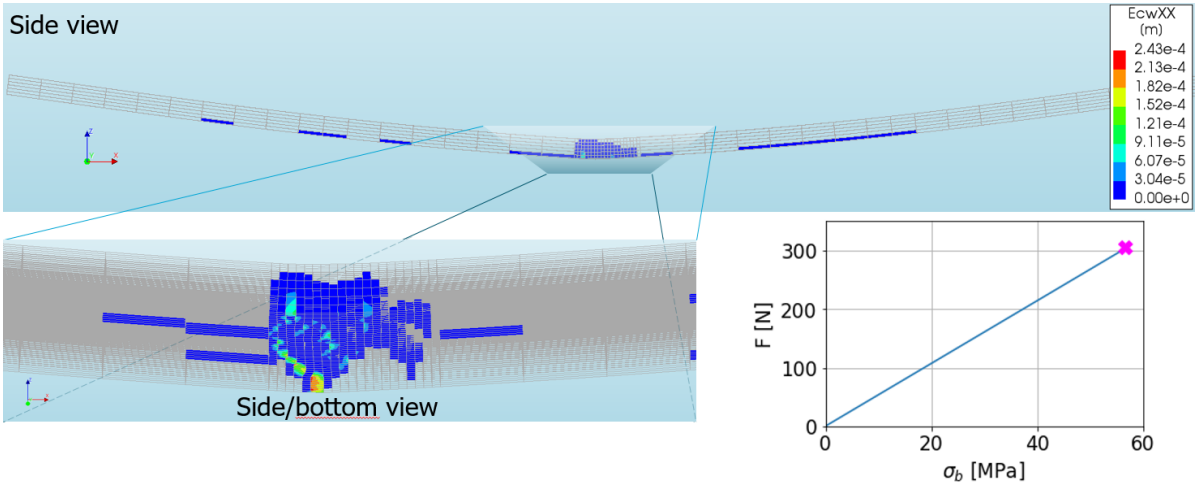

(c) Numerical instability of the model a.k.a. total failure.

Figure 4.9: Cracking of the finite elements at three different load steps. The graphs on the lower right of each image shows the load-stress diagram, with the pink marker indicating at what point on the graph the contour plots were taken.

The fracture behaviour of the finite element models is shown using visualisations. In these images, the elements that are cracked are coloured, while the elements that are still intact are transparent. The colour of the element indicates how severe the cracks are. The crack widths in X-direction are given in meters (EcwXX). These visualisations are shown in Figure 4.9, which belong to one of the 20 models. In the lower right corner of each image the load-stress diagrams are given, which give an indication of the load where the first micro cracks started to appear. The pink marker indicates which load and stress belongs to the accompanying image. The depicted deflection is an exaggeration of the real calculated deflection.

It can be observed that the first micro cracks start to appear at a load that is close to half of the failure load. These cracks appear all over the panel, not only in the middle where the tensile stresses are largest. As the load increases, more cracks start to appear, which are mostly located in the middle at the bottom of the panel. The panel fails when the cracks become too severe, which causes numerical instability of the finite element model.

Weibull Probability Plots

Model nr.	F [N]	$\sigma_{b,lin}$ [MPa]	$\sigma_{b,nonlin}$ [MPa]	Ratio	Model nr.	F [N]	$\sigma_{b,lin}$ [MPa]	$\sigma_{b,nonlin}$ [MPa]	Ratio
1	303	55.31	50.91	0.92	**11**	271	49.39	45.48	0.93
2	270	49.23	45.54	0.93	**12**	259	47.16	44.98	0.95
3	270	49.29	46.62	0.95	**13**	304	55.45	51.14	0.92
4	293	53.50	51.80	0.97	**14**	293	53.50	49.34	0.92
5	304	55.48	51.59	0.93	**15**	292	53.30	49.31	0.93
6	269	48.99	43.68	0.89	**16**	259	47.15	44.01	0.93
7	282	51.32	46.53	0.91	**17**	282	51.40	48.52	0.94
8	280	51.00	45.56	0.89	**18**	304	55.37	52.43	0.95
9	282	51.34	48.29	0.94	**19**	282	51.39	47.88	0.93
10	270	49.17	43.37	0.88	**20**	281	51.13	46.61	0.91

Table 4.2: Finite element results of the 20 different models. The loads (F) are subtracted from the FE models, while the stresses ($\sigma_{b,lin}$) are calculated from these loads with the relation given in Equation 4.2. $\sigma_{b,nonlin}$ includes the reduced stresses in the cracked elements in the middle of the panel. The right-most columns show the ratio between these two stresses.

Table 4.2 gives the failure (bending) stresses which were calculated from the failure loads subtracted from the finite element models using Equation 4.2. These were the loads belonging to the cracking stage as depicted in Figure 4.9(b), just before the model became numerically unstable. The bending stresses ($\sigma_{b,lin}$) given in this table are used to make Weibull probability plots of the finite element results. When looking to the contour plot of the stresses given in Figure 4.10, the stresses $\sigma_{b,lin}$ given in the table refer to the yellow elements. Those are the elements that show a linear distribution of stresses along the cross-section of the panels, since those are not cracked. The difference between the calculated stresses in the table, and the stresses in the yellow elements resulted from the finite element models, is only ±1%. From this it can be concluded that those elements indeed show linear behaviour in the stress distribution. The elements in Figure 4.10 that show cooler colours are cracked, which causes the lower stresses. This phenomenon refers to the nonlinear behaviour that was accounted for in the literature [8] with the factor of 0.8 in Equation 4.1. To get an impression of the difference in tensile stresses between this linear and nonlinear behaviour according to the finite element models, it was decided to take the average stress of all the finite element nodes that are located at the bottom of the panel inside the black square that is depicted in Figure 4.10. That is the area where most cracks appear. This average stress is given per model in the table as $\sigma_{b,nonlin}$. The ratio between $\sigma_{b,lin}$ and $\sigma_{b,nonlin}$ is given as well. A higher value of this ratio refers to less cracked elements in that region for that particular model.

For this studies $\sigma_{b,lin}$ is more interesting, since this is the stress where the panel will fail as a whole. This stress is, furthermore, linked in the same way to the calculated load as the stresses depicted in Figure 4.6 are linked to the experimentally obtained loads. Therefore, this is the stress that is plotted on the Weibull scales shown in the following paragraphs.

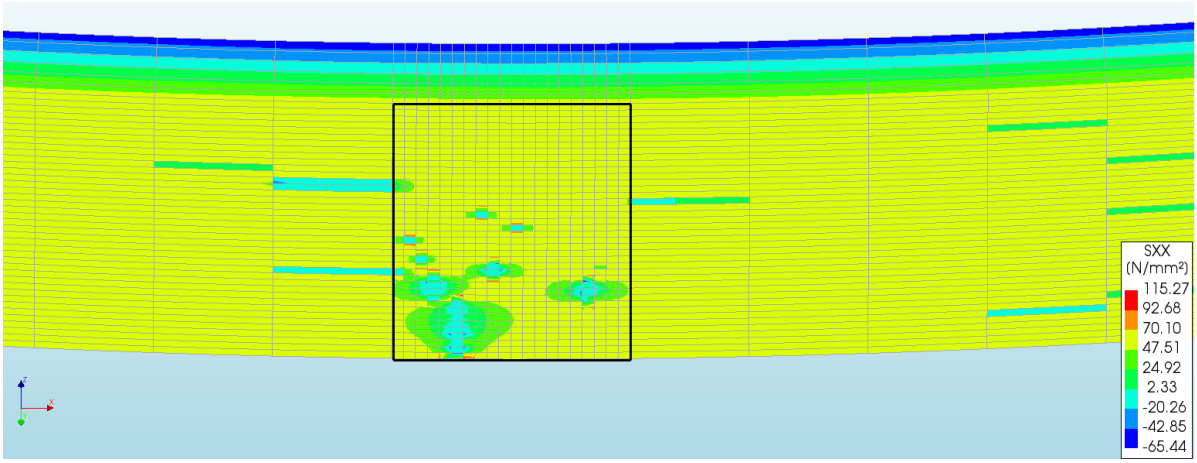

Figure 4.10: Contour plot of the bottom/side of the glass panel, when zoomed-in to the middle of the panel. The colours show the bending stresses in the panel. The cooler-coloured elements show lower stresses, which refer to cracked elements. This image belongs to the same FE model as used for the fracture behaviour plots of Figure 4.9.

The following figures show the Weibull probability plots of the failure stresses. First, in Figure 4.11, the finite element results are plotted on a Weibull scale. Two figures are shown, of which Figure (a) depicts the graphs belonging to the Weibull distributions as used to create the finite element models. Figure (b) only shows the blue line, which refers to the distribution used to model the scratch. Changing the value of k will influence the slope of the line, while adjusting λ will result in translation of the line in horizontal direction. It can be seen that in Figure 4.11(b) the value of λ is altered to get a better fit with the plotted finite element results. The fact that the distribution belonging to the scratch shows a relatively good fit, with altered values of λ, might point to the fact that the scratch does influence the failure strength of the glass; although the scratch is located at the compression side of the panel. It is logical that the value of λ, which can be seen as the mean failure stress, is lower than the original λ. The finite element models of the glass panels will show failure when a critical amount of elements, with a relatively low tensile strength, are cracked. Therefore, the failure stresses that are subtracted from the models are low percentile values of the distribution that is used to draw the tensile strengths from. This will lead to the same k, but a lower value of λ.

(a) Graphs belonging to the used Weibull distributions to create the finite element models.

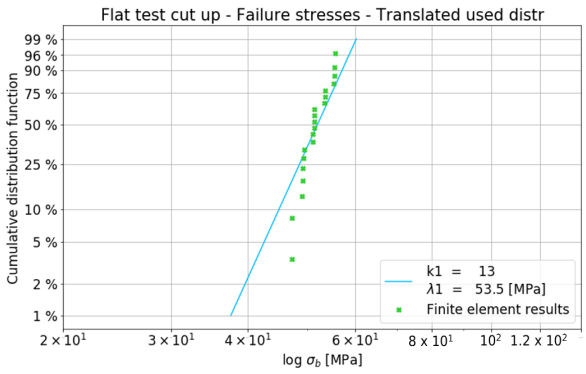

(b) Same as Figure (a), however only showing the distribution belonging to the scratch translated horizontally to fit the results. This is done by altering the value of λ.

Figure 4.11: Weibull probability plots of the finite element results.

Figure 4.12 shows Weibull probability plots where the experimental results are combined with the finite element results as shown in Figure 4.6. This was done in order to see the position of the finite element results in the distribution of the experimental results. Just as in the previous figures, the position of the points belonging to the results remain the same in every image. However, the graphs belonging to the Weibull distributions are altered. The images show that the finite element results

show relatively low failure stresses in comparison with the experimental results. This results in a safe estimate of the failure load of the glass panels.

The lines in Figure 4.12(a) show the exact same Weibull graphs as depicted in Figure 4.6(a), which were fitted to the experimental results only. It can be seen that the addition of the finite element results makes the fit inappropriate. Figure 4.12(b) is similar to Figure 4.11(b), where the k's are the same as for the Weibull distributions used to make the finite element models, but the λ's are optimised to fit the combined results. It can be observed that most experimental results fit best to the red line, while the majority of the finite element results make the best fit with the blue line. Interesting is that although the finite elements crack in the bottom of the panels, the Weibull plot assumed to be belonging to the diamond scratch appears to be the best fit for the finite element results. Even though this scratch is located at the top of the glass panels and not at the bottom where the failure stresses come from. Figure 4.12(c) shows two graphs for the Weibull distributions that fit both the experimental and finite element results best. The blue line is the same as in Figure (b).

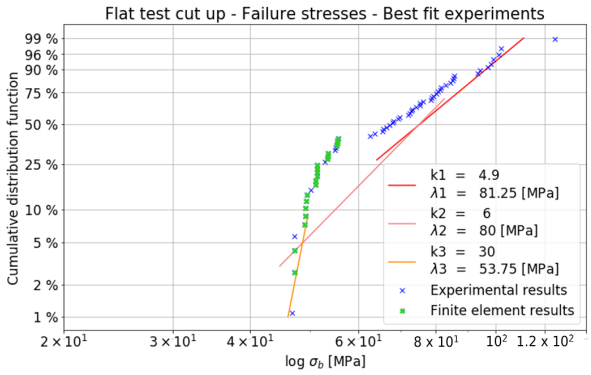

(a) Graphs belonging to the appropriate Weibull distributions for the experimental results as depicted in Figure 4.6(a).

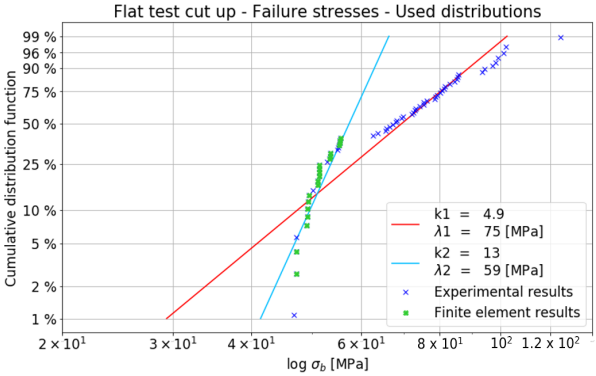

(b) Graphs belonging to the used Weibull distributions to create the finite element models with $k1 = 4.9$ and $k2 = 13$, however with different λ's to translate the line horizontally to match the results while remaining the same slope.

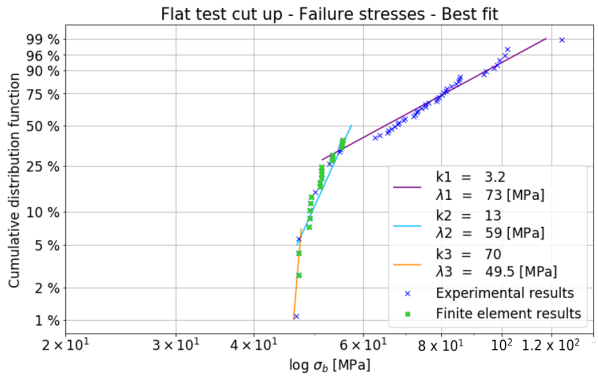

(c) Graphs belonging to new Weibull distributions appropriate for the combined experimental and finite element results.

Figure 4.12: Weibull probability plots of the experimental results combined with the finite element results.

4.3. Conclusions

In this section, preliminary conclusions are drawn about the method of finite element modelling presented in this chapter. The conclusions are preliminary, since too few glass finite element models are created to completely validate the accuracy of the modelling method. Firstly, conclusions are given regarding the finite element models of the glass panels given in Section 4.2. Secondly, the preliminary conclusions about the presented finite element modelling method for structural glass until failure are presented.

4.3.1. Finite Element Modelling of Glass Panels

The fracture behaviour of the panels shown in the contour plots of Figure 4.9 is realistic. It could be that small micro cracks occur during testing, which are not visible by the naked eye, before the panels break. This can, however, not be validated by the results presented in the literature. However, when consulting the author of that paper [8], F.A. Veer, it was confirmed that this is indeed plausible. The distribution of cracks along the bottom of the panel is more realistic in comparison to a finite element model where all finite elements would have the same tensile strength, since in that case all cracks would have been accumulated at the place with the highest tensile stresses.

From Figure 4.11 it can be concluded that the finite element results do not necessarily belong to the same statistical distribution as the one that was used to create the model. The finite element results show a distribution with a lower mean strength (lower value of λ), but a similar shape (same k). This may be caused by the fact that the elements in the models that fail first will have the lowest drawn tensile strength. This can be a reason that the failure stresses of the models are low in comparison to the experimental results.

It can be observed from Figure 4.12 that the finite element results fit in between the blue markers belonging to the experimental results. Furthermore, since the calculated failure stresses fit in the lower tail of the experimental results, the calculated failure loads and stresses give a safe estimation of reality.

The fact that all finite element results are relatively low, can be because the tensile stresses are drawn from full Weibull distributions, while in Figure 4.6(a) the line belonging to $k = 4.9$ and $\lambda = 81.25$ MPa only fits nicely from the 27th percentile value and upwards. In follow-up research it would be interesting to see if finite element analyses where values are drawn only from this part of the distribution, will give results closer to the mean of the experimental results. Additionally, the partial Weibull distributions of the other graphs shown in Figure 4.6(a) can also be added to draw tensile strength values from.

4.3.2. Method for FE Modelling of Structural Glass until Failure

Weibull distributions show potential in finding an appropriate probability distribution that can fit the failure strength of glass. However, finding good parameter values proves to be difficult. Furthermore, to fit all the results, multiple Weibull distributions are needed per glass element. The latter is probably why the finite element results belonging to the glass panels, shown in this section, only represent one part of the experimentally obtained results in Figure 4.12. The problem is that the theoretical knowledge regarding the choice of statistical (Weibull) distributions is, at this point in time, not sufficient to get the best results out of the models. The statistical problem has to be researched in a deterministic way. It is, however, very promising that the finite element results match the experimental results to this extend already without the prior knowledge.

The way of finite element modelling does show a more realistic fracture pattern than when the tensile strength of the glass would be modelled in the conventional way. The latter referring to one conservative value of the tensile strength of glass for all elements instead of varying tensile strengths. Furthermore, the models are able to produce results that lay in the range of experimentally obtained results. This all shows the potential that this method of finite element modelling of structural glass until failure can have for future calculations.

At last, the finite element models can help understand the fracture behaviour of the glass and may, therefore, be a good contribution to material sciences and for glass researchers.

III

Bend & Break Columns

5

Compression Tests until Failure

In August 2019 displacement controlled compression tests were performed as part of this study on twenty Bend & Break columns. This chapter shows the test setup as well as the results of the tests. The columns were compressed until failure, which caused the columns to break and shatter with explosive behaviour. It was a challenge to find a good test setup that ensured the safety of the ones who were performing the tests. Nevertheless, the testing appeared to be not only interesting, but also spectacular. This chapter contains information regarding the test setup, the obtained results and the conclusions that are drawn from these tests. The experimental results are used to validate finite element models of the Bend & Break columns.

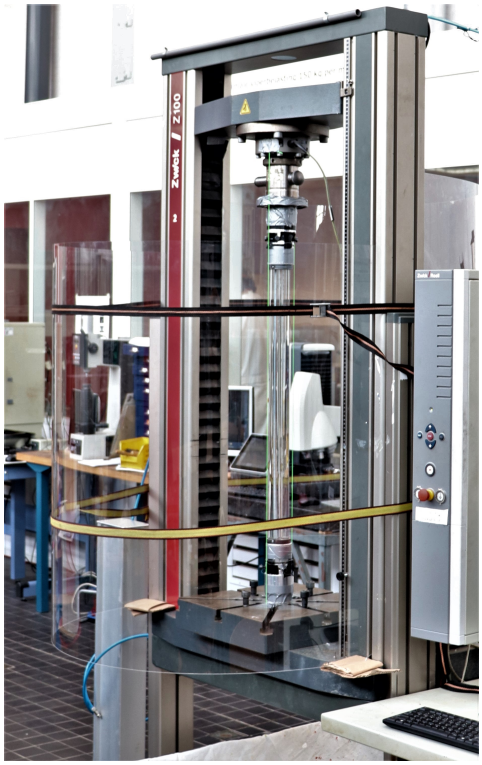

(a) The first try-out for the test setup with 2 mm thick sheets of acryl glass bend around the column as safety measure.

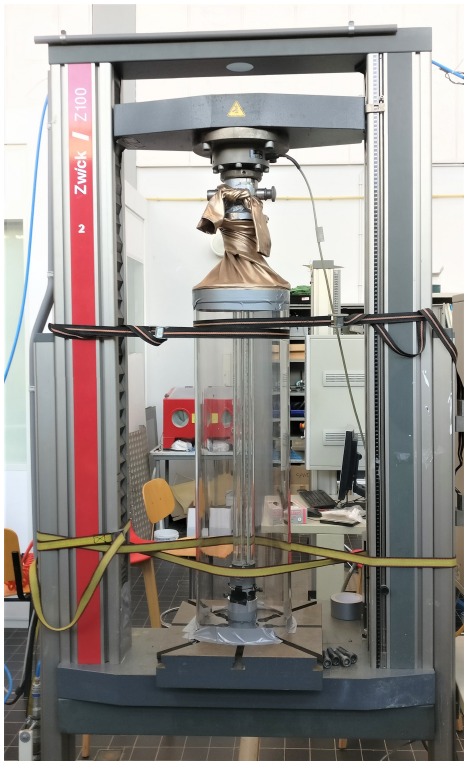

(b) The final test setup including a 5 mm thick polycarbonate tube as safety measure.

Figure 5.1: The two try-outs of the test setup to ensure the safety of the persons performing the tests, with on the right the final test setup. Both the acryl glass and the polycarbonate tube were used to stop the shattering glass from flying through the lab. The acryl glass was however not strong enough to withstand the impact of the shattering glass.

5.1. Test Setup

Figure 5.2 shows a schematic overview of the final test setup as well as a picture of the testing machine itself. The Zwick Z100 testing machine is able to perform displacement controlled compression tests, while measuring the applied force. In this way, it automatically produces load-displacement diagrams of the tests. A test rate of 1 mm/min was used. It was chosen to test twenty columns instead of just a single column, due to the statistical failure behaviour of (structural) glass. A total of twenty tests is the least amount of tests necessary in order to draw appropriate conclusions from such experiments.

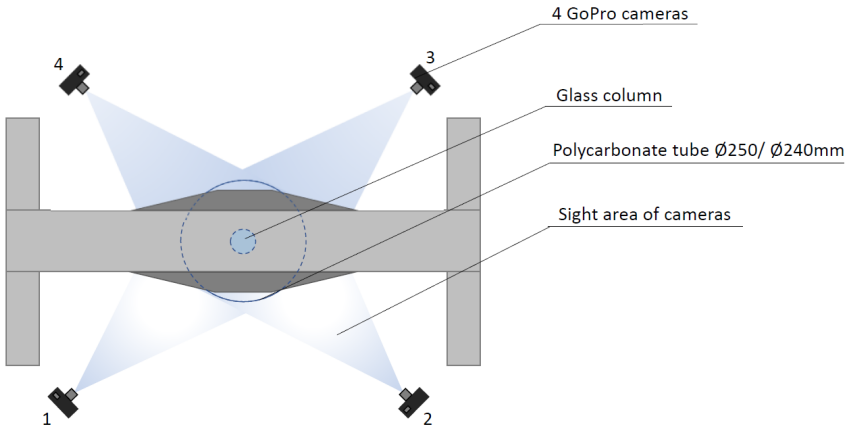

(a) Schematic top-view of the test setup.

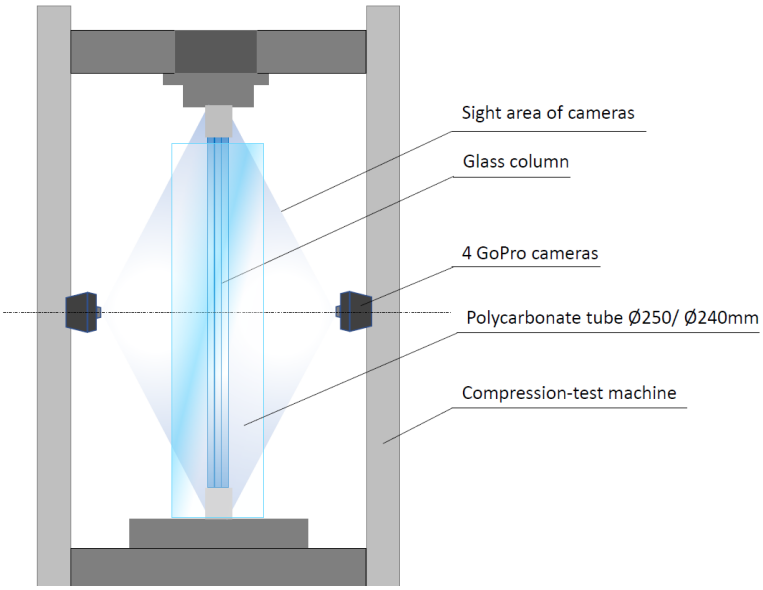

(b) Schematic side-view of the test setup.

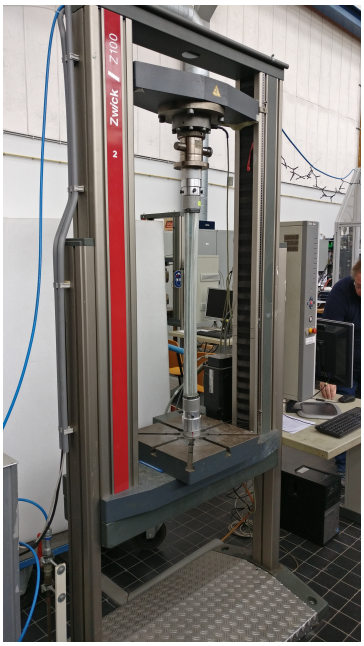

(c) Zwick Z100 testing machine including a Bend & Break glass column.

Figure 5.2: Setup of the displacement controlled compression tests on the Bend & Break bundled glass columns. The used machine is a Zwick Z100 testing machine. A compression rate of 1 mm/min was used. The polycarbonate tube ensured the safety of the people performing the tests by blocking the shattered pieces of glass. The tests were filmed from 4 sides using GoPro cameras capturing 60 frames per second.

5.1.1. Preparation

Before testing, preparations were done in order to get the best results. All twenty tested columns had the same design, but unfortunately that does not mean that they are identical in reality. Therefore, the columns were made as similar to each other as possible before testing. Furthermore, the dimensions of the columns were measured in order to get an idea of the differences between the columns. Since the columns were already fabricated before this thesis process, only limited actions could be taken on the optimisation of these columns.

Straightening of the columns

As mentioned in Section 2.3 all columns were straightened as much as possible by removing the twist from the columns.

Numbering of columns and glass rods

All columns were numbered and were assigned a top and a bottom. Furthermore, each of the five rods within the columns was marked with a line of a specific pattern along the length of the column to be able to distinguish the rods during and after testing. Such a line is visible in Figure 2.13. The used patterns and way of numbering the rods is shown in Figure 5.3.

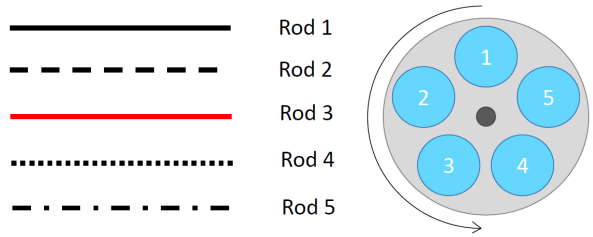

Figure 5.3: Marking and numbering of the five rods within each glass column. The figure on the right shows a top view cross-section.

Measuring the columns

An indication was made on the tilt of the steel caps on both ends of the columns by measuring the column lengths on different sides of the columns. It was, unfortunately, not possible to measure each individual glass rod within the columns.

Applying strain gauges

Two of the twenty tested columns were supplied with strain gauges. Each glass rod within the column got one strain gauge that measured the longitudinal strain in the middle of the column. In total 5 x 2 = 10 strain gauges were applied.

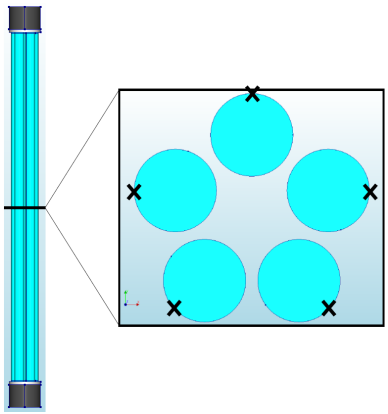

(a) Schematic image of the position of the five strain gauges on the glass column.

(b) Picture of the strain gauges on a column.

Figure 5.4: Strain gauges placed on two of the tested Bend & Break columns.

Fixing appropriate boundary conditions
Due to the slenderness of the columns, it was expected that the columns would fail due to buckling. To ensure the lowest buckling load, hinged connections were created at the top and bottom of the columns. The rotational stiffness of the boundary conditions has influence on the buckling load of the columns. The hinges consist of aluminium cylinders with a metal ball in the middle which enables the cylinders to rotate with reference to one another, see Figure 5.5.

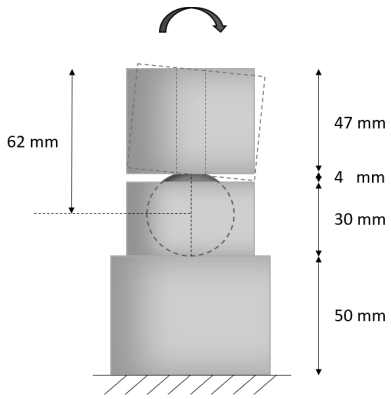

(a) Schematic drawing of the hinged support.

(b) Picture of a hinged support attached to a Bend & Break column.

Figure 5.5: Hinged supports used in the compression tests.

5.1.2. Capturing results

In order to capture the needed results of the compression tests, several measuring tools were used.

Force and displacement gauges
The used testing machine was supplied with a force gauge and a displacement gauge on the top of the machine. These gauges measured the applied normal force as well as the vertical deformation at the top of the columns.

Strain gauges
Two columns were supplied with five strain gauges to measure the longitudinal strain in the middle of the columns, see Figure 5.4. Strain gauges with a gauge resistance of 120±0.3 Ω and a gauge factor of 2.09% were used. With these results information was gained about the differences in stress distribution between the five glass rods within the columns.

Examining glass pieces after fracturing
During the tests care was taken to keep the glass from breaking again after the initial failure. This was achieved by applying a soft material on the bottom of the test setup to keep the glass from shattering on the hard steel bottom of the machine. All shattered glass was collected in separate bags per column to be examined afterwards using fractographic knowledge. The lines that were made on the glass to distinguish the different rods, were used to indicate where the shattered pieces came from.

Four GoPro cameras
As depicted in Figure 5.2, the tests were filmed from four sides using GoPro cameras. A resolution of 1080p and a frame rate of 60 fps was taken. The camera footage was used in order to capture the failure mode, to see which of the five rods within the columns failed first and to observe the lateral deformation due to the buckling. Unfortunately, it was hard to see the markings made on the rods to distinguish the rods on the camera footage; it is recommended to use a higher resolution in case of performing similar experiments in the future. Furthermore, to capture the crack propagation within the glass, high speed cameras are needed with a frame rate of ±100,000 fps. Such type of cameras were not available during testing. The used resolution and frame rate were chosen due to limited memory capacity.

5.2. Experimental Results

This sections shows the results obtained from the displacement controlled compression tests performed on the Bend & Break bundled glass columns. First, information regarding the (buckling and failure) loads as well as vertical deformations of the columns are given. Secondly, the differences in stress distribution between the five different glass rods within the columns are discussed. Thirdly, the fracture behaviour of the columns is investigated by examining the glass pieces after fracturing. At last, conclusions are drawn from the various observations.

5.2.1. Loads and Displacements

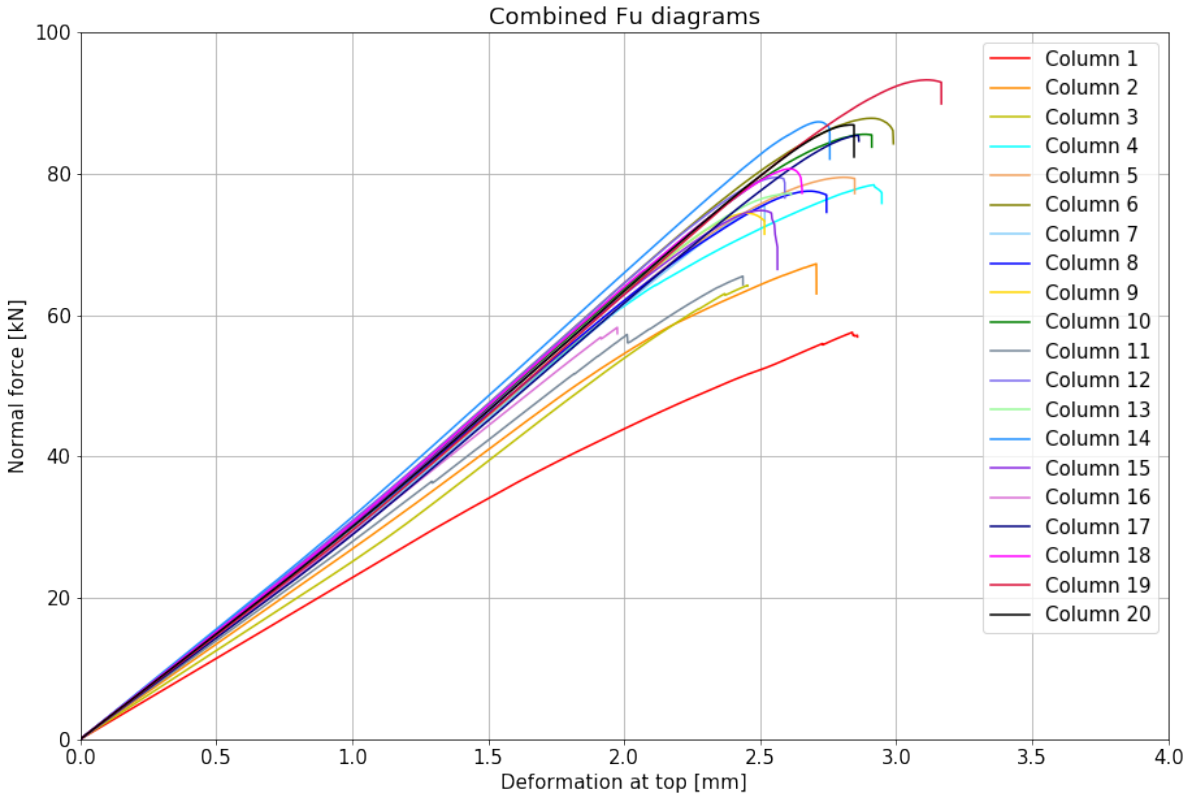

Figure 5.6: Combined load-displacement diagrams of all tested columns.

Figure 5.6 shows the load-displacement diagrams of all twenty columns which are experimentally obtained by performing the displacement controlled compression tests. It can be observed that the initial behaviour of the columns is linear-elastic, where most columns show similarity in slopes. However, Columns 1, 2, 3, 11 and 16 have gentler slopes. After a certain applied load, the buckling behaviour is indicated in most of the graphs by a decrease in slope. The sudden drop at the end of each plot indicates total failure of the column. In some graphs, for example the grey graph belonging to Column 11, a jump can be observed which indicates cracking in one of the five rods during the tests while the other rods remained intact. That cracked rod did not fail completely at that point in time; it still carried part of the load. The failure loads have a large scatter in values ranging between 58 and 93 kN. Also the initiation of buckling, shown by a sudden decrease in slope in the graphs, differs per specimen. At last, Column 1 shows different behaviour in comparison to the other columns. The slope of the graph decreases gradually as the compressive force increases, where after the column collapses without the drop in slope that would indicate buckling. This indicates that the failure mode of Column 1 was bending instead of buckling.

These observations imply a relatively large variety in structural behaviour between the Bend & Break columns. The explanations for these varieties will be given using the subsequent experimental results

and the finite element models presented in Chapter 6.

When comparing the results with the compression tests performed on the initial bundled glass columns, shown in Chapter 2 in Figure 2.5, some differences can be observed. The diagrams shown in that figure are divided in five stages of which only stages 4 and 5 can be seen in the diagrams shown in Figure 5.6. The first stage, shown in Figure 2.5, belongs to the setting of the machine, this was filtered out of the results of the tests done for this study. Stage 3 of Figure 2.5 is not observed due to the lack of a layer of lead in the Bend & Break column design. The absence of this stage indicates that the POM discs show linear elastic behaviour during the tests, which was also validated by checking the state of the POM discs after testing. The slope of stage 4 of Figure 2.5 is similar to the slope shown in Figure 5.6, which is logical since the same type of glass was used for the realisation of both column designs.

5.2.2. Strains and Stress Distribution

In Section 5.1 it was mentioned that two of the columns were supplied with five strain gauges. Figure 5.4 shows the position of these gauges. The results of these measurements are shown in Figure 5.8, with the time given on the horizontal axes. Here, the strains are depicted as microstrains on the left vertical axes, while the right vertical axes show the stresses. These stresses are calculated by multiplying the measured strains with a Young's modulus of 63 GPa, thereby assuming that the glass behaves linear elastically. Properties of glass shown in literature, and used in the finite element models elaborated in the following chapters, ensure that this is a plausible assumption.

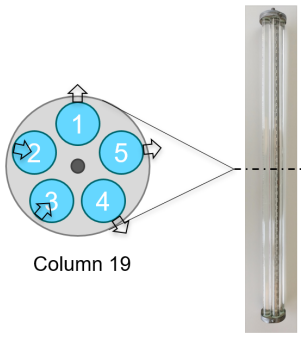

Figure 5.7: Directions in which the rods within Column 19 buckles, discovered from examining the tail propagation of the results of the strain gauges.

Figure 5.8 shows that the distribution of the compressive load through the columns is not equally spread over the five glass rods within the columns. Right from the moment of loading, the plotted lines start to deviate. The buckling point can be seen clearly by changes of slopes within all the lines. For Column 13 this is around 130 seconds, while for Column 19 it happens after 150 seconds of loading. With a test rate of 1 mm/min, this refers to 2.17 mm and 2.5 mm of compression respectively, which is in agreement with the moment of buckling shown in the load-displacement diagrams of these columns. After the buckling point, it can be discovered in which direction each rod buckles by the direction in which the tail propagates. As an example this was done for Column 19, shown in Figure 5.7. The behaviour of Column 13 is very similar. It can, furthermore, be observed that some rods show more lateral deformation than others. In both columns, the rod which is subjected to most of the load (the lowest line in the graph) starts to buckle first and has the largest overall lateral deformation. The GoPro camera footage, furthermore, showed that rod 2 of Column 19 was also the rod that failed first, where after the other rods immediately failed as well.

The observed tensile stresses at failure of rods 4 and 5 in Column 13 and rod 1 in Column 19 can not be used to determine the tensile stress in glass at failure. The reason for this is that it is most likely that the column which has the largest lateral deformation (rod 3 for Column 13 and rod 2 for Column 19) has the largest tensile stresses at one side of the rod. Unfortunately, for both rods, the strain gauges were placed at the compression sides of the rods (the tails of the graphs go down), so these tensile stresses were not measured. Furthermore, for the remainder of the rods it is unlikely that the strain gauges are placed exactly at the point on the rod where the tensile strains are largest.

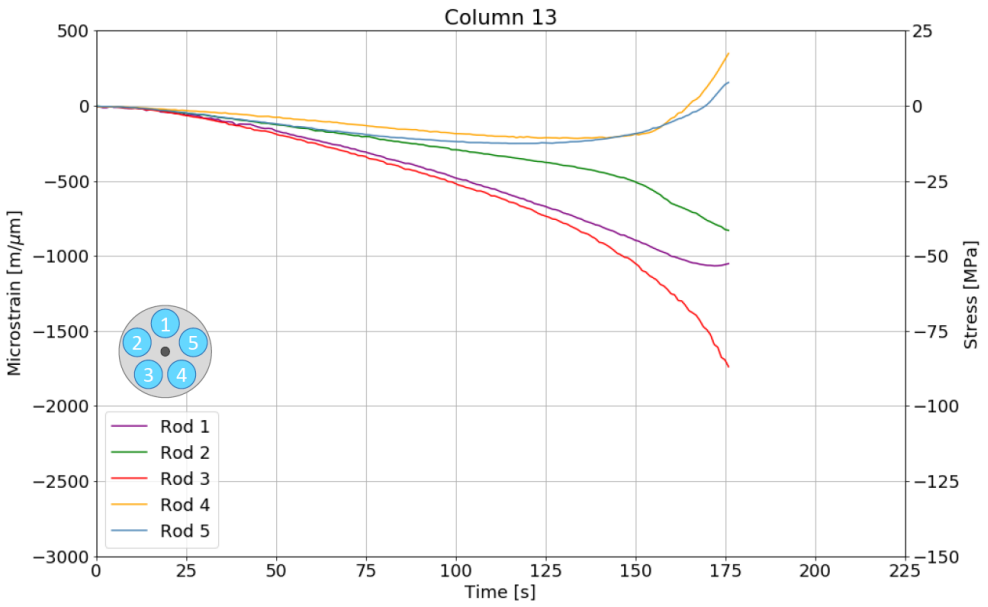

(a)

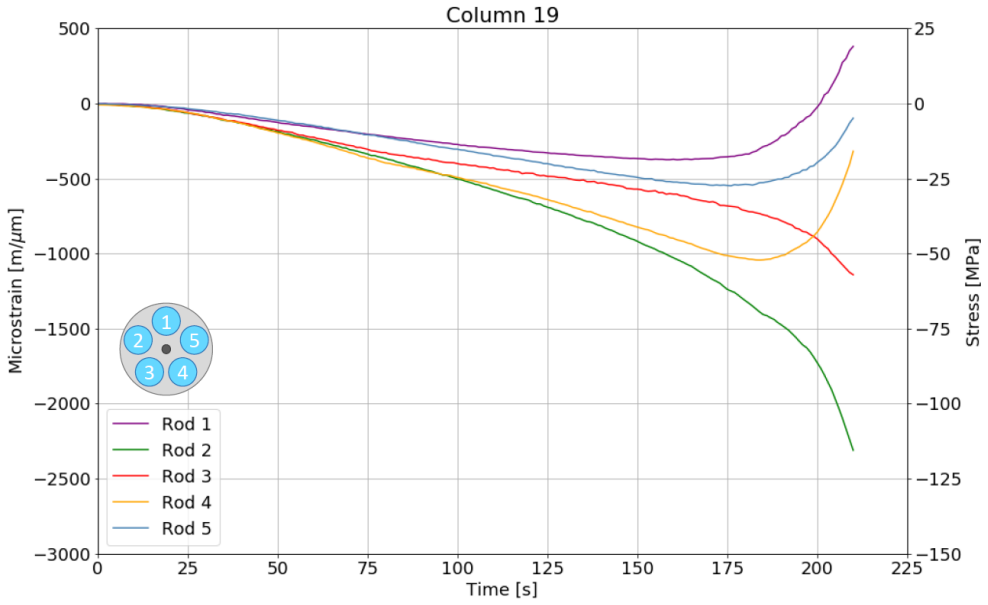

(b)

Figure 5.8: Time versus strain/stress diagrams for Column 13 and Column 19. The strains are measured by strain gauges during the compression tests. Each glass rod was supplied with one strain gauge. The stresses are calculated by multiplying strains with a Young's modulus of 63 GPa, assuming that the behaviour of the glass is linear elastic.

5.2.3. Fracture Behaviour

After each compression test, the fractured glass was collected per column and examined afterwards. Information on the failure mode of a glass element can be obtained from investigation of the fractured glass. George D. Quinn examined the fractography of glass and published a book about his findings, [16]. The fractured glass from the tests was compared with his research in order to draw conclusions from the fracture patterns.

From the load-displacement diagram of Column 1, it is concluded that this particular column failed due to bending. Figure 5.9 shows examples of fracture patterns for glass-like rods that showed bending failure. The origin of the crack can be observed in these images, which arose at the tensile side

of the rod. The cracks made an angle and propagated further in longitudinal direction, until it makes a 'compression curl' to the other side (which is in compression) of the rod. More features along the cracks refer to higher stresses within the glass [16].

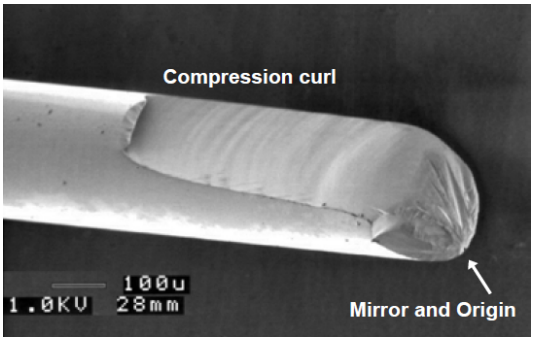

Figure 5.9: A chalcogenide fiber fractured in bending at 368 MPa showing classic fracture patterns for this failure mode [16].

When examining the pieces of glass from the compression tests on the Bend & Break columns, patterns similar to the one shown in Figure 5.9 were found in Column 1, see Figure 5.10(a). Furthermore, a great percentage of the glass rods were split in half in longitudinal direction. One of the larger pieces that was found in this state is depicted in Figure 5.10(c). Clearly visible here, are the curved lines along the crack which are called Wallner lines. These lines give an indication about the stress distribution along the width of the crack propagation direction, see Figure 5.11. The Wallner lines shown in Figure 5.10(c), therefore, indicate slightly more tension at the bottom of the image. Furthermore, they show in which direction the crack propagated; in this example the crack propagated from left to right. Figure 5.10(b) shows indications that cracks originated simultaneously at different locations within the glass and propagated towards each other. Most pieces of glass show a lot of features, which refers to great stresses within the glass at failure [16].

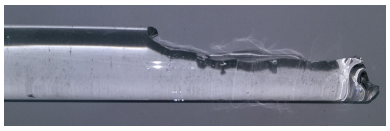

(a) Bending fracture in Column 1 with the compression curl at the top of the image.

(b) Fracture from Column 18 where the Wallner lines show flexure cracks from different origins which propagate in different directions.

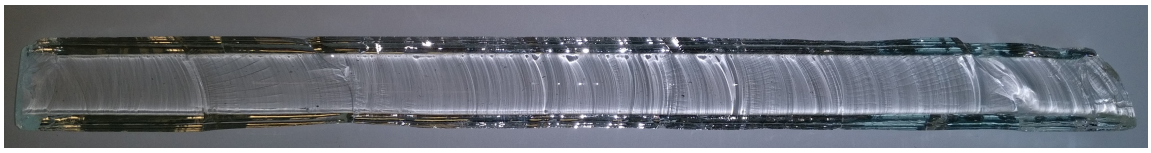

(c) Fracture from Column 2; a long piece split in longitudinal direction showing Wallner lines.

Figure 5.10: Examples of flexure fracture patterns caused by large stresses in the glass rods in the tested Bend & Break columns.

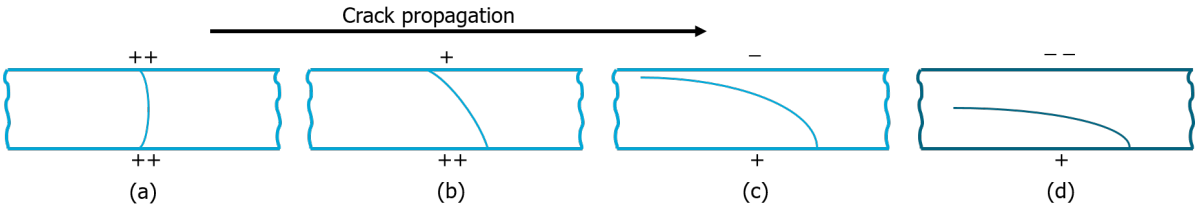

Figure 5.11: Wallner lines for different stress distributions through the thickness. (a) Uniform tension. (b) Tension greater at the bottom. (c) Bending: tension on the bottom, compression at the top [16]. (d) Expected shape belonging to compression at the top greater than the tension at the bottom.

The shape of the Wallner lines give information about the stress distribution along the width of the crack. It is, however, expected that the images of Figure 5.11 can be used to indicate stress distribu-

tions along other sides of the fracture. The shape of the crack shown in Figure 5.10(a) is similar to the image of Figure 5.11(c), when imagining that the crack originated at the bottom of this image. It can be expected that, if the compression on the upper side of this image was larger in comparison to the tension on the bottom, the tail that now propagates horizontally will be located lower towards the centre of the rod. This is depicted in Figure 5.11(d). This would explain the long longitudinal crack propagation that is observed in the rods of the Bend & Break columns. The stress distribution shown in Figure 5.11(d) is to be expected in the rods within the tested columns, since they were tested in pure compression. The buckling caused relatively small tension stresses at one side which originated the failure.

Figure 5.12 shows assembled pieces of broken glass for Column 13 and Column 19. These are the two columns that were supplied with strain gauges, and, therefore, the columns of which most information is available. In the figure, five rows of broken glass pieces can be distinguished, which each refer to one of the five glass rods within the column. These assemblies could be made since the rods were each marked with a specific pattern, as was pointed out in Section 5.1. It should be noted that only the larger pieces, and the pieces which included markings were used in the assembly. Furthermore, only for the pieces which included the rods ends was it possible to discover their original place. The other pieces were placed randomly within the line of that rod. The remainder of the shattered glass varied between pieces of ±2 cm and very small grit.

The figure representing Column 19 shows less glass pieces in comparison to Column 13, which indicates that there were more smaller pieces of glass of Column 19. Larger stresses cause more shattering of the glass. Since Column 19 failed at the highest loads, this is to be expected.

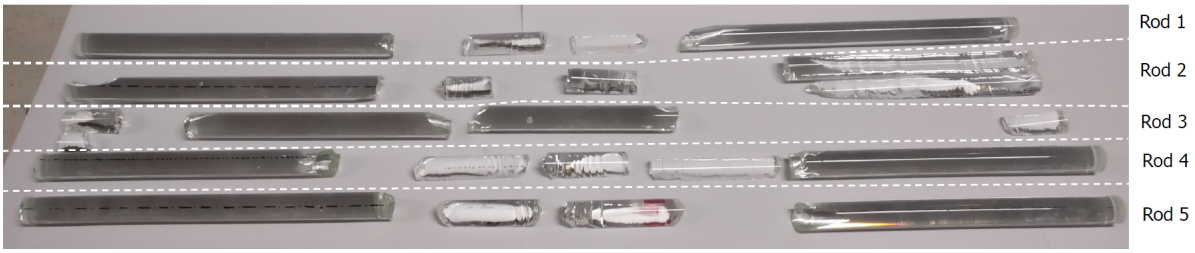

(a) Column 13.

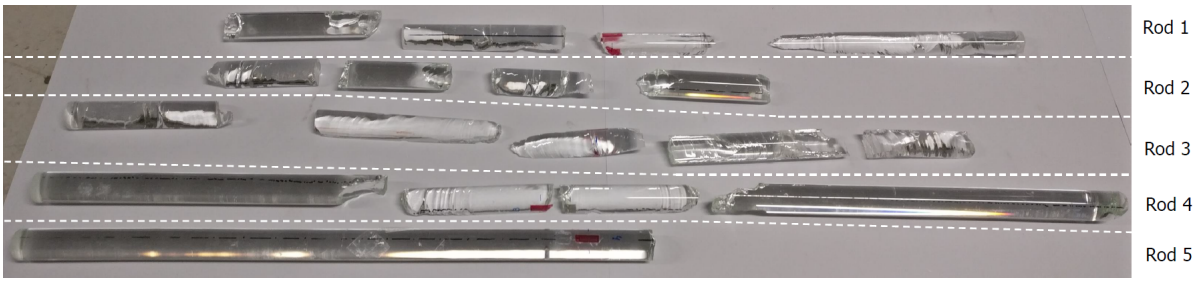

(b) Column 19.

Figure 5.12: Large broken pieces of glass assembled together to reform the five rods within Columns 13 and 19, which were the columns supplied with strain gauges. Smaller pieces and pieces without markings were not included in these assemblies.

Some of the rods showed failure from the ends of the glass rods towards the middle. The propagation direction of these cracks was detected using the Wallner lines, see Figure 5.13(a) and (b). In some rods within certain columns cracks propagating towards the ends were detected as well. Those, however, made their 'compression curl' just before they reached the end. Furthermore, some rods within the columns showed signs that are expected to relate to failure due to twisting, see Figure 5.13(c). The twisting of the columns was observed during testing. This happened due to the lack of torsional rigidity in the design of the Bend & Break columns.

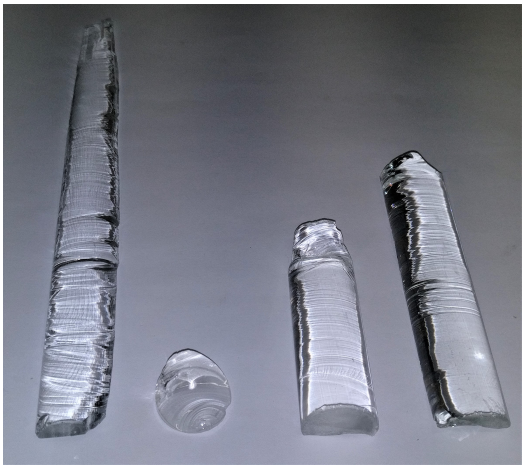

(a) Fractured rods ends belonging to Column 5.

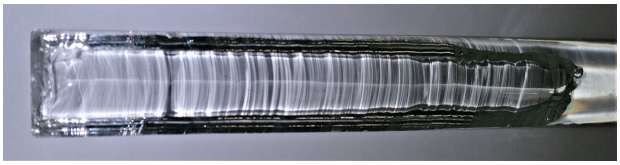

(b) Crack propagating from rod end toward the middle of Column 11, where the rods end is depicted at the left.

(c) Fracture expected to be due to twist of Column 2.

Figure 5.13: Examples of glass pieces indicating specific failure patterns.

For three of the tested columns (Columns 2, 5 and 10) one of the glass rods remained intact after failure of the column. This is depicted in the cover picture of this thesis. This, together with the results from the strain gauges, proves the non-equal distribution of stresses along the five glass rods within each column.

Figure 5.14 shows a sequence of frames that are captured from the camera footage of the failure of Column 3. When looking closely, first cracks can be observed in the rod depicted in the middle of the column already in the second image. The failure of this column happened in a fracture of a second.

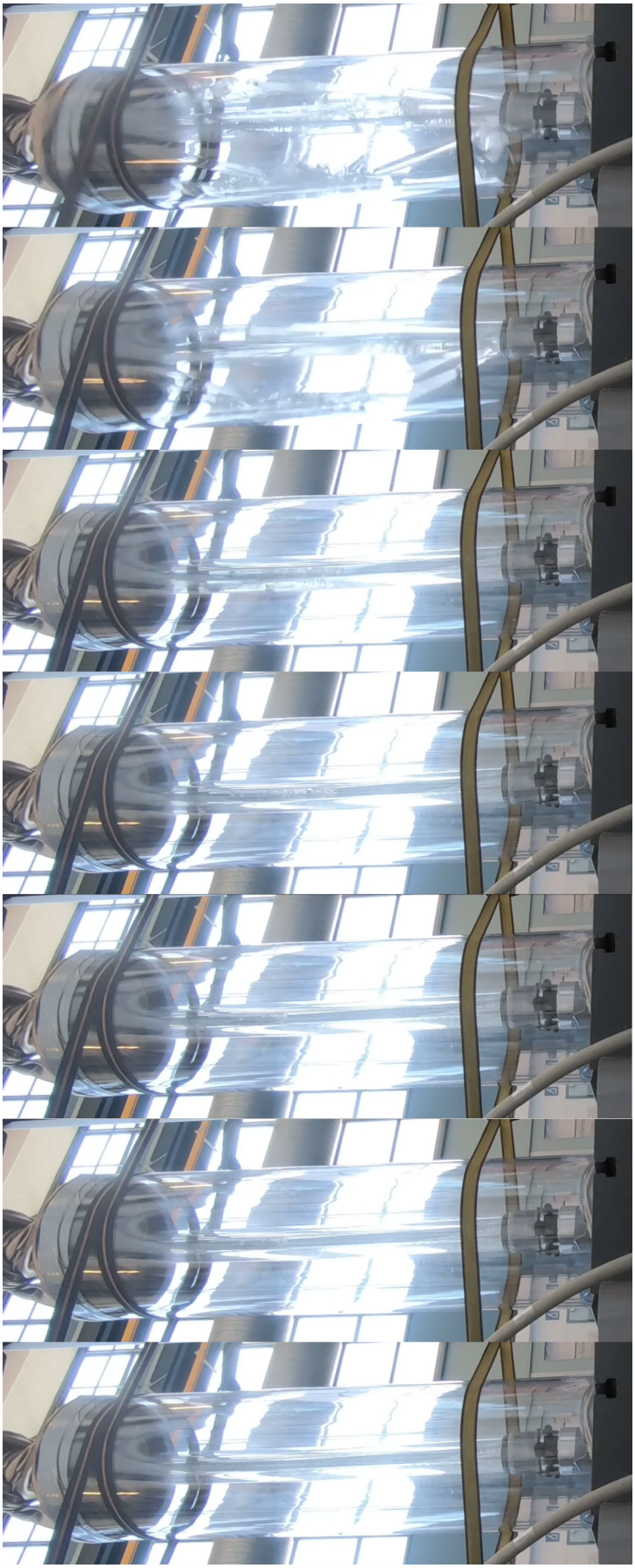

Figure 5.14: Snapshots from adjacent frames from the camera footage of Column 3 from camera position 3. Time duration from first to last image: $\frac{7}{60}$ seconds.

5.3. Conclusions

From all of the experimentally obtained results, the following is concluded:

The stresses are not equally distributed over the five glass rods within each column.
This is proven by:

- The deviating compressive strains measured for Columns 13 and 19.
- The fact that one of the glass rods within certain columns remained intact after failure of the rest of the rods.

The failure mode of Column 1 is bending.
This is proven by:

- The constantly decreasing slope of the load-displacement diagram.
- The fracture pattern of the glass rods belonging to Column 1.

The failure mode of the other 19 columns is buckling.
This is proven by:

- The decrease in slope in the load-displacement diagrams shortly before total failure occurred.
- The deviation in slopes shown in the results of the strain gauges shortly before total failure occurred.
- The severe lateral deformation in the middle of the columns that was observed during testing.

After the initiation of buckling the columns mainly failed due to the flexure of the rods that is caused by buckling.
This is proven by:

- The severe flexure (lateral deformation in the middle of the columns) that is observed during the tests.
- The failure crack patterns which showed mainly long cracks splitting the glass rods in half in longitudinal direction. These were most probably caused by bending where the bending compressive stress is much larger than the bending tensile stress along the cross-section.

Some rods within the columns failed due to twisting of the column.
This is proven by:

- The twist that is observed during the tests.
- Several glass rods that showed failure patterns that probably belonged to failure due to torsion.

Some rods within the columns showed cracks that originated from the ends of the rods.
This is proven by:

- Fracture patterns on pieces of glass which belonged to the rods ends.

Cracks originates from multiple locations simultaneously along the glass rods.
This is proven by:

- Fracture patterns that showed, among others, Wallner lines propagating towards each other.

6

FE Modelling of Bend & Break Columns until Failure

The way of modelling structural glass, presented in Chapter 4, is used to make finite element models for structural bundled glass columns. This chapter describes the models created to simulate the structural behaviour of the Bend & Break columns. Furthermore, its results are compared with the experimentally obtained results from the compression tests as described in Chapter 5.

6.1. The Finite Element Model

Section 4.1.1 of Chapter 4 shows an example on how to model a glass rod by assigning the glass finite elements varying tensile strengths. The glass rods of the Bend & Break columns consist of the same glass rods as described in that example.

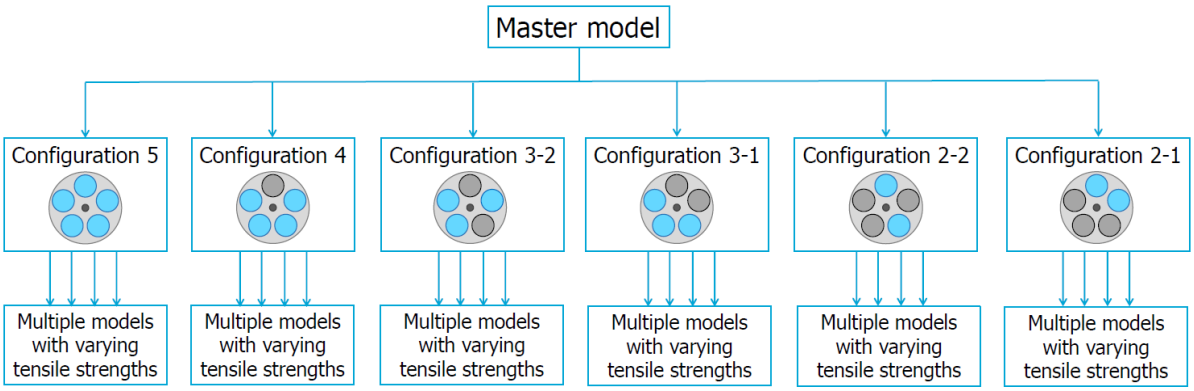

Figure 6.1: Scheme of the various finite element models that are created for the Bend & Break columns. The images belonging to the six different configurations are cross-sections which depict the glass rods that are removed from the finite element models. A blue circle means the glass rod at that place is modelled, a grey circle means that the rod is entirely left out of that finite element model.

Since the experimental results show varieties in structural behaviour, multiple finite element models are created in order to find the cause of these diversities. One of the possible sources is the variety in tensile strengths along a glass rod due to surface flaws. These would cause some columns to fail at a lower load than others. This, however, should theoretically not influence the buckling load, which is found to be varying as well in the experimental results. What does affect the buckling load is the unequal stress distribution over the five glass rods, which was one of the conclusions drawn from the experimental results. In order to model this phenomenon in a simplified way, it was decided to completely leave out glass rods in varying configurations within the finite element models. Figure 6.1 shows a scheme of the various finite models that are created. All models have the same 'master finite element model' as a base, which is adjusted to match the depicted configurations. Furthermore, for

each configuration, multiple models are created with varying tensile strengths along the finite elements. All these models have tensile strengths randomly drawn from the same Weibull distributions.

6.1.1. Details

In this subsection the geometry and mesh of the (master) model is elaborated. Furthermore, tables are given with information about the used materials and element types.

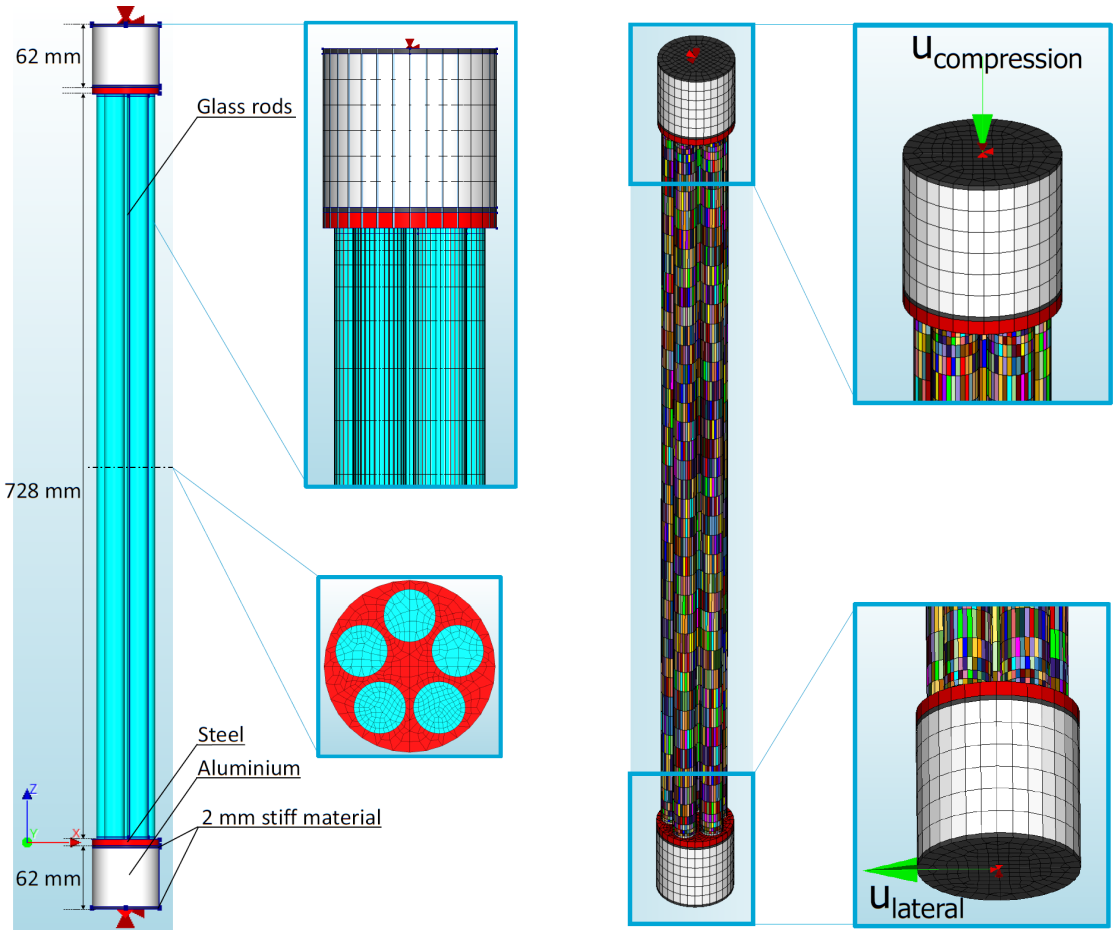

(a) Geometry of the FE model and mesh details.

(b) Mesh showing different colours for different tensile strengths for the finite elements. The zoom-ins show the applied loads in the finite element models.

Figure 6.2: Details of the finite element geometry, mesh and loads.

Figure 6.2(a) shows the finite element geometry of the Bend & Break columns. The model consists of five glass rods attached to 6 mm thick steel endplates, aluminium cylinders and hinged supports on top and bottom. The height of the aluminium cylinders is chosen to be 62 mm in accordance to the height of the rotation point in the hinges used in the compression tests shown in Figure 5.5 of Chapter 5. The ends of the finite element aluminium cylinders are made of 2 mm thick stiff material that will ensure the equal distribution of stresses from the point support. Moreover, it will prevent neighbouring elements from deforming too much due to the deformation of the aluminium. The figure, furthermore, shows the gradation in mesh size along the column. The element size in the middle of the column is 20 mm in the longitudinal direction, the elements slowly decrease to a size of 2 mm when it approaches the rods ends. The small element sizes near the ends are chosen to ensure a good distribution of stresses from the steel endplates to the glass rods. Furthermore, it was expected that the glass would fracture near the ends. Small elements show better results for nonlinear material behaviour such as cracking.

Figure 6.2(b) shows the randomised elements with varying tensile strengths. This is done in the same fashion as described in Chapter 4. Every colour refers to a different material set. In this model the glass ends have 20 material sets (so 20 different values of f_t), while the rest of the glass elements (the glass core) owns 50 material sets. These amounts of different materials will determine the amount of drawn tensile strengths from the Weibull distributions shown in Figure 6.3. Again, the dots in the figure refer to the drawn tensile strengths (f_t) for this particular example. For every finite element model of the Bend & Break columns that is created, the probability density functions are the same as in this figure. However, the drawn values (the dots in the figures) are different for every model. As indicated previously, the choice of Weibull parameters for the tensile strengths of the finite elements appears to be difficult. Several distributions are tried of which the one that gives the most probable results is chosen; the one shown in Figure 6.3. However, tests on the glass rods on itself to validate these choices are lacking. Luckily, the finite element models of the columns do show results that are comparable to reality. It is found that the unequal stress distribution over the five rods in the columns has significantly more influence on the structural behaviour of the columns, than the choice of Weibull parameters. This will be clarified by the obtained results showed later on in this chapter. Due to the relatively low influence of the choice of Weibull parameters, and the lack of experimental information to validate the choices, it was decided to use $\lambda = 20$ MPa and $k = 2$ for the rods ends and $\lambda = 60$ MPa and $k = 2.5$ for the rest of the rod (core).

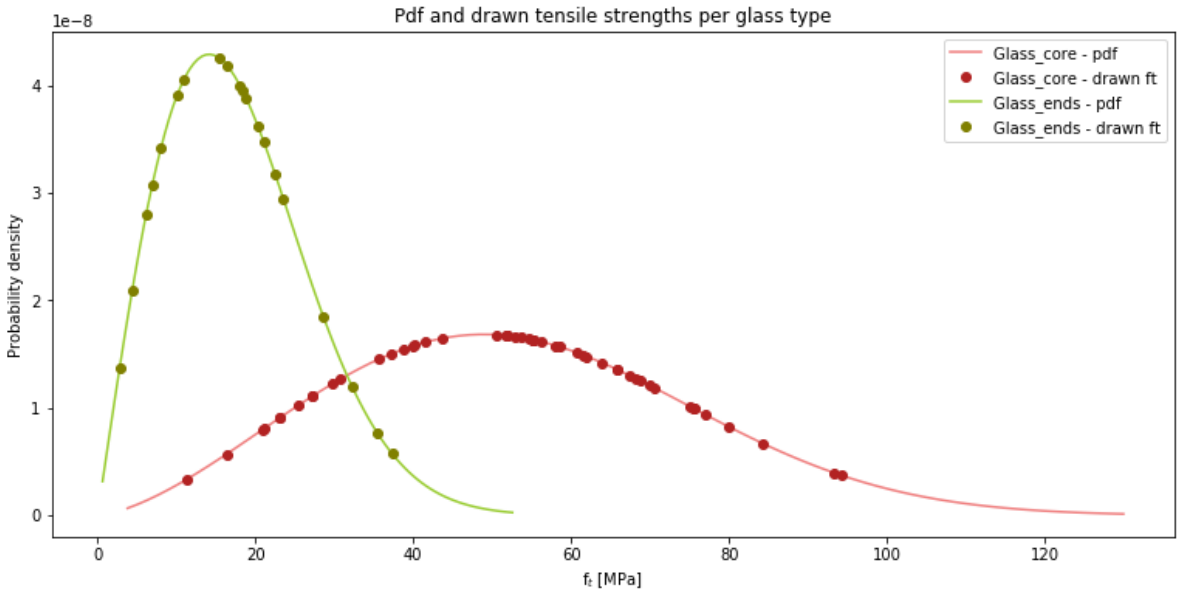

Figure 6.3: Probability density functions of the Weibull distributions used to model the Bend & Break columns with the dots referring to the drawn values of f_t. The green plot belongs to the glass ends and has parameters $\lambda = 20$ MPa and $k = 2$. The red plot belongs to the rest of the glass elements (the core) and has parameters $\lambda = 60$ MPa and $k = 2.5$.

The rest of the material parameters for the glass came from the datasheet generated by glass producer SCHOTT. As mentioned in Chapter 2, the Young's modulus provided by this sheet was validated using ultrasonic pulse velocity testing. It is, therefore, assumed that the other material properties would be accurate as well. The used material properties in the finite element models are given in Table 6.1. The element types used in the finite element models are presented in Figure 6.4. It was chosen to use quadratic elements to increase the accuracy of the models.

	Unit	Value	Type
Glass			
Young's modulus	GPa	63	
Poisson's ratio	-	0.2	
Compressive behaviour			Linear elastic
Tensile behaviour			Brittle (no residual strength)
Crack model			Smeared cracking (rotating)
Mass density	kg/m^3	2230	
Steel S235			
Young's modulus	GPa	210	
Poisson's ratio	-	0.3	
Mass density	kg/m^3	7850	
Stiff material			
Young's modulus	GPa	$2 \cdot 10^{11}$	
Poisson's ratio	-	0.1	
Mass density	kg/m^3	2000	
Aluminium			
Young's modulus	GPa	68.3	
Poisson's ratio	-	0.34	
Mass density	kg/m^3	2690	

Table 6.1: Material properties used in the FEM calculations of the Bend & Break columns. Except the glass, all materials behave linear elastically. (The influence of gravity is neglected in the models).

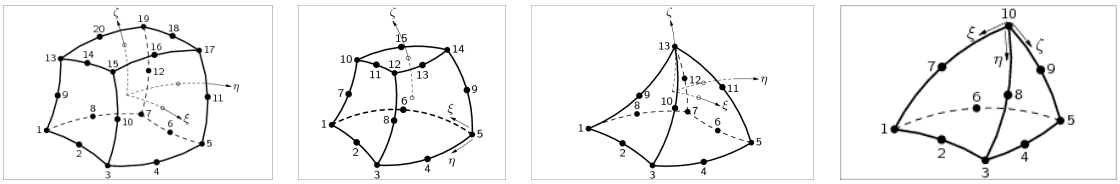

(a) CHX60 - brick, 20 nodes. (b) CTP45 - wedge, 15 nodes. (c) CPY39 - pyramid, 13 nodes. (d) CTE30 - pyramid, 3 sides, 10 nodes

Figure 6.4: DIANA finite elements used in the model of the Bend & Break columns. [17]

Loads and Analyses

To capture the buckling behaviour of the columns, it is needed to perform displacement controlled analyses. This is done by loading the columns with a prescribed deformation at the top of the column, as is depicted in Figure 6.2(b) as $u_{compression}$. This compressive, prescribed deformation is increased in a step wise fashion until the model becomes numerically unstable. The latter indicates total failure of the column. The choice of step size is such that smaller step sizes are taken if the model behaves in a nonlinear way (when it starts to buckle). The analyses done are both physically and geometrically nonlinear. This enables cracking of the glass and buckling respectively.

Figure 6.2(b) also shows a lateral prescribed deformation, $u_{lateral}$, which was 1 mm. This load was needed in the models of rod configuration 5, where all five rods were participating in carrying the load. This model was too symmetrical to buckle or fail without this lateral load. The other models were only subjected to the compressive load, $u_{compression}$.

6.1.2. Simplifications

Every finite element model, made for whatever purpose, will always be a simplification of reality. It is possible to get very close to reality, however, this generally leads to an extremely complicated model. Such a complex model is not only time consuming to create, but in addition needs a lot of computational

time to obtain results. Therefore, the challenge in finite element modelling is to create a model that is as simple as possible, but does give results that are accurate enough to draw conclusions from. It is, however, important to realise which simplifications with reference to reality are implemented in the finite element models. This is the reason why the various simplifications used to model the Bend & Break columns are summarised in this subsection.

Rod configurations
To model the inequality in stress distribution over the five glass rods within the columns, it was decided to completely leave out rods in the models in various configurations. These configurations are shown in Figure 6.1. This implies that a left-out rod does not contribute at all in carrying the load. In reality the columns will show intermediate behaviour of the shown configurations. Some rods will contribute more than others, but it is unlikely that one or multiple rods carry 0% of the load in reality.

Leaving out POM discs
The POM discs, which are used to avoid peak stresses (see Chapter 2), are chosen not to be modelled in the finite element model. The reason for this is that, in the finite element model, the surface of the ends of the rods is smooth and perfectly orthogonal to the rest of the rod. Therefore, in contradiction to reality, no peak stresses will occur in the finite element models due to steel to glass contact. Furthermore, if the POM discs would be modelled, they would deform due to the compressive force they are subjected to. This will cause them to bulk out to the sides. Since the element nodes at the bottom of the POM discs are connected to the top nodes of the glass rods, the lateral deformation of the POM discs will cause tensile stresses in the glass. These will generate unrealistic cracks in the glass rods ends, see Figure 6.5. The material properties of POM are given in Table 6.2. Using interface elements could be a solution, but would complicate the model. Furthermore, it will be difficult to determine the correct friction properties of these interfaces. By connecting the glass rods directly to the steel plates, the finite element model remains simple while the results will be closer to the experimental results compared to the models that included the POM discs (without interface elements). To ensure this decision does not influence the buckling loads of the models, the differences between these values were compared between finite element models with and without POM discs. The conclusions regarding the comparison between the models are the following:

- Approximately the same buckling and failure loads for finite element models with or without POM discs (difference of ±2 kN).
- The finite element models including POM discs show severe cracking of the glass rods ends already from an early loading stage, which is not realistic.
- The finite element models including POM discs needed more prescribed vertical deformation ($u_{compression}$) to get to the same compressive load due to the deformation of the POM.
- The models including POM discs show more numerical instability when the buckling load is reached due to severe cracking of the glass rods ends.

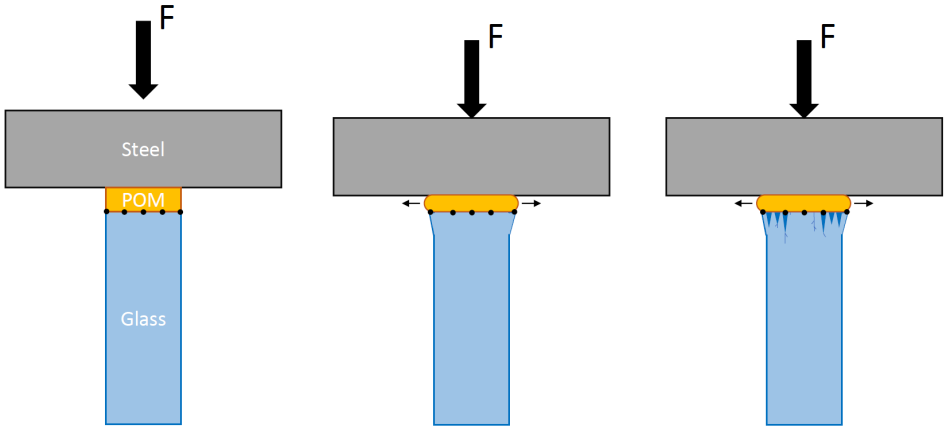

Figure 6.5: Visualisation of unrealistic cracking of the glass due to deformation of POM discs in finite element models that included POM discs without using interface elements.

	Unit	Value
POM (polyoxymethylene)		
Compression modulus	GPa	2.6
Poisson's ratio	-	0.37
Compression strength	MPa	20/35

Table 6.2: Properties of POM-Delrin®. [18]

No interface elements
It is chosen not to use any interface elements in the finite element models. This is a simplification, since in reality no glue is used in the configuration of the Bend & Break columns. In the finite element models, however, all the element nodes are connected. This implies that everything (the glass, the steel plates, the aluminium cylinders) that is modelled in direct contact with each other is basically 'glued together'. Using interface elements seems to lead to more realistic models, but would complicate them significantly.

Leaving out steel post-tensioning rod
The steel rod in the middle of the columns which enables post-tensioning of the column is not modelled. This steel rod keeps the glass rods together in reality. In the finite element model this is however not necessary. Furthermore, the design of the bundled glass columns is such that the glass will bear all the compressive forces.

Choice of Weibull distributions
The tensile strengths of the glass core as well as the rods ends are drawn from only one Weibull distribution respectively. In reality, the differences in tensile strengths within the glass could be not from one but several Weibull distributions. Furthermore, due to lack of experimental validation, an estimation of the Weibull parameters λ and k is used. This estimation is, however, not verified. More information on this topic is given in Chapters 3 and 4.

6.2. Finite Element Results

This section shows the results obtained from the finite element analyses that were performed for the Bend & Break columns. The lay-out of this section is similar to Section 5.2; first showing the load-displacement diagrams, followed by the strains/stresses and at last the fracture behaviour. In the next section the finite element results are compared with the experimental results in order to validate the finite element calculations. Furthermore, conclusions are drawn regarding the quality of the finite element models.

6.2.1. Loads and Displacements

In this subsection a distinction is made between the influence of the different rod configurations and the influence of the varying tensile strengths of the finite elements.

Influence of the Rod Configurations

Figure 6.6 shows the load-displacement diagrams of the six different rod configurations. It can be observed that the load bearing capacity of the columns decreases significantly when rods are removed from the models. Table 6.3 shows this reduction in percentages with reference to the maximum load of the configuration where all five glass rods are participating. Not only the load bearing capacities of the configurations differ, but also the structural behaviour of the columns. It can be observed that rod configuration 5 shows sudden brittle failure, this is due to the symmetry of the configuration. This enables perfect distribution of stresses along the five rods in the finite element model. The high stresses will cause sudden failure, due to the high energy storage within the rods. It should, however, be noted that nonlinear finite element modelling might show inaccuracies in results for brittle failure [19]. Configurations 4 and 3-2 do show the buckling behaviour by the decrease in slope. The load at which this decrease starts is seen as the buckling load and is given in Table 6.3. The other rod configurations show bending behaviour, which can be recognised by the gradual decrease in slope of the load-displacement diagrams. This is due to the eccentricity caused by the positions of participating glass rods in those configurations.

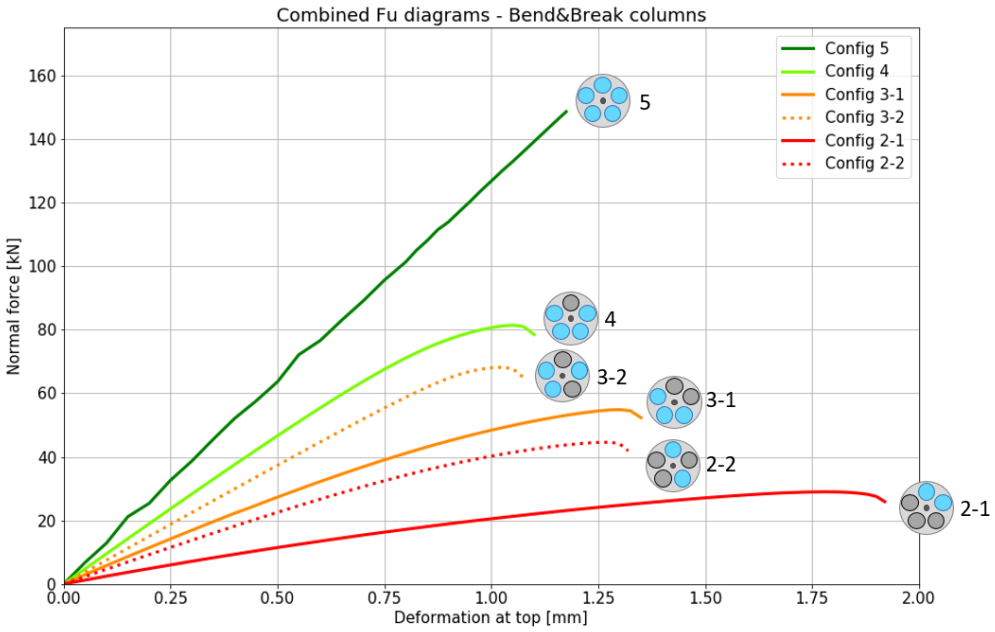

Figure 6.6: Load-displacement diagrams for the six different rod configurations.

Configuration	# of rods participating	Buckling load [kN]	Maximum load [kN]	%
5	5 rods	149	149	100
4	4 rods	60	81	55
3-2	3 rods	55	68	46
3-1	3 rods	*	55	37
2-2	2 rods	*	45	30
2-1	2 rods	*	29	20

* Fails due to bending. No buckling load.

Table 6.3: Buckling loads and maximum loads of all the rod configurations. The buckling loads are defined as the loads at which the slope of the lines of Figure 6.6 starts to decrease. The percentages at the right-hand side refer to the maximum loads with reference to rod configuration 5.

Influence of the Varying Tensile Strengths

As indicated in Figure 6.1, it was decided to run various models for every rod configuration with varying tensile strengths. These tensile strengths are drawn from the Weibull distributions for the glass rods ends and core which are shown in Figure 6.3. Due to time related issues it was decided to run most models for the configurations which are most likely to occur in reality. When briefly comparing the ultimate loads of the experimental results (which vary between 58 kN and 93 kN) to the finite element results, it is presumed that rod configurations 4 and 3-2 have the highest probability of occurrence.

Figure 6.7 shows the load-displacement diagrams of all the models. It can be observed that the differences in results are minor in comparison to the divergence the various rod configurations cause. The different models belonging to one rod configuration show exactly the same behaviour towards the buckling point. After buckling occurs, the results start to deviate. The zoom-ins on the tails of rod configurations 4 and 3-2 in Figures 6.7(b) and (c), give a better view of the differences in the failure

and ultimate loads of the models. That the deviation in results only starts after buckling occurs is logical, since tensile stresses arise due to the lateral deformation caused by buckling. Before that, the glass rods will be in compression only. The tensile stresses in the glass will cause the elements with the lowest tensile strengths, which are located where the highest tensile stresses occur, to crack in the finite element models. Visualisations of the cracking of the finite elements within the models are given in Subsection 6.2.3. The number of cracked elements, and the crack width increases as the load proceeds to increase. This, besides buckling on itself, causes the decrease in slope within the models after the buckling load. Since the elements crack differently for each model due to the varying tensile strengths, this causes the divergence in the tails shown in Figure 6.7.

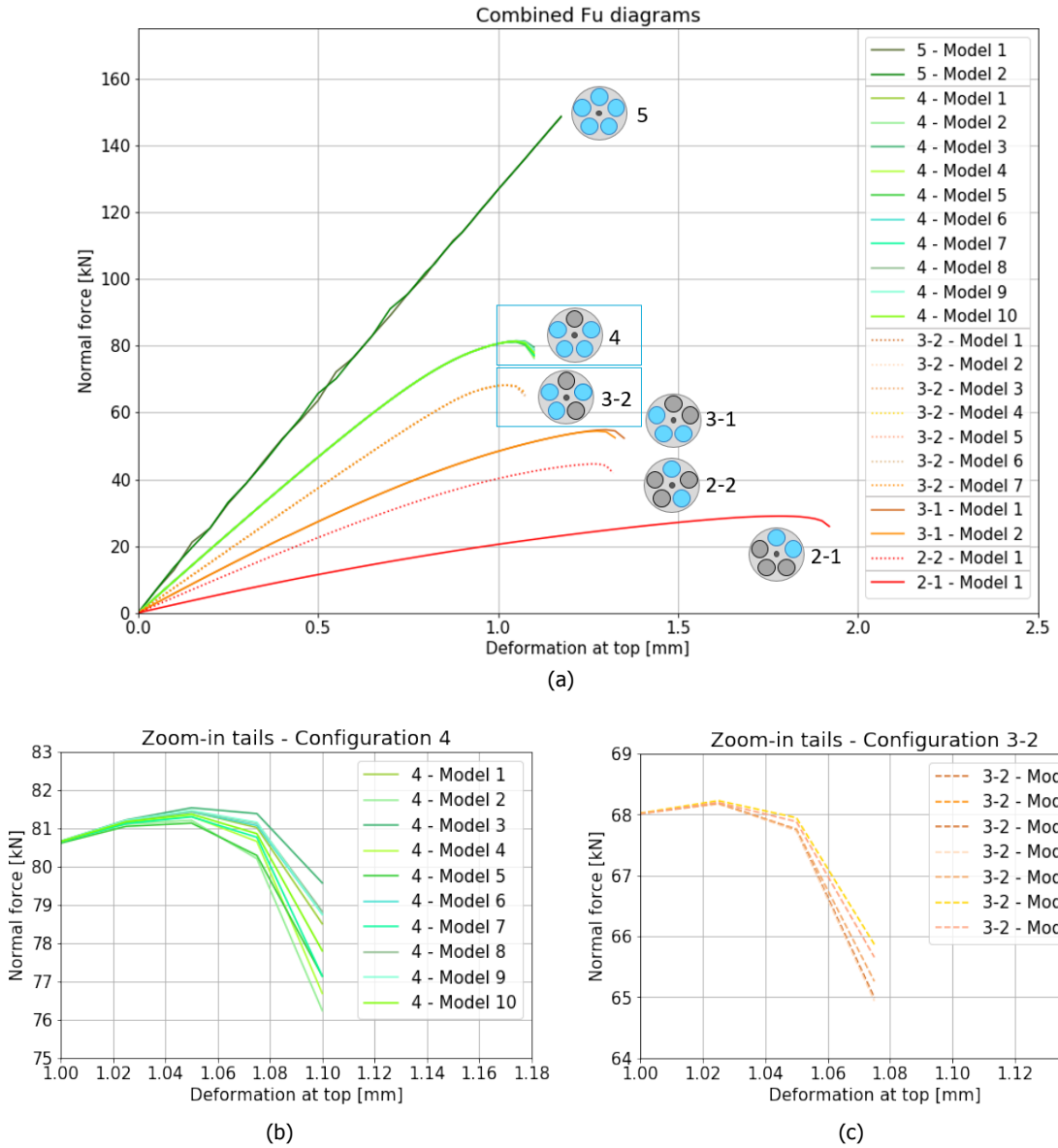

Figure 6.7: Load-displacement diagrams showing the influence of the varying tensile strengths. Figures (b) and (c) show zoom-ins on the tails for rod configuration 4 and 3-2 respectively.

Using different Weibull distributions than the ones shown in Figure 6.3 gives differences in results. Examples of these are given in Figure 6.8, where the tails of the load-displacement diagrams of models of rod configuration 4 are given. The rest of the diagrams is not shown, since that remains the same for each choice of Weibull distribution. The varying tensile strengths only have influence on the structural behaviour after buckling occurs. The buckling load is, therefore, not dependent on this choice. It can

also be observed that the maximum capacity of the columns remains within a range of 1 kN. It can, therefore, be concluded that the choice of Weibull distribution only influences the failure load.

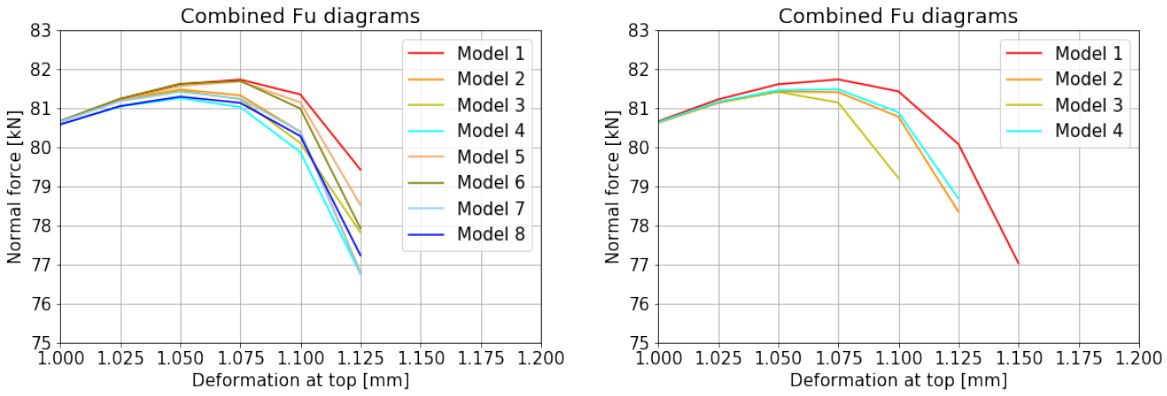

(a) $k = 2$ and $\lambda = 80$ MPa. (b) $k = 1.5$ and $\lambda = 80$ MPa.

Figure 6.8: Tails of the load-displacement diagrams subtracted from models of rod configuration 4 with different Weibull distributions.

6.2.2. Strains and Stress Distribution

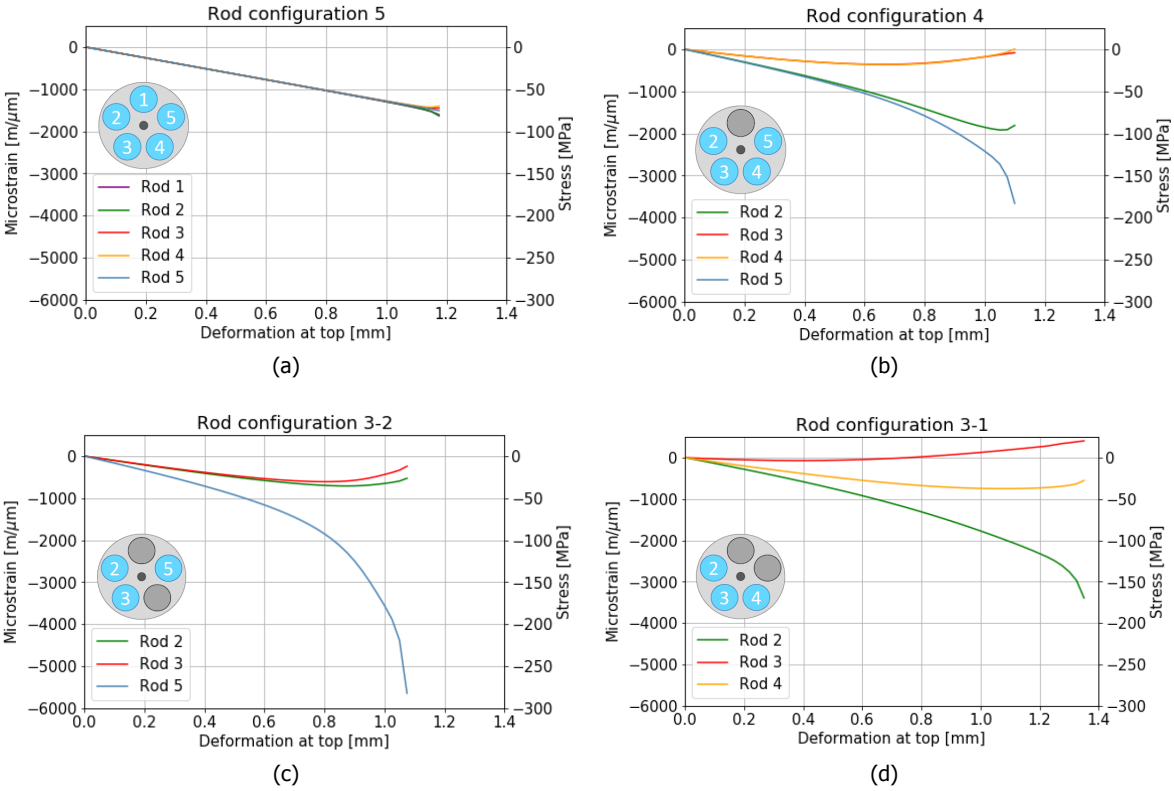

Figure 6.9: Deformation versus strain/stress diagrams for four of the rod configurations. The calculated strains/stresses come from the same location on the glass rods as the strain gauges were positioned in the experiments. This are the strains/stresses in longitudinal direction.

Figure 6.9 shows the strains and stresses of four of the rod configurations. The strains depicted here result from the same location on the glass rods as the strain gauges were positioned in the experiments. It is the calculated strain in longitudinal direction of the rods in the middle of the column. The

stresses, which are proportional to the strains due to the linear elastic material properties, are depicted on the right vertical axes. The horizontal axes show the prescribed deformations ($u_{compression}$) at the top of the columns. The figure, furthermore, shows an image of the cross-section of the models with the participating rods and their numbers. The strains and stresses for the rod configurations where only two rods are participating are not depicted, since it is unlikely that these configurations will occur in reality.

Rod configuration 5 shows an equal distribution of stresses along the rods. Only when the ultimate load is almost reached, do the stresses show deviation. This divergence is minor in comparison to the deviation shown in the other graphs. In the graph belonging to rod configuration 4 it can be observed that rods 2 and 5 carry most of the load. This is logical, since these are closest to the removed rod. Rods 3 and 4 show almost identical stresses. The eccentricity in rod configuration 3-2 results in rod 5 carrying a large percentage of the load in comparison to the other two rods. This can be seen in the graph by the large strains/stresses in this rod. The graph belonging to rod configuration 3-1 shows that the glass rod in the middle, rod 3, carries the least of the load. This is due to the eccentricity of the load, which causes the column to bend outwards in the direction of rod 3 with reference to the centre of the column. This explains the tensile stresses in that rod at that position.

6.2.3. Fracture Behaviour

As briefly addressed in Subsection 6.2.1, the varying tensile strengths in the finite element models cause differences in fracture behaviour between the models after buckling has occurred. In this subsection the fracture behaviour of the models is elaborated using visualisations. In these images, the elements that are cracked are coloured, while the elements that are still intact are transparent. The colour of the element indicates how severe the cracks are. The crack widths in longitudinal direction are given in meters (EcwZZ). Examples are shown per rod configuration. In the lower right corner the force-displacement diagrams are shown; the pink marker indicates which load/stress belongs to the accompanying image. Again, the results belonging to rod configurations 2-2 and 2-1 are not included, since it is unlikely that these configurations will occur in reality.

Rod Configuration 5

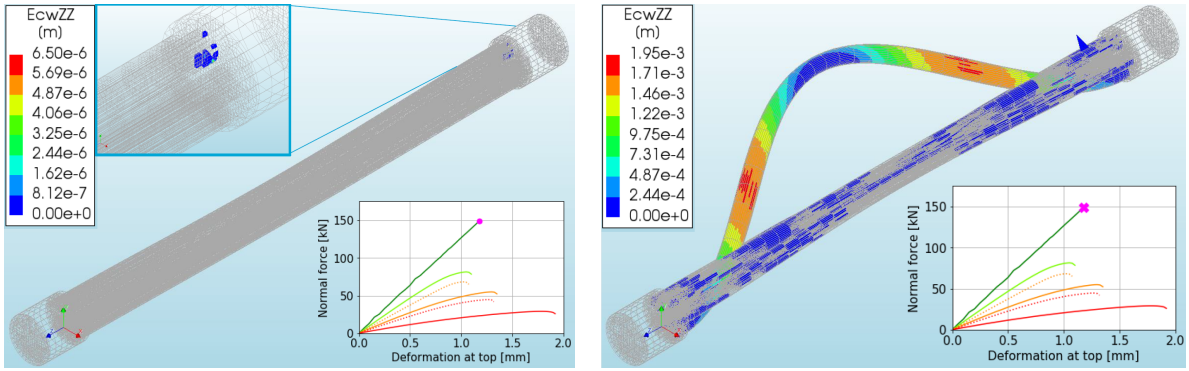

(a) Just before total failure.

(b) Numerical instability of the model a.k.a. total failure.

Figure 6.10: Contour plots showing crack widths for rod configuration 5, model 1. (Deformation scaling factor = 1).

As pointed out in the subsection regarding the load-displacement diagrams (Subsection 6.2.1), rod configuration 5 shows sudden failure. There are only few cracks with very small crack widths in the finite element model before the model becomes abruptly numerically unstable. The instability of the results can be observed by the large displacement of one of the rods in Figure 6.10(b). In reality, if the rods would be loaded in the ideal way like in the model, it is expected that the column would abruptly explode without any warning.

Rod Configuration 4

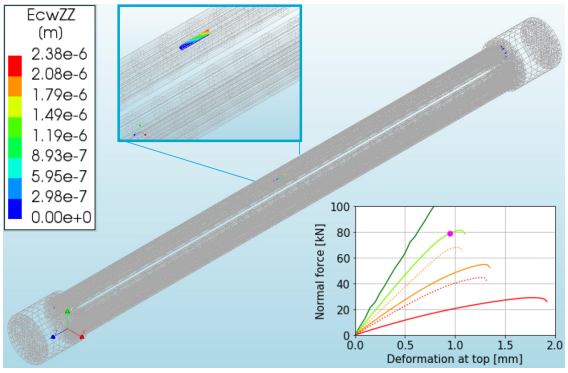

(a) First micro cracks in the middle of the column.

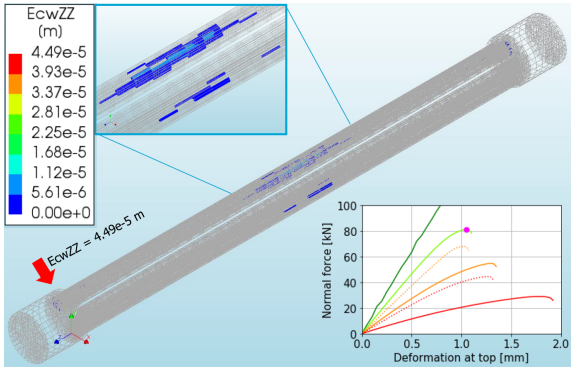

(b) Just after reaching the maximum capacity. More micro cracks in the middle of the column. More severe cracks at the rods ends.

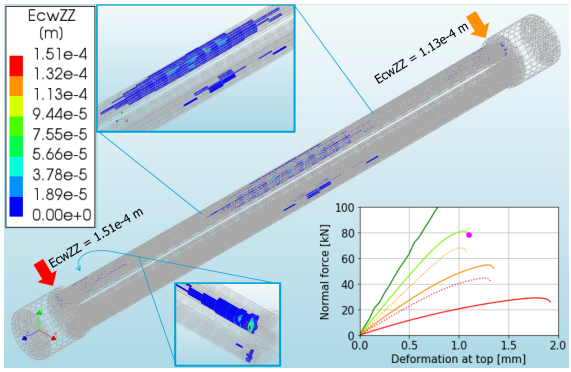

(c) Just before total failure. Rods ends crack significantly parallel to the steel endplates.

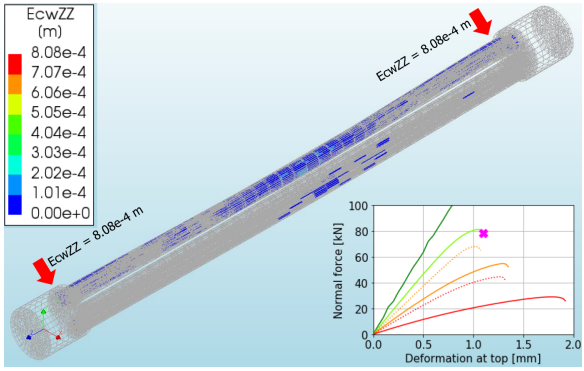

(d) Numerical instability of the model a.k.a. total failure.

Figure 6.11: Contour plots showing crack widths for rod configuration 4, model 1. (Deformation scaling factor = 1).

Rod configuration 4 shows more gradual failure behaviour. The first cracks in the middle of the column appear after the buckling load is reached. Mainly due to the cracking of the rods ends, the column start to deform more significantly in lateral direction after that point is reached. The cracks at the rods ends are mostly parallel to the steel endplates. These cracks may not occur in reality, but they enable the rods to deform more freely since they are less severely attached to the steel endplates. In reality the glass rods are not connected to those plates (or POM discs), so the cracking of the rods ends actually causes the model to behave more realistically regarding the deformation of the rest of the glass rod. The severity of cracking in the rods ends with reference to the rest of the rods is caused by the assigned tensile strengths that are weaker for the rods ends. Similar cracking behaviour in the rods ends is observed in rod configurations 3-2 and 3-1.

The cracks appear in the rods within the column that are most severely loaded, which are rods 2 and 5 as can be seen in the strain/stress diagrams given in Figure 6.9. This is to be expected, since the rods that are most heavily loaded will buckle first. All cracks appear at the tension side of the rods, which is logical since the elements can only crack due to tension and not due to compression. Again, similar behaviour is observed for rod configurations 3-2 and 3-1.

Rod Configuration 3-2

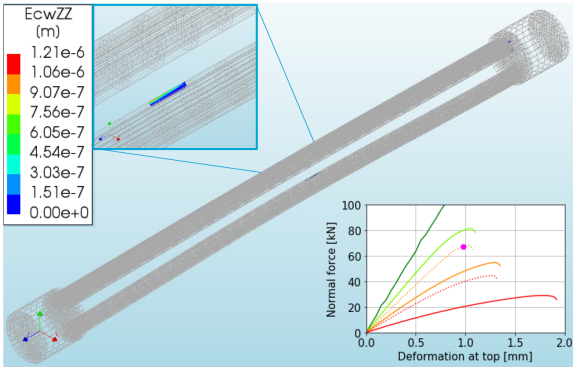

(a) First micro cracks in the middle of the column.

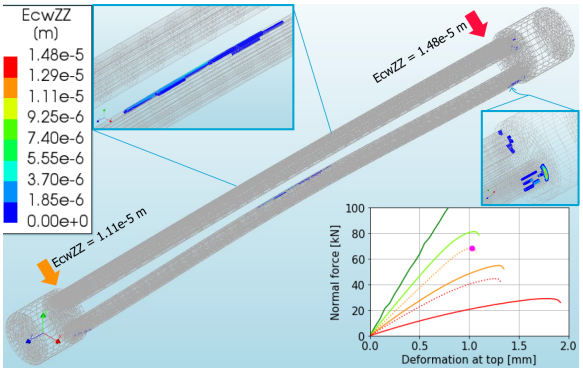

(b) Maximum capacity. More micro cracks in the middle of the column. More severe cracks at the rods ends.

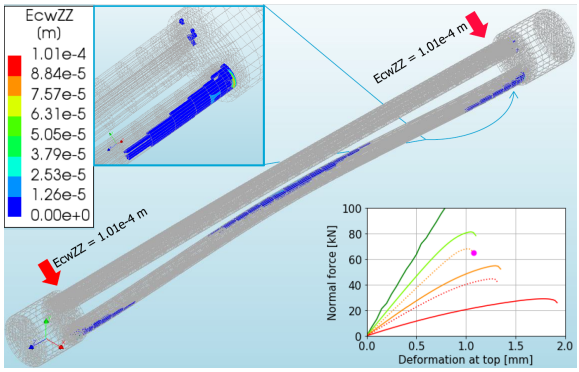

(c) Just before total failure. Rods ends crack significantly parallel to the steel endplates.

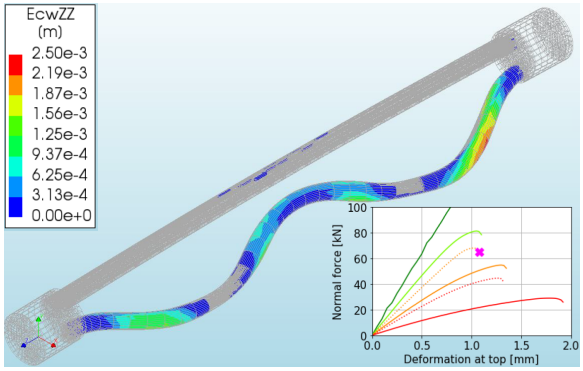

(d) Numerical instability of the model a.k.a. total failure.

Figure 6.12: Contour plots showing crack widths for rod configuration 3-2, model 1. (Deformation scaling factor = 1).

Since, in this configuration, one rod carries the biggest share of the load, this rod is the only one that cracks in the model before that rod fails completely. The cracking pattern is similar to that of the other rod configurations. The numerical instability of the model after failure is again obvious due to the large deformations in the model shown in Figure 6.12(d). For the other models this was observed by among others a sudden drop or increase in the compressive load due to the prescribed deformation ($u_{compression}$).

Rod Configuration 3-1

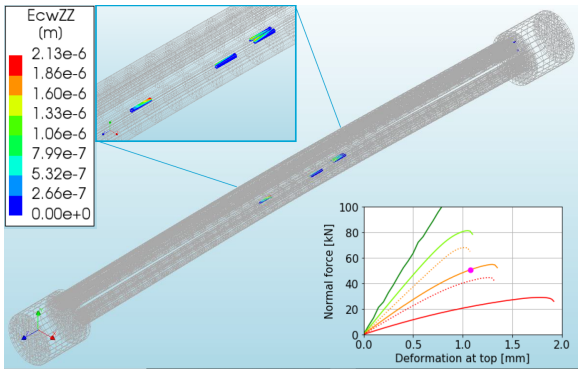

(a) First micro cracks in the middle of the column.

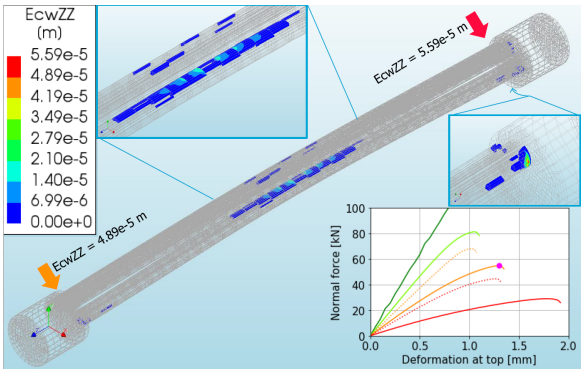

(b) Maximum capacity. More micro cracks in the middle of the column. More severe cracks at the rods ends.

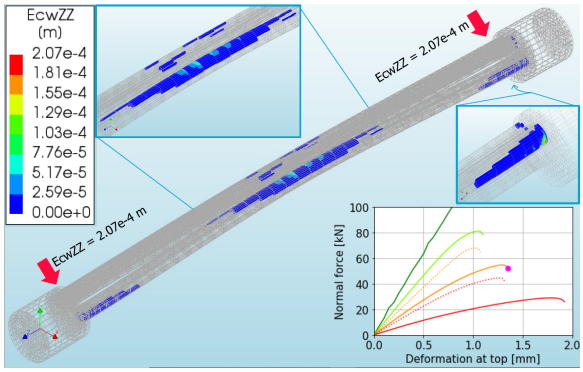

(c) Just before total failure. Rods ends crack significantly parallel to the steel endplates.

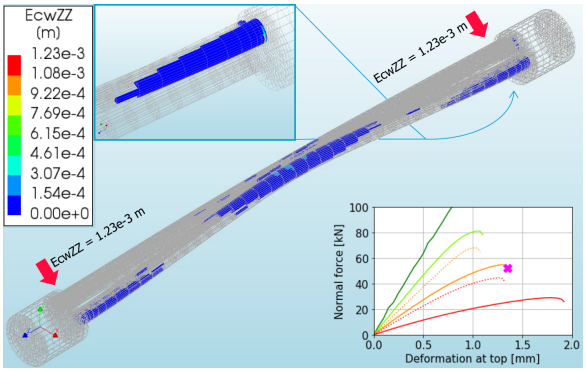

(d) Numerical instability of the model a.k.a. total failure.

Figure 6.13: Contour plots showing crack widths for rod configuration 3-1, model 1. (Deformation scaling factor = 1).

The eccentricity in this configuration causes bending behaviour of the column. The cracking pattern is similar to the configurations showing buckling behaviour, although the column remains intact longer after the first micro cracks start to appear. Again, the rod carrying most of the load cracks severest.

6.3. Validation and Conclusions

In this section the experimental results are compared to the finite element results in order to validate the finite element models. Conclusions regarding the quality of the finite element results are drawn using the comparisons. Using the validated models, conclusions regarding the structural behaviour of the Bend & Break columns are given.

6.3.1. Validation

The validation is done in the same order in topics as before, by first comparing the load-displacement diagrams, followed by the strains and stresses and at last the fracture behaviour.

Loads and Displacements

Figure 6.14 shows both the experimental and finite element results plotted on the same scale. Using this figure it can easily be spotted that the deformation at top (the prescribed displacement, $u_{compression}$) is significantly larger in the experimental results. This can be due to various reasons. First of all, the POM discs are not included in the finite element models. With a simple calculation using the calculated stresses within the POM discs subtracted from the finite element models, the dimensions of the POM discs and the properties of the POM given in Table 6.2, it was calculated that this will cause an additional vertical deformation of ±0.125 mm. Furthermore, the twist of the columns that happens in reality does

not occur in the finite element models, which can cause more vertical deformation as well.

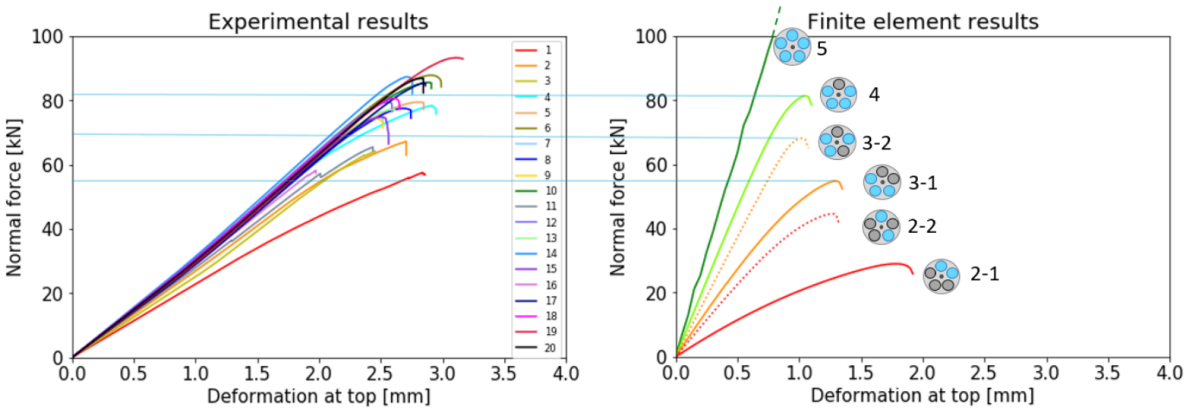

Figure 6.14: Load-displacement diagrams for both the experimental and the finite element results plotted on the same scale. The horizontal blue lines belong to the maximum capacities of rod configurations 4, 3-2 and 3-1 of the finite element models.

The loads and overall structural behaviour of the finite element models do, however, show great similarity to the experimental results. Especially rod configurations 4, 3-2 and 3-1 are close to the experimental results. It can be seen that none of the columns that were tested, has a capacity that is close to the 150 kN belonging to the perfectly loaded 5 rod configuration. However, some models show a higher capacity than the capacity of rod configuration 4. Furthermore, intermediate results between the finite element results of rod configurations 4 and 3-2 can be observed. It can, therefore, be concluded that the columns in reality show intermediate structural behaviour between rod configurations 5 to 3-1; where most columns show behaviour closest to configurations 4 and 3-2. Only Column 1 of the test series shows the bending behaviour belonging to rod configurations 3-1. None of the columns show behaviour that resembles the rod configurations where only two rods participate in carrying the load. Table 6.4 shows the experimentally obtained maximum loads with reference to the maximum loads subtracted from the finite element models.

FE configuration	Exp. column no.	Maximum load [kN]	%
5		149	100
	19	93	63
	6	88	59
	14	87	59
	20	87	58
	10	86	58
	17	85	57
4		81	55
	18	81	54
	5	79	53
	12	79	53
	4	78	53
	8	78	52
	13	77	52
	7	75	51
	15	75	50
	9	74	50
3-2		68	46
	2	67	45
	11	66	44
	3	64	43
	16	58	39
	1	58	39
3-1		55	37

Table 6.4: Maximum loads of all finite element rod configurations and the experimental results in order from high to low. The percentages at the right hand-side refer to the maximum loads with reference to rod configuration 5.

Strains and Stress Distribution

In the experiments, only two of the twenty columns were supplied with strain gauges. These were Columns 13 and 19. The load-displacement diagram of Column 13 is hidden between the other graphs, with a maximum capacity of 77 kN. This lays closest to the maximum capacity of rod configuration 4 (81 kN), therefore, from now on, Column 13 is assigned to belong in the group of rod configuration 4. The same holds for Column 19, which was the column with the highest capacity of 93 kN. Since both these columns are assigned to rod configuration 4, it was decided to compare the strains resulted from the finite element models of rod configuration 4 with the strains measured in the experiments. Due to the similarities in measured strains between the two tested columns, the finite element results are compared to the strains of Column 19 only.

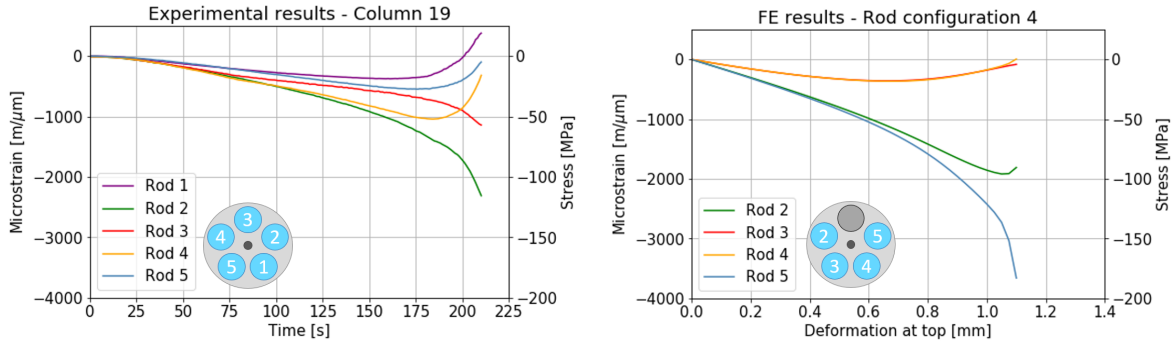

(a) (b)

Figure 6.15: Strain/stress diagrams for both the experimental and the finite element results.

A first point of interest when comparing the two graphs depicted in Figure 6.15, is the severity in strains/stresses calculated in the finite element model in comparison to the ones measured in Column 19. This difference, however, is logical, since the load compressing the rod has to be distributed over only four rods instead of five. Although Column 19 is assigned to the 4 rod configuration group, it does not mean that one rod is not participating at all. This can also be seen in the figure, where all rods carry at least a small amount of the load. The most heavily loaded rods are rod 2 for Column 19 and rod 5 for the finite element model. Furthermore, rod 4 of Column 19 can be compared to rod 2 of the finite element model. The depicted cross-sections in the figure show the numbering of the rods. Here the cross-section of Column 19 is rotated in such a way that it resembles this comparison between the most heavily loaded rods in the finite element model. It can be seen that, by looking at it from this point of view, rod 3 of Column 19 is the one that is missing in the FE model. This rod is in the experimental results, however, the rod that shows intermediate results compared to the other rods. When switching back to the results for Column 13, the same can be concluded. This can be checked by the reader of this thesis by looking into Figure 5.8(a).

When observing the tails of Figures 6.15(a) and (b) it can be seen that the direction in which they propagate are the same. This means that the rods in the finite element models bend out in the same directions as they do in reality.

Fracture Behaviour

Both the finite element results as the experimental results show that the glass fails due to the lateral deformation (flexure) of the column, which is in most cases caused by buckling. The severe cracking that the finite element models show near the rods ends, parallel to the steel endplates, does, however, not happen in reality. In reality the glass rods can move freely, since they are not glued to the POM discs or the steel endplates. The just mentioned cracks in the finite element model enables the modelled glass rods to move freely as well, which makes the flexure behaviour of the model more close to reality in comparison to a case where this cracking would not have been allowed.

Cracks in the middle of the glass rods and additional cracks at the rods ends can be observed in the contour plots shown in Subsection 6.2.3. Cracks that originated at the rods ends were also observed

by examining the fractured glass of the experimental results. Furthermore, it was observed that most columns had rods that were most severely fractured in the middle of the rods.

The finite element models do not show the crack propagation that is concluded by examining the fractured glass resulted from the experiments. Here, the cracks propagated relatively large distances along the longitudinal direction of the rods after they originated at the tensile side of the rod. The exact crack propagation within the glass, however, fell out of the scope of this thesis. Moreover, the positions of the origins of the cracks in the finite element models do show resemblance to reality. Both the finite element results as the experimental results indicate fractures that originate simultaneously on different points along the glass rods.

6.3.2. Conclusions

From the comparison between the experimental results and the finite element results, the following can be concluded:

The finite element models give a realistic representation of reality regarding the structural behaviour, buckling loads and maximum capacity of the Bend & Break columns. This gives allowance to conclude the following:

- The used simplifications in the finite element models were a good decision.
- The rod configuration simplification gives information regarding the structural behaviour of the real columns. Most columns show behaviour which point to three or four out of the five rods that carry the majority of the load.
- The experimental results show intermediate behaviour between finite element rod configurations 5, 4, 3-2 and 3-1. Most tested columns can be placed within the group of rod configuration 4 or 3-2. Only one out of the 20 tested columns belonged to the group of rod configuration 3-1. None of the columns showed a capacity close to the perfectly loaded rod configuration 5, however, some columns showed a capacity higher than the 81 kN belonging to rod configuration 4.
- Column 1 of the tested columns shows bending behaviour instead of buckling behaviour due to the eccentricity caused by the differences in rod lengths, tilt in the positioning of the steel endplates or other design flaws within the column.
- The calculated top deformation of the finite element models is ±2 mm lower than the experimentally measured top deformation. The goal of this thesis is, however, to find information regarding the structural behaviour, the buckling loads and capacity of the columns. That this deformation is not exactly the same as reality is, therefore, not of great importance.
- The varying tensile strengths over the glass rods have less impact on the structural capacity of the columns than the unequal stress distribution over the rods. This means that the influence of the micro flaws on the glass rods is also in reality significantly less in comparison to the influence of the inequality in stress distribution over the rods. It is, therefore, not of great importance for this research that the choice of Weibull distributions to create the finite element models was not perfect.
- The Weibull distribution that is used for the tensile strengths of the elements in the core of the glass rods was optimised to match the experimental results. Although the optimisation is not complete, since experimental results regarding the failure stress of such rods are missing, the chosen values for k and λ give an indication about the strength of these glass rods. The distribution used for the rods ends can not be verified.

7

Weibull Probability Plots of Results

In previous chapters (Chapters 3 and 4) Weibull probability plots belonging to experiments on glass panels performed by F.A. Veer and Y.M. Rodichev are shown [8]. Such plots are made of the failure stresses recorded in the experiments. Furthermore, finite element models are created as part of this studies as shown in Section 4.2 of Chapter 4. Those calculated failure stresses are plotted on a Weibull scale as well. Similar plots are shown in this chapter for the results obtained from the Bend & Break finite element models.

7.1. Experimental Results

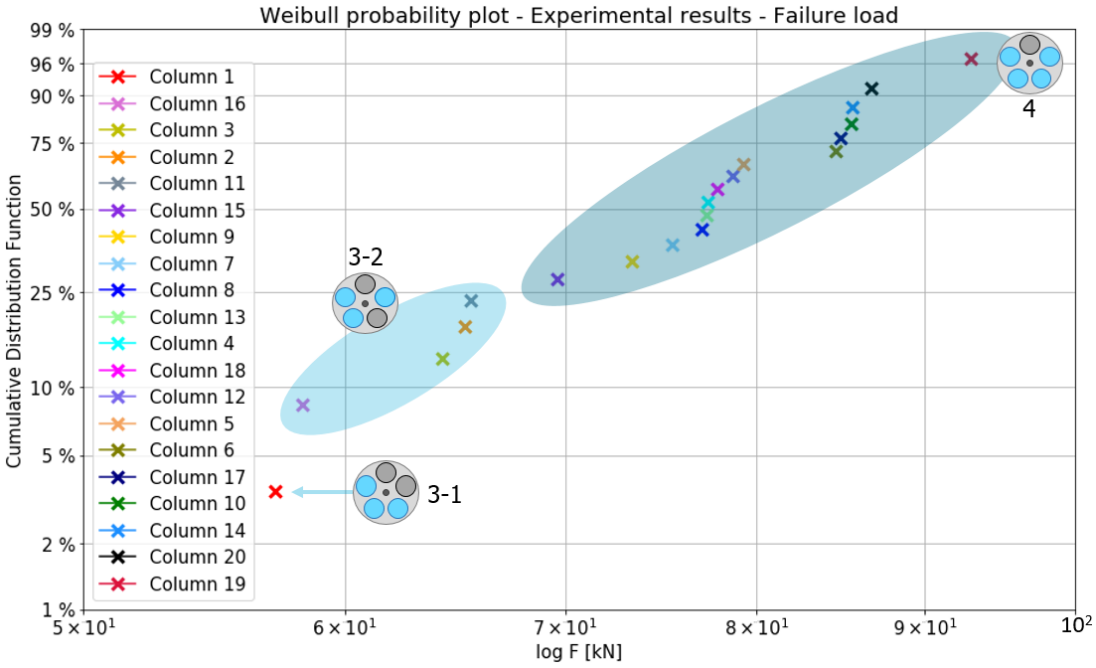

Figure 7.1: Compressive load at failure plotted against a Weibull scale for all twenty tested columns. The shaded areas indicate the groups to which the tested columns are assigned.

In the Weibull plots created for the glass panels from literature, the failure tensile stresses are plotted on the horizontal axis. In the compression tests on the Bend & Break columns, the failure stress itself was not measured. However, the compressive force was measured accurately; it is assumed that its behaviour is proportional to the failure tensile stresses. Calculating the failure stress from this force is not possible due to the varying distribution of forces within the five rods in the tested columns. It is, therefore, decided to plot the compressive normal force *at failure* on the horizontal axis. These results

are depicted in Figure 7.1. It can be seen that it does not show a perfect linearity, however, a step-like shape can be distinguished from the points.

As briefly mentioned in the validation of the finite element models in Section 6.3, all the tested columns can be assigned to groups belonging to rod configurations. This was already done for Columns 13 and 19, which were assigned to the group of rod configuration 4. The group assignments are based on the maximum loads, but also on the slope of the load-displacement diagrams. New Weibull probability plots are created by making these distinction between results, see Figure 7.2. The groups are also visualised in Figure 7.1 for clarification. Fifteen of the tested columns are placed in the group of **rod configuration 4 (75 %)**, four columns in **rod configuration 3-2 (20 %)** and column 1 is the only column placed in the group of **rod configuration 3-1 (5 %)**. It is, therefore, decided to make Weibull probability plots referring to the groups of rod configurations 4 and 3-2 only.

It is important to bear in mind that this distinction between the number of rods participating is a simplification of reality. It can be seen in Figure 5.8 of Chapter 5 that indeed some glass rods contribute more than others, but all carry at least a small part of the load.

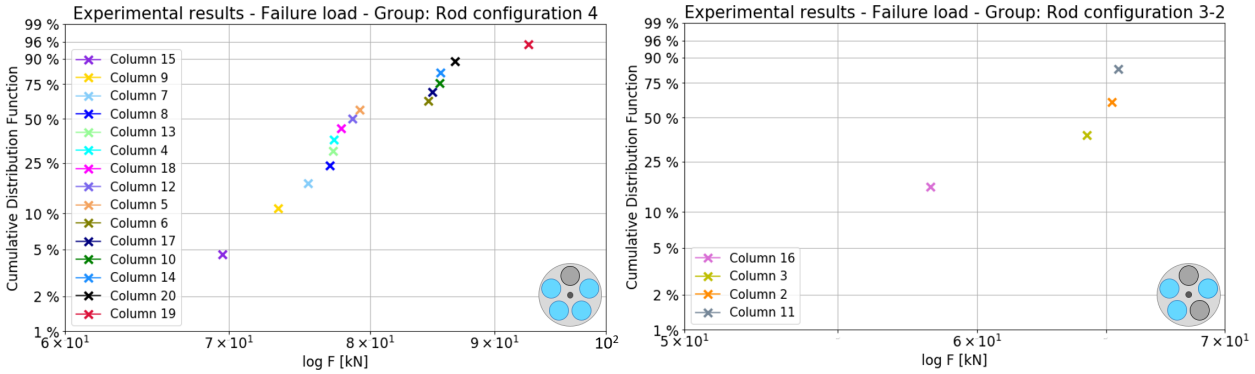

(a) (b)

Figure 7.2: Weibull probability plots of the experimental results when these are assigned in groups belonging to rod configurations 4 and 3-2.

When focusing on Figure 7.2, the points could be fitted to multiple straight lines. Doing this would be similar as was done for the tests on the glass panels from literature in Section 3.1.2 of Chapter 4. However, only limited results are available from the tests done on the Bend & Break columns. Twenty tests is the minimum amount to obtain appropriate conclusions regarding statistical distributions. However, due to the differences in participating rods within the columns, the structural behaviour is already very divers. Due to the design of the columns, there are a lot of variables that contribute to the behaviour of the columns, of which this variety in tensile strengths along the rods only plays a small part. The latter was concluded in the previous chapter. To be able to estimate the parameters k and λ, like was done in Section 4.2 of Chapter 4, it would be best to perform bending tests on the type of borosilicate glass rods used in the bundled glass columns. In this way the influence of the other parameters that are caused by the design of the bundled glass columns will be removed.

7.2. Finite Element Results

As mentioned in Chapter 6, the chosen Weibull distributions to make the finite element models of the Bend & Break columns were a guess. In the last paragraph of the previous section it is explained why the experimental results were not usable to choose the best Weibull parameters for these type of glass rods. The experimental results were, however, used to make a first assumption of these Weibull parameters.

The failure loads obtained from the various finite element models are plotted on a Weibull scale, using the same scales on both axes as in the plots made for the experimental results. Figure 7.3 shows

all the results of the finite element models of rod configurations 4, 3-2 and 3-1. When comparing this plot to the one belonging to the experimental results shown in Figure 7.1, it can be observed that the finite element results show more distinct groups.

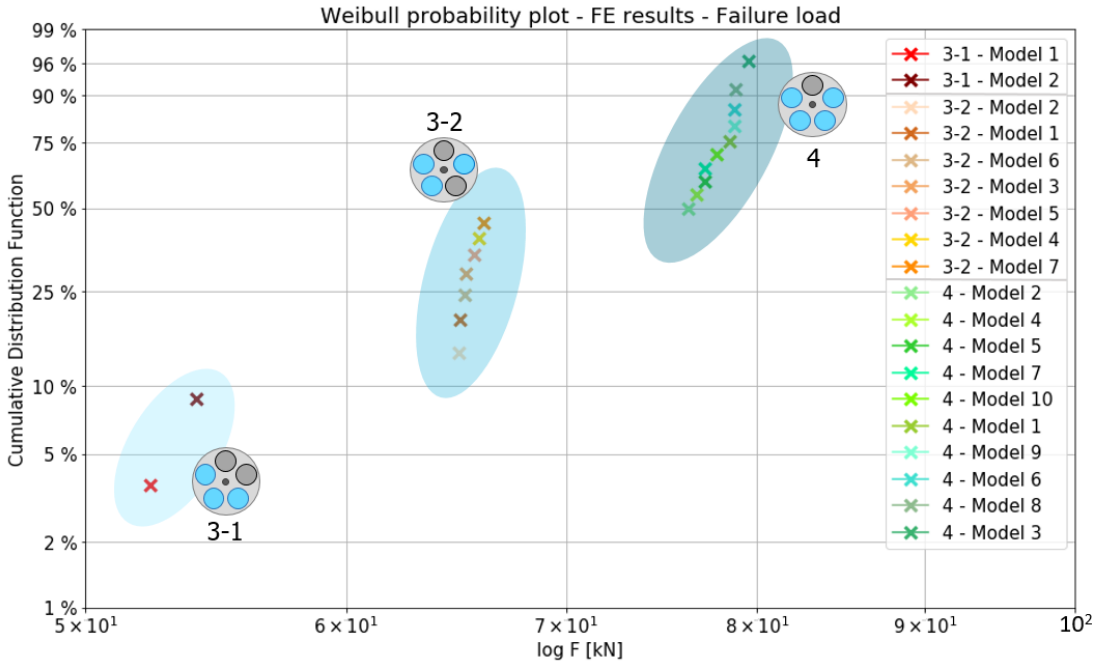

Figure 7.3: Compressive load at failure plotted against a Weibull scale for finite element models of rod configurations 4, 3-2 and 3-1. The shaded areas indicate the results belonging to the different rod configurations.

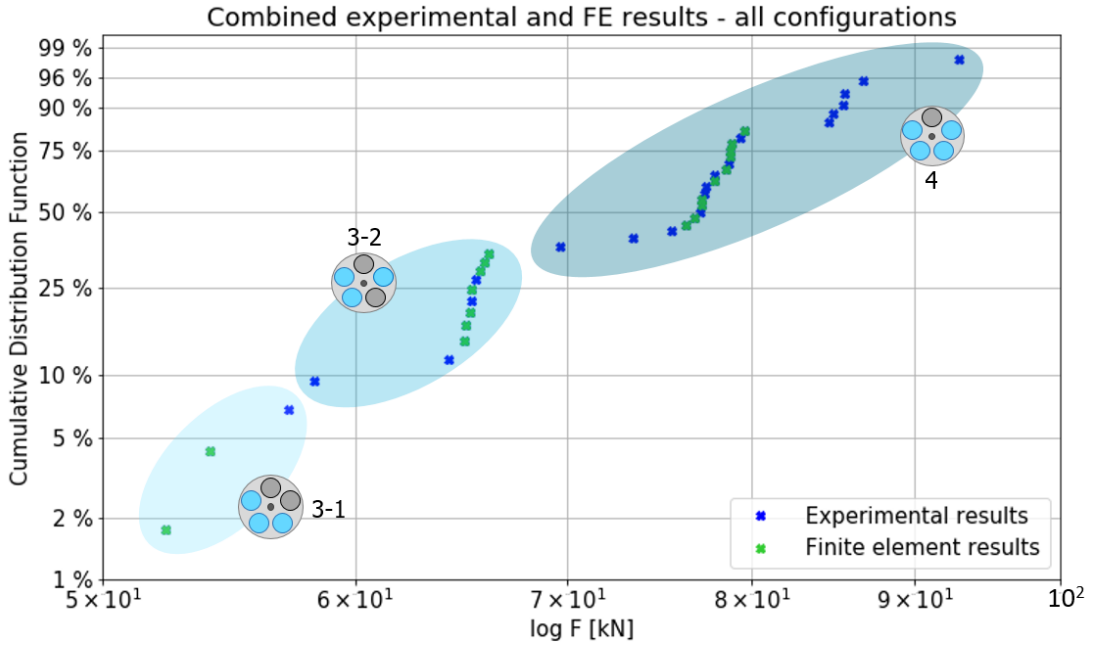

Figure 7.4: Compressive load at failure plotted against a Weibull scale for both the experimental results as the finite element results. The groups referring to the different rod configurations are indicated by the shaded areas.

To get a better indication of the finite element results with reference to the experimental results, Figure 7.4 shows a Weibull probability plot of both the experimental as the finite element results. It can be observed that for rod configurations 4 and 3-2 the finite element results lay well between the

experimentally obtained values. However, the two finite element models of rod configuration 3-1 show lower failure loads in comparison to the experimentally obtained result. It can, furthermore, be seen that the range of the experimental results is larger for rod configurations 4 and 3-2 in comparison to the finite element results. This can be explained by the diagnose that the experimental results show intermediate behaviour between the different rod configurations used in the finite element models.

7.3. Conclusions

Although the chosen Weibull distributions to create the finite element models of the Bend & Break columns are not verified, the resulted failure loads lay in line with the experimental results. Some results are however missing, since the experimental results show intermediate behaviour between the different rod configurations used to model the behaviour of the columns. Figure 7.1 summarises the buckling loads, maximum loads and probability of occurrences of the different rod configurations. The latter is based on the group assignments of the experimental results to different rod configurations.

Configuration	# of rods participating	Buckling load [kN]	Maximum load [kN]	Probability of occurence [%]
5 	5 rods	149	149	0
4 	4 rods	60	81	75
3-2 	3 rods	55	68	20
3-1 	3 rods	*	55	5
2-2 	2 rods	*	45	0
2-1 	2 rods	*	29	0

* Fails due to bending. No buckling load.

Table 7.1: Buckling loads and maximum loads of all Bend & Break rod configurations. The right-most column shows the probability of occurrence of each rod configuration based on the experimental results.

IV

Glass Truss Bridge Diagonals

8

FE Modelling of Glass Truss Bridge Diagonals until Failure

This chapter shows the finite element models that are created to simulate the behaviour of the diagonals in the Glass Truss Bridge. As mentioned in Chapter 2, the design of these type of bundled glass 'columns' is different to that of the Bend & Break columns. However, it is assumed that the structural behaviour is similar. Moreover, the same type of glass rods, from the same manufacturer are used in these columns. Therefore, the same approach in finite element modelling will be used for the Glass Truss Bridge diagonals as was used to model the Bend & Break columns.

8.1. The Finite Element Model

From the Bend & Break finite element models it is concluded that the different rod configurations have more influence on the structural behaviour than the varying tensile strength within the glass. It was, therefore, chosen to make only one finite element model per rod configuration for the Glass Truss Bridge diagonals. To make these models, the same Weibull distributions for the rods ends and the rest of the glass rods are used as depicted in Figure 6.3 of Chapter 6. The different rod configurations, and, therefore, the various finite element models, are shown in the scheme given in Figure 8.2. It can be seen that the star-shaped profile is never removed from the finite element models. In the scheme it can, furthermore, be observed that for every rod configuration three models are made, all with different lengths. The abbreviations $L1$, $L2$ and $L3$ stand for the following, where they represent the lengths of the glass rods (not the total column length):

$L1 = 728$ mm (same length as the glass rods in the Bend & Break columns)
$L2 = 1235$ mm (length of the shortest diagonals in the Glass Truss Bridge [9])
$L3 = 1392$ mm (length of the longest diagonals in the Glass Truss Bridge [9]).

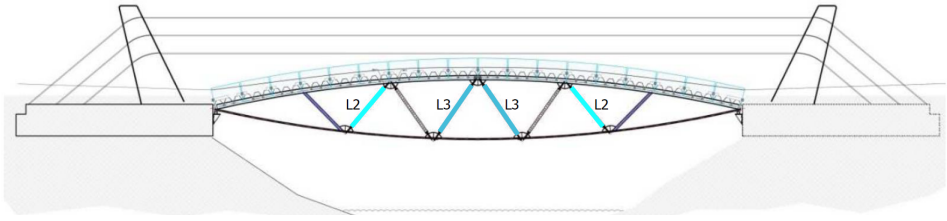

Figure 8.1: Side view of the Glass Truss Bridge with the shortest ($L2$) and longest ($L3$) diagonals high-lighted [1].

Models are created for both the shortest and longest diagonals in the Glass Truss Bridge. Those results are the upper and lower bound values for the medium length diagonals in the bridge. In addition models are created of the Glass Truss Bridge diagonals design with the length of the Bend & Break

columns ($L1$) in order to compare to structural behaviour of the designs. Those results are elaborated in Chapter 9.

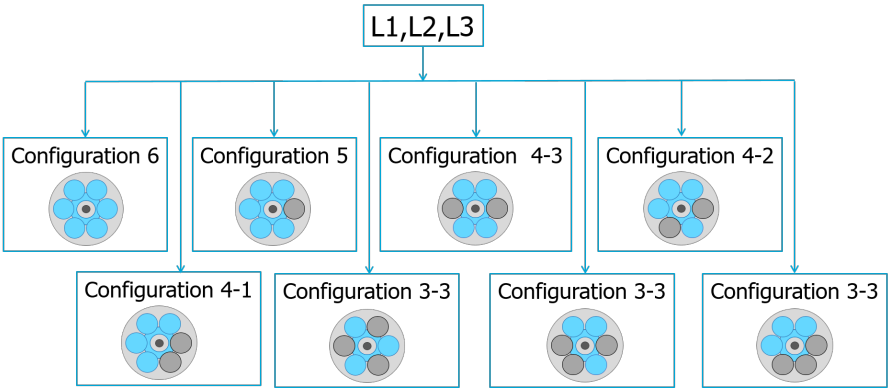

Figure 8.2: Scheme of the various finite element models that are created of the Glass Truss Bridge diagonals. The images belonging to the eight different configurations are cross-sections which depict the glass rods that are removed from the finite element models. For every rod configuration models of three different lengths ($L1$, $L2$ and $L3$) are created.

8.1.1. Details and Simplifications

This subsection shows the geometry and mesh details of the finite element models. Since the setup of the models is similar to the Bend & Break models, it is only briefly elaborated. Figure 8.3 shows the most important details of the finite element models of the Glass Truss Bridge diagonals. Most of the boundary conditions are the same as for the Bend & Break models, however, the aluminium cylinder is smaller to match the one in the Glass Truss Bridge design. Furthermore, the design of the Glass Truss Bridge diagonals prevents the star-shaped profile to be loaded directly, see Figure 2.9 of Chapter 2. This is done to avoid peak stresses in the legs of the star-shaped cross-section. To create this in the finite element model, it was decided to model the steel endplates as two parts with a thickness of 4 mm each. The first part is seen in the upmost zoomed in image of Figure 8.3, where the steel is an extension of the glass rods (steel is depicted in dark red). Attached to those small steel plates, the steel endplate is positioned which transfers the load through the aluminium towards the supports. Instead of the POM discs, used in the Bend & Break columns to create a more equal distribution of stresses over the glass rods, in this design soft aluminium was used. For the same reasons as the POM was not modelled in the Bend & Break models, this layer of aluminium is not modelled in the models of the Glass Truss Bridge diagonals.

It is pointed out in Chapter 2 that the glass rods are glued together in this particular bundled glass column design as opposed to the design of the Bend & Break columns. In that chapter it is, furthermore, indicated that the cross-section of the Glass Truss Bridge diagonals is the same as the initial bundled glass column design shown in Figure 2.3(a). In those designs the rods were glued together using the same adhesive. The failure pattern of such a column is shown in Figure 2.6 and indicates that the glass itself will fail, not the bond created by the adhesive. For that reason, the finite element nodes between the star-shaped profile and the circular glass rods within the model are directly connected to each other. This will create a perfect bond between the glass rods in the finite element models. Therefore, no interface elements were needed to model the adhesive. This decision resulted in a solid glass bar with the cross-section as given in the image in the middle of Figure 8.3.

The material properties, loads and analyses are the same as described in the chapter elaborating the Bend & Break models (Chapter 6). All models were subjected to a compressive prescribed deformation ($u_{compression}$) to enable displacement controlled analyses. The symmetrical models, rod configurations 6, 4-3 and 3-3, however, needed an additional lateral deformation ($u_{lateral}$) of 4 mm at the bottom to enable buckling within the finite element models. The same was done in the Bend & Break models of rod configuration 5, which is symmetrical as well.

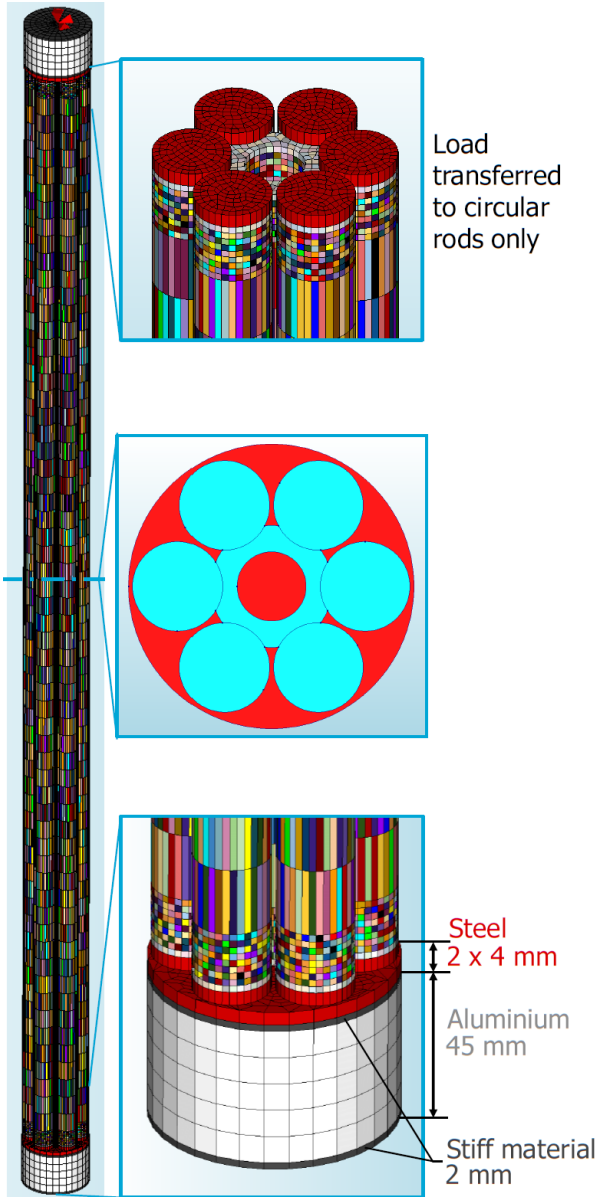

Figure 8.3: Geometry and mesh details of the finite element model.

8.2. Finite Element Results and Partial Validation

The finite element results obtained from the models of the Glass Truss Bridge diagonals are presented in this section. Again the presented results will consist of load-displacement diagrams, strains/stresses and the fracture behaviour. Compression tests were performed on the diagonals that are currently in the Glass Truss Bridge, see Section 2.2 of Chapter 2. During these tests the strains on three of the glass rods within the columns were measured. Although these tests were only up to a compressive load of 40 kN, the results partly validate the presented finite element results. Not only these experimental results, but also the results from the compression tests done on the initial bundled glass columns (see Section 2.1 of Chapter 2) can be used as partial validation. The cross-section of those diagonals is the same as that of the Glass Truss Bridge diagonals. Furthermore, the same adhesive was used to glue the rods together.

8.2.1. Loads and Displacements

Some of the graphs shown in this subsection will show small jumps. These jumps are caused by a difference in load step size within the finite element analyses. These, therefore, can be disregarded.

L2 = 1235 mm - Shortest Diagonals

The load displacement diagrams given in Figure 8.4 show the differences in structural behaviour and capacity the different rod configurations cause. Interesting is that three different kinds of structural behaviour can be observed. The first is that of the symmetrical cross-sections (rod configurations 6, 4-3 and 3-3), where perfectly brittle failure can be observed. This behaviour shows similarities to the behaviour of rod configuration 5 of the Bend & Break columns, which also had a symmetrical cross-section. It should again be noted that nonlinear finite element analyses may show inaccuracies in results for brittle failure. [19] The second behaviour that is observed in Figure 8.4 is the more ductile buckling behaviour of rod configurations 5 and 4-2. Here, the columns behave linear elastically until the buckling load is reached. From that point, the slope of the graphs start to decrease, until the columns eventually fail. The buckling loads, as well as the failure loads, of the different rod configurations are given in Table 8.1. The last type of structural behaviour that can be observed, belongs to rod configurations 4-1, 3-2 and 3-1, which shows bending behaviour. This behaviour is caused by the eccentricity in the cross-sections. However, configurations 4-1 and 3-2 also show some additional buckling behaviour before the maximum capacity is reached.

Contradictory to the Bend & Break column design, the adhesive used in the Glass Truss Bridge diagonal design enables the glass rods to work together. The star-shaped profile allows loads to transfer from one rod to the other within the column, which most probably causes a better distribution of stresses along the glass rods in comparison to the Bend & Break columns. It can, therefore, be expected that the rod configurations with only 3 rods participating are unlikely to occur in reality. Due to the contribution in stress distribution of the star-shaped profile over the six circular rods, it is expected that the stresses will be relatively symmetrically distributed over the rods with reference to the Bend & Break columns. This makes the probability of occurrence of rod configuration 4-1 less in comparison to the other configurations with four rods participating. This would be advantageous, since the capacity of rod configuration 4-1 is rather low in comparison to those others. In the experiments performed on the Bend & Break columns, it was observed that the configuration where all rods contribute equally in carrying the load (rod configuration 5), is not likely to occur. It is, therefore, expected that for the Glass Truss Bridge diagonals the probability of occurrence of rod configuration 6 is small. It is important to bear in mind that those are expectations, which have to be validated by performing experiments on columns with the Glass Truss Bridge diagonal design.

Table 8.1 shows a summary of the buckling and maximum loads of the finite element results for the shortest diagonals. The right-most column shows percentages of the maximum loads of all the rod configurations with reference to rod configuration 6.

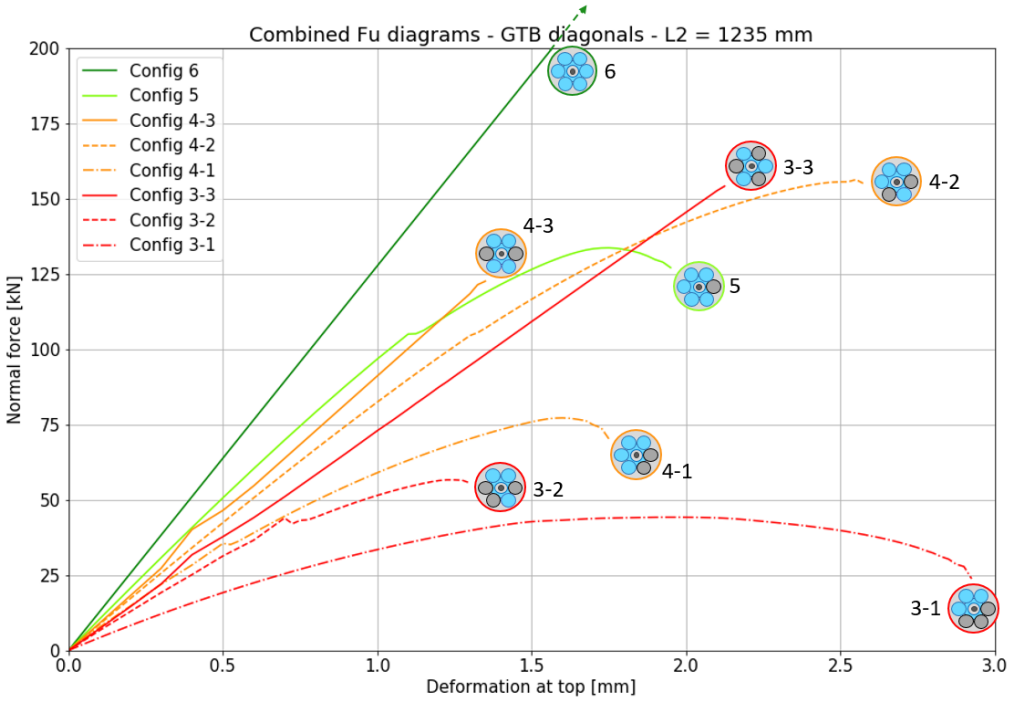

Figure 8.4: Load-displacement diagrams for the eight rod configurations belonging to the Glass Truss Bridge diagonals. These diagrams belong to a length of $L2 = 1235$ mm. The dark green graph belonging to rod configuration 6 extends out of the graph to a load of 294 kN and remains linear elastic to the point of sudden failure.

Number	Configuration	# of rods participating	Buckling load [kN]	Maximum load [kN]	%
6		6 rods	294	294	100
5		5 rods	100	134	45
4-3		4 rods	123	123	42
4-2		4 rods	100	156	53
4-1		4 rods	75	77	26
3-3		3 rods	154	154	52
3-2		3 rods	50	57	19
3-1		3 rods	*	44	15

* Fails due to bending. No buckling load.

Table 8.1: Buckling loads and maximum loads of all the rod configurations for $L2 = 1235$ mm. The buckling loads are defined as the loads at which the slope of the lines of Figure 8.4 start to decrease. The percentages shown in the right-most column refer to the maximum loads of all configurations with reference to rod configuration 6 of this design and this length.

L3 = 1392 mm - Longest Diagonals

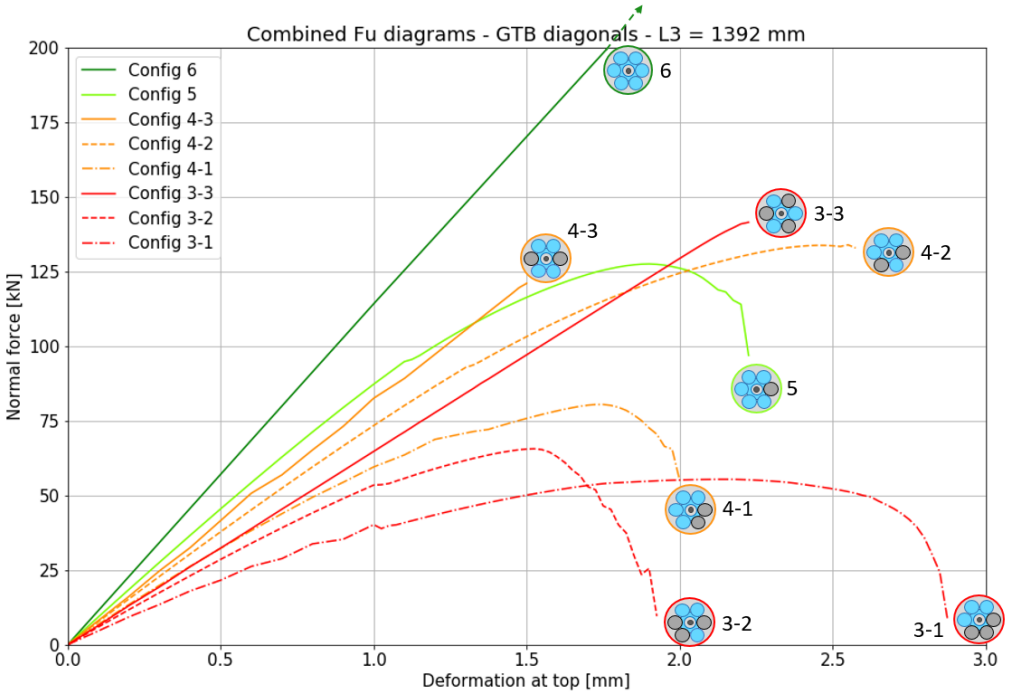

Figure 8.5: Load-displacement diagrams for the eight rod configurations belonging to the Glass Truss Bridge diagonals. These diagrams belong to a length of $L3 = 1392$ mm. The dark green graph belonging to rod configuration 6 extends out of the graph to a load of 248 kN and remains linear elastic to the point of sudden failure.

Number	Configuration	# of rods participating	Buckling load [kN]	Maximum load [kN]	%
6		6 rods	248	248	84
5		5 rods	100	128	43
4-3		4 rods	121	121	41
4-2		4 rods	90	134	46
4-1		4 rods	70	80	27
3-3		3 rods	141	141	48
3-2		3 rods	65	66	22
3-1		3 rods	*	55	19

* Fails due to bending. No buckling load.

Table 8.2: Buckling loads and maximum loads of all the rod configurations for $L3 = 1392$ mm. The buckling loads are defined as the loads at which the slope of the lines of Figure 8.5 start to decrease. The percentages shown in the right-most column refer to the maximum loads of all configurations with reference to rod configuration 6 of the short diagonals (see Table 8.1).

The right-most columns of both Table 8.1 and Table 8.2 are percentages with reference to the strongest configuration (configuration 6) of the shortest diagonals ($L2$). Those are chosen as reference, since the shortest diagonals will be the strongest of the bridge. It can be observed that the difference in capacity between the longest and shortest diagonals is minor. However, the longer the diagonal (or column), the more ductile the behaviour of the columns becomes after buckling occurs. This can be seen by the relatively long tails shown in the load-displacement diagrams. The diagrams belonging

to the short length of $L1 = 728$ mm (Figure 9.1 of Chapter 9) have the smallest tails and, therefore, show more brittle behaviour. It is to be expected that columns with a higher slenderness have lower capacity, but higher ductility. The same differences in behaviour can be observed when, for example, compressing a short plastic straw and a long plastic straw. The smaller straw will need more force to buckle and there after almost immediately collapses, while the longer straw will start to buckle at a rather low load but deforms more and more until it eventually collapses.

Partial Validation

In order to get an idea about the accuracy of the calculated loads, these finite element results are compared with the values given in Table 2.2 of Chapter 2. That table gives the experimentally obtained results of three of the tested series of the initial bundled glass columns by F. Oikonomopoulou et al. From those series, B_1 has a length that is closest to that of the Glass Truss Bridge diagonals, namely 1500 mm. However, the supports of these columns were clamped, whereas the supports of the Glass Truss Bridge diagonals were hinged. According to the buckling formulas of Euler, the buckling load for a column with two clamped supports is four times higher than for the same column with two hinged supports. When, furthermore, taking the differences in length into account, this will mean that the measured maximum loads will have to be divided by 3.52. The calculation to obtain this value is given in Equation 8.1, where the total length of the longest diagonal (1408 mm) is taken as reference length L. When dividing the maximum loads (F_{max}) of specimen series B_1 by 3.52, the following list of loads is obtained: 93.9 kN, 110.5 kN and 144.4 kN.

$$F_{buc} = \frac{\pi^2 EI}{(0.5\frac{1500}{1408}L)^2} \quad \Rightarrow \quad 3.52F_{buc} = \frac{\pi^2 EI}{L^2} \tag{8.1}$$

These values are compared to the maximum loads of the longest diagonals given in Table 8.2, since their length is closest to the length of 1500 mm of the tested columns. It can be seen that the values belonging to specimen series B_1 lay well within the range of calculated finite element results. From this it is assumed that the finite element results are accurate, however, this validation is not enough to draw full conclusions.

8.2.2. Strains and Stress Distribution

In this subsection the strains obtained from the finite element analyses of the shortest diagonals ($L2$) are presented for all configurations. Only those of the shortest are given, since the strain distributions belonging to other lengths will be very similar. This subsection not only shows results of the finite element models in Figure 8.6, but also the experimentally obtained strains in Figure 8.7. In this way, the finite element results and the experimental results can be compared.

The strain gauges in the experiments were placed at the same locations as for the Bend & Break columns, on the outside of three of the glass rods in the middle of the diagonal (see Figure 2.10 of Chapter 2). Therefore, Figure 8.6 shows the strains obtained from the finite element models at the outside of all the present circular rods in the middle of the diagonals. Both the finite element results as the experimental results are presented as force-strain diagrams.

Figure 8.6 shows those diagrams for the eight rod configurations obtained from the accompanying finite element models. It can be observed that the plots in the images are either red or green. The depicted cross-section in every image shows those colours as well and illustrates the number of each rod within the configuration. Since the strain gauges in the experiments were placed on only three out of six rods, those measured strains can either refer to the green combination of finite element strains or the red combination. The experimental results are depicted in Figure 8.7, where the unloading part of the tests is not depicted. Since those tests were performed up to a load of 40 or 48 kN, it was decided to only depict that range of the finite element strains in Figure 8.6.

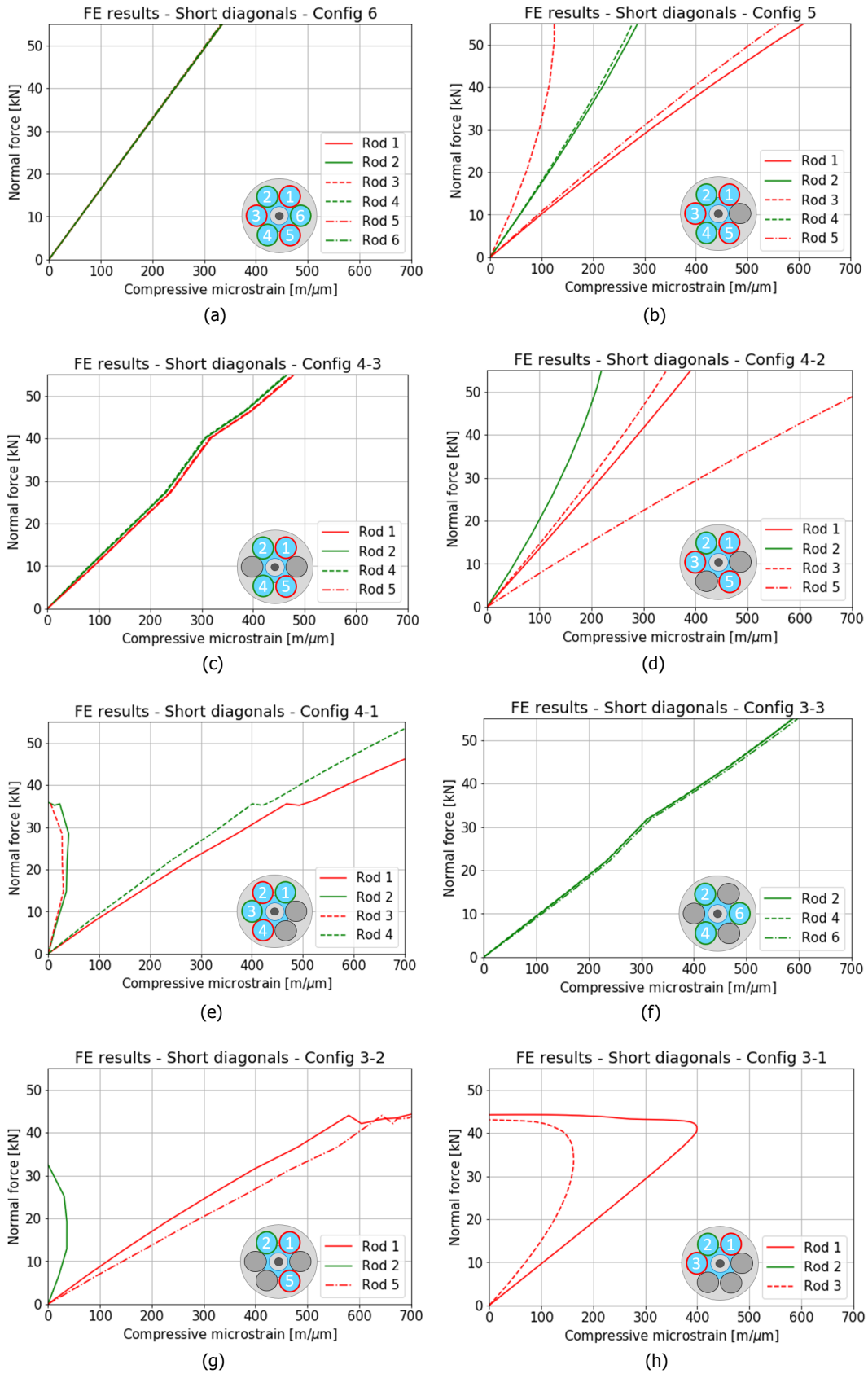

Figure 8.6: Compressive force-strain diagrams for the finite element models of all eight rod configurations in the range between 0 and ±60 kN.

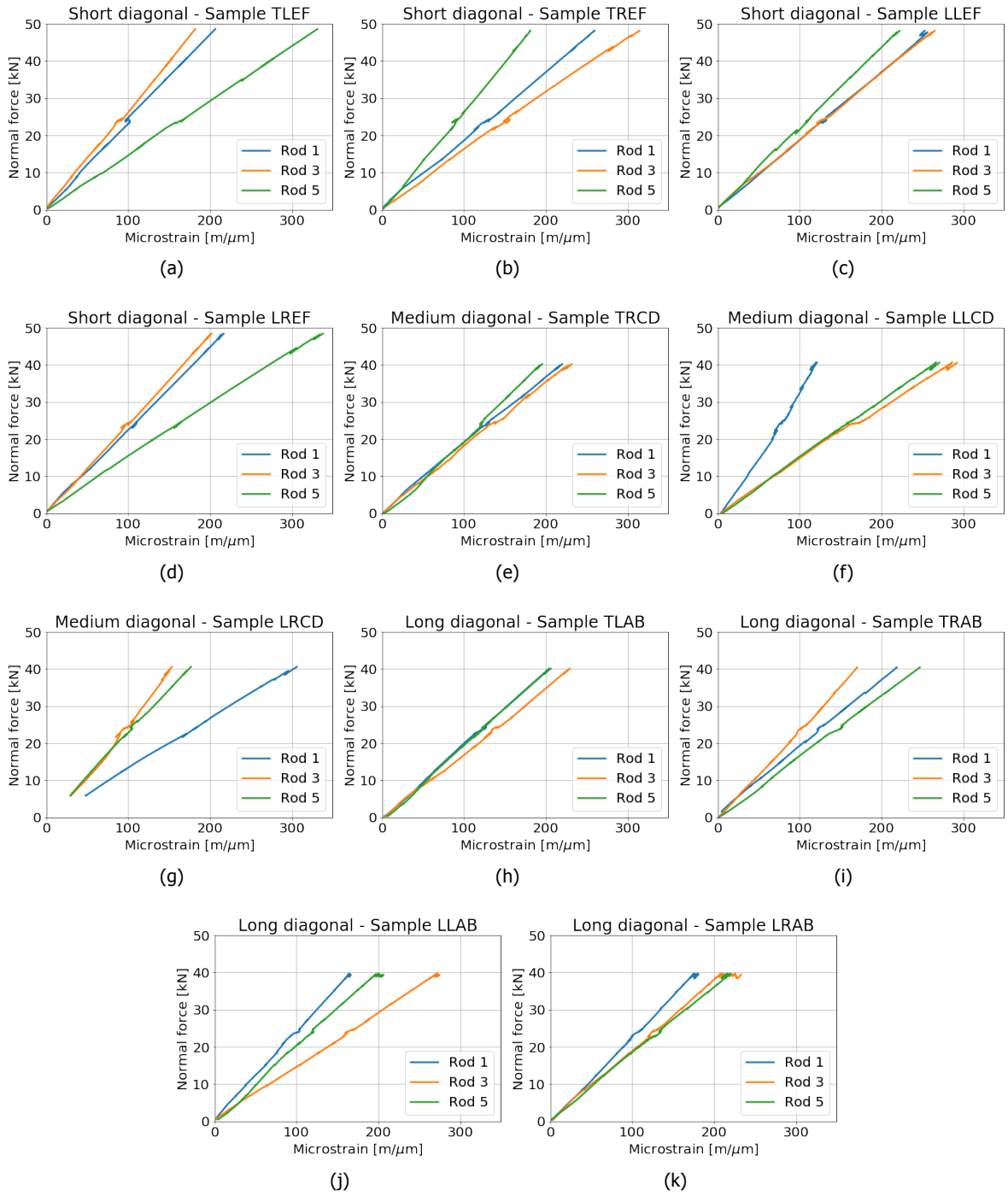

Figure 8.7: Compressive force-strain diagrams obtained from the compression test done on the Glass Truss Bridge diagonals. Unfortunately the results of one of the medium length diagonals was not usable.

Comparison between Finite Element Results and Experimental Results

First the comparison is made between the magnitude of the strains given in Figures 8.6 and 8.7. It can be observed that the strains originating from the finite element models are larger. This is partly due to the removed rods in most configurations of the finite element models, which causes the load to be spread over less cross-sectional area than it would in the real diagonals. However, even rod configuration 6, where all rods participate equally in carrying the load, shows larger strains than the experimentally obtained strains. This means that the glass shows stiffer behaviour in reality than in the models. In follow-up research it would be interesting to investigate the cause of this difference.

It could be that the addition of the adhesive to the columns causes it to behave stiffer than it would behave if the column would be composed of a solid glass rod.

By comparing the differences in slopes and divergences of the graphs shown in the figures, it might be possible to assign the real Glass Truss Bridge diagonals to rod configuration groups. This would be similar as the tactic performed for the Bend & Break columns. However, the lack of experimental data due to the attachment of only three strain gauges instead of six makes this difficult. Furthermore, the finite element rod configurations also lack strain results due to the removal of rods from the models. From the experimental results of the Bend & Break columns it was shown using Figure 6.15 of Chapter 6 that the missing strains of the finite element model of rod configuration 4, belonged to the rod that showed intermediate results compared to the other rods. This is, however, not verified for the other Bend & Break rod configurations. Furthermore, the differences in designs between the Bend & Break columns and the Glass Truss Bridge diagonals might result in completely different distributions.

As was already pointed out in Subsection 8.2.1, it is expected that the structural behaviour belonging to rod configurations 5, 4-3 and 4-2 are the ones that have the highest probability of occurrence in reality. The strain diagrams of rod configurations 4-1, 3-2 and 3-1, depicted in Figure 8.6(e), (g) and (h) respectively, show behaviour that is not observed in the experimental results of Figure 8.7. Some of the rods in those configurations namely show graphs that disappear in the left side of the graph, which refers to tensile strains in those rods. These tensile strains arise due to the bending behaviour caused by the eccentricity in those configurations. The non-occurrence of this behaviour in the experiments supports the theory that rod configurations 4-1, 3-2 and 3-1 will have a low probability of occurrence in reality. It is not possible to draw conclusions about the differences in occurrences of the symmetrical rod configurations (6, 4-3 and 3-3) due to their similarity in strain results.

It can be concluded from the divergence in graphs in Figure 8.7 that the strain/stress distribution over the rods within the Glass Truss Bridge diagonals is not perfect. However, some of the diagonals show graphs that have relatively equal slopes, namely Figures 8.7(c), (e), (h) and (k). The other images show larger deviations of which some have two graphs that remain close together above the third graph ((a), (d), (g) and (j)), and others that remain close together below the third graph ((b), (f) and (i)). That first group shows similarity to the red graphs of Figure 8.6(d) of rod configuration 4-2, while the second group shows affinity with the red graphs of Figure 8.6(b) of rod configuration 5. It would, however, be unwise to place the tested diagonals within those rod configuration groups based on these findings, since the finite element results that would give all of the three green plots is lacking. If those would be known, these might point to different conclusions.

8.2.3. Fracture Behaviour

This subsection shows the fracture behaviour obtained from the finite element model of rod configuration 5 of the short diagonals ($L2$). It is chosen to show the results of this rod configuration, since it shows ductile buckling behaviour, which is more interesting to observe than the sudden failure of the symmetrical configurations. Furthermore, it is expected that rod configuration 5 is one of the configurations that has a high probability of occurrence in reality. It is chosen to show the results of the short diagonals only, since the other lengths will give similar results.

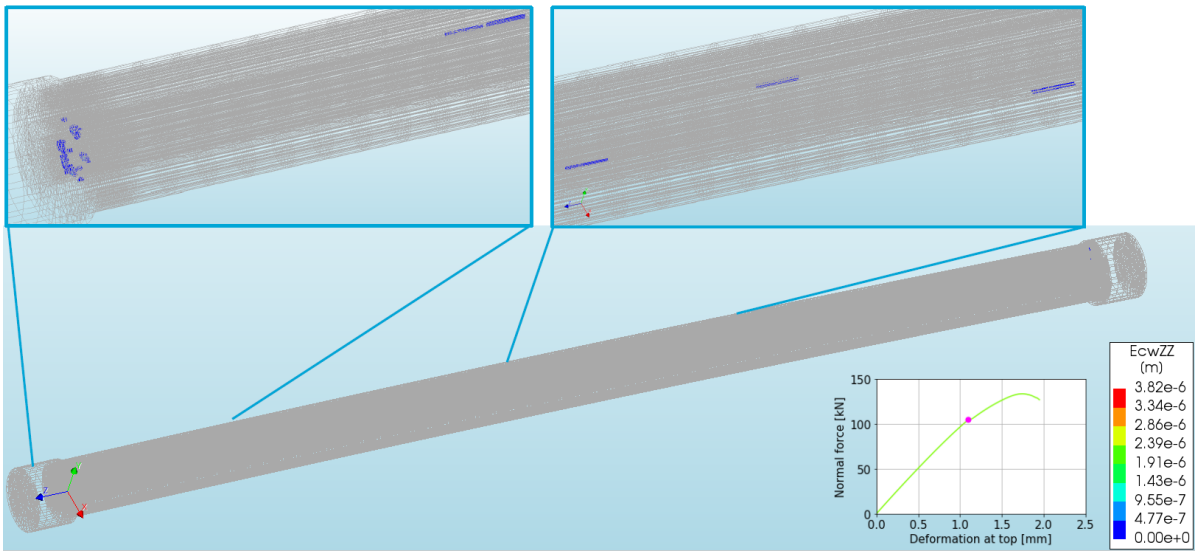

(a) First micro cracks in the middle of the column just after the buckling load is reached. Cracks only appear in the legs and the ends of the star-shaped profile.

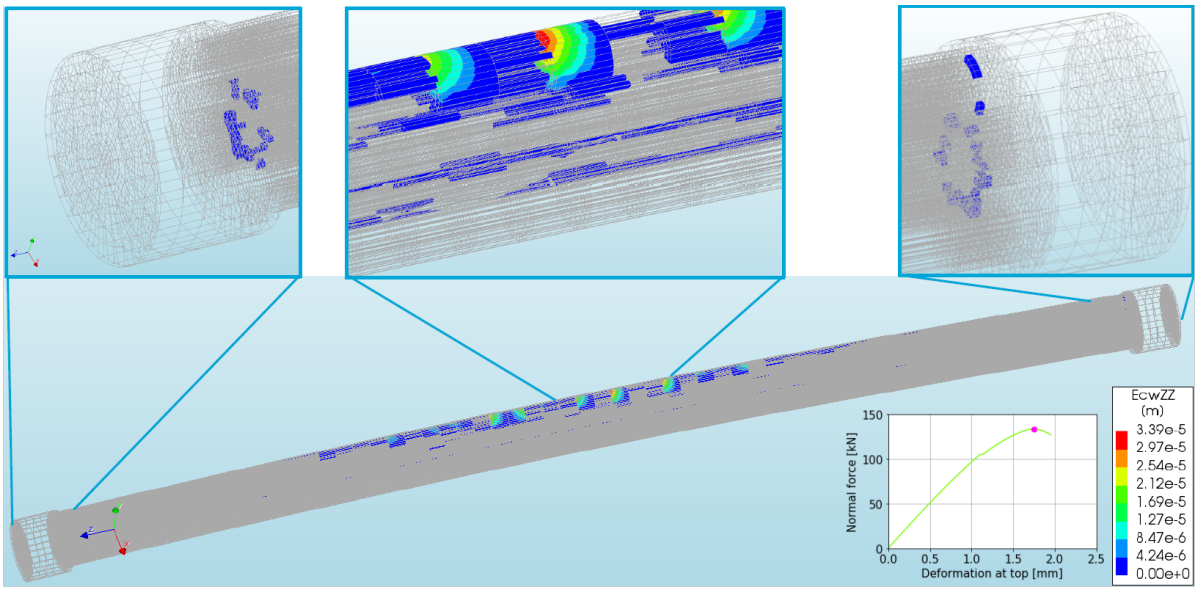

(b) Maximum capacity. The largest cracks are in the middle of the column in one of the circular rods. The star-shaped profile has micro cracks in the ends and in the legs of the star along the length of the profile.

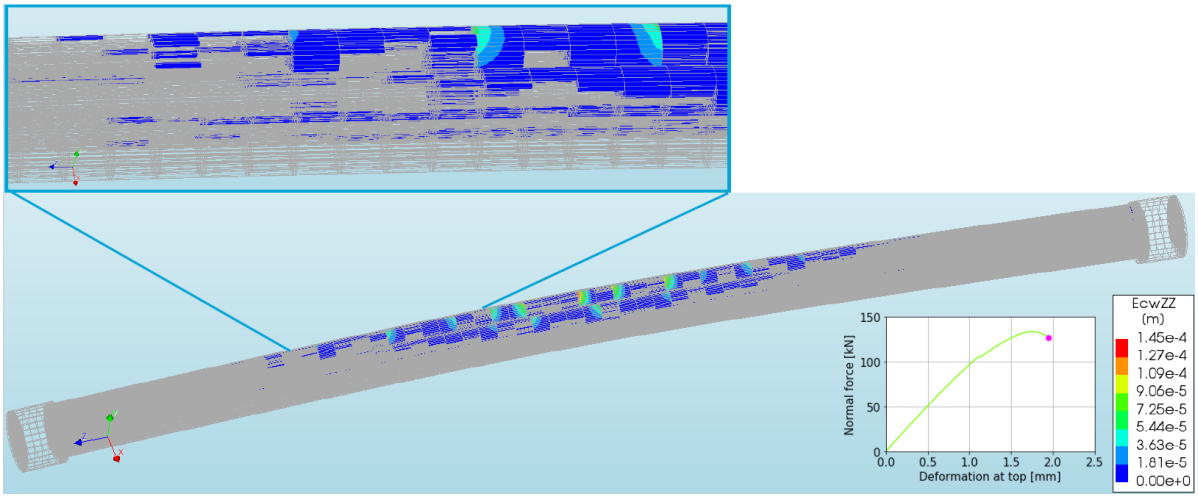

(c) Just before total failure. The largest cracks remain in the middle of the column in three of the circular rods. The cracks in the star-shaped profile remain small.

Figure 8.8: Contour plots showing crack widths for rod configuration 5 of length $L2 = 1235$ mm. (Deformation scaling factor = 1).

8.3. Conclusions

From the findings described in this chapter, it can be concluded that the experimental results that are currently available for the Glass Truss Bridge diagonals do not give enough information to draw full conclusions regarding the structural capacity of these diagonals. Using the experimentally obtained results of the initial bundled glass columns done in 2016, does, however, give an indication about the accuracy of the finite element models. Those experimental results lay well within the range of the finite element results and may, therefore, point to accurate finite element models. After complete validation of these finite element models when additional experiments (of which recommendations are given in Chapter 11) are conducted in the future, the following (for now **preliminary**) conclusions can be drawn.

- In reality the Glass Truss Bridge diagonals will show intermediate behaviour between the finite element rod configurations.
- The variance in structural behaviour between different diagonals is less with reference to the Bend & Break columns. The addition of the star-shaped profile and use of an adhesive enables the columns to behave as a solid glass bar. It, furthermore, causes the ability to transfer loads from one rod to another within the column. This will lead to a more equal stress distribution in comparison to the distribution over the separate glass rods in the Bend & Break columns.
- Rod configurations 5, 4-3 and 4-2 are expected to have the highest probability of occurrence. These refer to the following buckling and maximum loads:
  - Shortest diagonals:
    - Rod confguration 5: F_{buc} = 100 kN, F_{max} = 134 kN.
    - Rod confguration 4-3: F_{buc} = 123 kN, F_{max} = 123 kN.
    - Rod confguration 4-2: F_{buc} = 100 kN, F_{max} = 156 kN.
  - Longest diagonals:
    - Rod confguration 5: F_{buc} = 100 kN, F_{max} = 128 kN.
    - Rod confguration 4-3: F_{buc} = 121 kN, F_{max} = 121 kN.
    - Rod confguration 4-2: F_{buc} = 90 kN, F_{max} = 134 kN.
- The diagonals of medium length will show intermediate behaviour between the results of the shortest and longest diagonals.
- Longer columns/diagonals show a lower capacity, but more ductility after buckling point.

9

Comparison between Bundled Glass Column Designs

This chapter shows the differences in structural behaviour and capacity that are expected between the designs of the Bend & Break columns and the Glass Truss Bridge diagonals. Furthermore, reasons that cause these differences and the (dis)advantages for both designs are given.

9.1. Comparison of Results

To be able to make a legit comparison between the two designs, it is needed to compare them with the same lengths. Therefore, as mentioned in the previous chapter, finite element models of the Glass Truss Bridge diagonals with the same length as the Bend & Break columns are created. The load-displacement diagrams obtained from these models are shown in Figure 9.1. Table 9.1 shows the buckling and maximum loads.

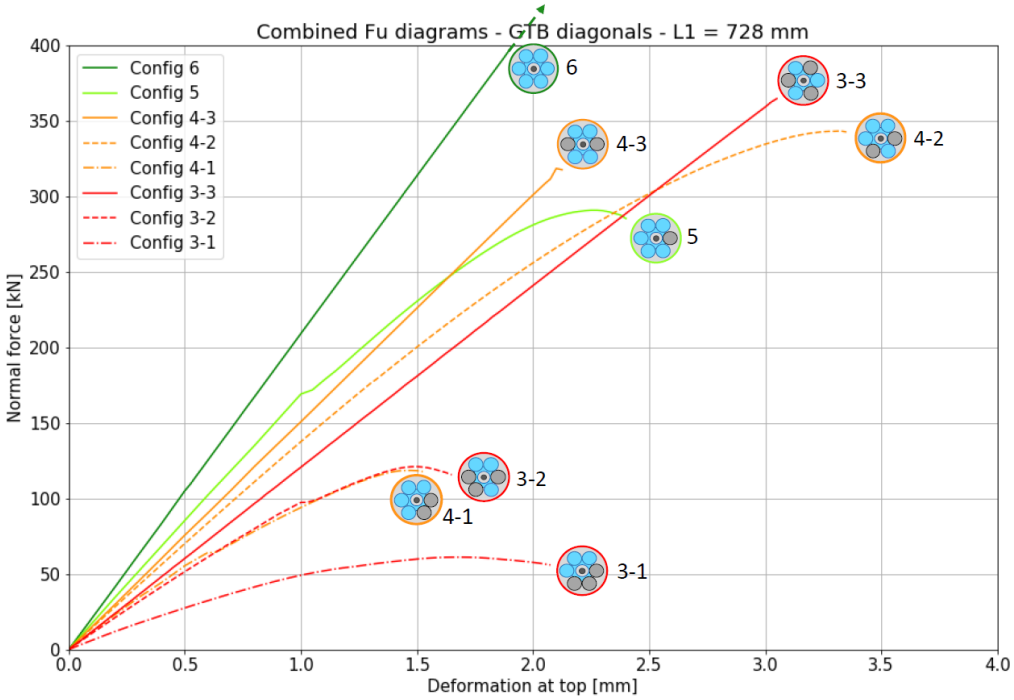

Figure 9.1: Load-displacement diagrams for the eight rod configurations belonging to the Glass Truss Bridge diagonals. These diagrams belong to a length of $L1 = 728$ mm. The dark green graph belonging to rod configuration 6 extends out of the graph to a load of 676 kN and remains linear elastic to the point of sudden failure.

Number	Configuration	# of rods participating	Buckling load [kN]	Maximum load [kN]	%
6		6 rods	676	676	453
5		5 rods	200	291	195
4-3		4 rods	319	319	214
4-2		4 rods	250	344	231
4-1		4 rods	100	118	80
3-3		3 rods	365	365	245
3-2		3 rods	100	121	81
3-1		3 rods	*	61	41

* Fails due to bending. No buckling load.

Table 9.1: Buckling loads and maximum loads of all the rod configurations for $L1 = 728$ mm. The buckling loads are defined as the loads at which the slope of the lines of Figure 9.1 start to decrease. The percentage shown in the right-most column refers to the maximum loads of all configurations with reference to rod configuration 5 of the *Bend & Break* columns (see Table 6.3).

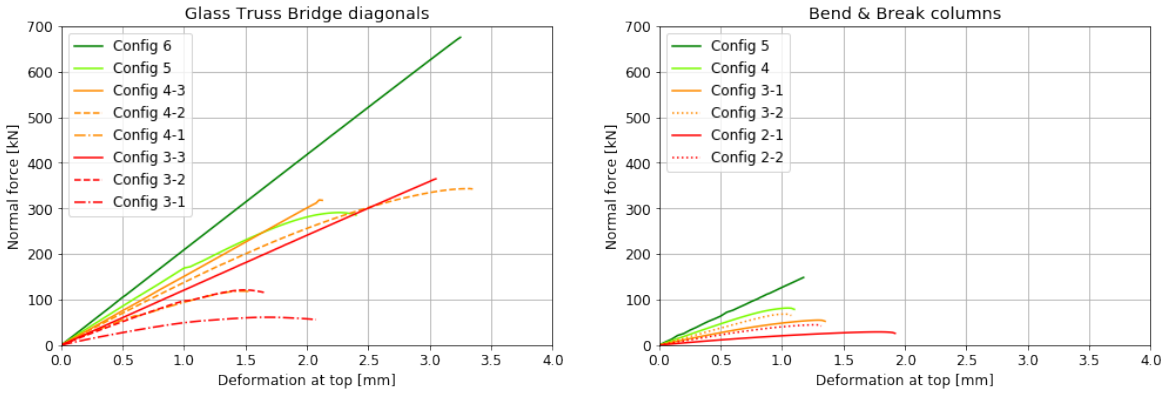

(a) (b)

Figure 9.2: Load-displacement diagrams for both designs with $L = L1 = 728$ mm obtained from the finite element models. The scales on the axes of both plots are the same.

The right-most column in Table 9.1 shows percentages. Here, 100% belongs to the maximum capacity of the 5 rods configuration of the Bend & Break columns, which is 149 kN. Since the loads given in this table belong to columns with the same length as the Bend & Break columns, these percentages give a good comparison between the structural capacity of the different bundled glass column designs. Figure 9.2 provides a good comparison as well by showing the load-displacement diagrams obtained from the finite element models with the same scales on the axes. It can be seen that the capacity of the Glass Truss Bridge diagonal design is approximately 4 times as large as the capacity of the Bend & Break column design. This can, among others, be explained by the larger cross-sectional area of the Glass Truss Bridge diagonals. Furthermore, the adhesive used in that design enables the glass rods to work together, while in the design of the Bend & Break columns the rods work individually. This means that one of the rods within the Glass Truss Bridge diagonals can be fractured before total failure of the column occurs. The adhesive allows the fractured glass to stay together; in that way the other rods will be able to bear the load and the fractured rod can still carry a small part. On the contrary, for the Bend & Break columns, in most cases the buckling/failure of one of the rods ignites a chain reaction of buckling/failure of the rest of the rods.

In the previous section it is stated that rod configurations 5, 4-3 and 4-2 are most probable to occur in reality for the Glass Truss Bridge diagonals. This would imply that it is most probable that the buckling load of this design, with a length of $L1 = 728$ mm, will be between 200 and 319 kN. This is ±4 times as large as the range in buckling loads of the Bend & Break columns, which lays between 55 and 60 kN for rod configurations 4 and 3-2.

9.2. Advantages and Disadvantages of the Designs

Bend & Break columns

+ Advantages:

- Slender, transparent and aesthetically attractive design.
- No use of adhesive, which enables the columns to be demountable and, therefore, to be more sustainable in comparison with the Glass Truss Bridge diagonal design.
- The POM discs show elastic behaviour during loading, which makes this material a good design choice to avoid peak stresses due to steel to glass contact.

- Disadvantages:

- The load bearing capacity of the columns is ±4 times lower than that of the Glass Truss Bridge diagonals.
- The unequal stress distribution causes large differences in structural behaviour and capacity between individual columns of this design.
- Twist occurs in the columns due to the lack of torsional rigidity in the design
- Only a limited amount of post-tensioning can be applied, since the turning of the nut to apply those stresses will cause a twist in the columns.
- The fabrication of the columns needs to be highly regulated, since differences in e.g. rod lengths or tilted steel endplates have large effects on the structural behaviour and capacity of the columns.
- The buckling/failure of one of the rods within the columns ignites in most cases a chain reaction in buckling/failure of the other rods.
- The explosive failure behaviour of the columns can be dangerous.

Glass Truss Bridge diagonals

+ Advantages:

- Slender, transparent and aesthetically attractive design.
- The load bearing capacity of the diagonals is ±4 times higher than that of the Bend & Break columns.
- The addition of the star-shaped profile and the adhesive:
  - provides torsional rigidity of the columns.
  - enables the column to stay intact after one of the rods fails, which provides ductility and safety.
  - enables the stresses to be transferred from one rod to the other, which enables a more equal stress distribution along the rods with reference to the Bend & Break columns.

- Disadvantages:

- The fabrication of the columns needs to be closely regulated, since differences in e.g. rod lengths, tilted steel endplates or insufficient use of adhesives have large effects on the structural behaviour and capacity of the columns.

- The need of application of the adhesive makes the production time relatively long in comparison with the Bend & Break columns.
- The use of adhesives disregards the increase in sustainability that the choice of using glass can provide, since demounting and recycling is no longer possible.

V

Conclusions and Recommendations

10

Conclusions

10.1. Finite Element Modelling of Structural Glass until Failure

In this study a new approach to model structural glass until failure using the finite element method is presented. This proposed way of finite element modelling does show a more realistic fracture pattern than when the tensile strength of the glass would be modelled in the conventional way. The latter referring to one conservative value of the tensile strength of glass for all elements instead of varying tensile strengths. Furthermore, the models are able to produce results for the stress at failure within the glass that lay in the range of experimentally obtained results. This all shows the potential that this method of finite element modelling of structural glass until failure can have for future calculations. However, at this point in time, insufficient studies are available regarding the choice of statistical (Weibull) distribution for the creation of these finite element models. This results in finite element results that only represent a part of experimentally obtained results. It is, however, very promising that the finite element results match the experimental results to this extend already without the prior knowledge.

Finite element models created according to this approach can help understand the fracture behaviour of the glass and may, therefore, be a good contribution to material sciences and for glass researchers. It is concluded in Chapter 6 that the influence to the structural behaviour of these varying tensile strengths is minor in comparison to the inequality in stress distribution over the rods within bundled glass columns. This finite element modelling method may, therefore, not seem of great importance to the engineering knowledge regarding these columns. On the other hand, it does contribute to material studies regarding the failure behaviour of glass in general.

10.2. Bend & Break Columns

The design of the Bend & Break columns, where five separate glass rods carry the load, causes the stresses to distribute unequally over these rods when the column is subjected to a axial compressive load. This is caused by, among others, small differences in lengths between the five rods or tilted steel endplates. This inequality in stress distribution influences the buckling load and maximum capacity of the columns severely. It is, furthermore, the cause of the large diversity in structural behaviour between all tested columns, which all had the same design.

To simulate this variance, finite element models were created where glass rods were removed in different configurations. These simplified models appeared to give a good estimation of what happens in reality. The experimental results showed intermediate results between four of the configurations, which were rod configurations 5, 4, 3-2 and 3-1. Here the first number refers to the amount of rods that participate in bearing the load. Most tested columns showed results that were closest to the simulated behaviour of rod configurations 4 and 3-2. By assigning the tested columns to rod configuration groups, Table 10.1 is created where the percentages show the probability of occurrence of each rod configuration.

Configuration	# of rods participating	Buckling load [kN]	Maximum load [kN]	Probability of occurence [%]
5 	5 rods	149	149	0
4 	4 rods	60	81	75
3-2 	3 rods	55	68	20
3-1 	3 rods	*	55	5
2-2 	2 rods	*	45	0
2-1 	2 rods	*	29	0

* Fails due to bending. No buckling load.

Table 10.1: Buckling loads and maximum loads of all Bend & Break rod configurations. The right-most column shows the probability of occurrence of each rod configuration based on the experimental results.

Besides the simplification regarding the rod configurations, another significant simplification in the finite element models was made by not including the POM discs in the models. The differences in calculated buckling and failure loads for models with and without POM appeared to be negligible. Since this simplification contributed significantly to the decrease in calculation time, increase in numerical stability and simplicity of the models, this was a good modelling decision.

The main failure mode of the Bend & Break columns is buckling, however, 5% of the tested columns show bending behaviour that causes failure. This bending is caused by eccentricity that occurs due to the configuration of rods that carry the majority of the load. The failure itself originates when tensile stresses occur in the glass rods due to lateral deformation in the middle of the rods, which is caused by either buckling or bending.

The varying tensile strengths over the glass rods created in the finite element models have less impact on the structural capacity of the columns than the unequal stress distribution over the rods. It is, therefore, not of great importance for this research that the choice of statistical distributions to create the finite element models was not perfect. This, however, means that the influence of the micro flaws on the glass rods is also in reality significantly less in comparison to the influence of the inequality in stress distribution over the rods.

10.3. Glass Truss Bridge Diagonals

In order to make estimations of the structural capacity of the diagonals that are currently present in the Glass Truss Bridge, finite element models were created. This was done in a similar fashion as the validated finite element models of the Bend & Break columns. The experimental results that are currently available for the Glass Truss Bridge diagonals do not give enough information to draw full conclusions regarding the structural capacity of these diagonals. Using the experimentally obtained results of the initial bundled glass columns done in 2016, does, however, give an indication about the accuracy of the finite element models. Those experimental results lay well within the range of the finite element results and may, therefore, point to accurate finite element models. However, the conclusions presented here are **preliminary**.

The results from the compression tests done on each of the diagonals shows that also for this design the stress distribution over the glass rods is not equal. This is again simulated by removing glass rods from the finite element models in different configurations. In reality the Glass Truss Bridge diagonals will show intermediate behaviour between these finite element rod configurations. It is expected that rod configurations 5, 4-3 and 4-2 have the highest probability of occurrence. These refer to the following

expected buckling and maximum loads for the longest and shortest diagonals in the Glass Truss Bridge:

- Shortest diagonals:
  - Rod confguration 5: F_{buc} = 100 kN, F_{max} = 134 kN.
  - Rod confguration 4-3: F_{buc} = 123 kN, F_{max} = 123 kN.
  - Rod confguration 4-2: F_{buc} = 100 kN, F_{max} = 156 kN.
- Longest diagonals:
  - Rod confguration 5: F_{buc} = 100 kN, F_{max} = 128 kN.
  - Rod confguration 4-3: F_{buc} = 121 kN, F_{max} = 121 kN.
  - Rod confguration 4-2: F_{buc} = 90 kN, F_{max} = 134 kN.

It is expected that the variance in structural behaviour for these diagonals is less with reference to the Bend & Break columns. The addition of the star-shaped profile and use of an adhesive enables the columns to behave as a solid glass bar. It, furthermore, causes the ability to transfer loads from one rod to another within the column. This will lead to a more equal stress distribution in comparison to the distribution over the separate glass rods in the Bend & Break columns.

The failure behaviour of the Glass Truss Bridge diagonals is similar to that of the Bend & Break columns; most diagonals will fail due to buckling, while a minority can fail due to bending caused by an eccentricity within the configuration of that column. These differences in behaviour can in reality be caused by, among others, differences in rod lengths, tilted steel endplates or insufficient use of adhesives along the rods.

10.4. Comparison Between Bundled Glass Column Designs

Both the Bend & Break column as the Glass Truss Bridge diagonal designs result in slender, transparent and aesthetically attractive columns. However, the design decision for the Glass Truss Bridge diagonal design to glue the rods together, results in differences in sustainability and structural behaviour. The use of adhesives disregards the increase in sustainability that the choice of using glass can provide, since demounting and recycling is no longer possible. This is, however, possible for the Bend & Break columns, which makes those more sustainable in comparison to the Glass Truss Bridge diagonals.

The Glass Truss Bridge diagonal design results in a ±4 times higher load bearing capacity than the Bend & Break column design due to, among others, a larger cross-sectional area and the possibility to transfer loads between glass rods within the columns. The latter is made possible by the use of the star-shaped profile and adhesive, which also provides torsional rigidity. These design choices, furthermore, lead to a safer failure mode, where one of the glass rods may fail, while the others remain intact to carry the load. This is not possible for the Bend & Break column design, since the failure of one rod generally causes a chain reaction in failure of the other rods.

11

Recommendations

11.1. Future research

Finite Element Modelling of Structural Glass until Failure

In order to get the best results using the presented method of finite element modelling of glass until failure, the appropriate statistical distributions to describe the failure stresses of glass need to be known. It is recommended to extend current research regarding this topic and to implement this future knowledge in the creation of finite element models of glass.

The presented finite element models all had values drawn from only one Weibull distribution per type of glass. Studies, like the one presented in Chapters 3 and 4 [8] on glass panels, show that it is more likely that experimentally obtained failure stresses in glass can be fitted to multiple Weibull distributions. Those experimental results generally fit to a fragment of a Weibull distribution above, below or in between certain percentile values. For future research regarding this method of finite element modelling, it would be interesting to perform finite element analyses of the glass panels as is done in Section 4.2, but with tensile strength values drawn from multiple distributions and the fragments of those distributions that belong to the experimental results. It is expected that these finite element results will lay in the full range of experimental results, instead of representing only a part of the experimental results which is the case with the current finite element models.

Glass Truss Bridge Diagonals

More experiments on bundled glass columns with the same design as the Glass Truss Bridge diagonals should be performed to validate the presented finite element models. Those experiments can be used to verify the theories that are opposed about the probability of occurrence of the eight rod configurations. It is recommended to perform similar tests as done in this project on the twenty Bend & Break columns; compression tests until failure on at least twenty columns. To perform these tests new columns will need to be created.

By performing more tests on the Glass Truss Bridge diagonals themselves it might be possible to assign the diagonals to certain rod configuration groups in order to predict their structural behaviour and capacity. It is recommended to start off by performing tests with strain gauges on all of the glass rods within the diagonals instead of only three. When the strains on all six rods within the Glass Truss Bridge diagonals are measured, it would be possible to make an estimation of the buckling and maximum loads of each diagonal within the bridge. This can be done by comparing the measured strains with the distribution of finite element strains given in Figure 8.6 of Chapter 8.

It is recommended to study the influence of the used adhesive on the stiffness of the diagonals. It is expected that the addition of the adhesive in the design makes the column behave stiffer in comparison to a design where one solid glass bar was used as column. It is not expected that a column of the same design of the Glass Truss Bridge diagonals behaves stiffer without the use of the adhesive, since than the rods can move with reference to each other.

11.2. Improvement of Bundled Glass Column Designs

The biggest disadvantage that the bundled glass columns have is the diversity in structural behaviour and capacity, which is caused by an unequal distribution of stresses over the glass rods within each column. By minimising the differences in rods lengths as much as possible, this problem could be decreased in severity. It is also recommended to place the glass rods within a column of the Bend & Break column design as close together as possible, while avoiding the glass rods to be in direct contact with one another. This will decrease the bad influence of tilted endplates on the stress distribution over the rods. What can, furthermore, influence the stress distribution, is the use of relatively soft materials in the supports like the POM discs. These POM discs appear to be a relatively good design choice in comparison with soft lead or aluminium that was used in other bundled glass column designs.

It is shown that gluing the glass rods together and adding a star-shaped rod significantly contributes to the overall structural capacity of the bundled glass columns. It makes the columns approximately 4 times stronger. The use of an adhesive, however, creates disadvantages regarding the sustainability of the columns in comparison to a design without adhesives. The amount of disadvantages that the current design without glue (the Bend & Break columns) gives, points out that this bundled glass column design might not be the best design choice. It is recommended to try a design including the star-shaped profile in the middle, with the circular shaped rods adjacent to this profile. It is expected that this will increase the torsional rigidity and, therefore, the overall stiffness of the columns. This will result in the same cross-section as the Glass Truss Bridge diagonals, only with the difference that no adhesive is used. By using for example 3D printed steel, it is possible to create steel endplates that perfectly fit the cross-sections of the glass rods to keep them in place. This is just a preliminary design idea, it would be best if an experienced engineer would create a design that can ensure an equal stress distribution. An idea is to, for example, find a way to regulate post-tensioning per rod instead of over the entire column.

11.3. Engineering with Bundled Glass Columns

The influence of the production process to the quality of bundled glass columns is large and should, therefore, always be well observed and regulated. Irregular lengths of the rods within the columns, the amount of adhesive used between a circular rod and the star-shaped profile or tilted endplates can cause a column to unexpectedly behave as one of the rod configurations with a relatively low capacity.

It is recommended, when designing with columns like the Bend & Break columns, to design with lengths equal or smaller than the length of the tested Bend & Break columns. Those columns consisted of glass rods of 728 mm. For this lengths the capacity is now known; smaller columns will have a higher capacity. Engineering with longer columns, however, will give insecurities regarding the capacity and, therefore, the safety of the design. A longer length will not only mean a lower buckling load, but also less torsional rigidity.

It is important to design with the bundled glass columns in such a way that the load that is carried by the columns is lower than the buckling load. It is recommended to design with safety factors as given in guidelines provided by international codes, such as the Eurocode. For the Bend & Break columns it is recommended to use a buckling load of 50 kN for columns with the same length or shorter than 728 mm. The following recommendations regarding the buckling loads of columns with the Glass Truss Bridge diagonal design are not completely validated. It is recommended to perform tests to ensure their capacity. For the Glass Truss Bridge diagonals with a length of 1392 mm or shorter it is recommended to work with a buckling load of 80 kN. For columns with the design of the Glass Truss Bridge diagonals with a length of 728 mm or shorter, it is recommended to use a buckling load of 180 kN. Safety factors are not yet included in these recommended buckling loads. These loads are chosen by taking 90% of the critical (mainly buckling) load of the rod configuration that shows the lowest capacity that has a probability of occurrence higher than 0%. This all is summarised in Table 11.1.

Design	Length range [mm]	Critical rod configuration	F_{buc} [kN]	$0.9 * F_{buc}$ [kN]
Bend & Break	$\leq$ 728	3-1	55	50
Glass Truss Bridge	728 - 1392	4-2	90	80
Glass Truss Bridge	$\leq$ 728	5	200	180

Table 11.1: The right-most column contains the recommended buckling loads to use for calculations for engineering purposes for certain lengths of the discussed bundled glass column designs. These are excluding any safety factors given in design codes.

For designing with columns with other lengths than given in Table 11.1, it is recommended to perform additional tests and make new finite element models. The finite element modelling method elaborated in this thesis is not necessary to get to know the buckling loads of the columns. A conventional way of finite element modelling can be used. However, it is recommended to use the same values for the Young's modulus and the Poisson's ratio for the borosilicate glass rods as presented in this document. When it is needed to model the behaviour of the columns until failure, it is recommended to use the same method of finite element modelling as elaborated in Chapter 4.

To ensure the safety of new bundled glass column designs, it is recommended to perform tests on the columns that are to be used in the real structure. When supplying all glass rods within the columns with strain gauges in a similar way as done in the tests elaborated in Chapter 5, it will be able to assign a column to a rod configuration group by examining the divergence in strain results per rod. By comparing those to strain results from finite element models as the ones depicted in Figure 6.9 of Chapter 6 these assignments can be made, which will lead to information regarding the structural behaviour and capacity of that specific column. The divergence in strain results can already be observed in an early load stage. It is, therefore, recommended to load the column to ±5 % of the calculated maximum load that the column will be subjected to. This can be done using a compression testing machine in a laboratory. By keeping the applied load low, the chances are small that micro cracks will occur during those tests that will decrease the capacity of the column.

11.4. Dynamic Properties of the Glass Truss Bridge

Recommendations regarding research on the dynamic properties of the Glass Truss Bridge are given in Appendix C. These recommendations are based on preliminary studies that are performed during this graduation project, which are elaborated in that appendix as well.

Bibliography

[1] A. Snijder, R. Nijsse, and C. Louter, *The glass truss bridge,* in *Structural Glass*, Vol. 63 (HERON, 2018) pp. 139 – 157.

[2] R. Lehman, *The mechanical properties of glass,* http://glassproperties.com/references/MechPropHandouts.pdf (2017).

[3] MaterialDistrict, *World's first bridge with glass columns strong enough to hold student party,* https://materialdistrict.com/article/worlds-first-bridge-glass-columns/ (2017).

[4] F. Oikonomopoulou, E. A. M. van den Broek, T. Bristogianni, F. A. Veer, and R. Nijsse, *Design and experimental testing of the bundled glass column,* (2017).

[5] A. Bagger, *Glass columns at danfoss 2005,* http://www.annebagger.dk/en/projects/glass-columns-at-danfoss.aspx.

[6] *SCHOTT - CONTURAX® Technical Data,* (2017).

[7] DELO Industrial Adhesives, *DELO Technical Information, DELO® PHOTOBOND® 4468,* (2019), revision 50.

[8] F. Veer and Y. M. Rodichev, *The structural strength of glass: hidden damage,* Strength of Materials, Vol. 43 (2011).

[9] A. Snijder, *Proofloading glass diagonals 13-03-2017,* (2017).

[10] M. Aurik, *Structural Aspects of an Arched Glass Masonry Bridge*, Master's thesis, Delft University of Technology (2017).

[11] O. van der Velde, *Finding the strength of glass - A mechanical and fractographic research of glass' biaxial strength for structural purposes*, Master's thesis, Delft University of Technology (2015).

[12] E. Salamin, *The weibull distribution in the strength of glass,* (2006), lecture - University of Arizona - College of Optical Sciences.

[13] E. Moayedi and L. Wondraczek, *Quantitative analysis of stratch-induced microabrasion on silica glass,* Elsevier - Journal of Non-Crystalline Solids (2017).

[14] R. Jiang and D. Murthy, *A study of Weibull shape parameter: Properties and significance* (Reliability Engineering & System Safety, 2011).

[15] SAINT-GOBAIN, *Glass properties,* https://www.saint-gobain-sekurit.com/glossary/glass-properties.

[16] G. D. Quinn, *Fractography of Ceramics and Glasses* (National Institute of Standards and Technology, 2016).

[17] DIANA Finite Element Analysis, *Diana fea,* dianafea.com.

[18] *Ridderflex POM Delrin datasheet,* https://www.ridderflex.nl/producten/pom-delrin/.

[19] B. Danks, *Validation of Sequentially Linear Analysis*, Master's thesis, Delft University of Technology (2019).

[20] Nationale Staalprijs 2018, *Glass truss bridge delft,* https://www.nationalestaalprijs.nl/deelnemende-projecten/detail/duurzaamheidsprijs/glass-truss-bridge.

[21] C. Bedon, *Diagnostic analysis and dynamic identification of a glass suspension footbridge via on-site vibration experiments and fe numerical modelling,* Elsevier - Composite Structures (2019).

[22] Detail Inspiration, *Glass bridge in the basilica of aquileia,* https://inspiration.detail.de/glass-bridge-in-the-basilica-of-aquileia-107122.html?lang=en.

[23] S. Chen, M. Zang, D. Wang, Z. Zheng, and C. Zhao, *Finite element modelling of impact damage in polyvinyl butyral laminated glass,* Elsevier - Composite Structures (2015).

[24] M. Timmel, S. Kolling, P. Osterrieder, and P. D. Bois, *A finite element model for impact simulation with laminated glass,* Elsevier - Composite Structures (2006).

[25] *NEN-EN 1991-2+C1: Actions on structures - Part 2: Traffic loads on bridges,* (2015).

[26] J. M. W. Brownjohn, S. Zivanovic, and A. Pavic, *Crowd dynamic loading on footbridges,* Footbridge 2008 - Third International Conference (2008).

VI

Appendices

A

Glass Truss Bridge

Figure A.1: The bundled glass diagonals in the Glass Truss Bridge [20].

In May 2017 a glass truss bridge was realised at the campus of Delft University of Technology, the Netherlands. The bridge is located at the 'Green Village' of the university, which is a place for students and professors to realise sustainable and innovative ideas and designs. Unique about this bridge is the fact that the diagonals of the trusses are composed of bundled glass. The glass diagonals of the bridge are shown in Figure A.1.

A.1. The Glass Truss Bridge

The bridge is designed as a footbridge with a span of 14 m. The depth of the truss is 1.2 m, which was chosen to have a 1 to 10-15 ratio with the span. The structure of the bridge is a composite steel-glass truss structure. The upper chord consists of an HEA120 steel profile, which causes resistance against secondary bending between the truss nodes and against out of plane buckling. The lower cord is designed as a steel strip, since this cord only has to withstand tension forces. As mentioned previously, most of the diagonals are made of glass. More information about the design of these bundled glass diagonals are given in Chapter 2. The out-most diagonals are, however, made of steel square hollow sections. The reason for this is that, in the unlikely event of an out-most glass diagonal failure, the shear next to the support will cause very large deformations. The steel diagonals will ensure extra rigidity [1].

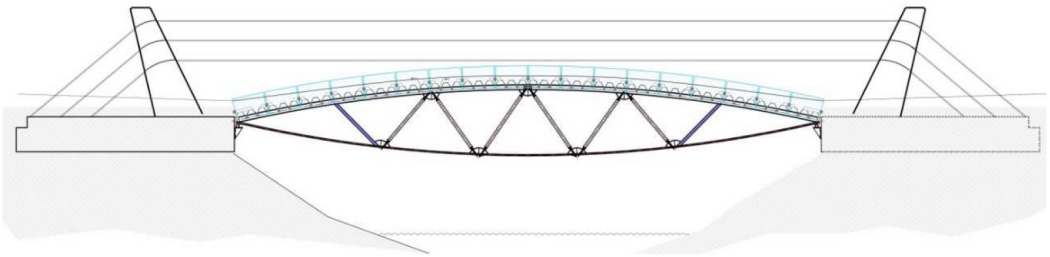

Figure A.2: Side view of the Glass Truss Bridge [1].

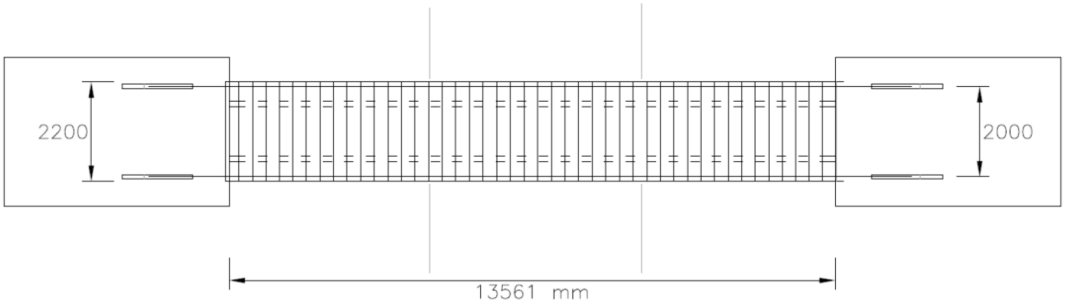

Figure A.3: Top view of the Glass Truss Bridge [1].

The glass diagonals are post-tensioned in order to ensure a compression force in the glass at all times, since tension is an unfavourable load condition for glass. The post-tensioning could be realised by placing a 12 mm chrome coated, steel rod in the centre of each bundled glass diagonal. A post-tensioning force on these steel rods was applied; the well designed steel to glass connections enabled these forces to transfer through the glass. The steel rods and the post-tensioning were necessary, since in a truss structure some diagonals will be in tension, while others are in compression. Whether a certain diagonal is in tension or compression can change in time when different load cases are present on the bridge. Therefore, every diagonal must be able to resist tension and compression. Glass is very strong in compression, but behaves poorly in tension. The steel rods can transfer the tension forces in the diagonals without the need to transfer these tension forces through the glass. The applied post-tensioning force is as much as the maximum tension force in a diagonal that was calculated in the design stage of the bridge [1].

The truss nodes were a challenging part of the design. One challenge was already discussed in the previous paragraph. The problem that the diagonals could be either in compression or tension, while glass behaves poorly in tension. Furthermore, it was a starting point that the diagonals should not meet in an eccentric way to avoid unnecessary bending moments in the upper/lower chords. Another starting point in the design of the nodes was that they should be as transparent as possible. This could be accomplished by using glass as the main material [1]. The design of the truss nodes are elaborated in the following section.

The glass diagonals used in the bridge were tested in 2017 in the Stevin II laboratory of Delft University of Technology, see Section 2.2.2 of Chapter 2. Furthermore, the current bridge design was tested to ensure the safety of its unique design. Some information about these tests is given in Appendix C.

A.2. Detailing of the Bridge

In this section the design of the glass nodes in the bridge are shown. Details of the diagonals themselves are given in Chapter 2.

A.2.1. Nodes

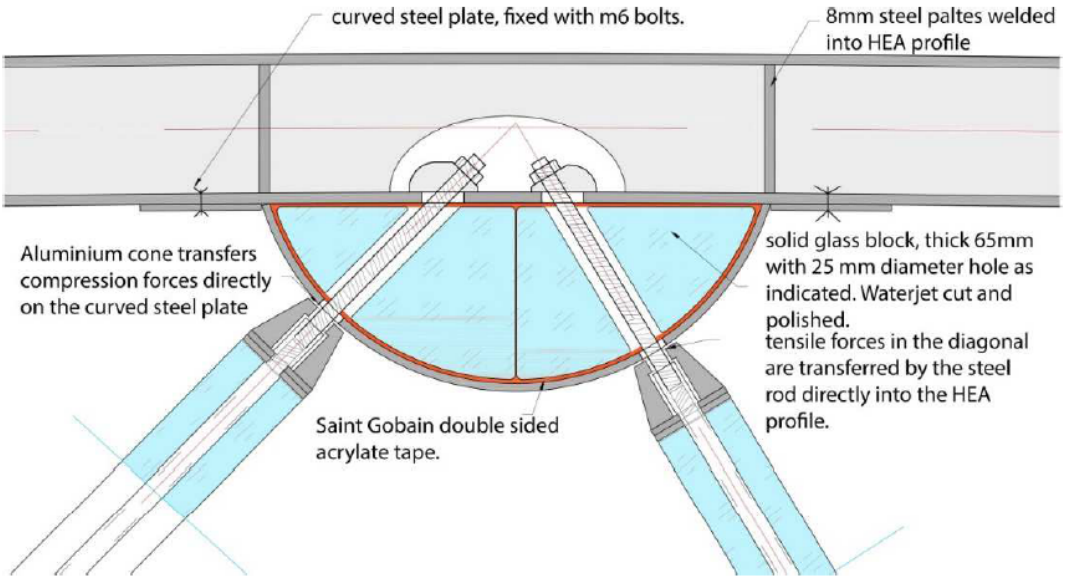

Figure A.4: Detail of the glass truss node [1].

Figure A.4 shows the design solutions for the three starting points for the design of the nodes mentioned earlier in this chapter. To ensure the transparency of the node, a large part of it is made of waterjet cut glass blocks. These blocks are of high quality glass, since they were left-over from the Crystal Houses project in Amsterdam. The above figure shows how the post-tensioned steel rods are connected to the upper chord without touching any of the glass. This is done by cutting holes in the glass blocks where the extension nuts pass through. Furthermore, the figure shows that the diagonals are connected in a non-eccentric way [1].

A truncated cone shaped aluminium head is placed at the ends of the diagonals to ensure free rotation of the diagonals. A truss structure is always designed with hinged nodes to make sure that there are no bending moments in the diagonals. The buckling length of the diagonals is, therefore, equal to its own length [1].

A 6 mm steel strip is placed around the glass blocks bonded with double sided acrylate tape. These will spread the compression forces in the diagonals over the glass blocks in the nodes [1].

Figure A.5: A glass node in the bridge [1].

B

Examples of Structural Glass Finite Element Modelling

This appendix shows other designs with structural glass and the ways the designers have made calculations for their designs. The cases in which the finite element method is used to model structural glass are high-lighted. This is interesting, since every glass manufacturer produces a different kind of glass with different properties. In Table B.1 the material properties of the glass used to make the structural bundled glass columns tested during this thesis process according to the glass producer SCHOTT are given. The material properties used in the calculations of the examples given further on in this appendix are given as well. Differences between values are due to the fact that the glass used in the structural bundled glass columns is borosilicate glass, while the glass used in the examples is soda-lime glass. Borosilicate glass is known for its high resistance against heat and chemicals. In comparison with soda-lime glass it has lower Young's modulus, mass density and generally also a lower failure strength. The latter also highly depends on the manufacturing process of the glass, which influences the quality and, therefore, the occurrence and significance of flaws.

	Unit	**Value**
Young's modulus	GPa	63
Poisson's ratio	-	0.2
Mass density	kg/m^3	2230
Thermal expansion coefficient	10^{-6} K^{-1}	3.3

Table B.1: Material properties of the borosilicate glass used in the Bend & Break columns and the Glass Truss Bridge diagonals according to the glass producer SCHOTT [6].

In order to model the failure behaviour of the glass using the finite element method, the material properties assigned to the glass should enable brittle failure. This means that the glass should be given a particular ultimate tensile strength. As can be seen in Table 2.1 SCHOTT does not give an ultimate tensile strength of the glass used in the bundled glass columns. Most examples found in literature did not model the glass until failure. However, the latter two examples in this chapter do show the fracturing of glass and, therefore, an ultimate tensile strength of the glass is assigned in those models.

B.1. Diagnostic analysis and dynamic identification of a glass suspension footbridge via on-site vibration experiments and FE numerical modelling

[21]

This case study done by C. Bedon has some resemblance with the Glass Truss Bridge, since it involves a footbridge made of structural glass. This glass footbridge, realised in 2004, was investigated on its dynamic properties using tests and finite element modelling. The footbridge is located in a church in Italy (Basilica of Aquileia) and is shown in Figure B.1. C. Bedon has done on-site vibration experiments which are presented based on Operational Modal Analysis (OMA). This is done to estimate the fundamental dynamic parameters and asses the actual structural performance of the footbridge. Using parametric finite element numerical studies, further advantages for the dynamic characterisation of the footbridge are derived. These finite element analyses are performed on selected structural modules of the structure to explore its sensitivity to geometrical/mechanical key influencing parameters.

Figure B.1: Glass Bridge in the Basilica of Aquileia [22].

Calculations were performed using the finite element method. In this case study the glass panel was modelled using 2D shell elements with a thickness of 6 mm. Furthermore the material properties of the glass were chosen to be the following:

	Unit	Value
Young's modulus	GPa	70
Poisson's ratio	-	0.23
Mass density	kg/m^3	2500

Table B.2: Material properties of glass used in the FEM calculations [21].

As can be seen, no ultimate stress or strain is assigned to the glass. Therefore, the glass in this finite element model will not crack.

B.2. Structural Aspects of an Arched Glass Masonry Bridge
[10]

In this graduation thesis for Delft University of Technology a study is done about the structural aspects of an arched glass masonry bridge, see Figure B.2. The glass bricks were fabricated by casting the glass, later on the glass bricks were glued together in order to form an arch.

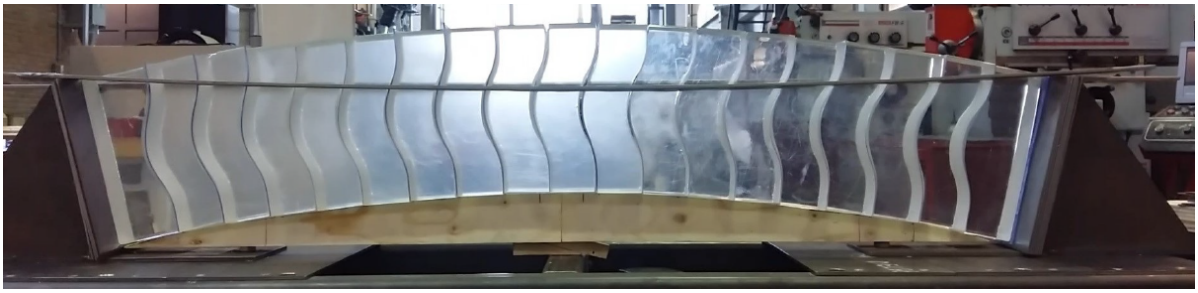

Figure B.2: Arched glass masonry [10].

Here M. Aurik made a finite element model of this glass structure. The properties used in his model are shown in Table B.3. The glass bricks are modelled by 2D plane stress elements, the behaviour of the adhesive is modelled using interface elements.

Glass	**Unit**	**Value**
Young's modulus	GPa	70
Poisson's ratio	-	0.2
Thermal expansion coefficient	10^{-6} K^{-1}	9.0
Mass density	kg/m^3	2500
Interface (adhesive)	**Unit**	**Value**
Normal stiffness modulus	kN/m^3	$7{\cdot}10^{11}$
Shear stiffness modulus	kN/m^3	$7{\cdot}10^{11}$
Tensile strength	kN/m^2	10^{-8}
Interface non-linearities		Discrete cracking
Mode-I Model		Brittle
Mode-II Model		Brittle

Table B.3: Material properties used in the FEM calculations by M. Aurik [10].

It can be seen that the author of this thesis assumes that the glue in the arch bridge will fail before the glass does. Therefore, it was chosen in this example to assume infinite linear elastic properties for the glass elements. Again, the glass in this finite element model will not crack.

B.3. Finite element modelling of impact damage in polyvinyl butyral laminated glass

[23]

This case study done by S. Chen et al. refers, as well as the next case study, to impact loads on laminated glass and how to model it. In both cases finite element models are made for PVB (polyvinyl butyral) laminated glass, which is commonly used in automotive and architectural industries. Unlike the examples given earlier on in this chapter, in these examples the glass itself is loaded until failure and will break accordingly. In this case study a beam of laminated glass is modelled which is subjected to a 3-point bending test. An example of the crack propagation as well as the horizontal stresses in the beam are shown Figure B.3. Here three layers can be distinguished; the top and bottom beams represent the glass, while the middle layer is the PVB. Furthermore, the material properties for glass used in the finite element model are given in Table B.4. Brick finite elements were used with an element size of 1 mm^3. These elements were preferable over tetrahedral elements due to various reasons among which the higher accuracy of the brick elements. The results of these calculations are compared with test results. It is found that the crack pattern, locations and propagation sequence of the cracks are in good agreement with the experiments. Little information is given about the calculated and measured strength capacity of the beams.

	Unit	Value
Young's modulus	GPa	74
Poisson's ratio	-	0.2
Mass density	kg/m^3	2500
Tensile strength	MPa	80

Table B.4: Material properties of glass used in the FEM calculations [23].

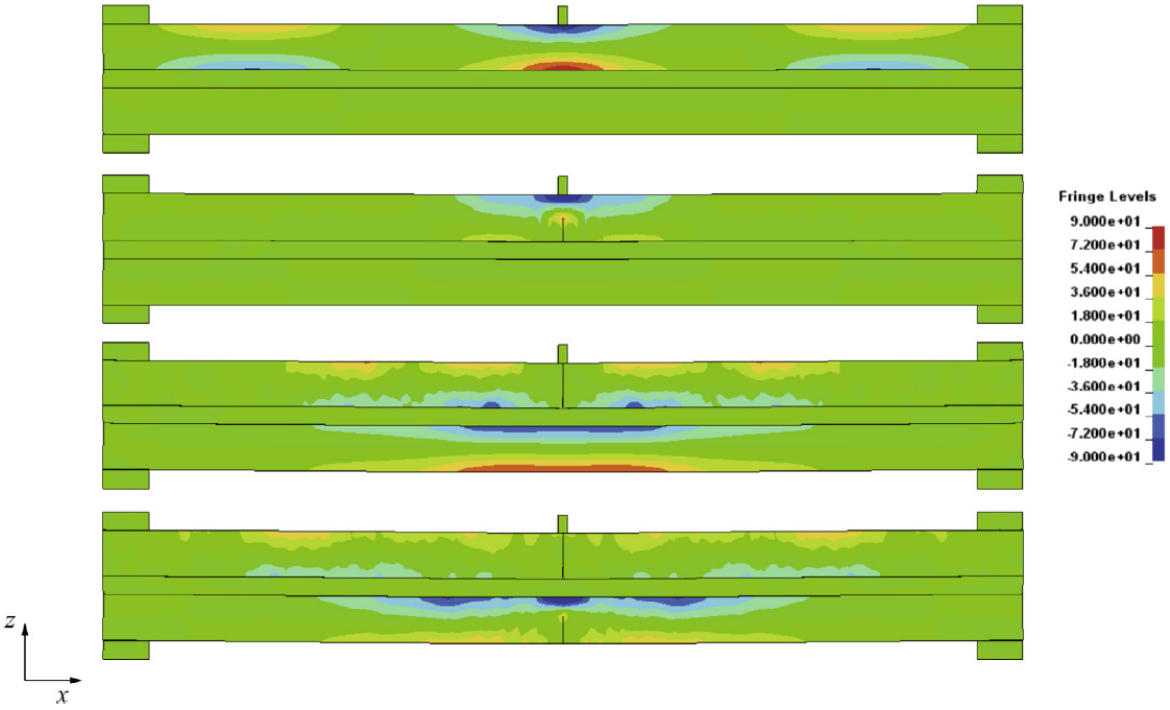

Figure B.3: The impact crack process of the laminated glass beam with stress fringes of σ_{xx}. The pictures from the top to the bottom are captured at t = 55 μs, 65 μs, 200 μs and 234 μs [23].

B.4. A finite element model for impact simulation with laminated glass [24]

This case study by M. Timmel et al. shows similarities to the previous case study, an impact load of a sphere that hits a car window is modelled. The cracking pattern of the glass that was found in the finite element model made for this case study is depicted in Figure B.4. Furthermore, the material properties used in the model to simulate the glass are given in Table B.5. In the paper the tensile strength was given as a strain, but by assuming that the glass behaves linear elastically before it breaks in a brittle way, the ultimate tensile stress could be calculated as shown in Table B.5. In the paper the tensile strength given in the table was used for static loading of the glass. For dynamic loading (the impact load) a lower tensile strength of 70 MPa was taken. Furthermore, shell finite elements with brittle failure behaviour while using a smeared cracking model were used.

	Unit	Value
Young's modulus	GPa	70
Poisson's ratio	-	0.23
Tensile strength	MPa	$E * \varepsilon = 70000 \cdot 0.0015 = 105$

Table B.5: Material properties of glass used in the FEM calculations [24].

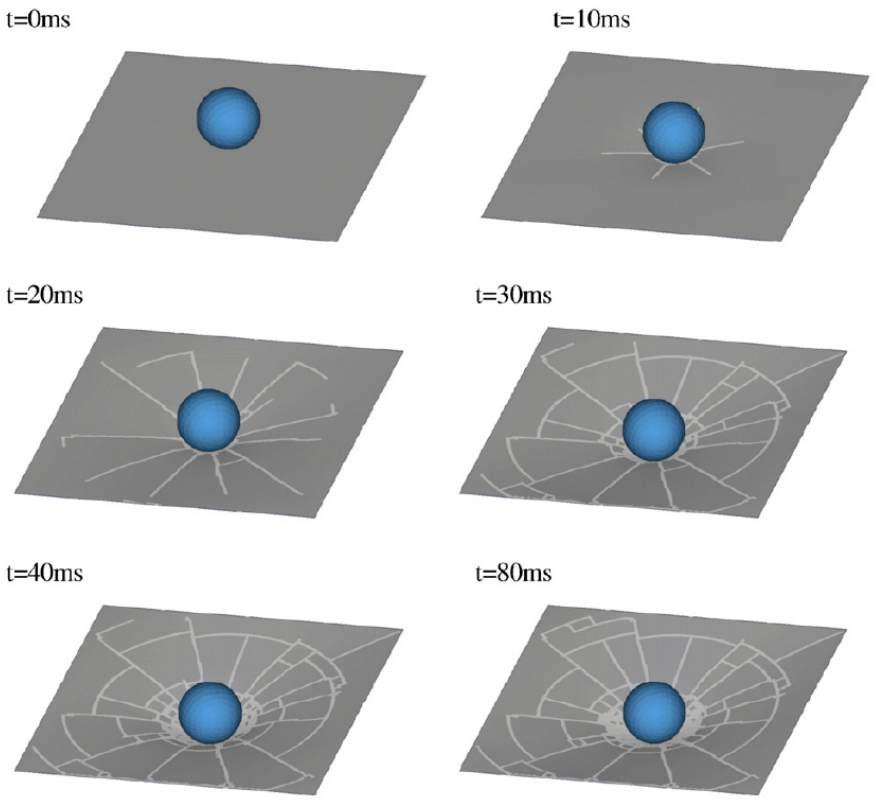

Figure B.4: Temporal evolution of cracks in case of impact load using irregular meshing [24].

B.5. Conclusions

By taking a look into the different ways engineers have tried to model structural glass, it can be seen that there are no particular values set for the material properties of glass. The material properties of a particular piece of glass depends on its chemical consistency, but also on the way it is manufactured. Especially in the tensile strength inconsistent values can be seen.

The tensile strength of glass is difficult to determine. This not only differs per glass type or geometry, but even per window/rod. Calculation guidelines set this value to be around 20 MPa, which is a low (and therefore a safe) value to use. In reality this value can be much higher. More information about the varying tensile strength of glass is given in Chapter 3.

The Poisson's ratio and the mass density of the glass are more consistent and also easier to measure. During this studies the Young's modulus of a glass rod from glass manufacturer SCHOTT was validated using ultrasonic pulse velocity testing. When the geometry and density of a certain material is known, the Young's modulus can be determined by measuring the travelling speed of sound through that material. Using this method the Young's modulus given by SCHOTT was validated and indeed appeared to be around 63 GPa. Therefore, it can be assumed that the material properties given by the glass manufacturer SCHOTT given in Table B.1 can be used in further calculations.

Figure B.5: Determining the Young's modulus of a glass rod using ultrasonic pulse velocity testing.

The last two examples given in this appendix (Sections B.3 and B.4) do show ways to model the fracture behaviour of glass. The downside of these models is that the origin of the crack is known, since the position of the (impact) load is prescribed. Furthermore, in the tests elaborated in Section 3.1.2 of Chapter 3, a scratch was made into the glass so the origin of the fracture could be (partly) regulated as well. In reality the origin of failure of the glass will not be known beforehand. The glass can even start to fail simultaneously at multiple points within the same structural glass element. Therefore, in this studies a new way of modelling the failure behaviour of structural glass is proposed.

C

Dynamic Properties of Glass Truss Bridge

At first, the objective of this studies was to investigate the dynamic behaviour of the Glass Truss Bridge. In order to do proper static and dynamic analyses of the bridge, it is, however, needed to know how the newly designed bundled glass diagonals of the bridge behave structurally. Some tests were performed on the bridge and the diagonals separately, but proper analyses of these tests were lacking. Furthermore, no legitimate calculations have been made in order to predict the behaviour of the glass diagonals. Calculations were made to make a safe design for the bridge, but these appeared to be too conservative. The fact that dynamic analyses are not yet made for the Glass Truss Bridge is due to the fact that static load cases are generally governing. Only for very slender footbridges the dynamic loads might dominate, but this does not mean that the dynamic behaviour of this newly designed bridge is not interesting to study.

This chapter shows the brief analyses that have been done on the dynamic behaviour of the Glass Truss Bridge. This information can be a starting point for a follow-up research on the dynamic behaviour of this bridge.

C.1. Dynamic Tests performed on the Glass Truss Bridge

When the Glass Truss Bridge was realised in 2017, its performance was tested by students and professors of Delft University of Technology. This was done by letting 60 students enter the bridge on several ways. The output of the tests were strains measured in the middle of the diagonals of the bridge, the positions of the strain gauges are given in Figure 2.10 of Chapter 2. They are placed in such a way that the axial strains in the diagonals is measured. Regarding the symmetry of the bridge in longitudinal direction, the strains were only measured on one side of the bridge. The positions of the strain gauges are clarified in Figure C.1. Note that every diagonal has three strain gauges placed in the middle, so in total 18 strain gauges are used to measure the output of the tests.

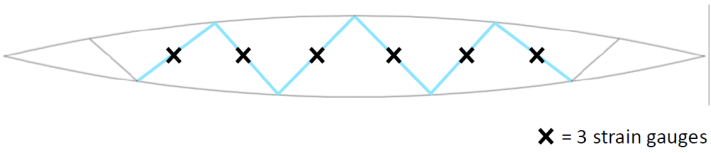

Figure C.1: Position of the strain gauges on the Glass Truss Bridge. Every cross marks three strain gauges on a single diagonal.

The tests performed in 2017 were not only static, but also dynamic. These dynamic tests were 60 students that entered the bridge who were either running, marching or dancing (see Figure C.3). For all the tests the strains were measured over time while students moved back and forth over the bridge. An example of the output of one of the diagonals of the tests when students were marching back and forth over the bridge is given in Figure C.2(a). The points in time with large vibrations indicate the moments when the students were on the bridge. In order to make calculations with these results, the

average values of outputs of the three strain gauges was taken per diagonal. Some important issues to notify here are the following:

- The values of the averaged strains are calibrated in such a way that the first values of the averaged strain is equal to zero for every measurement (see Figure C.2(b)). Here it is assumed that the bridge is unloaded and not in motion at the start of each measurement.
- By taking the averages of the strains it is assumed that there are no bending moments in the diagonals. Theoretically this is true for truss structures, since the connections are hinged. However, in reality there is no hinge that has a rotational stiffness of exactly zero.
  - In the example given in Figure C.2(a) it can be seen that the strains show different values already from the beginning of the test. These differences are due to unequal stress distribution over the various glass rods within a diagonal. The distance of the three coloured lines stays approximately equal during the measurement. This points to only small bending moments present in the diagonals due to the loads. Therefore the bending moments in the diagonals are neglected in this stage of the research.
- The strain gauges are placed after the prestress was applied to the diagonals. Therefore, in reality the zero point in the graph is equal to the post-tensioning force in the diagonal, which is around 16 kN. Due to this post-tensioning the glass in the diagonals will always be in compression.

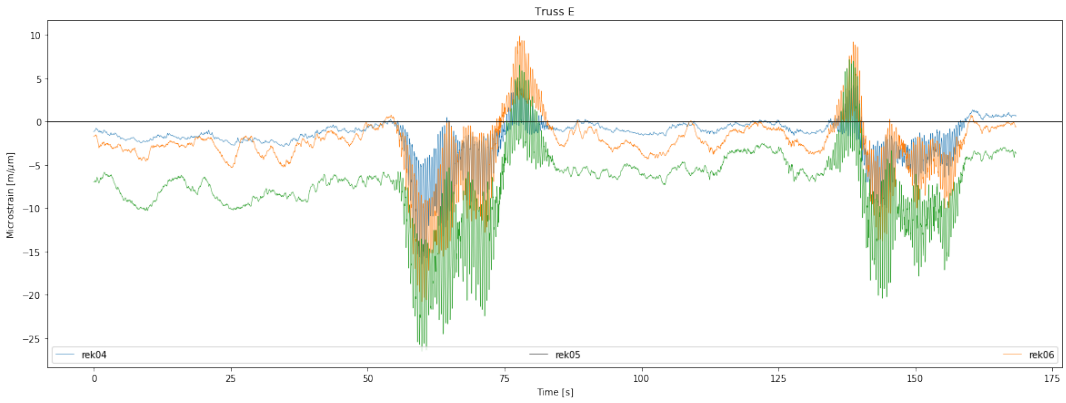

(a) The 3 outputs of the 3 strain gauges are plotted in different colours.

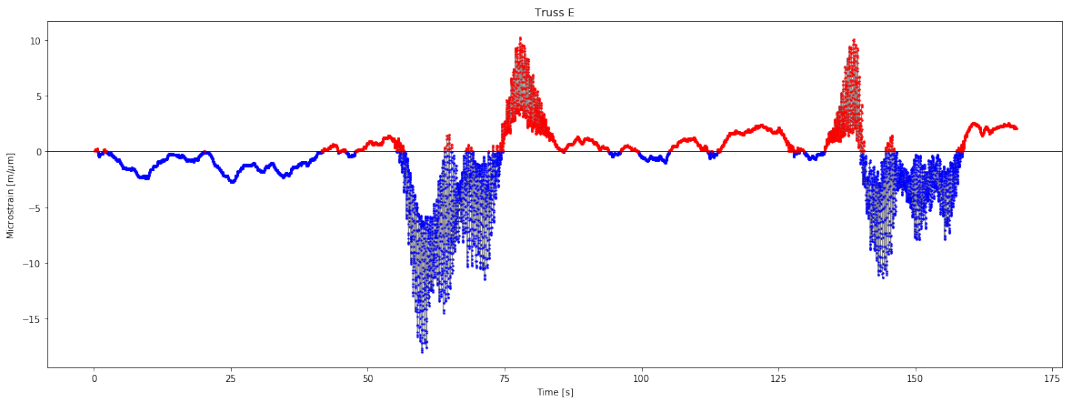

(b) Averaged strain of the outputs of the 3 strain gauges. The values are calibrated in such a way that the first value is equal to zero for every measurement. Blue indicates that the measured values are in compression in comparison with the first measured value of that measurement. Red indicates tension with reference to the first measured value of that measurement.

Figure C.2: Example of output of one diagonal for the marching students load case. Note that the prestress of 16 kN is not included in the values given in the plot.

(a) 60 running students.

(b) 60 marching students.

(c) 60 dancing students.

Figure C.3: The dynamic load cases of the tests performed on the Glass Truss Bridge in 2017 [1].

C.2. Analyses of Dynamic Tests

The tests described previously were performed in order to verify the safety of the bridge. From these tests and the compression tests performed on the diagonals, which are elaborated in Section 2.2.2, it could be concluded that the bridge design is safe. However, the bridge is over-designed and could be optimised if the overall structural behaviour of the bridge would be known. One aspect of the structural behaviour that is briefly analysed during this studies is the dynamic behaviour of the bridge by using the results of the tests discussed previously. The outcomes of these analyses are elaborated in

this section. Furthermore recommendations are given for follow-up researches regarding the dynamic behaviour of the Glass Truss Bridge.

C.2.1. Dynamic Pedestrian Loads

According to the Eurocode it is obliged for a new bridge design to obtain the relevant eigen frequencies (corresponding to vertical, horizontal and torsional vibrations) of the main supporting structure. This needs to be done by using an appropriate structural model [25]. It is important to get to know these eigen frequencies, since it might be possible that pedestrian loads cause frequencies which are equal (or very close) to the eigen frequency of the bridge. This can cause resonance which is a risky phenomena.

The Eurocode [25] states that the frequency area in vertical direction for normally walking pedestrians is from 1 to 3 Hz. In the horizontal direction this would be 0.5 to 1.5 Hz. Higher frequencies can occur for running pedestrians. It is however difficult to give exact values of pedestrian loads, because every pedestrian walks in another way. Furthermore, the way a person moves depends a lot on its surroundings and the amount of persons around that individual. Various studies are done in order to simulate a person walking, some did this using Monte Carlo simulations (a probabilistic approach), others by random vibrations theory or by using motion capturing technology. It appears to be difficult to predict the behaviour of a walking person or crowd and, therefore, to describe the loads that are produced.

From this information, it can be concluded that using pedestrian loads to analyse the structural (dynamic) behaviour of a bridge can be difficult. It is easier to analyse a structure if the applied load in a test is known, or if the load produces a very wide frequency spectrum (white noise spectrum). The pedestrian loads can however be used to verify the ability of the strain gauges on the Glass Truss Bridge to capture motion. An example of a frequency spectrum produced by pedestrians is given in Figure C.4. In the following section this spectrum will be compared to the ones find by analysing the results of the tests on the Glass Truss Bridge.

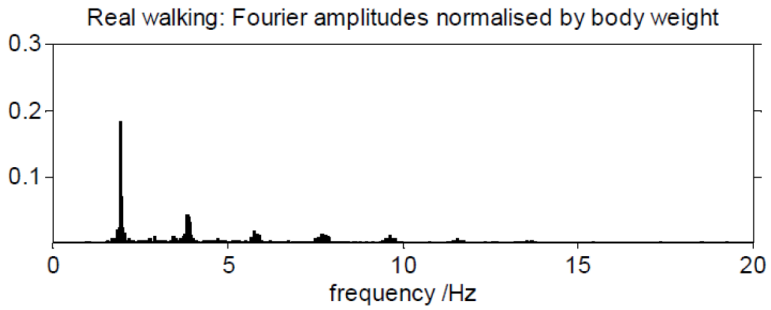

Figure C.4: Fourier-spectrum of real forces corresponding to a pacing rate of 1.91 Hz [26].

C.2.2. Fourier Transform

By using the fast Fourier transform it is possible to transfer the values from a time domain into a frequency domain. This is done, since it might be possible to get information about the eigen frequencies of the Glass Truss Bridge, although this is only possible if the frequencies induced by the pedestrians would be higher than that eigen frequency. Furthermore, by comparing the spectra that can be obtained using the Fourier transform with spectra of pedestrian loads from literature, some information can be obtained on the validity of the test results. Figure C.5 gives the real part of the spectrum of the marching students load case. Since all students march in approximately the same pace, the higher peaks depicted in the figure show resemblance with the peaks shown in Figure C.4. Also, second and third harmonics can be seen in the spectrum given in Figure C.5, multiple harmonics are also shown by the different degrading peaks of Figure C.4. This indicates that the strain gauges capture the motions of the Glass Truss Bridge well.

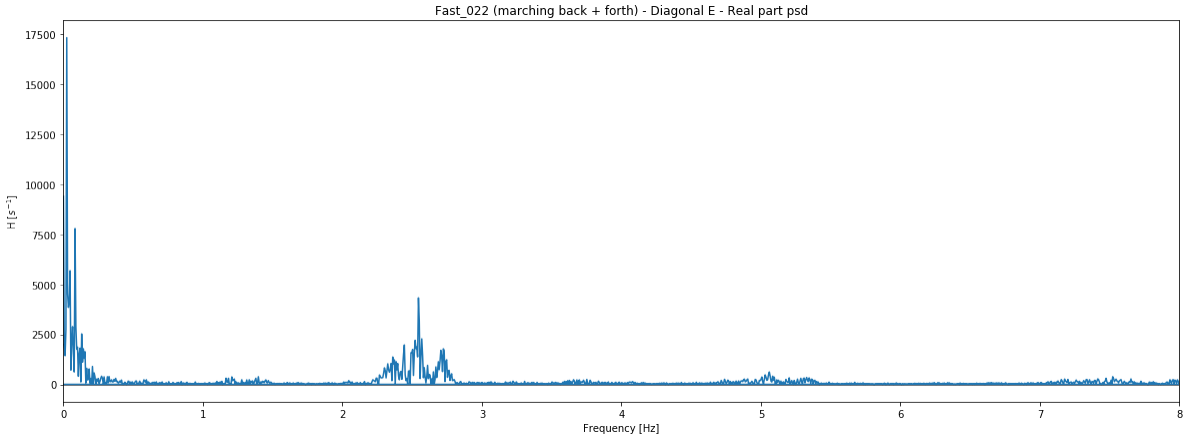

Figure C.5: Fourier-spectrum by fast Fourier transform of the averaged strains in one of the diagonals in the Glass Truss Bridge caused by students marching back and forth over the bridge.

In order to find the eigen frequency of the bridge, this frequency needs to be excited by the load on the bridge. The best chance for this to happen is if the spectrum of the load is as wide as possible. For the load cases present in the tests on the Glass Truss Bridge performed in 2017, that would be the dancing students load case. The spectrum of this load case is shown in Figure C.6. From the various peaks in the graph it can be seen that the data is quite noisy, which is a disadvantage. Also, no obvious peak belonging to the eigen frequency of the bridge can be distinguished from this graph.

It was, furthermore, tried to make a frequency spectrum of a moment in time were the bridge was unloaded and, therefore, moving at its eigen frequency. Unfortunately only very small frequencies (<0.5 Hz) were found by doing this. Since the bridge behaves relatively stiff it can be assumed that the eigen frequency of the bridge is higher than 0.5 Hz.

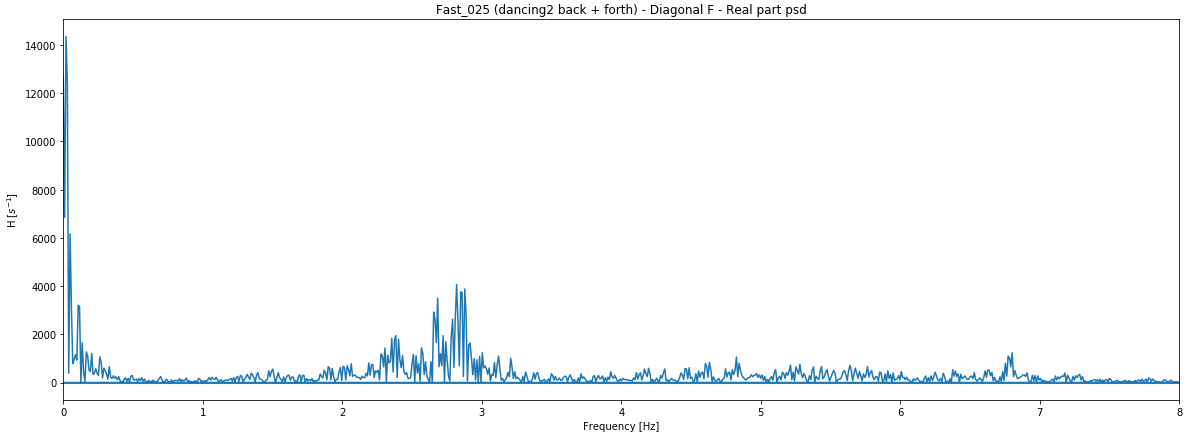

Figure C.6: Fourier-spectrum by fast Fourier transform of the strains in one of the diagonals in the Glass Truss Bridge caused by students dancing back and forth over the bridge.

C.2.3. Frequency Domain Decomposition

Since it is difficult to draw conclusions from the frequency spectra given in Figures C.5 and C.6 a frequency domain decomposition of the spectrum belonging to the dancing students was performed. By using a frequency domain decomposition it is possible to identify frequency modes, and to see whether a certain peak in the frequency domain belongs to one or multiple modes.

In order to perform the frequency domain decomposition, an estimation needs to be made on the input force (in this case, the pedestrian load). This estimation states that the spectrum of this load approximates a white noise spectrum (a.k.a. a horizontal line spectrum where all the frequencies are

excited in the same magnitude). The better the test input corresponds to this white noise spectrum, the better the estimations of the frequency modes of the bridge will be. Furthermore, the estimation will get better if more data points are available, so the longer the measurement, the better the results of the frequency domain decomposition. This results in the problems that the measurements done in 2017 are giving. The spectrum shown in Figure C.6 is not wide enough; it does not correspond well enough to a white noise spectrum. Furthermore, the amount of measured points is too low, because the time domain of the measurements were not long enough.

For these reasons no frequency domain decomposition could be performed for the Glass Truss Bridge. It would be best to perform tests in the future with which a wide frequency spectrum is produced. This can be done by doing hammer tests. It is important to take long measurements with a high measurement frequency. More information can be obtained by exciting the bridge at different places in the structure. With the information obtained from such tests, a representative frequency domain decomposition could be established.

C.3. Conclusions & Recommendations

The current design of the Glass Truss Bridge is too conservative. This can be due to various reasons (or a combination of the following):

1. The design loads for footbridges given in the Eurocode, which are used to design the Glass Truss Bridge, are too conservative.
2. The mechanical properties of the glass diagonals used for the structural calculations of the Glass Truss Bridge are inaccurate.
3. The mechanical properties and rotational stiffnesses of the glass nodes used in the Glass Truss Bridge calculations are inaccurate.
4. The boundary supports used in the structural calculations of the bridge might be too ideal.
5. Errors can be present in the (FE) calculations used to design the Glass Truss Bridge.

The results presented in Part IV of this thesis can be used for calculations of the Glass Truss Bridge. This knowledge can not only be used for understanding of the Glass Truss Bridge, but also for new designs that will be created using structural bundled glass columns.

In order to investigate the dynamic behaviour of the Glass Truss Bridge it is recommended to perform new dynamic tests on the bridge. One way to do this is by performing hammer tests on the bridge, since this will excite the bridge with as many frequencies as possible. Furthermore, the load with which you excite the bridge with the hammer can be measured. It would be advantageous to excite the bridge in different places in the structure to get more information about the movements of the bridge. Perform long term measurements while exciting the bridge with a hammer and let its movements damp out completely before exciting it again. Make the measurements as long as possible with a high measuring frequency in order to get as many data points as possible in one measurement. The measuring frequency used in the previous tests was 100 per second, which can measure frequencies up to 50 Hz. This measuring frequency should be sufficient for future tests as well.

At this point the strain gauges used to measure the movements of the Glass Truss Bridge during the previous tests are still on the bridge. Strain gauges are accurate in measuring low frequency movements, in order to capture high frequency movements it would be better to use accelerometers which measure the accelerations. The Glass Truss Bridge behaves relatively stiff, therefore, it might be possible that this eigen frequency can not be captured with the strain gauges. Since no dynamic model of the bridge is present and no information about the eigen frequency of the bridge is obtained from previous tests, no assumptions can be made about the range in which the eigen frequency of the bridge will be. Therefore, it is recommended to make a dynamic model to estimate the value of the eigen frequencies in order to see if measuring with strain gauges would be sufficient. A second option can be to try to measure with strain gauges only at first and see if the eigen frequency can be found in

these results. If this appears not to be the case, then second tests can be performed using accelerometers. It might be useful to know the measuring range of the strain gauges before performing any tests.

It is important to negotiate about in what extent it is needed to know the exact dynamic behaviour of the bridge. In a lot of cases knowing the eigen frequencies and mode shapes is enough. If it is necessary to know the magnitude of the modes instead of only the shape, this knowledge can be obtained by making use of the magnitude of the input force applied by the hammer.

D

GUI and Python Script

GUI stands for Graphical User Interface. In Chapter 4 it was mentioned that a Python script was created to enable the creation of the finite element models used for this studies. To make this sheet user-friendly for future calculations by other researchers, a GUI for this script was created using the Tkinter package of Python. Both the GUI and the Python script are given in this appendix. Python itself can be downloaded by downloading Anaconda, which can be downloaded for free. It is recommended to use version 3.6 of Python. The sheet itself is created using the Jupyter Notebook interface of Python, it is recommended to use this interface as well when using the script presented here.

D.1. Graphical User Interface

On the following pages the GUI will be shown, along with a guideline on how to use it.

When creating your DIANA model make sure you create the glass materials and glass geometries before you create any geometries or materials for other materials. Doing otherwise might give errors when using this Python script.

Step 1: Copy 'K Verleg - User friendly Weibull glass ft.ipynb' and 'tudelft_invflame_XFY_icon.ico' files in the Users folder of your computer.

Step 2: Open the Python script in Jupiter Notebook using Anaconda.

Step 3: To run the script press Cell → Run All

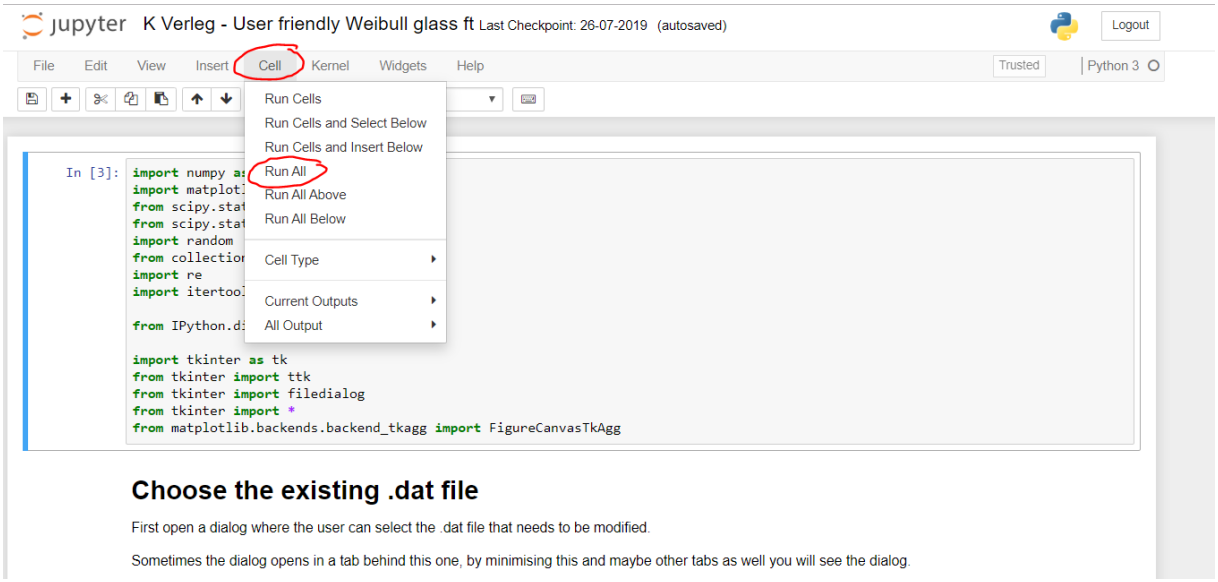

Step 4: Choose the DIANA .dat file that you want to modify in the dialog that is opened automatically after running the script. It might be that this dialog opens behind the tab that you have currently open. To find it minimise your open tabs.

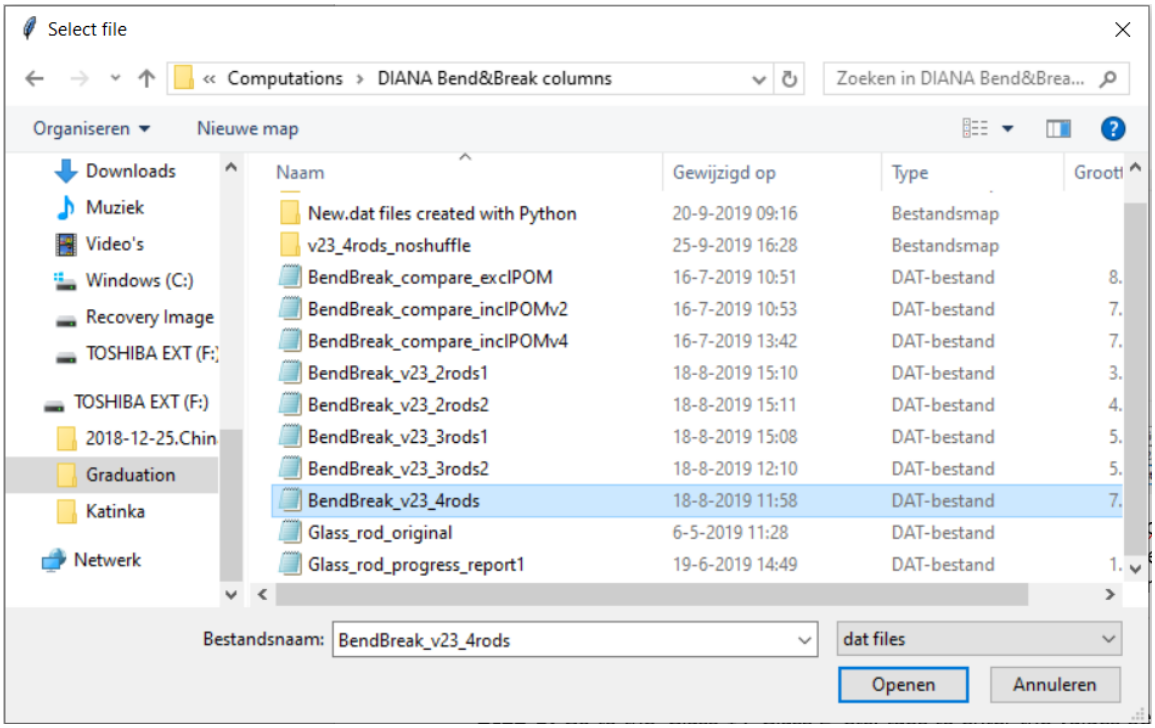

After pressing 'Open' the following window appears automatically.

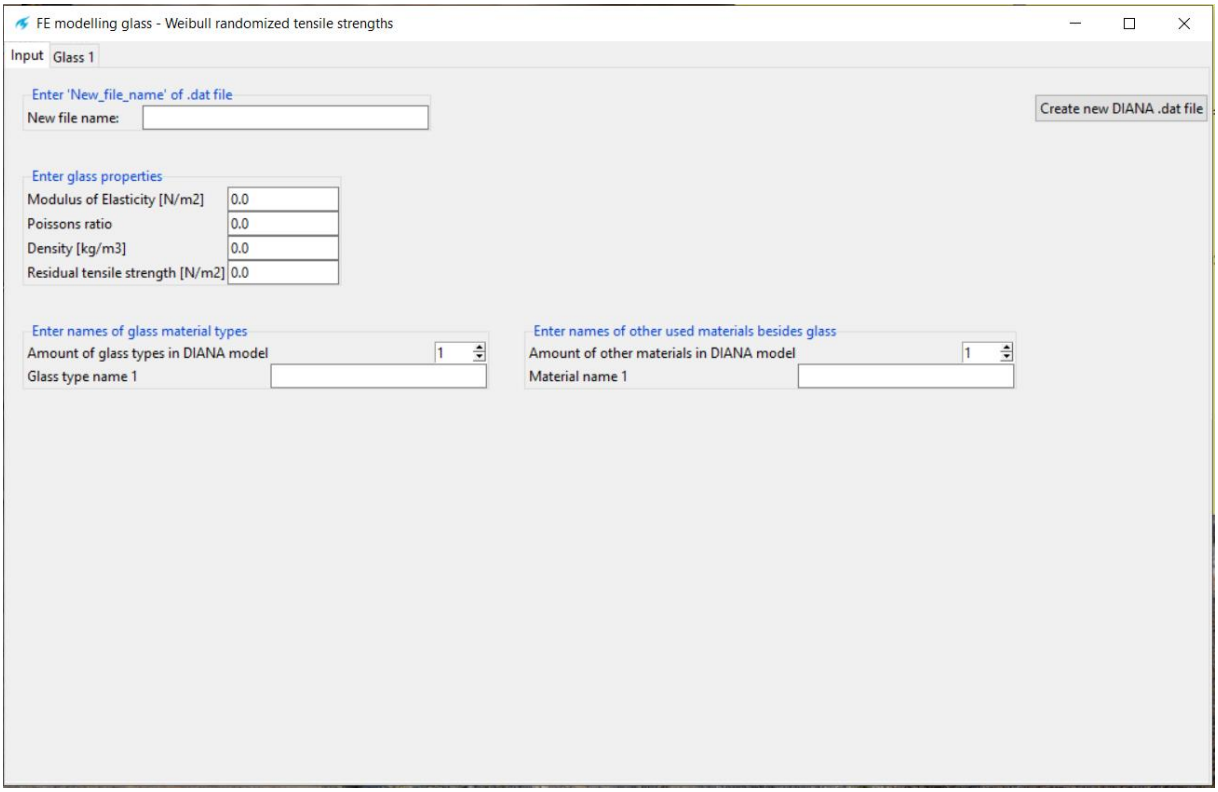

Step 5: Enter the name of the new .dat file you are generating and enter the material properties of the glass that you are using. In the frame 'Enter names of glass material types' you can enter the types of glass materials you have in your DIANA model. See the example below. The window below shows the materials used in the DIANA model.

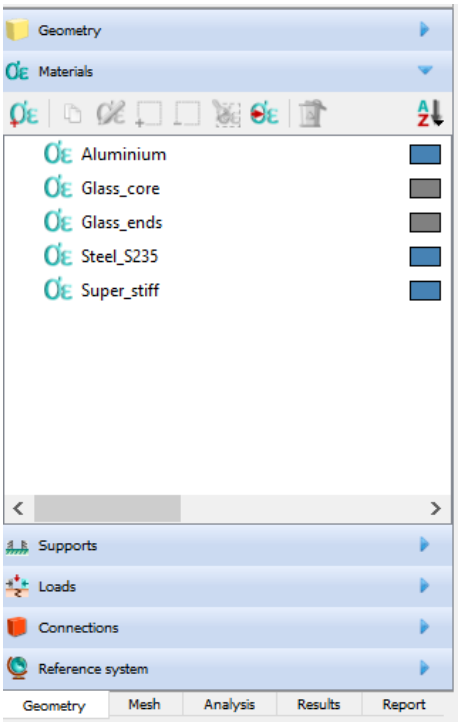

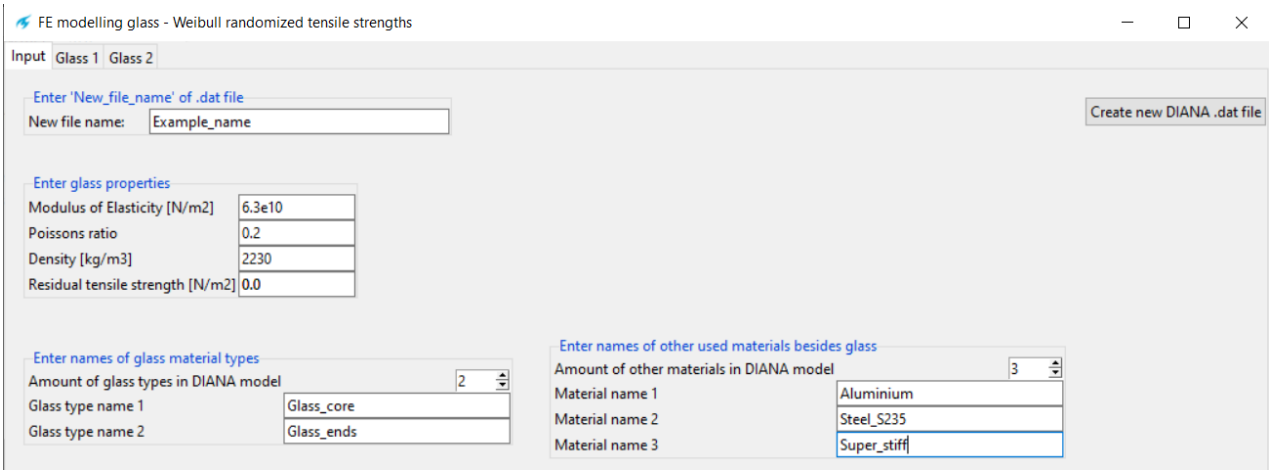

Increasing the amount of glass types or other materials in the spinbox will automatically generate a box where you can specify the name. When you decrease the amount again the boxes will, however, not disappear. If you make sure that the amount in the spinbox is right again, this will not create a problem. Increasing the amount of glass types with the spinbox will also generate new tabs. See the figure above where now a new tab named 'Glass 2' is created which belongs to the material 'Glass_ends'. You can enter a maximum of 10 different glass types. When entering the other used materials, make sure to use the same order as they are printed in the original .dat file.

Step 6: Go to the 'Glass 1', 'Glass 2' etc. tabs to enter the values belonging to your glass types and which DIANA geometries are made of those types of glass. See the example below. The first image shows the glass geometries in the DIANA model.

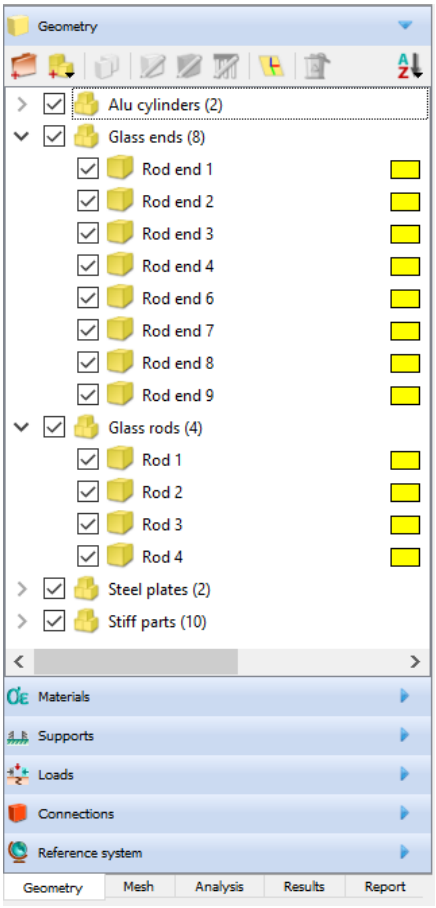

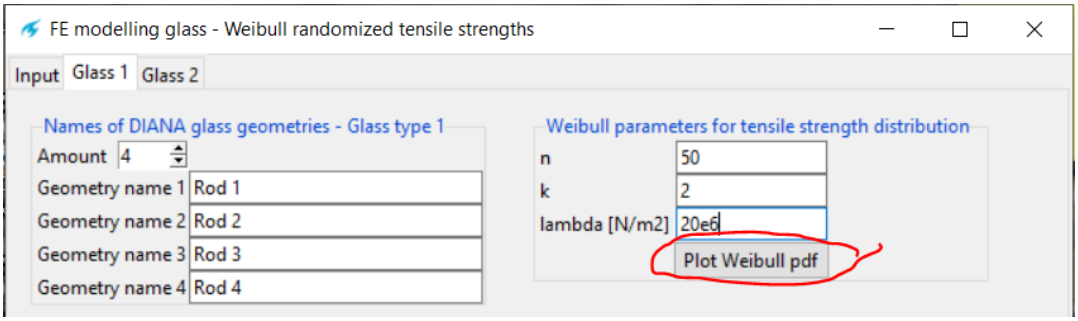

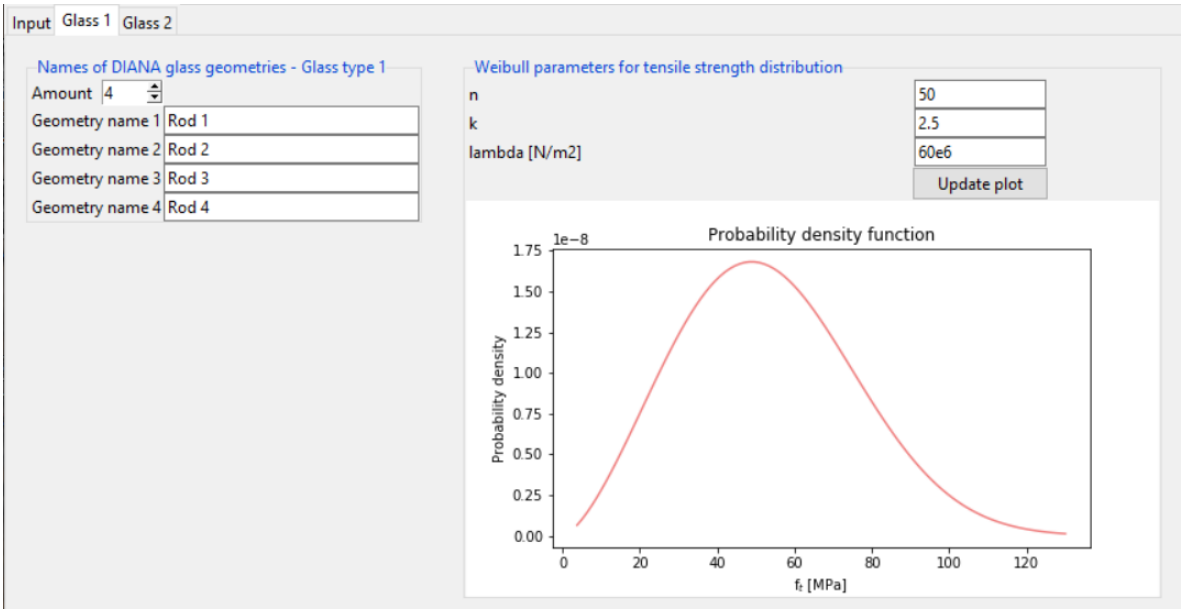

n stands for the amount of different material sets with different tensile strengths you want to create for that type of glass. k and lambda are the Weibull parameters. These parameters can be altered, the plot will be updated by pressing the button 'Update plot'. The amount of glass geometries in the spinbox will generate new boxes for the geometry names. Again, decreasing the amount in the spinbox will not make them disappear. Make sure the amount in the spinbox is correct, see the example below. You can enter a maximum of 30 different geometries per glass type.

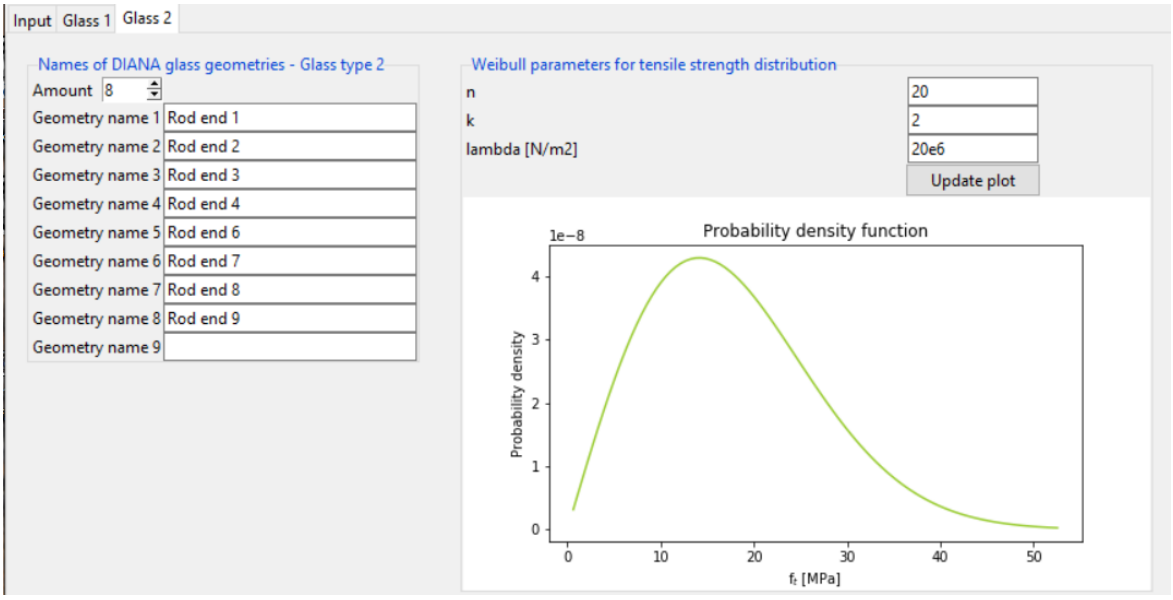

Step 7: Go back to the 'Input' tab. If everything you filled in is correct, press the button 'Create new DIANA .dat file'. A new file with the name 'Example_name.dat' will appear in the Users folder of your computer. Creating the file generally takes a few seconds, dependent on the amount of elements in your DIANA model. Pressing the button, furthermore, generates a new tab named 'Combined plots'.

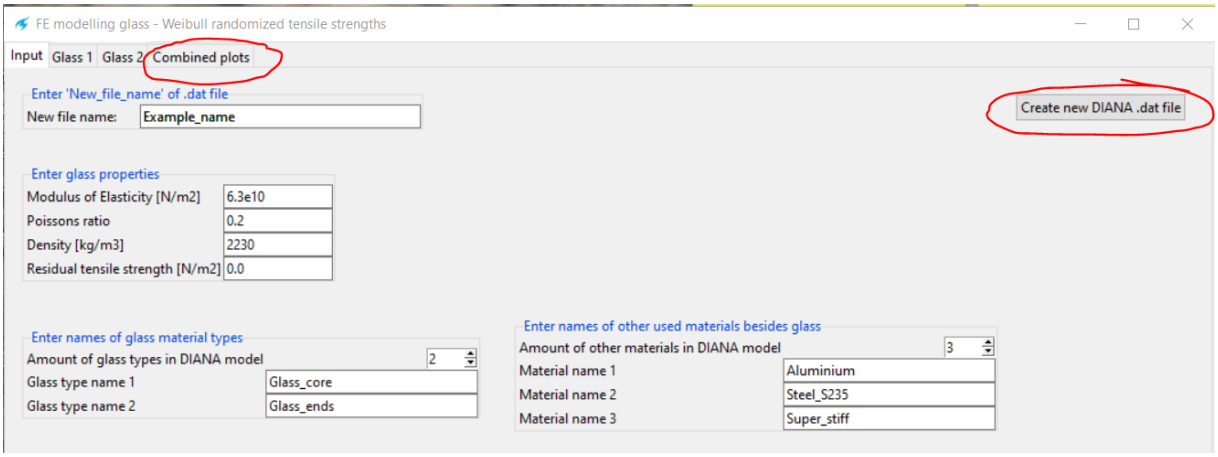

This tab shows the combined probability density functions of all the glass types. The points on the graph refer to the drawn tensile stresses for this new DIANA model. The amount of points is the same amount you entered for the value of n in the previous step. You can save this plot by pressing the button 'Save plot as png'. The figure will appear in the Users folder of your computer with the same name as your new .dat file. In this example that will be 'Example_name.png'.

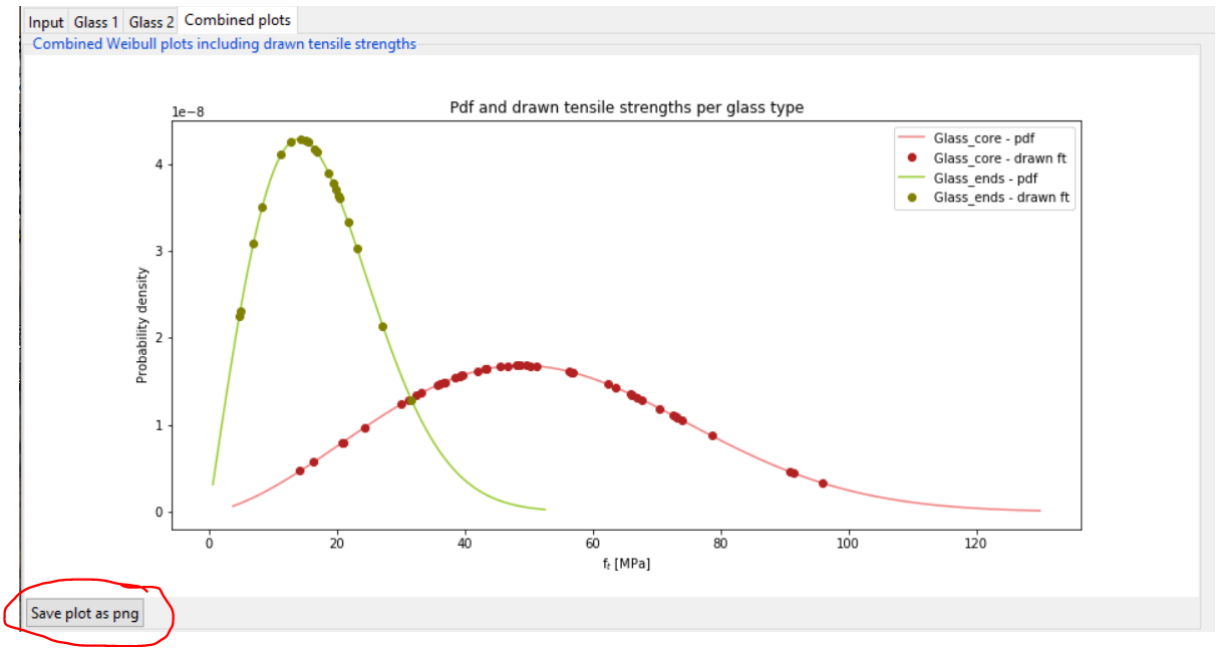

If you want to create multiple models with different tensile strengths assigned to different finite elements in your model, you can just change the name of your new .dat file in the 'New file name' box and again press the button 'Create new DIANA .dat file'.

D.2. Python Code

```
import numpy as np
import matplotlib.pyplot as plt
from scipy.stats import weibull_min
from scipy.stats import weibull_max
import random
from collections import Counter
import re
import itertools

from IPython.display import HTML

import tkinter as tk
from tkinter import ttk
from tkinter import filedialog
from tkinter import *
from matplotlib.backends.backend_tkagg import FigureCanvasTkAgg
```

Choose the existing .dat file

First open a dialog where the user can select the .dat file that needs to be modified.

Sometimes the dialog opens in a tab behind this one, by minimising this and maybe other tabs as well you will see the dialog.

```
# Open dialog to select correct Diana .dat input file of Diana model you want to modify

root = tk.Tk()
root.withdraw()
root.filename =  filedialog.askopenfilename(initialdir = "/",title = "Select file",
                                            filetypes = [("dat files","*.dat")])
file_diana = root.filename
f = open(file_diana)
data = f.read()
f.close()
lines = data.split('\n')
```

GUI outline

The code underneath generates the outline of the GUI, all the input boxes and gets all the values that you enter in the input boxes to use in the piece of code to write the new .dat file.

```
root.destroy()
win = tk.Tk()
win.title('FE modelling glass - Weibull randomized tensile strengths')

tabControl = ttk.Notebook(win)
tab1 = ttk.Frame(tabControl)
tabControl.add(tab1,text='Input')
tab2 = ttk.Frame(tabControl)
tabControl.add(tab2,text='Glass 1')
tabControl.pack(expand=1,fill='both')


# File frame ----------------------------------------------------
# ---------------------------------------------------------------

file_dat = ttk.LabelFrame(tab1,text="Enter 'New_file_name' of .dat file")
file_dat.grid(column=0,row=0,padx=15,pady=15,sticky=tk.W)

ttk.Label(file_dat,text='New file name:      ').grid(column=0,row=0,sticky=tk.W)

new_dat_file = tk.StringVar()
ttk.Entry(file_dat,width=40,textvariable=new_dat_file).grid(column=1,row=0)

# Materials frame -----------------------------------------------
# ---------------------------------------------------------------

# Glass ---------------------------------------------------------
glass_prop = ttk.LabelFrame(tab1,text='Enter glass properties')
glass_prop.grid(column=0,row=1,padx=15,pady=15,sticky=tk.W)

glass_prop_text = ['Modulus of Elasticity [N/m2]','Poissons ratio','Density [kg/m3]'
                  ,'Residual tensile strength [N/m2]']

for i in range(len(glass_prop_text)):
    ttk.Label(glass_prop,text=glass_prop_text[i]).grid(column=0,row=i,sticky=tk.W)


E_modulus = tk.DoubleVar()
poisson = tk.DoubleVar()
density = tk.DoubleVar()
rest_ft = tk.DoubleVar()

glass_prop_list = [E_modulus,poisson,density,rest_ft]

for i in range(len(glass_prop_text)):
    ttk.Entry(glass_prop,width=15,textvariable=glass_prop_list[i]).grid(column=1,row=i)
```

```
# Label frames ------------------------------------------------

glass_geo = ttk.LabelFrame(tab1,text='Enter names of glass material types')
glass_geo.grid(column=0,row=2,padx=15,pady=15,sticky=tk.W)

glass_geo1 = ttk.LabelFrame(tab2,text='Names of DIANA glass geometries - Glass type 1')
glass_geo1.grid(column=0,row=0,padx=15,pady=15,sticky=tk.NW)

other_mat_frame = ttk.LabelFrame(tab1,text='Enter names of other used materials besides glass')
other_mat_frame.grid(column=1,row=2,padx=15,pady=15,sticky=tk.NW)

# Glass types -------------------------------------------------

ttk.Label(glass_geo,text='Amount of glass types in DIANA model').grid(column=0,row=0,sticky=tk.W)

# Enable 10 different types of glass materials with each 30 different geometries. So 300 variants possible.

glassname = tk.StringVar()
glassname2 = tk.StringVar()
glassname3 = tk.StringVar()
glassname4 = tk.StringVar()
glassname5 = tk.StringVar()
glassname6 = tk.StringVar()
glassname7 = tk.StringVar()
glassname8 = tk.StringVar()
glassname9 = tk.StringVar()
glassname10 = tk.StringVar()

glass_name_list = [glassname,glassname2,glassname3,glassname4,glassname5,
                   glassname6,glassname7,glassname8,glassname9,glassname10]

gl1_geo1,gl1_geo2,gl1_geo3,gl1_geo4,gl1_geo5,gl1_geo6,gl1_geo7,gl1_geo8,gl1_geo9,gl1_geo10 = tk.StringVar(),tk.StringVar(),tk.Str
gl1_geo11,gl1_geo12,gl1_geo13,gl1_geo14,gl1_geo15,gl1_geo16,gl1_geo17,gl1_geo18,gl1_geo19,gl1_geo20 = tk.StringVar(),tk.StringVar
gl1_geo21,gl1_geo22,gl1_geo23,gl1_geo24,gl1_geo25,gl1_geo26,gl1_geo27,gl1_geo28,gl1_geo29,gl1_geo30 = tk.StringVar(),tk.StringVar

gl1_geo_list = [gl1_geo1,gl1_geo2,gl1_geo3,gl1_geo4,gl1_geo5,gl1_geo6,gl1_geo7,gl1_geo8,gl1_geo9,gl1_geo10,
                gl1_geo11,gl1_geo12,gl1_geo13,gl1_geo14,gl1_geo15,gl1_geo16,gl1_geo17,gl1_geo18,gl1_geo19,gl1_geo20,
                gl1_geo21,gl1_geo22,gl1_geo23,gl1_geo24,gl1_geo25,gl1_geo26,gl1_geo27,gl1_geo28,gl1_geo29,gl1_geo30]

gl2_geo1, gl2_geo2, gl2_geo3, gl2_geo4, gl2_geo5, gl2_geo6, gl2_geo7, gl2_geo8, gl2_geo9, gl2_geo10 = tk.StringVar(),tk.StringVar
gl2_geo11,gl2_geo12,gl2_geo13,gl2_geo14,gl2_geo15,gl2_geo16,gl2_geo17,gl2_geo18,gl2_geo19,gl2_geo20 = tk.StringVar(),tk.StringVar
gl2_geo21,gl2_geo22,gl2_geo23,gl2_geo24,gl2_geo25,gl2_geo26,gl2_geo27,gl2_geo28,gl2_geo29,gl2_geo30 = tk.StringVar(),tk.StringVar

gl2_geo_list = [gl2_geo1, gl2_geo2, gl2_geo3, gl2_geo4, gl2_geo5, gl2_geo6, gl2_geo7, gl2_geo8, gl2_geo9, gl2_geo10,
                gl2_geo11,gl2_geo12,gl2_geo13,gl2_geo14,gl2_geo15,gl2_geo16,gl2_geo17,gl2_geo18,gl2_geo19,gl2_geo20,
                gl2_geo21,gl2_geo22,gl2_geo23,gl2_geo24,gl2_geo25,gl2_geo26,gl2_geo27,gl2_geo28,gl2_geo29,gl2_geo30]

gl3_geo1, gl3_geo2, gl3_geo3, gl3_geo4, gl3_geo5, gl3_geo6, gl3_geo7, gl3_geo8, gl3_geo9, gl3_geo10 = tk.StringVar(),tk.StringVar
gl3_geo11,gl3_geo12,gl3_geo13,gl3_geo14,gl3_geo15,gl3_geo16,gl3_geo17,gl3_geo18,gl3_geo19,gl3_geo20 = tk.StringVar(),tk.StringVar
gl3_geo21,gl3_geo22,gl3_geo23,gl3_geo24,gl3_geo25,gl3_geo26,gl3_geo27,gl3_geo28,gl3_geo29,gl3_geo30 = tk.StringVar(),tk.StringVar

gl3_geo_list = [gl3_geo1, gl3_geo2, gl3_geo3, gl3_geo4, gl3_geo5, gl3_geo6, gl3_geo7, gl3_geo8, gl3_geo9, gl3_geo10,
                gl3_geo11,gl3_geo12,gl3_geo13,gl3_geo14,gl3_geo15,gl3_geo16,gl3_geo17,gl3_geo18,gl3_geo19,gl3_geo20,
                gl3_geo21,gl3_geo22,gl3_geo23,gl3_geo24,gl3_geo25,gl3_geo26,gl3_geo27,gl3_geo28,gl3_geo29,gl3_geo30]

gl4_geo1, gl4_geo2, gl4_geo3, gl4_geo4, gl4_geo5, gl4_geo6, gl4_geo7, gl4_geo8, gl4_geo9, gl4_geo10 = tk.StringVar(),tk.StringVar
gl4_geo11,gl4_geo12,gl4_geo13,gl4_geo14,gl4_geo15,gl4_geo16,gl4_geo17,gl4_geo18,gl4_geo19,gl4_geo20 = tk.StringVar(),tk.StringVar
gl4_geo21,gl4_geo22,gl4_geo23,gl4_geo24,gl4_geo25,gl4_geo26,gl4_geo27,gl4_geo28,gl4_geo29,gl4_geo30 = tk.StringVar(),tk.StringVar

gl4_geo_list = [gl4_geo1, gl4_geo2, gl4_geo3, gl4_geo4, gl4_geo5, gl4_geo6, gl4_geo7, gl4_geo8, gl4_geo9, gl4_geo10,
                gl4_geo11,gl4_geo12,gl4_geo13,gl4_geo14,gl4_geo15,gl4_geo16,gl4_geo17,gl4_geo18,gl4_geo19,gl4_geo20,
                gl4_geo21,gl4_geo22,gl4_geo23,gl4_geo24,gl4_geo25,gl4_geo26,gl4_geo27,gl4_geo28,gl4_geo29,gl4_geo30]

gl5_geo1, gl5_geo2, gl5_geo3, gl5_geo4, gl5_geo5, gl5_geo6, gl5_geo7, gl5_geo8, gl5_geo9, gl5_geo10 = tk.StringVar(),tk.StringVar
gl5_geo11,gl5_geo12,gl5_geo13,gl5_geo14,gl5_geo15,gl5_geo16,gl5_geo17,gl5_geo18,gl5_geo19,gl5_geo20 = tk.StringVar(),tk.StringVar
gl5_geo21,gl5_geo22,gl5_geo23,gl5_geo24,gl5_geo25,gl5_geo26,gl5_geo27,gl5_geo28,gl5_geo29,gl5_geo30 = tk.StringVar(),tk.StringVar

gl5_geo_list = [gl5_geo1, gl5_geo2, gl5_geo3, gl5_geo4, gl5_geo5, gl5_geo6, gl5_geo7, gl5_geo8, gl5_geo9, gl5_geo10,
                gl5_geo11,gl5_geo12,gl5_geo13,gl5_geo14,gl5_geo15,gl5_geo16,gl5_geo17,gl5_geo18,gl5_geo19,gl5_geo20,
                gl5_geo21,gl5_geo22,gl5_geo23,gl5_geo24,gl5_geo25,gl5_geo26,gl5_geo27,gl5_geo28,gl5_geo29,gl5_geo30]

gl6_geo1, gl6_geo2, gl6_geo3, gl6_geo4, gl6_geo5, gl6_geo6, gl6_geo7, gl6_geo8, gl6_geo9, gl6_geo10 = tk.StringVar(),tk.StringVar
gl6_geo11,gl6_geo12,gl6_geo13,gl6_geo14,gl6_geo15,gl6_geo16,gl6_geo17,gl6_geo18,gl6_geo19,gl6_geo20 = tk.StringVar(),tk.StringVar
gl6_geo21,gl6_geo22,gl6_geo23,gl6_geo24,gl6_geo25,gl6_geo26,gl6_geo27,gl6_geo28,gl6_geo29,gl6_geo30 = tk.StringVar(),tk.StringVar

gl6_geo_list = [gl6_geo1, gl6_geo2, gl6_geo3, gl6_geo4, gl6_geo5, gl6_geo6, gl6_geo7, gl6_geo8, gl6_geo9, gl6_geo10,
                gl6_geo11,gl6_geo12,gl6_geo13,gl6_geo14,gl6_geo15,gl6_geo16,gl6_geo17,gl6_geo18,gl6_geo19,gl6_geo20,
                gl6_geo21,gl6_geo22,gl6_geo23,gl6_geo24,gl6_geo25,gl6_geo26,gl6_geo27,gl6_geo28,gl6_geo29,gl6_geo30]

gl7_geo1, gl7_geo2, gl7_geo3, gl7_geo4, gl7_geo5, gl7_geo6, gl7_geo7, gl7_geo8, gl7_geo9, gl7_geo10 = tk.StringVar(),tk.StringVar
gl7_geo11,gl7_geo12,gl7_geo13,gl7_geo14,gl7_geo15,gl7_geo16,gl7_geo17,gl7_geo18,gl7_geo19,gl7_geo20 = tk.StringVar(),tk.StringVar
gl7_geo21,gl7_geo22,gl7_geo23,gl7_geo24,gl7_geo25,gl7_geo26,gl7_geo27,gl7_geo28,gl7_geo29,gl7_geo30 = tk.StringVar(),tk.StringVar

gl7_geo_list = [gl7_geo1, gl7_geo2, gl7_geo3, gl7_geo4, gl7_geo5, gl7_geo6, gl7_geo7, gl7_geo8, gl7_geo9, gl7_geo10,
                gl7_geo11,gl7_geo12,gl7_geo13,gl7_geo14,gl7_geo15,gl7_geo16,gl7_geo17,gl7_geo18,gl7_geo19,gl7_geo20,
                gl7_geo21,gl7_geo22,gl7_geo23,gl7_geo24,gl7_geo25,gl7_geo26,gl7_geo27,gl7_geo28,gl7_geo29,gl7_geo30]

gl8_geo1, gl8_geo2, gl8_geo3, gl8_geo4, gl8_geo5, gl8_geo6, gl8_geo7, gl8_geo8, gl8_geo9, gl8_geo10 = tk.StringVar(),tk.StringVar
gl8_geo11,gl8_geo12,gl8_geo13,gl8_geo14,gl8_geo15,gl8_geo16,gl8_geo17,gl8_geo18,gl8_geo19,gl8_geo20 = tk.StringVar(),tk.StringVar
gl8_geo21,gl8_geo22,gl8_geo23,gl8_geo24,gl8_geo25,gl8_geo26,gl8_geo27,gl8_geo28,gl8_geo29,gl8_geo30 = tk.StringVar(),tk.StringVar
```

```
gl8_geo_list = [gl8_geo1, gl8_geo2, gl8_geo3, gl8_geo4, gl8_geo5, gl8_geo6, gl8_geo7, gl8_geo8, gl8_geo9, gl8_geo10,
                gl8_geo11,gl8_geo12,gl8_geo13,gl8_geo14,gl8_geo15,gl8_geo16,gl8_geo17,gl8_geo18,gl8_geo19,gl8_geo20,
                gl8_geo21,gl8_geo22,gl8_geo23,gl8_geo24,gl8_geo25,gl8_geo26,gl8_geo27,gl8_geo28,gl8_geo29,gl8_geo30]

gl9_geo1, gl9_geo2, gl9_geo3, gl9_geo4, gl9_geo5, gl9_geo6, gl9_geo7, gl9_geo8, gl9_geo9, gl9_geo10 = tk.StringVar(),tk.StringVar
gl9_geo11,gl9_geo12,gl9_geo13,gl9_geo14,gl9_geo15,gl9_geo16,gl9_geo17,gl9_geo18,gl9_geo19,gl9_geo20 = tk.StringVar(),tk.StringVar
gl9_geo21,gl9_geo22,gl9_geo23,gl9_geo24,gl9_geo25,gl9_geo26,gl9_geo27,gl9_geo28,gl9_geo29,gl9_geo30 = tk.StringVar(),tk.StringVar

gl9_geo_list = [gl9_geo1, gl9_geo2, gl9_geo3, gl9_geo4, gl9_geo5, gl9_geo6, gl9_geo7, gl9_geo8, gl9_geo9, gl9_geo10,
                gl9_geo11,gl9_geo12,gl9_geo13,gl9_geo14,gl9_geo15,gl9_geo16,gl9_geo17,gl9_geo18,gl9_geo19,gl9_geo20,
                gl9_geo21,gl9_geo22,gl9_geo23,gl9_geo24,gl9_geo25,gl9_geo26,gl9_geo27,gl9_geo28,gl9_geo29,gl9_geo30]

gl10_geo1, gl10_geo2, gl10_geo3, gl10_geo4, gl10_geo5, gl10_geo6, gl10_geo7, gl10_geo8, gl10_geo9, gl10_geo10 = tk.StringVar(),tk
gl10_geo11,gl10_geo12,gl10_geo13,gl10_geo14,gl10_geo15,gl10_geo16,gl10_geo17,gl10_geo18,gl10_geo19,gl10_geo20 = tk.StringVar(),tk
gl10_geo21,gl10_geo22,gl10_geo23,gl10_geo24,gl10_geo25,gl10_geo26,gl10_geo27,gl10_geo28,gl10_geo29,gl10_geo30 = tk.StringVar(),tk

gl10_geo_list = [gl10_geo1, gl10_geo2, gl10_geo3, gl10_geo4, gl10_geo5, gl10_geo6, gl10_geo7, gl10_geo8, gl10_geo9, gl10_geo10,
                gl10_geo11,gl10_geo12,gl10_geo13,gl10_geo14,gl10_geo15,gl10_geo16,gl10_geo17,gl10_geo18,gl10_geo19,gl10_geo20,
                gl10_geo21,gl10_geo22,gl10_geo23,gl10_geo24,gl10_geo25,gl10_geo26,gl10_geo27,gl10_geo28,gl10_geo29,gl10_geo30]

def get_gl1_geo():
    gl1_geo_amount = int(gl1_geo_spin.get())
    for i in range(1,gl1_geo_amount):
        ttk.Label(glass_geo1,text='Geometry name ' + str(i+1)).grid(column=0,row=1+i,sticky=tk.W)
        ttk.Entry(glass_geo1,width=30,textvariable=gl1_geo_list[i]).grid(column=1,row=i+1)

def get_gl2_geo():
    gl2_geo_amount = int(gl2_geo_spin.get())
    for i in range(1,gl2_geo_amount):
        ttk.Label(glass_geo2,text='Geometry name ' + str(i+1)).grid(column=0,row=1+i,sticky=tk.W)
        ttk.Entry(glass_geo2,width=30,textvariable=gl2_geo_list[i]).grid(column=1,row=1+i)

def get_gl3_geo():
    gl3_geo_amount = int(gl3_geo_spin.get())
    for i in range(1,gl3_geo_amount):
        ttk.Label(glass_geo3,text='Geometry name ' + str(i+1)).grid(column=0,row=1+i,sticky=tk.W)
        ttk.Entry(glass_geo3,width=30,textvariable=gl3_geo_list[i]).grid(column=1,row=1+i)

def get_gl4_geo():
    gl4_geo_amount = int(gl4_geo_spin.get())
    for i in range(1,gl4_geo_amount):
        ttk.Label(glass_geo4,text='Geometry name ' + str(i+1)).grid(column=0,row=1+i,sticky=tk.W)
        ttk.Entry(glass_geo4,width=30,textvariable=gl4_geo_list[i]).grid(column=1,row=1+i)

def get_gl5_geo():
    gl5_geo_amount = int(gl5_geo_spin.get())
    for i in range(1,gl5_geo_amount):
        ttk.Label(glass_geo5,text='Geometry name ' + str(i+1)).grid(column=0,row=1+i,sticky=tk.W)
        ttk.Entry(glass_geo5_width=30,textvariable=gl5_geo_list[i]).grid(column=1,row=1+i)
```

```
def get_gl6_geo():
    gl6_geo_amount = int(gl6_geo_spin.get())
    for i in range(1,gl6_geo_amount):
        ttk.Label(glass_geo6,text='Geometry name ' + str(i+1)).grid(column=0,row=1+i,sticky=tk.W)
        ttk.Entry(glass_geo6,width=30,textvariable=gl6_geo_list[i]).grid(column=1,row=1+i)

def get_gl7_geo():
    gl7_geo_amount = int(gl7_geo_spin.get())
    for i in range(1,gl7_geo_amount):
        ttk.Label(glass_geo7,text='Geometry name ' + str(i+1)).grid(column=0,row=1+i,sticky=tk.W)
        ttk.Entry(glass_geo7,width=30,textvariable=gl7_geo_list[i]).grid(column=1,row=1+i)

def get_gl8_geo():
    gl8_geo_amount = int(gl8_geo_spin.get())
    for i in range(1,gl8_geo_amount):
        ttk.Label(glass_geo8,text='Geometry name ' + str(i+1)).grid(column=0,row=1+i,sticky=tk.W)
        ttk.Entry(glass_geo8,width=30,textvariable=gl8_geo_list[i]).grid(column=1,row=1+i)

def get_gl9_geo():
    gl9_geo_amount = int(gl9_geo_spin.get())
    for i in range(1,gl9_geo_amount):
        ttk.Label(glass_geo9,text='Geometry name ' + str(i+1)).grid(column=0,row=1+i,sticky=tk.W)
        ttk.Entry(glass_geo9,width=30,textvariable=gl9_geo_list[i]).grid(column=1,row=1+i)

def get_gl10_geo():
    gl10_geo_amount = int(gl10_geo_spin.get())
    for i in range(1,gl10_geo_amount):
        ttk.Label(glass_geo10,text='Geometry name ' + str(i+1)).grid(column=0,row=1+i,sticky=tk.W)
        ttk.Entry(glass_geo10,width=30,textvariable=gl10_geo_list[i]).grid(column=1,row=1+i)


# ------------------------------------------------------------------------

gl1_n,gl1_k,gl1_lam = tk.DoubleVar(),tk.DoubleVar(),tk.DoubleVar()
gl2_n,gl2_k,gl2_lam = tk.DoubleVar(),tk.DoubleVar(),tk.DoubleVar()
gl3_n,gl3_k,gl3_lam = tk.DoubleVar(),tk.DoubleVar(),tk.DoubleVar()
gl4_n,gl4_k,gl4_lam = tk.DoubleVar(),tk.DoubleVar(),tk.DoubleVar()
gl5_n,gl5_k,gl5_lam = tk.DoubleVar(),tk.DoubleVar(),tk.DoubleVar()
gl6_n,gl6_k,gl6_lam = tk.DoubleVar(),tk.DoubleVar(),tk.DoubleVar()
gl7_n,gl7_k,gl7_lam = tk.DoubleVar(),tk.DoubleVar(),tk.DoubleVar()
gl8_n,gl8_k,gl8_lam = tk.DoubleVar(),tk.DoubleVar(),tk.DoubleVar()
gl9_n,gl9_k,gl9_lam = tk.DoubleVar(),tk.DoubleVar(),tk.DoubleVar()
gl10_n,gl10_k,gl10_lam = tk.DoubleVar(),tk.DoubleVar(),tk.DoubleVar()
```

```
gl1_weibull_list = [gl1_n,gl1_k,gl1_lam]
gl2_weibull_list = [gl2_n,gl2_k,gl2_lam]
gl3_weibull_list = [gl3_n,gl3_k,gl3_lam]
gl4_weibull_list = [gl4_n,gl4_k,gl4_lam]
gl5_weibull_list = [gl5_n,gl5_k,gl5_lam]
gl6_weibull_list = [gl6_n,gl6_k,gl6_lam]
gl7_weibull_list = [gl7_n,gl7_k,gl7_lam]
gl8_weibull_list = [gl8_n,gl8_k,gl8_lam]
gl9_weibull_list = [gl9_n,gl9_k,gl9_lam]
gl10_weibull_list = [gl10_n,gl10_k,gl10_lam]

weibull_list = ['n','k','lambda [N/m2]']

pdf_colors = ['lightcoral','yellowgreen','plum','mediumspringgreen','sandybrown','deepskyblue','silver','orange','lime','mediumsl
ft_colors =  ['firebrick','olive','darkorchid','seagreen','sienna','steelblue','gray','brown','g','mediumblue']

def plot_weibull(k,lam,frame,ind):
    fig = plt.figure(figsize = (7,4))
    axis = fig.add_subplot(111)
    x = np.linspace(weibull_min.ppf(0.001,k,scale = lam),weibull_min.ppf(0.999,k,scale = lam),100)
    axis.plot(x/10**6,weibull_min.pdf(x,k,scale = lam),color=pdf_colors[ind])
    axis.set_xlabel('f$_t$ [MPa]')
    axis.set_ylabel('Probability density')
    axis.set_title('Probability density function')
    canvas = FigureCanvasTkAgg(fig, master = frame)
    canvas._tkcanvas.grid(column=0,row=4,columnspan=2,sticky=tk.W)

def plot_wei1():
    k = gl1_k.get()
    lam = gl1_lam.get()
    plot_weibull(k,lam,glass_wei1,0)
    plot1_button.configure(text = 'Update plot')

# ------------------------------------------------------------------------
# ------------------------------------------------------------------------

def get_glass_amount():

    gl_amount = int(spin.get())

    for i in range(1,gl_amount):
        ttk.Label(glass_geo,text='Glass type name ' + str(i+1)).grid(column=0,row=i+1,sticky=tk.W)
        ttk.Entry(glass_geo,width=30,textvariable=glass_name_list[i]).grid(column=1,row=i+1)

    if gl_amount == 2:
        tabControl.add(tab3,text='Glass 2')
        tabControl.pack(expand=1,fill='both')
        glass_geo2.grid(column=0,row=0,padx=15,pady=15,sticky=tk.NW)
        gl2_amount_label.grid(column=0,row=0,sticky=tk.W)
        gl2_geo_spin.grid(column=0,row=0,sticky=tk.E)
        gl2_geo1_label.grid(column=0,row=1,sticky=tk.W)
        gl2_geo1_entry.grid(column=1,row=1)

        # WEIBULL
        def plot_wei2():
            k = gl2_k.get()
            lam = gl2_lam.get()
            plot_weibull(k,lam,glass_wei2,1)
            plot2_button.configure(text = 'Update plot')

        glass_wei2.grid(column=1,row=0,padx=15,pady=15,sticky=tk.NW)

        for i in range(len(gl2_weibull_list)):
            ttk.Label(glass_wei2,text=weibull_list[i]).grid(column=0,row=i,sticky=tk.W)
            ttk.Entry(glass_wei2,width=15,textvariable=gl2_weibull_list[i]).grid(column=1,row=i)
        plot2_button = ttk.Button(glass_wei2,text='Plot Weibull pdf - ' + glassname2.get() ,width = 15,command=plot_wei2)
        plot2_button.grid(column=1,row=3)

    if gl_amount == 3:
        tabControl.add(tab4,text='Glass 3')
        tabControl.pack(expand=1,fill='both')
        glass_geo3.grid(column=0,row=0,padx=15,pady=15,sticky=tk.NW)

        gl3_amount_label.grid(column=0,row=0,sticky=tk.W)
        gl3_geo_spin.grid(column=0,row=0,sticky=tk.E)
        gl3_geo1_label.grid(column=0,row=1,sticky=tk.W)
        gl3_geo1_entry.grid(column=1,row=1)

        # WEIBULL
        def plot_wei3():
            k = gl3_k.get()
            lam = gl3_lam.get()
            plot_weibull(k,lam,glass_wei3,2)
            plot3_button.configure(text = 'Update plot')

        glass_wei3.grid(column=1,row=0,padx=15,pady=15,sticky=tk.NW)

        for i in range(len(gl3_weibull_list)):
            ttk.Label(glass_wei3,text=weibull_list[i]).grid(column=0,row=i,sticky=tk.W)
            ttk.Entry(glass_wei3,width=15,textvariable=gl3_weibull_list[i]).grid(column=1,row=i)
        plot3_button = ttk.Button(glass_wei3,text='Plot Weibull pdf - ' + glassname3.get(),width = 15,command=plot_wei3)
        plot3_button.grid(column=1,row=3)
```

```
if gl_amount == 4:
    tabControl.add(tab5,text='Glass 4')
    tabControl.pack(expand=1,fill='both')
    glass_geo4.grid(column=0,row=0,padx=15,pady=15,sticky=tk.NW)

    gl4_amount_label.grid(column=0,row=0,sticky=tk.W)
    gl4_geo_spin.grid(column=0,row=0,sticky=tk.E)
    gl4_geo1_label.grid(column=0,row=1,sticky=tk.W)
    gl4_geo1_entry.grid(column=1,row=1)

    # WEIBULL
    def plot_wei4():
        k = gl4_k.get()
        lam = gl4_lam.get()
        plot_weibull(k,lam,glass_wei4,3)
        plot4_button.configure(text = 'Update plot')

    glass_wei4.grid(column=1,row=0,padx=15,pady=15,sticky=tk.NW)

    for i in range(len(gl4_weibull_list)):
        ttk.Label(glass_wei4,text=weibull_list[i]).grid(column=0,row=i,sticky=tk.W)
        ttk.Entry(glass_wei4,width=15,textvariable=gl4_weibull_list[i]).grid(column=1,row=i)
    plot4_button = ttk.Button(glass_wei4,text='Plot Weibull pdf - ' + glassname4.get(),width = 15,command=plot_wei4)
    plot4_button.grid(column=1,row=3)

if gl_amount == 5:
    tabControl.add(tab6,text='Glass 5')
    tabControl.pack(expand=1,fill='both')
    glass_geo5.grid(column=0,row=0,padx=15,pady=15,sticky=tk.NW)

    gl5_amount_label.grid(column=0,row=0,sticky=tk.W)
    gl5_geo_spin.grid(column=0,row=0,sticky=tk.E)
    gl5_geo1_label.grid(column=0,row=1,sticky=tk.W)
    gl5_geo1_entry.grid(column=1,row=1)

    # WEIBULL
    def plot_wei5():
        k = gl5_k.get()
        lam = gl5_lam.get()
        plot_weibull(k,lam,glass_wei5,4)
        plot5_button.configure(text = 'Update plot')

    glass_wei5.grid(column=1,row=0,padx=15,pady=15,sticky=tk.NW)
    for i in range(len(gl5_weibull_list)):
        ttk.Label(glass_wei5,text=weibull_list[i]).grid(column=0,row=i,sticky=tk.W)
        ttk.Entry(glass_wei5,width=15,textvariable=gl5_weibull_list[i]).grid(column=1,row=i)
    plot5_button = ttk.Button(glass_wei5,text='Plot Weibull pdf - ' + glassname5.get(),width = 15,command=plot_wei5)
    plot5_button.grid(column=1,row=3)

if gl_amount == 6:
    tabControl.add(tab7,text='Glass 6')
    tabControl.pack(expand=1,fill='both')
    glass_geo6.grid(column=0,row=0,padx=15,pady=15,sticky=tk.NW)

    gl6_amount_label.grid(column=0,row=0,sticky=tk.W)
    gl6_geo_spin.grid(column=0,row=0,sticky=tk.E)
    gl6_geo1_label.grid(column=0,row=1,sticky=tk.W)
    gl6_geo1_entry.grid(column=1,row=1)

    # WEIBULL
    def plot_wei6():
        k = gl6_k.get()
        lam = gl6_lam.get()
        plot_weibull(k,lam,glass_wei6,5)
        plot6_button.configure(text = 'Update plot')

    glass_wei6.grid(column=1,row=0,padx=15,pady=15,sticky=tk.NW)

    for i in range(len(gl6_weibull_list)):
        ttk.Label(glass_wei6,text=weibull_list[i]).grid(column=0,row=i,sticky=tk.W)
        ttk.Entry(glass_wei6,width=15,textvariable=gl6_weibull_list[i]).grid(column=1,row=i)
    plot6_button = ttk.Button(glass_wei6,text='Plot Weibull pdf - ' + glassname6.get(),width = 15,command=plot_wei6)
    plot6_button.grid(column=1,row=3)

if gl_amount == 7:
    tabControl.add(tab8,text='Glass 7')
    tabControl.pack(expand=1,fill='both')
    glass_geo7.grid(column=0,row=0,padx=15,pady=15,sticky=tk.NW)

    gl7_amount_label.grid(column=0,row=0,sticky=tk.W)
    gl7_geo_spin.grid(column=0,row=0,sticky=tk.E)
    gl7_geo1_label.grid(column=0,row=1,sticky=tk.W)
    gl7_geo1_entry.grid(column=1,row=1)

    # WEIBULL
    def plot_wei7():
        k = gl7_k.get()
        lam = gl7_lam.get()
        plot_weibull(k,lam,glass_wei7,6)
        plot7_button.configure(text = 'Update plot')

    glass_wei7.grid(column=1,row=0,padx=15,pady=15,sticky=tk.NW)
```

```
        for i in range(len(gl7_weibull_list)):
            ttk.Label(glass_wei7,text=weibull_list[i]).grid(column=0,row=i,sticky=tk.W)
            ttk.Entry(glass_wei7,width=15,textvariable=gl7_weibull_list[i]).grid(column=1,row=i)
        plot7_button = ttk.Button(glass_wei7,text='Plot Weibull pdf - ' + glassname7.get(),width = 15,command=plot_wei7)
        plot7_button.grid(column=1,row=3)

    if gl_amount == 8:
        tabControl.add(tab9,text='Glass 8')
        tabControl.pack(expand=1,fill='both')
        glass_geo8.grid(column=0,row=0,padx=15,pady=15,sticky=tk.NW)

        gl8_amount_label.grid(column=0,row=0,sticky=tk.W)
        gl8_geo_spin.grid(column=0,row=0,sticky=tk.E)
        gl8_geo1_label.grid(column=0,row=1,sticky=tk.W)
        gl8_geo1_entry.grid(column=1,row=1)

        # WEIBULL
        def plot_wei8():
            k = gl8_k.get()
            lam = gl8_lam.get()
            plot_weibull(k,lam,glass_wei8,7)
            plot8_button.configure(text = 'Update plot')

        glass_wei8.grid(column=1,row=0,padx=15,pady=15,sticky=tk.NW)

        for i in range(len(gl8_weibull_list)):
            ttk.Label(glass_wei8,text=weibull_list[i]).grid(column=0,row=i,sticky=tk.W)
            ttk.Entry(glass_wei8,width=15,textvariable=gl8_weibull_list[i]).grid(column=1,row=i)
        plot8_button = ttk.Button(glass_wei8,text='Plot Weibull pdf - ' + glassname8.get(),width = 15,command=plot_wei8)
        plot8_button.grid(column=1,row=3)

    if gl_amount == 9:
        tabControl.add(tab10,text='Glass 9')
        tabControl.pack(expand=1,fill='both')
        glass_geo9.grid(column=0,row=0,padx=15,pady=15,sticky=tk.NW)

        gl9_amount_label.grid(column=0,row=0,sticky=tk.W)
        gl9_geo_spin.grid(column=0,row=0,sticky=tk.E)
        gl9_geo1_label.grid(column=0,row=1,sticky=tk.W)
        gl9_geo1_entry.grid(column=1,row=1)

        # WEIBULL
        def plot_wei9():
            k = gl9_k.get()
            lam = gl9_lam.get()
            plot_weibull(k,lam,glass_wei9,8)
            plot9_button.configure(text = 'Update plot')
        glass_wei9.grid(column=1,row=0,padx=15,pady=15,sticky=tk.NW)

        for i in range(len(gl9_weibull_list)):
            ttk.Label(glass_wei9,text=weibull_list[i]).grid(column=0,row=i,sticky=tk.W)
            ttk.Entry(glass_wei9,width=15,textvariable=gl9_weibull_list[i]).grid(column=1,row=i)
        plot9_button = ttk.Button(glass_wei9,text='Plot Weibull pdf - ' + glassname9.get(),width = 15,command=plot_wei9)
        plot9_button.grid(column=1,row=3)

    if gl_amount == 10:
        tabControl.add(tab11,text='Glass 10')
        tabControl.pack(expand=1,fill='both')
        glass_geo10.grid(column=0,row=0,padx=15,pady=15,sticky=tk.NW)

        gl10_amount_label.grid(column=0,row=0,sticky=tk.W)
        gl10_geo_spin.grid(column=0,row=0,sticky=tk.E)
        gl10_geo1_label.grid(column=0,row=1,sticky=tk.W)
        gl10_geo1_entry.grid(column=1,row=1)

        # WEIBULL
        def plot_wei10():
            k = gl10_k.get()
            lam = gl10_lam.get()
            plot_weibull(k,lam,glass_wei10,9)
            plot10_button.configure(text = 'Update plot')

        glass_wei10.grid(column=1,row=0,padx=15,pady=15,sticky=tk.NW)

        for i in range(len(gl10_weibull_list)):
            ttk.Label(glass_wei10,text=weibull_list[i]).grid(column=0,row=i,sticky=tk.W)
            ttk.Entry(glass_wei10,width=15,textvariable=gl10_weibull_list[i]).grid(column=1,row=i)
        plot10_button = ttk.Button(glass_wei10,text='Plot Weibull pdf - ' + glassname10.get(),width = 15,command=plot_wei10)
        plot10_button.grid(column=1,row=3)

# ---------------------------------------------------------------------------
# ---------------------------------------------------------------------------

other_mat1,other_mat2,other_mat3,other_mat4,other_mat5,other_mat6,other_mat7,other_mat8,other_mat9,other_mat10 = tk.StringVar(),t
other_mat11,other_mat12,other_mat13,other_mat14,other_mat15,other_mat16,other_mat17,other_mat18,other_mat19,other_mat20 = tk.Stri
other_mat21,other_mat22,other_mat23,other_mat24,other_mat25,other_mat26,other_mat27,other_mat28,other_mat29,other_mat30 = tk.Stri

other_mat_list = [other_mat1,other_mat2,other_mat3,other_mat4,other_mat5,other_mat6,other_mat7,other_mat8,other_mat9,other_mat10,
                  other_mat11,other_mat12,other_mat13,other_mat14,other_mat15,other_mat16,other_mat17,other_mat18,other_mat19,othe
                  other_mat21,other_mat22,other_mat23,other_mat24,other_mat25,other_mat26,other_mat27,other_mat28,other_mat29,othe
```

```
def get_other_mat():
    other_mat_amount = int(other_mat_spin.get())

    for i in range(1,other_mat_amount):
        ttk.Label(other_mat_frame,text='Material name ' + str(i+1)).grid(column=0,row=i+1,sticky=tk.W)
        ttk.Entry(other_mat_frame,width=30,textvariable=other_mat_list[i]).grid(column=1,row=i+1)

# ---------------------------------------------------------------------------
spin = Spinbox(glass_geo,from_=1,to=10,width=5,command=get_glass_amount)
spin.grid(column=1,row=0,sticky=tk.E)

ttk.Label(glass_geo,text = 'Glass type name 1').grid(column=0,row=1,sticky=tk.W)
ttk.Entry(glass_geo,width=30,textvariable=glass_name_list[0]).grid(column=1,row=1)

# Glass geometries ----------------------------------------------------------
tab11 = ttk.Frame(tabControl)
glass_geo10 = ttk.LabelFrame(tab11,text='Names of DIANA glass geometries - Glass type 10')
gl10_geo_spin = Spinbox(glass_geo10,from_=1,to=30,width=5,command=get_gl10_geo)
gl10_amount_label = ttk.Label(glass_geo10,text='Amount')
gl10_geo1_label = ttk.Label(glass_geo10,text = 'Geometry name 1')
gl10_geo1_entry = ttk.Entry(glass_geo10,width=30,textvariable=gl10_geo_list[0])
glass_wei10 = ttk.LabelFrame(tab11,text='Weibull parameters for tensile strength distribution')

tab10 = ttk.Frame(tabControl)
glass_geo9 = ttk.LabelFrame(tab10,text='Names of DIANA glass geometries - Glass type 9')
gl9_geo_spin = Spinbox(glass_geo9,from_=1,to=30,width=5,command=get_gl9_geo)
gl9_amount_label = ttk.Label(glass_geo9,text='Amount')
gl9_geo1_label = ttk.Label(glass_geo9,text = 'Geometry name 1')
gl9_geo1_entry = ttk.Entry(glass_geo9,width=30,textvariable=gl9_geo_list[0])
glass_wei9 = ttk.LabelFrame(tab10,text='Weibull parameters for tensile strength distribution')

tab9 = ttk.Frame(tabControl)
glass_geo8 = ttk.LabelFrame(tab9,text='Names of DIANA glass geometries - Glass type 8')
gl8_geo_spin = Spinbox(glass_geo8,from_=1,to=30,width=5,command=get_gl8_geo)
gl8_amount_label = ttk.Label(glass_geo8,text='Amount')
gl8_geo1_label = ttk.Label(glass_geo8,text = 'Geometry name 1')
gl8_geo1_entry = ttk.Entry(glass_geo8,width=30,textvariable=gl8_geo_list[0])
glass_wei8 = ttk.LabelFrame(tab9,text='Weibull parameters for tensile strength distribution')

tab8 = ttk.Frame(tabControl)
glass_geo7 = ttk.LabelFrame(tab8,text='Names of DIANA glass geometries - Glass type 2')
gl7_geo_spin = Spinbox(glass_geo7,from_=1,to=30,width=5,command=get_gl7_geo)
gl7_amount_label = ttk.Label(glass_geo7,text='Amount')
gl7_geo1_label = ttk.Label(glass_geo7,text = 'Geometry name 1')
gl7_geo1_entry = ttk.Entry(glass_geo7,width=30,textvariable=gl7_geo_list[0])
glass_wei7 = ttk.LabelFrame(tab8,text='Weibull parameters for tensile strength distribution')
```

```
tab7 = ttk.Frame(tabControl)
glass_geo6 = ttk.LabelFrame(tab7,text='Names of DIANA glass geometries - Glass type 6')
gl6_geo_spin = Spinbox(glass_geo6,from_=1,to=30,width=5,command=get_gl6_geo)
gl6_amount_label = ttk.Label(glass_geo6,text='Amount')
gl6_geo1_label = ttk.Label(glass_geo6,text = 'Geometry name 1')
gl6_geo1_entry = ttk.Entry(glass_geo6,width=30,textvariable=gl6_geo_list[0])
glass_wei6 = ttk.LabelFrame(tab7,text='Weibull parameters for tensile strength distribution')

tab6 = ttk.Frame(tabControl)
glass_geo5 = ttk.LabelFrame(tab6,text='Names of DIANA glass geometries - Glass type 5')
gl5_geo_spin = Spinbox(glass_geo5,from_=1,to=30,width=5,command=get_gl5_geo)
gl5_amount_label = ttk.Label(glass_geo5,text='Amount')
gl5_geo1_label = ttk.Label(glass_geo5,text = 'Geometry name 1')
gl5_geo1_entry = ttk.Entry(glass_geo5,width=30,textvariable=gl5_geo_list[0])
glass_wei5 = ttk.LabelFrame(tab6,text='Weibull parameters for tensile strength distribution')

tab5 = ttk.Frame(tabControl)
glass_geo4 = ttk.LabelFrame(tab5,text='Names of DIANA glass geometries - Glass type 4')
gl4_geo_spin = Spinbox(glass_geo4,from_=1,to=30,width=5,command=get_gl4_geo)
gl4_amount_label = ttk.Label(glass_geo4,text='Amount')
gl4_geo1_label = ttk.Label(glass_geo4,text = 'Geometry name 1')
gl4_geo1_entry = ttk.Entry(glass_geo4,width=30,textvariable=gl4_geo_list[0])
glass_wei4 = ttk.LabelFrame(tab5,text='Weibull parameters for tensile strength distribution')

tab4 = ttk.Frame(tabControl)
glass_geo3 = ttk.LabelFrame(tab4,text='Names of DIANA glass geometries - Glass type 3')
gl3_geo_spin = Spinbox(glass_geo3,from_=1,to=30,width=5,command=get_gl3_geo)
gl3_amount_label = ttk.Label(glass_geo3,text='Amount')
gl3_geo1_label = ttk.Label(glass_geo3,text = 'Geometry name 1')
gl3_geo1_entry = ttk.Entry(glass_geo3,width=30,textvariable=gl3_geo_list[0])
glass_wei3 = ttk.LabelFrame(tab4,text='Weibull parameters for tensile strength distribution')

tab3 = ttk.Frame(tabControl)
glass_geo2 = ttk.LabelFrame(tab3,text='Names of DIANA glass geometries - Glass type 2')
gl2_geo_spin = Spinbox(glass_geo2,from_=1,to=30,width=5,command=get_gl2_geo)
gl2_amount_label = ttk.Label(glass_geo2,text='Amount')
gl2_geo1_label = ttk.Label(glass_geo2,text = 'Geometry name 1')
gl2_geo1_entry = ttk.Entry(glass_geo2,width=30,textvariable=gl2_geo_list[0])
glass_wei2 = ttk.LabelFrame(tab3,text='Weibull parameters for tensile strength distribution')

ttk.Label(glass_geo1,text='Amount').grid(column=0,row=0,sticky=tk.W)
gl1_geo_spin = Spinbox(glass_geo1,from_=1,to=30,width=5,command=get_gl1_geo)
gl1_geo_spin.grid(column=0,row=0,sticky=tk.E)
ttk.Label(glass_geo1,text='Geometry name 1').grid(column=0,row=1,sticky=tk.W)
ttk.Entry(glass_geo1,width=30,textvariable=gl1_geo_list[0]).grid(column=1,row=1)
```

```
# ------------------------------------------------------------------------------
glass_wei1 = ttk.LabelFrame(tab2,text='Weibull parameters for tensile strength distribution')
glass_wei1.grid(column=1,row=0,padx=15,pady=15,sticky=tk.NW)

for i in range(len(gl1_weibull_list)):
    ttk.Label(glass_wei1,text=weibull_list[i]).grid(column=0,row=i,sticky=tk.W)
    ttk.Entry(glass_wei1,width=15,textvariable=gl1_weibull_list[i]).grid(column=1,row=i)
plot1_button = ttk.Button(glass_wei1,text='Plot Weibull pdf',width = 15,command=plot_wei1)
plot1_button.grid(column=1,row=3)

# ------------------------------------------------------------------------------
mat_amount_label = ttk.Label(other_mat_frame,text='Amount of other materials in DIANA model').grid(column=0,row=0,sticky=tk.W)

other_mat_spin = Spinbox(other_mat_frame,from_=1,to=10,width=5,command=get_other_mat)
other_mat_spin.grid(column=1,row=0,sticky=tk.E)

ttk.Label(other_mat_frame,text = 'Material name 1').grid(column=0,row=1,sticky=tk.W)
ttk.Entry(other_mat_frame,width=30,textvariable=other_mat_list[0]).grid(column=1,row=1)
```

Writing the .dat file

All the things that will happen when you press the 'Write DIANA .dat file' button in the GUI.

```
# WRITING THE .DAT FILE ========================================================
# ==============================================================================
# ==============================================================================

tab_plots = ttk.Frame(tabControl)
plot_frame = ttk.LabelFrame(tab_plots,text='Combined Weibull plots including drawn tensile strengths')

def write_dat_file():
    # Get all the input ------------------------------------------------------------
    # ------------------------------------------------------------------------------

    # New .dat file name
    filename = new_dat_file.get()

    # Amount of glass types and their names
    gl_amount = int(spin.get())
    glass_name = glassname.get()
    glass_name2 = glassname2.get()
    glass_name3 = glassname3.get()
    glass_name4 = glassname4.get()
    glass_name5 = glassname5.get()
    glass_name6 = glassname6.get()
    glass_name7 = glassname7.get()
    glass_name8 = glassname8.get()
    glass_name9 = glassname9.get()
    glass_name10 = glassname10.get()
    gl_names = [glass_name,glass_name2,glass_name3,glass_name4,glass_name5,glass_name6,
          glass_name7,glass_name8,glass_name9,glass_name10]
    for i in range(len(gl_names)):
        if gl_names[i] == '':
            gl_names = gl_names[:i]
            break

    # Material properties of the glass
    E = '%.5E' % E_modulus.get()
    nu = '%.5E' % poisson.get()
    rho = '%.5E' % density.get()
    restatst = '%.5E' % rest_ft.get()

    # Names of the DIANA geometries made of glass
    set_names1 = [gl1_geo1.get(),gl1_geo2.get(),gl1_geo3.get(),gl1_geo4.get(),gl1_geo5.get(),gl1_geo6.get(),gl1_geo7.get(),gl1_ge
                gl1_geo11.get(),gl1_geo12.get(),gl1_geo13.get(),gl1_geo14.get(),gl1_geo15.get(),gl1_geo16.get(),gl1_geo17.get(),gl
                gl1_geo21.get(),gl1_geo22.get(),gl1_geo23.get(),gl1_geo24.get(),gl1_geo25.get(),gl1_geo26.get(),gl1_geo27.get(),gl
    set_names2 = [gl2_geo1.get(),gl2_geo2.get(),gl2_geo3.get(),gl2_geo4.get(),gl2_geo5.get(),gl2_geo6.get(),gl2_geo7.get(),gl2_ge
                gl2_geo11.get(),gl2_geo12.get(),gl2_geo13.get(),gl2_geo14.get(),gl2_geo15.get(),gl2_geo16.get(),gl2_geo17.get(),gl
                gl2_geo12.get(),gl2_geo22.get(),gl2_geo23.get(),gl2_geo24.get(),gl2_geo25.get(),gl2_geo26.get(),gl2_geo27.get(),gl
    set_names3 = [gl3_geo1.get(),gl3_geo2.get(),gl3_geo3.get(),gl3_geo4.get(),gl3_geo5.get(),gl3_geo6.get(),gl3_geo7.get(),gl3_ge
                gl3_geo11.get(),gl3_geo12.get(),gl3_geo13.get(),gl3_geo14.get(),gl3_geo15.get(),gl3_geo16.get(),gl3_geo17.get(),gl
                gl3_geo12.get(),gl3_geo22.get(),gl3_geo23.get(),gl3_geo24.get(),gl3_geo25.get(),gl3_geo26.get(),gl3_geo27.get(),gl
    set_names4 = [gl4_geo1.get(),gl4_geo2.get(),gl4_geo3.get(),gl4_geo4.get(),gl4_geo5.get(),gl4_geo6.get(),gl4_geo7.get(),gl4_ge
                gl4_geo11.get(),gl4_geo12.get(),gl4_geo13.get(),gl4_geo14.get(),gl4_geo15.get(),gl4_geo16.get(),gl4_geo17.get(),gl
                gl4_geo12.get(),gl4_geo22.get(),gl4_geo23.get(),gl4_geo24.get(),gl4_geo25.get(),gl4_geo26.get(),gl4_geo27.get(),gl
    set_names5 = [gl5_geo1.get(),gl5_geo2.get(),gl5_geo3.get(),gl5_geo4.get(),gl5_geo5.get(),gl5_geo6.get(),gl5_geo7.get(),gl5_ge
                gl5_geo11.get(),gl5_geo12.get(),gl5_geo13.get(),gl5_geo14.get(),gl5_geo15.get(),gl5_geo16.get(),gl5_geo17.get(),gl
                gl5_geo12.get(),gl5_geo22.get(),gl5_geo23.get(),gl5_geo24.get(),gl5_geo25.get(),gl5_geo26.get(),gl5_geo27.get(),gl
    set_names6 = [gl6_geo1.get(),gl6_geo2.get(),gl6_geo3.get(),gl6_geo4.get(),gl6_geo5.get(),gl6_geo6.get(),gl6_geo7.get(),gl6_ge
                gl6_geo11.get(),gl6_geo12.get(),gl6_geo13.get(),gl6_geo14.get(),gl6_geo15.get(),gl6_geo16.get(),gl6_geo17.get(),gl
                gl6_geo12.get(),gl6_geo22.get(),gl6_geo23.get(),gl6_geo24.get(),gl6_geo25.get(),gl6_geo26.get(),gl6_geo27.get(),gl
    set_names7 = [gl7_geo1.get(),gl7_geo2.get(),gl7_geo3.get(),gl7_geo4.get(),gl7_geo5.get(),gl7_geo6.get(),gl7_geo7.get(),gl7_ge
                gl7_geo11.get(),gl7_geo12.get(),gl7_geo13.get(),gl7_geo14.get(),gl7_geo15.get(),gl7_geo16.get(),gl7_geo17.get(),gl
                gl7_geo12.get(),gl7_geo22.get(),gl7_geo23.get(),gl7_geo24.get(),gl7_geo25.get(),gl7_geo26.get(),gl7_geo27.get(),gl
    set_names8 = [gl8_geo1.get(),gl8_geo2.get(),gl8_geo3.get(),gl8_geo4.get(),gl8_geo5.get(),gl8_geo6.get(),gl8_geo7.get(),gl8_ge
                gl8_geo11.get(),gl8_geo12.get(),gl8_geo13.get(),gl8_geo14.get(),gl8_geo15.get(),gl8_geo16.get(),gl8_geo17.get(),gl
                gl8_geo12.get(),gl8_geo22.get(),gl8_geo23.get(),gl8_geo24.get(),gl8_geo25.get(),gl8_geo26.get(),gl8_geo27.get(),gl
```

```
set_names9 = [gl9_geo1.get(),gl9_geo2.get(),gl9_geo3.get(),gl9_geo4.get(),gl9_geo5.get(),gl9_geo6.get(),gl9_geo7.get(),gl9_ge
              gl9_geo11.get(),gl9_geo12.get(),gl9_geo13.get(),gl9_geo14.get(),gl9_geo15.get(),gl9_geo16.get(),gl9_geo17.get(),gl
              gl9_geo12.get(),gl9_geo22.get(),gl9_geo23.get(),gl9_geo24.get(),gl9_geo25.get(),gl9_geo26.get(),gl9_geo27.get(),gl
set_names10 = [gl10_geo1.get(),gl10_geo2.get(),gl10_geo3.get(),gl10_geo4.get(),gl10_geo5.get(),gl10_geo6.get(),gl10_geo7.get(
              gl10_geo11.get(),gl10_geo12.get(),gl10_geo13.get(),gl10_geo14.get(),gl10_geo15.get(),gl10_geo16.get(),gl10_geo17.g
              gl10_geo12.get(),gl10_geo22.get(),gl10_geo23.get(),gl10_geo24.get(),gl10_geo25.get(),gl10_geo26.get(),gl10_geo27.g

set_names = [set_names1,set_names2,set_names3,set_names4,set_names5,
             set_names6,set_names7,set_names8,set_names9,set_names10]

for i in range(len(set_names)):
    for j in range(len(set_names[i])):
        if set_names[i][j] == '':
            set_names[i] = set_names[i][:j]
            break
    if set_names[i] == []:
        set_names = set_names[:i]
        break

# Weibull parameters
n_list = [gl1_n.get(),gl2_n.get(),gl3_n.get(),gl4_n.get(),gl5_n.get(),gl6_n.get(),gl7_n.get(),
          gl8_n.get(),gl9_n.get(),gl10_n.get()]
k_list = [gl1_k.get(),gl2_k.get(),gl3_k.get(),gl4_k.get(),gl5_k.get(),gl6_k.get(),gl7_k.get(),
          gl8_k.get(),gl9_k.get(),gl10_k.get()]
lam_list = [gl1_lam.get(),gl2_lam.get(),gl3_lam.get(),gl4_lam.get(),gl5_lam.get(),gl6_lam.get(),gl7_lam.get(),
          gl8_lam.get(),gl9_lam.get(),gl10_lam.get()]

n_list = n_list[:gl_amount]
for i in range(len(n_list)):
    n_list[i] = int(n_list[i])
k_list = k_list[:gl_amount]
lam_list = lam_list[:gl_amount]

# Other material names in DIANA model
material_names = [other_mat1.get(),other_mat2.get(),other_mat3.get(),other_mat4.get(),other_mat5.get(),other_mat6.get(),other
              other_mat11.get(),other_mat12.get(),other_mat13.get(),other_mat14.get(),other_mat15.get(),other_mat16.get(),othe
              other_mat21.get(),other_mat22.get(),other_mat23.get(),other_mat24.get(),other_mat25.get(),other_mat26.get(),othe

other_mat_amount = int(other_mat_spin.get())
material_names = material_names[:other_mat_amount]
# Material properties - Weibull ------------------------------------------------------------
# ------------------------------------------------------------------------------------------
```

```
f_t,pdf,x,P_ft,weight_sets = [[] for i in range(gl_amount)],[[] for i in range(gl_amount)],[[] for i in range(gl_amount)],[[]
pdf_max = np.zeros(gl_amount)
for i in range(gl_amount):
    f_t[i] = list(weibull_min.rvs(k_list[i], loc=0, scale=lam_list[i], size = n_list[i]))
    pdf[i] = list(weibull_min.pdf(f_t[i],k_list[i], loc=0, scale=lam_list[i]))
    x[i] = list(np.linspace(weibull_min.ppf(0.001,k_list[i],scale = lam_list[i]),weibull_min.ppf(0.999,k_list[i],scale = lam_
    pdf_max[i] = max(weibull_min.pdf(x[i],k_list[i],scale = lam_list[i]))
    pdf_max = list(pdf_max)

legend = list()
for i in range(gl_amount):
    legend.append(gl_names[i] + ' - pdf')
    legend.append(gl_names[i] + ' - drawn ft')

tabControl.add(tab_plots,text='Combined plots')
tabControl.pack(expand=1,fill='both')
plot_frame.grid(row=0,column=0)

fig = plt.figure(figsize = (13,6))
axis = fig.add_subplot(111)
for i in range(gl_amount):
    xi = x[i]
    fti = f_t[i]
    axis.plot(np.array(xi)/10**6,weibull_min.pdf(x[i],k_list[i],scale = lam_list[i]),color=pdf_colors[i])
    axis.plot(np.array(fti)/10**6,pdf[i],'o',color=ft_colors[i])

axis.set_xlabel('f$_t$ [MPa]')
axis.set_ylabel('Probability density')
axis.set_title('Pdf and drawn tensile strengths per glass type')
axis.legend(legend)
canvas = FigureCanvasTkAgg(fig, master = plot_frame)
canvas._tkcanvas.grid(column=0,row=0)

def save_graph():
    plt.savefig(filename + '.png', bbox_inches='tight')
    save_plot_button.configure(text='Plot has been saved')

save_plot_button = ttk.Button(plot_frame,text = 'Save plot as png',command=save_graph)
save_plot_button.grid(column=0,row=1,sticky=tk.W)

for i in range(len(f_t)):
    P_ft[i] = pdf[i]/pdf_max[i]
list(P_ft)
for i in range(len(f_t)):
    weight_sets[i]= list(P_ft[i]/sum(P_ft[i])) # Percentages of how many elements will get that tensile strength
```

```
# Print COORDINATES part of .dat file ------------------------------------------------------
# ------------------------------------------------------------------------------------------

# Copy the directions and coordinates of the existing file to the new file
def COORDINATES():
    for i in range(len(lines)):
        file.write(lines[i] + '\n')
        if "'MATERI'" in lines[i]:
            break

# Shuffling the elements -------------------------------------------------------------------
# ------------------------------------------------------------------------------------------

# Get the elements made of glass from the existing .dat file
mat_lst = list() # Insanely long materials list
for i in range(1,400):
    mat_lst.append("MATERIAL " + str(i))

index1 = lines.index("'MATERI'")
index2 = lines.index('CONNECT')

def elements(gl_name,set_names):
    # Find which material number belongs to the material Glass used in the Diana file
    def matnr_glass(gl_name):
        splt = list()
        for i in range(index1,index2):
            line = lines[i]
            split = line.split()
            splt.extend(split)
        glasss = splt.index('"' + gl_name + '"')
        matnr_glass = splt[glasss-2]
        return(matnr_glass)
    matnr_glass = matnr_glass(gl_name)

     # Find the last line in the existing .dat file where the material Glass is used for a set
    inv_lines = lines[::-1]
    index4 = len(lines) - inv_lines.index(mat_lst[int(matnr_glass)-1]) - 1
    ind_till_mat = lines.index(mat_lst[int(matnr_glass)-1])
    lines_till_mat = lines[:ind_till_mat]
    invlines_till_mat = lines_till_mat[::-1]
    index3 = ind_till_mat - invlines_till_mat.index('CONNECT')
```

```
    def element_list(set_names):
        # Get the list with elements who are made of glass
        element_list = lines[index3:index4]
        for i in range(len(set_names)):
            # Remove the lines without elements (MATERIAL, SET.. , CONNECT)
            element_list = [e for e in element_list if e not in ('CONNECT','SET  "' + set_names[i] + '"', mat_lst[int(matnr_g
        return(element_list)
    return(element_list(set_names),matnr_glass,index3,index4)

element_list = [[] for i in range(gl_amount)]
matnr_glass = np.zeros(gl_amount)
for i in range(gl_amount):
    element_list[i] = list(elements(gl_names[i],set_names[i])[0])
    matnr_glass[i] = elements(gl_names[i],set_names[i])[1]
    matnr_glass = list(matnr_glass)

# Place of the first element number of a glass type in the to be shuffled  glass element list
def first_element_number(element_list):
    line = element_list[0]
    split = line.split()
    el_no1 = int(split[0])
    return(el_no1)

el_no1 = [[] for i in range(gl_amount)]
for i in range(gl_amount):
    el_no1[i] = first_element_number(element_list[i])

# Shuffle the elements and put them in n number of element sets with different glass material properties
# ------------------------------------------------------------------------------------------
# ------------------------------------------------------------------------------------------

def random_list(element_list,set1,set2,weight_sets):
    # Number of elements differ from length of list due to new lines in the file, I want to know the number of elements

    fl = list(np.ones(len(element_list)))
    for i in range(len(element_list)):
        fl[i] = int(fl[i])
        if element_list[i][7] == ' ': # Find places were an extra line is present in the element set list
            fl[i] = 0

    # Number of elements in element list
    length = len(element_list) - fl.count(0)
```

```
# Get a list with the indices of the places were an extra line is present in the element set list
len_ind = fl.count(0)
ind = np.zeros(len_ind)
reverse = fl[::-1]
ind_end = len(fl) - reverse.index(0) - 1
for i in range(1,len_ind):
    ind[0] = fl.index(0)
    fl_new = fl[int(ind[i-1])+1:]
    ind[i] = ind[i-1] + fl_new.index(0) + 1
    if i == ind_end:
        break
ind = [0] + list(ind) + [len(fl)]

# Define the number of elements in every set.
# When the numbers are rounded the number of elements can be not equal to n
# Therefore if there is an element missing there is one added to the biggest group
# If there is an element too much one will be substracted from the smallest group
def no_el_sets():
    q = []
    for i in range(1,set2+1):
        p = int(round(length*weight_sets[i-1],0))
        q.append(p)
    if sum(q) < length:
        for i in range(len(q)):
            if q[i] == max(q):
                q[i] = q[i] + (length - sum(q))
                break
    if sum(q) > length:
        for i in range(len(q)):
            if q[i] == min(q) and q[i] >= (sum(q) - length):
                q[i] = q[i] - (sum(q) - length)
                break
    return(q)

# Make a shuffled list of 1 to n (set number) with the calculated number of elements per set
# For more glass materials, the counting should start from n and go to n2 etc.
c = []
for i in range(set1+1,set1+set2+1):
    b = int(i)*np.ones(no_el_sets()[i-set1-1])
    c.extend(b)
np.random.shuffle(c)
```

```
# Assign the random numbers between 1 and n to the right place in a list.
# Where an extra line is present put 0
cb = list()
for i in range(1,len(ind)):
    ca = c[sum(fl[:int(ind[i-1])]):sum(fl[:int(ind[i])])]
    cb.append(ca)
for i in range(len(cb)):
    cb[i].extend([0])

rndm = list(itertools.chain(*cb))
rndm = rndm[:-1]

# Give the extra lines the same number as the line before it
for i in range(len(rndm)):
    if rndm[i] == 0:
        rndm[i] = rndm[i-1]

# Assign the different elements to a set
setsss = list()
sets = [[] for i in range(set2)]
for i in range(len(element_list)):
    setss = str(rndm[i]) + str(element_list[i])
    setsss.append(setss)
    for j in range(set2):
        if rndm[i] == (j+set1+1):
            sets[j].append(setsss[i])

# Remove the old element numbers
for i in range(set2):
    for j in range(len(sets[i])):
        if sets[i][j][6] != ' ' and i+set1 < 9:
            sets[i][j] = sets[i][j][8:]
        elif sets[i][j][6] == ' ' and i+set1 < 9:
            sets[i][j] = sets[i][j][15:]
        elif sets[i][j][6] != ' ' and i+set1 < 99:
            sets[i][j] = sets[i][j][9:]
        elif sets[i][j][6] == ' ' and i+set1 < 99:
            sets[i][j] = sets[i][j][16:]
        elif sets[i][j][6] != ' ' and i+set1 < 999:
            sets[i][j] = sets[i][j][10:]
        elif sets[i][j][6] == ' ' and i+set1 < 999:
            sets[i][j] = sets[i][j][17:]

        if sets[i][j][0] == ' ':
            sets[i][j] = sets[i][j][1:]
```

```
    length = np.zeros(gl_amount)
    sets = [[] for i in range(gl_amount)]
    n = [0] + n_list
    for i in range(gl_amount):
        length[i] = random_list(element_list[i],n[i],n[i+1],weight_sets[i])[0]
        length = list(length)
        sets[i] = random_list(element_list[i],n[i],n[i+1],weight_sets[i])[1]

    # Create the list with new element numbers at the beginning of the lines. --------------------
    # ---------------------------------------------------------------------------------------------

    def element_nr_list(el_no,length,sets,element_list,n):
        # List of numbers counting from first element number in glass material set (el_no) to number of elements
        numbers1 = np.arange(length) + [el_no]
        numbers = list()
        for i in range(len(numbers1)):
            number = [numbers1[i]]
            numbers.extend(number)

        # Indices of the places in the element set matrix where extra lines are
        # (New places, since the lines are shuffled)
        sets_ind = [[] for s in range(n)]
        sets_ind2 = list()
        for i in range(len(sets)):
            for j in range(len(sets[i])):
                if sets[i][j][0].isdigit() == True:
                    sets_ind[i] = [i,j]
                sets_ind3 = sets_ind[i]
                sets_ind2.append(sets_ind3)
        sets_index = list(np.unique(sets_ind2))
        sets_index.remove([])

        # The length of each set
        num_ind = list()
        len_sets = list()
        for i in range(len(sets)):
            lensets = len(sets[i])
            len_sets.append(lensets)
        len_sets = [0] + len_sets[:-1] # Add zero at begin of list
        len_set = list()
        for i in range(0,len(len_sets)):
            len_set.append(len_sets[i] + sum(len_sets[:i])) # Sum to get length set + lengths of sets before that set

        # Add the found indices of the element set matrix to the number of elements in the element sets before it to get
        # the right indices in the row of elements where an extra line is present.
        # This creates a row of indices instead of a matrix with indices.
        # Necessary to do this again since all elements are shuffled.
        no = np.arange(n)
        def indd(no):
            extr_index = list()
            for i in range(len(sets_index)):
                if sets_index[i][0] == no:
                    index = sets_index[i][1] + len_set[no]
                    extr_index.append(index)
            return(extr_index)
        extr_index = list()
        for i in range(len(no)):
            extr_index.extend(indd(no[i]))
        extr_index = [0] + extr_index + [len(element_list)]
    #     print(extr_index)

        # Create a row with numbers counting from the first element number to number of elements in FE model
        # with 0's where an extra line is present
        def el_numbers():
            el_number = np.zeros(len(element_list))
            for i1 in range(1,len(extr_index)-1):
                for i in range(extr_index[0],extr_index[1]):
                    el_number[i] = numbers[i]
                ind_beg = extr_index[i1] - (i1 - 1)
                ind_end = extr_index[i1+1] - (i1)
                for i in range(ind_beg,ind_end):
                    el_number[i+i1] = numbers[i]
            return(el_number)

        el_number = list(el_numbers())
        len_set = len_set + [len(element_list)]
        return(el_number,len_set)

    len_set = [[] for i in range(gl_amount)]
    el_number = [[] for i in range(gl_amount)]
    for i in range(gl_amount):
        len_set[i] = element_nr_list(el_no1[i],length[i],sets[i],element_list[i],n[i+1])[1]
        el_number[i] = element_nr_list(el_no1[i],length[i],sets[i],element_list[i],n[i+1])[0]

    # Write MATERI part of .dat file --------------------------------------------------------------
    # ---------------------------------------------------------------------------------------------

    n_tot = sum(n)
    last_matnr_glass = matnr_glass[-1]
```

```
    # Get new numbers (starting from n+1) in front of the materials that are not glass
    mat_other_ind = lines.index('    ' + str(int(last_matnr_glass) + 1) + ' NAME    ' + '"' + material_names[0] + '"')
    mat_other_lines = lines[mat_other_ind:index2-2]

    mat_new_lines = list()
    mat_new_lins = list()
    for i in range(len(material_names)):
        if int(n_tot) + 1 + int(i) <= 9:
            mat_new_lins = '    ' + str(int(n_tot) + 1 + int(i)) + ' NAME    ' + '"' + material_names[i] + '"'
        elif int(n_tot) + 1 + int(i) <= 99:
            mat_new_lins = '   ' + str(int(n_tot) + 1 + int(i)) + ' NAME    ' + '"' + material_names[i] + '"'
        elif int(n_tot) + 1 + int(i) <= 999:
            mat_new_lins = '  ' + str(int(n_tot) + 1 + int(i)) + ' NAME    ' + '"' + material_names[i] + '"'
        elif int(n_tot) + 1 + int(i) <= 9999:
            mat_new_lins = ' ' + str(int(n_tot) + 1 + int(i)) + ' NAME    ' + '"' + material_names[i] + '"'
        mat_new_lines.append(mat_new_lins)

    for i in range(len(material_names)):
        mat_other_lines = [x if x != ('    ' + str(int(last_matnr_glass) + 1 + int(i)) + ' NAME    ' + '"' + material_names[i] + '"
                           else mat_new_lines[i] for x in mat_other_lines]

    def write_gl_mat(glass_name,set1,set2,f_t):
        # Print all the new glass materials to the new .dat file
        materi = list() # Material names
        for i in range(set1+1,set1+set2+1):
            materi.append(glass_name + ' ' + str(i-set1))
            if i <= 9:
                file.write('    ' + str(i) + ' NAME    ' + '"' + materi[i-set1-1] + '"' + '\n')
            elif i <= 99:
                file.write('   ' + str(i) + ' NAME    ' + '"' + materi[i-set1-1] + '"' + '\n')
            elif i <= 999:
                file.write('  ' + str(i) + ' NAME    ' + '"' + materi[i-set1-1] + '"' + '\n')
            elif i <= 9999:
                file.write(str(i) + ' NAME    ' + '"' + materi[i-set1-1] + '"' + '\n')
            file.write('      ' + 'MCNAME CONCR\n' +
                       '      ' + 'MATMDL TSCR\n' +
                       '      ' + 'ASPECT\n' +
                       '      ' + 'YOUNG     ' + str(E) + '\n' +
                       '      ' + 'POISON    ' + str(nu) + '\n' +
                       '      ' + 'DENSIT    ' + str(rho) + '\n' +
                       '      ' + 'TOTCRK ROTATE\n' +
                       '      ' + 'TENCRV BRITTL\n' +
                       '      ' + 'TENSTR    ' + str('%.5E' % f_t[i-set1-1]) + '\n' +
                       '      ' + 'RESTST    ' + str(reststst) + '\n' +
                       '      ' + 'POIRED NONE\n' +
                       '      ' + 'COMCRV ELASTI\n')
```

```
    def MATERI():
        for i in range(gl_amount):
            write_gl_mat(gl_names[i],n[i],n[i+1],f_t[i])

        # Print all the other materials to the new .dat file
        for i in range(len(mat_other_lines)):
            file.write(mat_other_lines[i]+'\n')

    # Write ELEMENTS part of .dat file ------------------------------------------------------------
    # ---------------------------------------------------------------------------------------------

    index3 = elements(gl_names[0],set_names[0])[2] # First element that belongs to glass
    index4 = elements(gl_names[-1],set_names[-1])[3] # Last element that belongs to glass
    index5 = lines.index("'LOADS'")

    def ELEMENTS_glass(n,len_set,el_number,sets):
        for k in range(n):
            for i in range(len_set[k],len_set[k+1]):
                    w = i - len_set[k]
                    if el_number[i] <= 9 and el_number[i] != 0 and sets[k][w][6] == ' ':
                        sets[k][w] = str('    ') + str(int(el_number[i])) + ' ' + str(sets[k][w][:5]) + '  ' + str(sets[k][w][7:])
                    elif el_number[i] <= 9 and el_number[i] != 0 and sets[k][w][6] != ' ':
                        sets[k][w] = str('    ') + str(int(el_number[i])) + ' ' + str(sets[k][w][:5]) + '  ' + str(sets[k][w][6:])

                    elif el_number[i] <= 99 and el_number[i] != 0 and sets[k][w][6] == ' ':
                        sets[k][w] = str('   ') + str(int(el_number[i])) + ' ' + str(sets[k][w][:5]) + '  ' + str(sets[k][w][7:])
                    elif el_number[i] <= 99 and el_number[i] != 0 and sets[k][w][6] != ' ':
                        sets[k][w] = str('   ') + str(int(el_number[i])) + ' ' + str(sets[k][w][:5]) + '  ' + str(sets[k][w][6:])

                    elif el_number[i] <= 999 and el_number[i] != 0 and sets[k][w][6] == ' ':
                        sets[k][w] = str('  ') + str(int(el_number[i])) + ' ' + str(sets[k][w][:5]) + '  ' + str(sets[k][w][7:])
                    elif el_number[i] <= 999 and el_number[i] != 0 and sets[k][w][6] != ' ':
                        sets[k][w] = str('  ') + str(int(el_number[i])) + ' ' + str(sets[k][w][:5]) + '  ' + str(sets[k][w][6:])

                    elif el_number[i] <= 9999 and el_number[i] != 0 and sets[k][w][6] == ' ':
                        sets[k][w] = str(int(el_number[i])) + ' ' + str(sets[k][w][:5]) + '  ' + str(sets[k][w][7:])
                    elif el_number[i] <= 9999 and el_number[i] != 0 and sets[k][w][6] != ' ':
                        sets[k][w] = str(int(el_number[i])) + ' ' + str(sets[k][w][:5]) + '  ' + str(sets[k][w][6:])

                    elif el_number[i] != 0 and sets[k][w][6] == ' ':
                        sets[k][w] = str(int(el_number[i])) + ' ' + str(sets[k][w][:5]) + ' ' + str(sets[k][w][7:])
                    elif el_number[i] != 0 and sets[k][w][6] != ' ':
                        sets[k][w] = str(int(el_number[i])) + ' ' + str(sets[k][w][:5]) + ' ' + str(sets[k][w][6:])

                    elif el_number[i] == 0:
                        sets[k][w] = str('            ') + str(sets[k][w])
        return(sets)
```

```
    for i in range(gl_amount):
        sets[i] = ELEMENTS_glass(n[i+1],len_set[i],el_number[i],sets[i])

    other_el_front = lines[index2-1:index3-2]
    other_el_back = lines[index4+1:index5]

    if len(material_names) != 0:
        materi_now = list()
        for i in range(gl_amount+1, gl_amount + 1 + len(material_names)):
            materi_no = 'MATERIAL ' + str(i)
            materi_now.append(materi_no)

        materi_other = list()
        for i in range(n_tot+1,n_tot+1 + len(material_names)):
            materi_othe = 'MATERIAL ' + str(i)
            materi_other.append(materi_othe)

        # Replace the material numbers of the old element list with the new material numbers
        for i in range(len(material_names)):
            other_el_front = [x if x != materi_now[i]
                              else materi_other[i] for x in other_el_front]
            other_el_back = [x if x != materi_now[i]
                              else materi_other[i] for x in other_el_back]

    def write_gl_el(sets,set1,set2,glass_name):
        # Write glass sets in .dat file
        setname = list()
        for i in range(1,set2+1):
            setname.append(glass_name + ' ' + str(i))
        for i in range(set2):
            if len(sets[i]) != 0:
                file.write('SET "' + setname[i] + '"\n' + 'CONNECT\n')
                for j in range(len(sets[i])):
                    file.write(sets[i][j] + '\n')
                file.write('MATERIAL ' + str(set1 + i + 1) + '\n')

    def ELEMENTS():
        file.write("'ELEMENTS'\n")
        if len(material_names) != 0:
            # Print elements before the glass sets first
            for i in range(len(other_el_front)):
                file.write(other_el_front[i] + '\n')

        for j in range(gl_amount):
            write_gl_el(sets[j],n[j],n[j+1],gl_names[j])
```

```
        if len(material_names) != 0:
            # Print elements after the glass sets last
            for i in range(len(other_el_back)):
                file.write(other_el_back[i] + '\n')

    # Write LOADS and END part of .dat file ------------------------------------------------------------
    # --------------------------------------------------------------------------------------------------

    def LOADS():
        end_lines = lines[index5:]
        for i in range(len(end_lines)):
            file.write(end_lines[i] + '\n')

#     Create new .dat and write everything ===========================================================
#     ==================================================================================================

    file = open(filename + '.dat',"a+")

    COORDINATES()
    MATERI()
    ELEMENTS()
    LOADS()
    file.close()

win.iconbitmap('tudelft_invflame_XFY_icon.ico')

ttk.Button(tab1,text='Create new DIANA .dat file',command=write_dat_file).grid(column=2,row=0)

win.mainloop()
```